EXPERIMENTAL INVESTIGATION OF PERFORMANCE AND EMISSION CHARACTERSTICS OF A NANO BIOFUELED CI ENGINE

**Thesis Submitted
in Partial Fulfilment of the Requirements for
theDegree of**

DOCTOR OF PHILOSOPHY

by
SURAJ BHAN
(2K18/PhD/ME/530)

Under the supervision of

Dr. PUSHPENDRA SINGH   **Dr. RAGHVENDRA GAUTAM**
(Associate Professor)   **(Assistant Professor)**

**TO the
DEPARTMENT OF MECHANICAL ENGINEERING**

DELHI TECHNOLOGICAL UNIVERSITY
(Formerly Delhi College of Engineering)
Shahbad Daulatpur, Main Bawana Road, Delhi-110042. India.

Feb, 2024

CANDIDATE'S DECLARATION

I hereby declare that the thesis entitled "**Experimental Investigation of Performance and Emission Characteristics of a Nano Biofueled CI Engine"** is an original work carried out by me under the supervision of Dr. Pushpendra Singh (Associate professor) and Dr. Raghvendra Gautam (Assistant Professor), Mechanical Engineering Department, Delhi Technological University, Delhi. This thesis has been prepared in conformity with the rules and regulations of the Delhi Technological University, Delhi. The research work reported, and results presented in the thesis have not been submitted either in part or full to any other university or institute for the award of any other degree or diploma.

(Suraj Bhan)
2K18/PhD/ME/530
Research Scholar
Mechanical Engineering Department
Delhi Technological University
Delhi-110042

Date:
Place: Delhi

CERTIFICATE

This is to certify that the work embodied in the thesis entitled **"Experimental Investigation of Performance and Emission Characteristics of a Nano Biofueled CI Engine"** by **Suraj Bhan,** (Roll No. **2K18/PhD/ME/530)** in partial fulfilment of requirements for the award of Degree of **DOCTOR OF PHILOSOPHY in Mechanical Engineering,** is an authentic record of student's own work carried by him under my supervision**.**

This is also certified that this work has not been submitted to any other university or institute for the award of any diploma or degree.

(Dr. Pushpendra Singh)   **(Dr. Raghvendra Gautam)**
Associate professor   Assistant Professor
Mechanical Engineering Department   Mechanical Engineering Department
Delhi Technological University   Delhi Technological University
Delhi-11004   Delhi-11004

EXPERIMENTAL INVESTIGATION OF PERFORMANCE AND EMISSION CHARACTERSTICS OF A NANO BIOFUELED CI ENGINE
(SURAJ BHAN)
ABSTRACT

This current research aims is to investigate the impact of nanoparticles as fuel additives on engine performance and emissions. The experimental investigation was conducted on a CRDI diesel engine that was fuelled by a newly developed tertiary blend of nanoparticles, waste-cooking biofuel, and diesel while varying engine parameter. Present study was conducted into five distinct phases.

In the first phase biofuel is extracted from waste cooking oil via transesterification process. As per ASTM standards, physicochemical parameters were evaluated and found to be within acceptable limits. The subsequent stage includes developing a new suitable blend, B20 (20% WCO + 80% Diesel), and testing the engine's performance and emissions. The investigation test was performed on a single-cylinder diesel engine fuelled by B20 under a steady speed of 1500rpm and various loads. Experiment results revels that, compared to D100, the engine's BTE increased and its SFC decreased. As far as emissions, B20 mix decreased engine emissions like CO_2, HC, and CO than D100, except for NO_X.

The third phase consists of the utilization of metallic nanopartcile as a fuel additive to boost engine performance and emissions. Al_2O_3 nanoparticle was selected as fuel additives to improve engine performance and emissions. After that, using an ultrasonicator, Al_2O_3 was mixed in B20 at the distinct proportions of 25, 50, and 100 ppm, respectively, and new ternary blends are developed: $B20 + 25Al_2O_3$, $B20 + 50Al_2O_3$, and $B20 + 100Al_2O_3$. The experiment test was performed on a CRDI engine fuelled by Diesel, B20, $B20 + 25Al_2O_3$, $B20+50Al_2O_3$, and $B20 +100Al_2O_3$ samples at a steady speed of 1500 rpm and different engine loads to

evaluate engine performance, combustion, and emission characteristics. The test result depicts that BTE extensively improved by 13.53% and SFC reduced by 20.93% for B20 +100Al_2O_3 than B20 at full load. The emission characteristics, for example, CO, and HC were altogether decreased with the mixing of nanoparticles in the correlation of B20 and D100 yet there is a slight increment in NOx emissions than B20 and D100. Higher peak points in CPmax and HRRmax reached for B20 +100Al_2O_3 because of reduced ignition delay than that of B20 and D100.

In the fourth stage, two different nanoparticles were compared as fuel additives to investigate their impact on engine emissions and performance. Two distinct metal-based nanoparticles cerium oxide (CeO_2) and aluminium oxide (Al_2O_3) were blended in B20 in different proportions. An ultrasonication procedure was used to homogenously mix the nanoparticles with a B20 fuel in mass fractions of 50 and 100 ppm. The developed nanoparticle fuel samples were designated as (B20+50 Al_2O_3, B20+100 Al_2O_3, B20+50 CeO_2, B20+100 CeO_2). The CRDI engine was run at a constant speed with four different engine loads: 3kg, 6kg, 9kg, and 12kg. The result showed that the presence of Al_2O_3 in the blended fuel improved the BTE by 11.39%, reduced the SFC by 13.74%, and increased the cylinder pressure and heat release rate (HRR) by 16.77% and 21.48% respectively compared to B20 fuel at peak load condition. Regarding harmful emissions, CO emissions decreased by 15.06% for B20+50 Al_2O_3 than B20 and HC emissions decreased by 50% for B20+50 CeO_2 than diesel at peak load. Further, NOx is reduced by 18.29 % for B20+50 CeO_2 than B20 at peak loads.

In the last stage, newly developed waste cooking biodiesel (B20) with nanoparticles (Al_2O_3) was tested to optimize the response of a CRDI single-cylinder four-stroke VCR

engine at various input parameters. A response surface methodology (RSM) was used to investigate the impact of various input parameters, such as injection pressure (IP), load, compression ratio (CR), and nanoparticle concentration as fuel additives on engine responses, including brake thermal efficiency (BTE), specific fuel consumption (SFC), carbon dioxide (CO), hydrocarbon (HC), and oxide of nitrogen (NO_X) emissions. The RSM found the best suitable value of all input parameters at which the engine produced maximum performance and minimum emissions. Accordingly, the optimal setting of all input parameters was identified as a nano biofuel blend ratio of 1.10, IP of 656 bars, CR of 18.50, and a load of 7.10 kg. At this combination of input parameters, the optimal BTE, SFC, CO, HC, and NOx are 23.6%, 0.3461 kg/kWh, 0.0281%, 25.3756 ppm, and 536.41 ppm respectively. The predicted optimum value from RSM is compared with the experimental value for validity and found a fair agreement.

Key words: Waste cooking oil, Al_2O_3, CeO_2, Response surface methodology, BTE, SFC, CO, HC, and NOx

ACKNOWLEDGEMENT

At the very outset of this thesis, I would like to express my sincere and heartfelt gratitude to my learned guide Dr. Pushpendra Singh and Dr Raghavendra Gautam, under whose esteemed supervision I had accomplished the present research work. Without his panegyric efforts, active participation, ever helping attitude and cooperation, I would not have made headway in my work. His constant encouragement and 'never give up' perspective, especially during difficult times, have always led me to become a good researcher. I am especially grateful to my mother Smt. Jai Vati, who has supported me emotionally. I would also like to extend my gratitude to Prof. S.K. Garg, Head, DRC Chairman, Prof. S.P.S Rajput NIT Bhopal, Prof. Faizan Ahamad Sherwani, Jamia Millia Islamia New Delhi, Prof. R C Singh DTU Delhi, Prof. M.S. Chaudhary DTU Delhi, Dr Abhishek Sharma, Associate Professor in Mechanical Engineering, LNJPIT Chapra, Bihar, Dr. Harveer Singh Pali, Assistant Professor, NIT Srinagar, Dr. Sumit Mahajan, Assistant Professor, Noida International university, Dr. Vishal Vasistha, Assistant professor for their guidence and unwavering support.

I owe a debt of appreciation to the supportive colleagues DTU, Delhi; in particular, Dr. Abhishek Sharma, Associate Professor, LNJPIT Chapra, Dr. Prem Shanker Yadav, Assistant Professor, JSS Academy of Technical education Noida, and existing researcher of centre for advance studies in vehicle diagnostic in research in automobile engineering lab Mr. Saket Kumar and Mr. Manoj Kumar for their valuable guidance, persistent help and support.

LIST OF CONTENT

LIST OF FIGURES

and their combined impact on NOx.

LIST OF PLATES

LIST OF TABLES

NOMENCLATURE

CI	Compression Ignition
CO_2	Carbon Dioxide
CO	Carbon Monoxide
COP	Conference of Parties
HC	Hydrocarbon
NOx	Oxides of Nitrogen
PM	Particulate Matter
SO_2	Sulphur Dioxide
UNFCCC	United Nations Structure Convention on Climate Change
mb/d	Million barrel per day
ICE	Internal Combustion Engine
CP	Cloud point
PP	Pour point
GHG	Green House Gas
CH_4	Methane
CN	Cetane number
g/km	Gram Per Kilometer
PPM	Parts Per Million
Afs	Alternative Fuels
WCO	Waste Cooking Oil
MT	Metric Ton
FFA	Free Fatty Acid
TWh	Terawatt-hours
BTE	Brake Thermal Efficiency
IMEP	Indicated Mean Effective Pressure
BSFC	Brake Specific Fuel Consumption
MMT	Million Metric Ton
Ml	Milli Liter

Gm	Gram
Mol. Wt	Molecular Weight
WCOME	Waste Cooking Oil Methyl Ester
KJ/Kg	Kilo Jule Per Kilogram
CN	Cetane Number
TPM	Total Polar Material
Hrs	Hours
Hz	Hertz
Ms	Milli Second
μm	Micrometer
KW	Kilo Watt
Rpm	Revolution Per Minute
RSM	Response surface methodology
B20+25Al$_2$O$_3$	20% biodiesel+80% diesel+25ppm Al$_2$O$_3$ nanoparticles
B20+50Al$_2$O$_3$	20% biodiesel+80% diesel+50ppm Al$_2$O$_3$ nanoparticles
B20+75Al$_2$O$_3$	20% biodiesel+80% diesel+75ppm Al$_2$O$_3$ nanoparticles
B20+100Al$_2$O$_3$	20% biodiesel+80% diesel+100ppm Al$_2$O$_3$ nanoparticles
B20+25CeO$_2$	20% biodiesel+80% diesel+25ppm CeO$_2$ nanoparticles
B20+50 CeO$_2$	20% biodiesel+80% diesel+50ppm CeO$_2$ nanoparticles
B20+100CeO$_2$	20% biodiesel+80% diesel+100ppm CeO$_2$ nanoparticles
bTDC	Before Top Dead Centre
ASTM	American Society for Testing and Materials
HRR	Heat release rate
FAME	Fatty Acid Methyl Ester
B100	Biodiesel (100%)
B20	Diesel (80%)+Biodiesel(20%)
D	Diesel
D100	100% Diesel
JOME	Jatropha Oil Methyl Ester
VCR	Variable Compression Ratio

CRDI	Common Rail Direct Injection
P_{inj}	Injection Pressure
P_{amb}	Ambient Pressure
mN/m	Milli Newton per Meter
CH_3OH	Methanol
TEM	Transmission Electron Microscopy
XRD	X-ray Diffraction
SEM	Scanning Electron Microscopy
ID	Ignition Delay
CCRD	Central Composite Rotational Design
RSM	Response Surface Methodology
CCD	Central Cubic Design
Wt%	Percentage of Weight
KOH	Potassium Hydroxide
PTSA	P-toluenesulfonic Acid
UHC	Unburnt Hydrocarbon
GC	Gas Chromatography
PSI	Pound per Square Inch
Hp	Horse Power
ANOVA	Analysis of Variance
CR	Compression RatiO
IP	Injection pressure
Mg	Milli Gram

CHAPTER 1
INTRODUCTION

Overview

This section delves into the research background, commencing with the motivation behind the current study and an examination of India's energy landscape. Additionally, it addresses environmental concerns linked to exhaust emissions and their potential health impacts. The narrative then proposes an alternative approach, leveraging advanced technology and alternative fuels to mitigate harmful pollutants. Emphasis is placed on the impact of nanoparticle as fuel additive on combustion, as well as performance and emissions in diesel engines. The chapter concludes by providing an overview of the thesis structure.

1.1 Energy crisis

Traditional energy sources often come from non-renewable sources of combustion, such as coal, raw oil, and combustible gases. It was estimated that global oil and different fluid reserves would be consumed at a rate of 36.5 billion barrels in 2018 [1]. Around 80% of the world's total energy use is represented by this information. Over the past 50 years, the use of petroleum products has fundamentally increased, about doubling starting around 1950 and generally multiplying starting around 1980. However, the types of fuel we rely on have also changed, from being solely coal to a mix of coal and oil, then to petrol. Today, less coal is being used in many parts of the world. Oil and gas, however, are still expanding quickly. That is seen in figure no 1.1 [2]. Industrialization, transportation, and indulgence in the luxury life of the growing population have led to a serious energy crisis and ecological pollution. The transport system plays a major role in energy consumption. 32% of the total energy consumed in the transport system is used to maintain human comfort and standardization as shown in figure 1.2 [3]. World energy efficiency is expected to rise from 575 trillion Btu in 2015 to 736 trillion Btu (define unit) in 2040, with a 28% increase in total energy. Most of the increase was provided by non-OECD countries, some of which was 41%, while in OECD countries it increased by 9 % [4]. Moderation commitments, for example, the Kyoto Protocol in 1997 and the Paris Agreement in 2015, have cultivated the development of sustainable power source use because of the squeezing atmosphere-related dangers, for example, untimely mortality from encompassing air contamination [5], work limit, vector-borne infections, and effect on food security due to rising worldwide temperature [6]. Under these arrangements and understandings, nations are required to meet their discharge's focus through national measures to manage the alleviation of ozone-depleting substances. For instance, as of late the Paris Agreement rulebook has been concluded during the COP24 composed by UNFCCC in Katowice, Poland, such that nations set out to keep unnatural weather change to well underneath 2° C above pre-mechanical levels by 2100 and to confine the expansion to 1.5° C [7]. As per the above conversation, because of the expanding population and standardization of mankind, the request for petroleum products is expanding fundamentally. The increasing cost and finite availability of petroleum oil have been driven by its rapid consumption. Public

transport vehicles commonly rely on internal combustion (IC) engines due to their durability, reliability, and capacity for high power generation across different loads and speeds.

1.2 Negative impact of energy consumption on environment

At the point when petroleum products are consumed in IC motors, dangerous toxins such as carbon monoxide (CO), unburned hydrocarbons (HC), nitrogen oxides (NOx), and smoke are created. Negative emissions represent a serious risk to the climate, human well-being, and the environment [8, 9]. The essential supporter of air contamination is the transportation system.
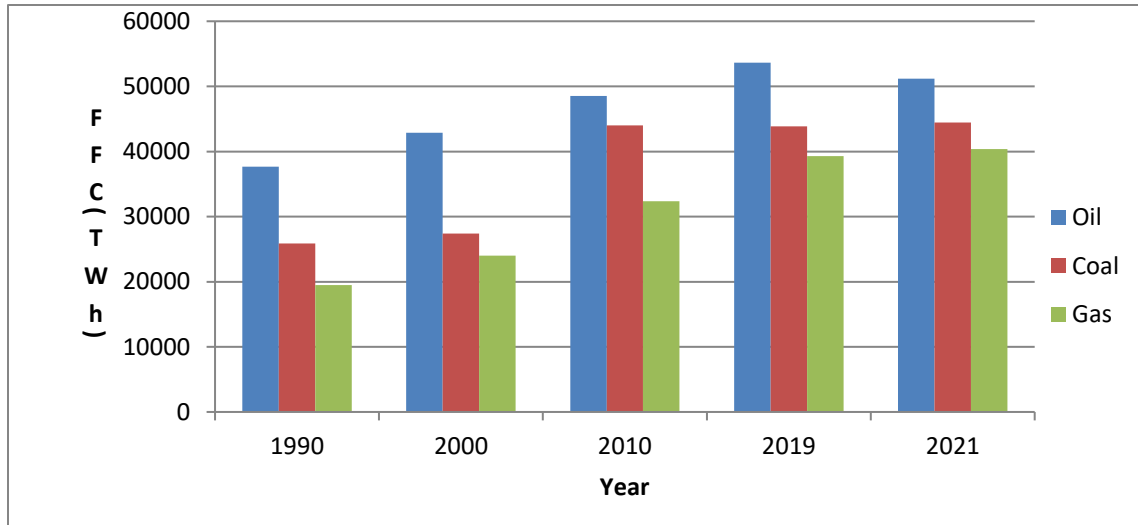
Fig. 1.1 Consumption of nonrenewable energy

The transportation framework is answerable for around 14% of all air contamination, as seen in fig1.3 [10]. As per the after effects of the lightning search calculation (LSA), marine hunters' calculation (MPA), balance streamlining agent (EO), cooperative creatures search calculation (SOS), and backtracking search calculation (BSA), CO_2 discharges and F-gases will ascend somewhere in the range of 2.5 and 2.87 times for CO_2 outflows and somewhere in the range of 2.8 and 3.5 times for F-gases in 2050. GHG emanations would normally increase by 2.1-2.4 times more in 2050 than today [11]. Specialists are in this way exploring elective fuel sources to decrease ecological corruption and end our dependence on petroleum products [12]. There are various sources of energy, which can be grouped into general categories such as primary and secondary, renewable and non-renewable, and fuels. Primary energy sources include fossil fuels (petroleum, natural gas, and coal), nuclear energy, and renewable sources of energy. In the United States, British thermal units (Btu), a measure of heat energy, is commonly used for comparing different types of energy to each other [13].

1.2.1 Importance of alternative fuel and renewable sources

The significance of adopting alternative fuels and harnessing renewable energy sources cannot be overstated. As our planet faces unprecedented challenges posed by climate change, dwindling fossil fuel reserves, and environmental degradation, transitioning to cleaner, greener energy solutions has become imperative.
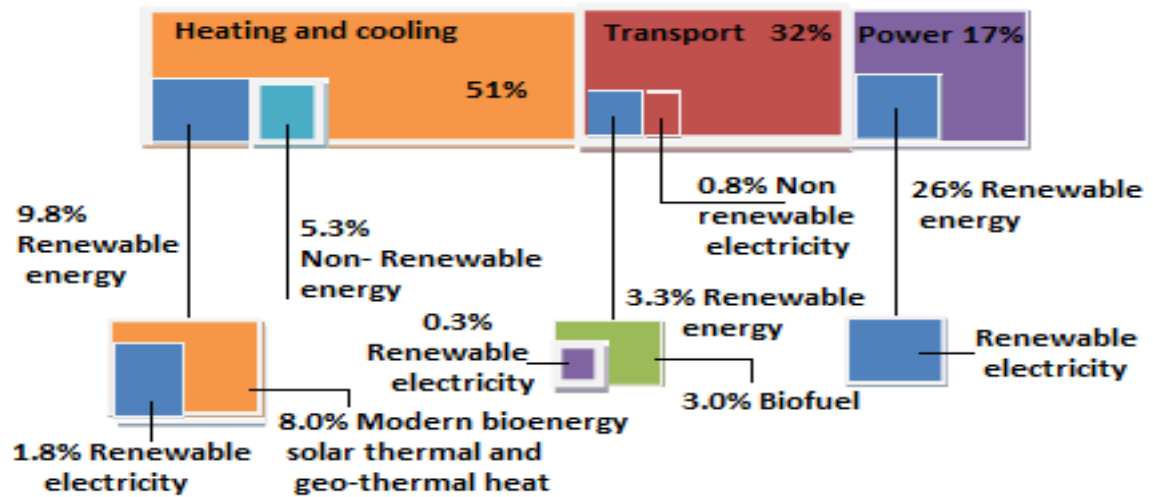
Fig.1.2 Renewable energy in total final energy consumption [3]
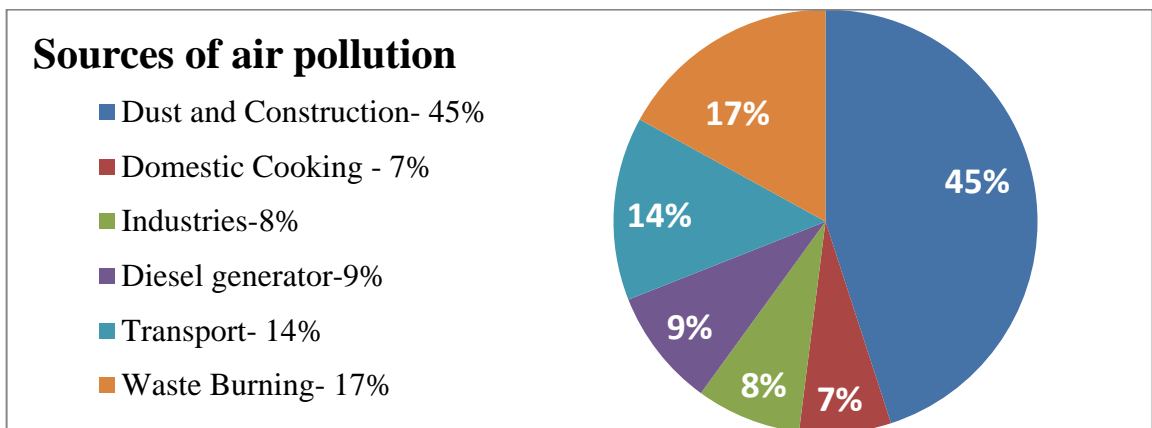
Fig.1.3 Sources of air pollution [10]

In this paradigm shift, the role of alternative fuels and renewable sources emerges as pivotal in shaping a more resilient and environmentally responsible society. First and foremost, embracing alternative fuels and renewable sources offers a pathway to mitigate the adverse effects of greenhouse gas emissions on our planet's delicate ecosystems. Traditional fossil fuels, such as coal, oil, and natural gas, are major contributors to air pollution and global warming. By shifting towards cleaner alternatives like biodiesel, ethanol, hydrogen, and compressed natural gas, we can significantly reduce carbon emissions, thereby curbing the pace of climate change and its catastrophic consequences. Furthermore, the utilization of renewable energy sources such as solar, wind, hydroelectric, and geothermal power presents a viable solution to the energy challenges we face. Unlike finite fossil fuels, renewable resources are abundant and inexhaustible, offering a sustainable energy supply for generations to come. Harnessing these sources not only reduces our dependence on non-renewable resources but also promotes energy security and fosters economic development through job creation and technological innovation. Moreover, the adoption of alternative fuels and

renewable energy sources aligns with the imperative to diversify our energy portfolio and enhance energy resilience. Relying solely on fossil fuels leaves us vulnerable to price fluctuations, geopolitical tensions, and supply disruptions. In contrast, decentralizing our energy infrastructure and investing in renewable technologies empower communities to generate their own clean energy, thereby

enhancing energy security and reducing vulnerability to external shocks. Additionally, transitioning to alternative fuels and renewable sources fosters a paradigm shift towards a circular economy, wherein resources are conserved, reused, and recycled in a closed-loop system. By promoting energy efficiency, reducing waste, and minimizing environmental degradation, we can transition towards a more sustainable and regenerative model of development that meets the needs of the present without compromising the ability of future generations to meet their own needs [13].

1.3. Sources of energy

1.3.1 Non-renewable sources of energy

1.3.1.1 *Coal production*

A coal-based energy source is non-renewable. A high energy demand has led to a rapid depletion of coal. In 2021, it reached about 1.13 billion short tons in the United States. However, coal production peaked in 2008 at about 1.17 billion short tons. In 2021, coal accounted for approximately 546 million short tons and 10.55 quads of U.S. energy consumption. A total of 578 million short tons of coal were produced in 2021, which is equal to approximately 11.62 quads. Since coal is a limited source of energy, researchers are looking for renewable, sustainable alternatives [13]. The non renewable energy production according to U.S. primary energy source, 2021 was shown in fig 1.4.

1.3.1.2 *Natural gas production*

In 2021, natural gas production (dry gas) reached a record high of 34.15 trillion cubic feet (Tcf) or 93.57 billion cubic feet per day (Bcf/day). The U.S. consumed 82.97 Bcf/day of natural gas in 2021, or about 32% of its total energy consumption. Natural gas prices declined through 2020 as a result of increased production, contributing to increased electric power and industrial use of natural gas [13].

1.3.1.3 *Renewable energy production*

Traditionally, energy has been derived from non-renewable sources. Almost all energy is derived from non-renewable resources. Due to greater reliance on non-renewable resources, the non-renewable energy crisis emerged. As a result of record-high solar and wind energy production, renewable energy production and consumption reached record highs in 2021 of about 12.32 and 12.16 quads, respectively. In 2021, hydroelectric power production was about 9% lower than in 2020 and about 19% lower than the 50-year average. Despite higher biomass production and consumption in 2021 than in 2020, they were lower than the record highs in 2018. The amount of geothermal energy used in 2021 was about 1.5% higher than in 2020, but was lower than the record high in 2014 [13].

1.3.1.4 *Nuclear energy production*

Nuclear energy production in commercial nuclear power plants in the United States began in 1957, grew each year through 1990, and generally levelled off after 2000. Even though there were fewer operating nuclear reactors in 2021 than in 2000, the amount of nuclear energy production in 2021 was about 778 billion kilowatt-hours (kWh), equal to about 8.13 quads. A combination of increased electric generation capacity upgrades and shorter

refuelling and maintenance cycles at nuclear power plants have helped to compensate for reductions in the numbers of nuclear reactors and to maintain a relatively consistent level of annual U.S. nuclear electricity generation for the past 20 years [13].

1.3.1.5 *Petroleum oil production*

Annual crude oil production generally decreased between 1970 and 2008. In 2009, the trend reversed and production began to rise, and in 2019, U.S. crude oil production reached a record high of 12.29 million barrels per day. U.S. petroleum demand decreased in 2020 and 2021 largely due to COVID-19 pandemic [13].
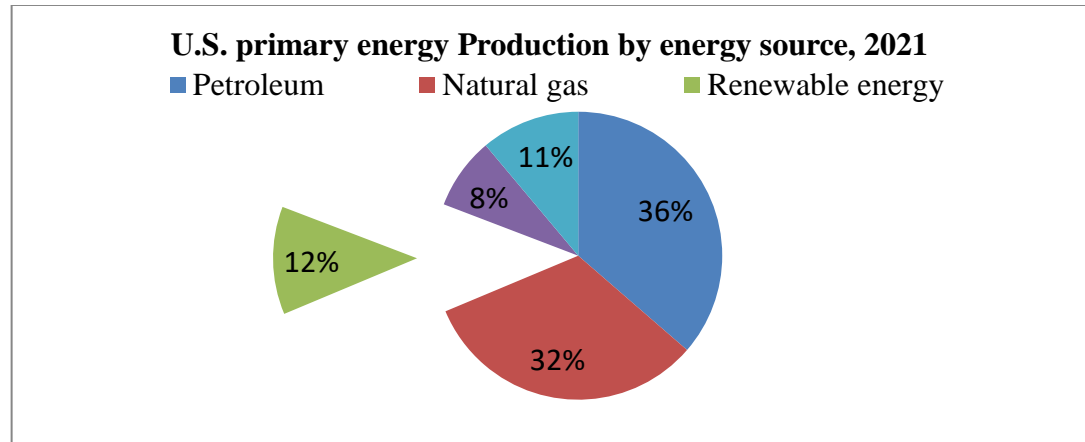
Fig. 1.4 Primary energy production data [13]

1.3.2 Renewable sources of energy

Renewable energy sources and technologies have potential to provide solutions to the long-standing energy problems being faced by the developing countries. The renewable energy sources like wind energy, solar energy, geothermal energy, ocean energy, biomass energy and fuel cell technology can be used to overcome energy shortage in India. To meet the energy requirement for such a fast-growing economy, India will require an assured supply of 3–4 times more energy than the total energy consumed today. The renewable energy is one of the options to meet this requirement. Today, renewable account for about 33% of India's primary energy consumptions. India is increasingly adopting responsible renewable energy techniques and taking positive steps towards carbon emissions, cleaning the air and ensuring a more sustainable future. In India, from the last two and half decades there has been a vigorous pursuit of activities relating to research, development, demonstration, production and application of a variety of renewable energy technologies for use in different sectors. In this paper, efforts have been made to summarize the availability, current status, major achievements and future potentials of renewable energy options in India. Various types of renewable energy participation is shown in fig 1.5 [13].

1.3.2.1Hydroelectric

Hydro power is currently the largest renewable energy source for power generation around the world. Hydro electricity generation has had a strong increase over the past 50 years. It was 340 TWh in 1950 and covered about one-third of the global electricity demand. It increased to 1,500 TWh in 1975 and further to 2,994 in 2005. We can compare this to the global consumption of 15,000 TWh of electricity with a global production of 18,306 TWh in

2005 [14]. Currently, hydro power development is difficult due to a large initial fixed investment cost and environmental concerns. Additionally, hydro power has caused problems for local residents associated with the need to relocate large populations, as well as the construction of dams is permanent with a sunk cost of utilities which cannot be removed. The environment is also influenced by hydro power construction because of large engineering works. On the other hand, hydro power is attractive due to a pre existing supply of water for agriculture, household and industrial use, and hydro power is clean and enables the storage of both water and energy. Also, the stored energy can be used for the application of both base-load and peak time power generation.

1.3.2.2 Wind energy

The trend shows that wind capacity installation has increased continuously throughout the last two decades. IEA estimates that the global capacity will increase from 238 GW in 2011 to almost 1,100 GW by 2035, of which 80% will be derived from onshore wind turbines [15].

1.3.2.3 Solar energy

During the two last decades, the economic feasibility of solar power for residential, commercial and industrial consumption has been investigated by researchers. Industrial countries like Japan and Germany are looking for alternative sources of energy such as solar power due to the limited availability of natural primary energy sources. In early 1990s, Japan started to take advantage of large-scale electricity generation by solar photovoltaic (PV), and was soon followed by Germany. Currently, both countries have taken the lead in the manufacture and production of solar power technologies. More recently, China has developed an extensive solar power capacity due to cheap labour and government subsidies, in turn, decreasing the cost of solar power generation. Alongside the cost reduction in power generated through conventional solar PV technologies, the advancement, and increase in efficiency, of concentrated solar power technologies in the US has further reduced the cost of electricity in the solar power industry [16].

1.3.2.4 Geothermal

Geothermal is a type of thermal energy generated and stored within the Earth. It has been used throughout history for bathing, heating and cooking. Geothermal energy is created by radioactive decay, with temperatures reaching 4,000˚C at the core of the Earth. While geothermal energy is available worldwide, there is an important factor called the geothermal gradient that indicates whether a region is a favored place for enactment. It measures the rate at which the temperature increases as the depth of the Earth increases. For example, the average geothermal gradient in France is 4˚C/100m with a range of 10˚C/100m in the Alsace region to 2˚C/100m in the Pyrenees Mountains. In Iceland and the volcanic regions, the gradient can reach as high as 30˚C/100m [14].

1.3.2.5 Biomass energy

Biomass is defined as living plants and organic waste which are made by plants, human, marine life, and animals. Based on Tester (2005), the main advantage of biomass is availability, as it can be readily found in all places. Many kinds of energy can be produced from biomass: electricity, cooking heat, chemical feedstock, etc. As a feedstock, biomass has lower sulfur content than coal and a lower emission is produced by combustion. In early 2000, the United States had an installed capacity of 11 GW from biomass including the forest product and agricultural industry, municipal and solid waste industry, and other sources [14].

Renewable Energy Data

- Geothermal energy
- Solar
- Hydroelectric
- Wind
- Biomass waste
- Biofuels
- Wood

2%
12%
17%
19%
19%
4%
27%
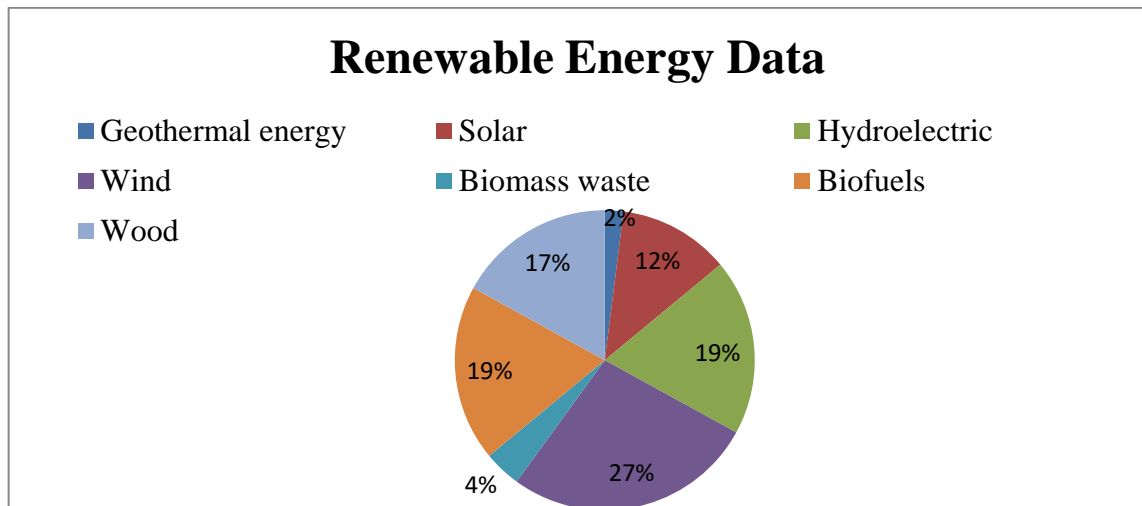
Fig. 1.5 Renewable energy sources data [13]

1.3.2.6 Biofuel

Biodiesel produced from a variety of raw material sources, such as vegetables, animal fats, algae oils and microbial oil sources. Biodiesel is methyl ester, usually derived from free fatty acids from various natural resources. Biofuels can act as alternative fuels to fossil fuels because they have many beneficial properties which are given below.

- Biofuel has physical and chemical properties that are similar to diesel.
- It may be locality available in various types of feedstock. It may be produced from waste fatty material. Although biofuel is produced, solid waste management may occur on other aspects.
- It is compatible to use in a diesel engine without modification in diesel engine design.
- It is miscible with diesel due to which it can use with a blend of diesel.
- Biofuel is biodegradable, sustainable, non-toxic, and eco-friendly.
- Biofuel is oxygenated fuel due to which it offers more oxygen during the combustion of fuel. Oxygen molecules help in the burning of fuel. So that proper burning of fuel takes place inside the combustion chamber.
- Biofuel flash point is high so that it is easy to handle in the transport system.
- Biofuel is more viscous in comparison to diesel due to which fantastic lubricity to diminish wear and to expand the life of fuel injection.
- Biodiesel holds extraordinary potential for animating economical country improvement and an answer for energy security issues.
- Biodiesel shouldn't be transported, refined, and drilled like diesel.
- Biodiesel creation is simpler in contrast with diesel.
- Biodiesel has a higher cetane number in comparison to diesel.
- It has the capacity to diminish CO_2 discharges contrasted with fossil diesel or remaining CO_2 nonpartisan [17,18,19].

On the other aspect biofuel has some limitations like as:

- Biofuel has a lower calorific value in comparison to diesel fuel.
- It has a high pour point so that it has poor storage stability and cold flow properties.
- Biofuel has lower oxidation stability.
- Biodiesel has a corrosive nature against copper and brass.

- Biodiesel produces lower engine speed and torque on the shaft. The biodiesels on the normal abatement power by 5% contrasted with that of diesel at rated load
- Coking of injectors on the piston and head of the engine is the major problem. Researchers are attentive towards it to remove this problem.
- Biofuel has high viscosity due to which it has inferior spray characteristics resulting in insufficient mixing of fuel, improper combustion of fuel.
- Biodiesel degradation under storage for prolonged periods.
- In the case of biofuel combustion of fuel take place at higher temperature due to more oxygen molecule in the structure of biofuel.
- The high viscosity, in long haul activity, presents the arrangement of injector deposits, stopping of channels, lines and injectors, ring sticking and contradiction with ordinary.
- It was seen by the researcher biofuel has the more BSFC and lower BTC. But it can say that its biofuel produced lesser CO and HC emissions but increase CO_2 emissions comparatively. At the higher flame temperature oxides of nitrogen formed.
- Biodiesel causes excessive engine wear [17, 18, 19].

1.4 Sources of biofuel

Biofuels are renewable fuels made from biological materials such as crops, agricultural waste, and organic matter. Here are some sources of biofuel:

- Corn - Corn is a commonly used feedstock for biofuels such as ethanol.
- Sugarcane - Sugarcane is another common source of biofuels, particularly ethanol.
- Soybean - Soybean oil is used to make biodiesel, a renewable alternative to petroleum-based diesel fuel.
- Algae - Algae is a promising source of biofuels due to its high oil content and rapid growth rate.
- Waste vegetable oil - Used vegetable oil can be converted into biodiesel.
- Animal waste - Animal waste, such as manure, can be used to produce biogas through a process called anaerobic digestion.
- Wood - Wood and other types of biomasses can be burned to produce bioenergy.
- Municipal solid waste - Municipal solid waste can be processed to produce a biofuel known as refuse-derived fuel.
- Switchgrass - Switchgrass is a perennial grass that can be converted into biofuels such as ethanol.
- Jatropha - Jatropha is a plant that produces oil-rich seeds that can be used to make biodiesel [18].

1.5 Need of biofuel

Biofuels have gained increasing attention as a viable alternative to traditional fossil fuels due to several reasons:

Renewable and sustainable: Biofuels are made from renewable sources, such as crops, agricultural waste, and organic matter, which can be grown or produced continuously, making them a sustainable source of energy.

Reduced greenhouse gas emissions: Biofuels can help reduce greenhouse gas emissions because they release less carbon dioxide into the atmosphere than traditional fossil fuels when they are burned. Some biofuels, such as biogas produced from animal waste, can actually reduce greenhouse gas emissions by capturing methane that would otherwise be released into the atmosphere.

Energy security: Biofuels can reduce dependence on foreign oil and enhance energy security by diversifying the fuel supply.

Economic benefits: The production and use of biofuels can create jobs and stimulate economic growth in rural areas by providing new markets for agricultural products.

Technological advancements: The development of biofuels has spurred technological advancements in the fields of biotechnology, agriculture, and engineering, which can have positive impacts on other industries as well [18].

Overall, biofuels can contribute to a more sustainable and secure energy future, reduce greenhouse gas emissions, and provide economic benefits.

1.6. Biofuel generations

Biodiesel feedstocks has categorized in three type of generation which are based on FFA content. These generations are given below:

- First generation (edible oil)- less than 1% FFA
- Second generation (nonedible oil)- more than 2% FFA
- Third generations (micro algae)

First generations incorporate the production of biodiesel from edible oils which include Sunflower, Soya been, Palm oil, and so forth. The FFA content of first generation (edible oil) oil is generally less than 1%wt. basic alkaline catalyst are often used to produce first generations biofuel because of it contains fewer FFA. When FFA responds with hydroxide particles, it produces soap, which decreases catalyst activity. A lot of water is produced in this procedure, prompting an additional purification procedure. Economically it preferred for commercial use only. The second generation incorporates non- eatable oils, for example, Pongamia pinnata (Karanja), elastic seed oil, and Jatropha curcas, which contains high FFA (>2%wt). Acid catalysts are normally used to create biofuels in a second-generation oil (no eatable oil). Acid catalyst production can expel the saponification process, increase productivity, and reduce production costs. In the third generation; algae are normally utilized in biofuel production. Algae give the greatest yield of biofuel production what's more, photosynthesis proficiency. So now day's algae growth is generally utilized as a feedstock for biodiesel production however a primary issue in the creation of oil is the extraction of the oil which can be evacuated by utilizing the solvents. Feedstock for fourth-generation biofuels is cellulosic biomass. Unlike first-generation biofuels, which rely on food crops like corn and sugarcane, cellulosic biomass can be sourced from a variety of non-food agricultural residues, forestry residues, and dedicated energy crops such as switchgrass and miscanthus. Cellulosic biomass is rich in cellulose, hemicellulose, and lignin, which can be enzymatically hydrolyzed and fermented into biofuels like cellulosic ethanol and biobutanol. This approach not only mitigates concerns about food security and land competition but also utilizes abundant waste streams, promoting resource efficiency and waste reduction. Furthermore, waste materials represent a valuable yet often overlooked feedstock for fourth-generation biofuels. Municipal solid waste, agricultural residues, food waste, and industrial by-products can be converted into biofuels through processes such as anaerobic digestion, gasification, and pyrolysis. By repurposing these waste streams, fourth-generation biofuels offer a sustainable solution to waste management while simultaneously producing renewable energy. This integrated approach not only reduces greenhouse gas emissions from landfills but also contributes to the circular economy by closing the loop on waste utilization [17,18,19]. Generations of biofuel arranged as indicated by FFA content is given in figure1.6 underneath.
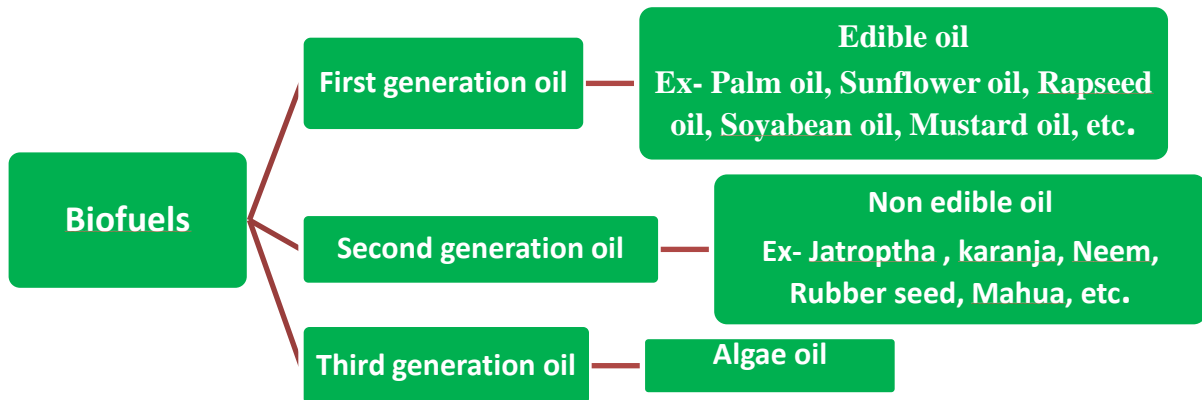
Fig.1.6 Generation of biofuel

Biofuel obtained from the various types of generations contains high viscosity, low volatility, and polyunsaturated properties in comparison to fossil fuels. To avoid this difficulty, biodiesel production uses a variety of production methods, such as pyrolysis, micro-emulsion, hydrocarbon blend, and the transesterification process.

1.7. Waste cooking oil as a biofuel source

The world has become contaminated with toxic pollutants from multiple sources due to increasing human activities. Amongst the most prominent pollutants released from anthropogenic activities are petroleum hydrocarbons and polycyclic aromatic hydrocarbons (PAHs), which include cooking oil as it is also categorised as a hydrocarbon compound. Waste cooking oil is the major waste generated from food processing industries, dairy industries, kitchen activities, bakeries and beverage industries. This problem is also one of the main concerns of environmentalists as it is discharged into drains, running water or sewages without prior treatment, which causes damage to the environment. The presence of toxic, organic and volatile compounds such as acrylamide, aldehyde, and 4- hydroxymethylfurfural in heated cooking oil (waste oil) has been known to have mutagenic and carcinogenic activities. Additionally, toxic compounds in the oil can be readily dissolved into the water and absorbed into living cells, eventually killing plants and animals. Furthermore, the consumption of heated cooking oil or the produced toxic compounds can cause inflammation, endothelial dysfunction, high blood pressure and neurodegenerative diseases [20].

Deep frying is one of the popular food processing methods across the globe. Vegetable oils such as palm, sunflower, coconut, peanut, soybean, corn, cottonseed, canola, and safflower are commonly used for frying food items. Reusing this deep-fried oil repeatedly for frying purposes is responsible for many health hazards in human population. Fried food may absorb many oxidative products such as hydro peroxide and aldehydes, which are produced during this process. This affects the quality of oil. The quality of oil deteriorates with increased length of frying time due to the accelerated formation of oxidized and polymerized lipid species in the frying medium. If the physio-chemical properties of cooking oil deteriorate, the oil must be discarded because it can prove to be harmful for human .Oxidation; hydrolysis and thermal degradation are the chemical reactions occurring as a result of repeated heating of cooking oil for low and cheap food production[21].

Hydrolysis: Moisture from the food being fried vaporizes and hydrolyses triglycerides (TGs) in the frying oil to glycerol, free fatty acids (FFA s) , monoglycerides (MGs) and diglycerides (DGs).

Oxidation: Triglyceride molecules in the frying oil undergo primary oxidation to unstable lipid species called —hydro peroxides‖ which Cleave to form secondary oxidation products which comprise non-volatile and volatile compounds. Some of these secondary products polymerize (t e r t i a r y o x i d a t i o n), increasing the oil viscosity, cause browning on the surface, and darken the oil [24].

Thermal Polymerization: High temperatures of the frying operation produce high molecular cyclic fatty acid (FA) monomers, and TG dimers and oligomers [22, 23, 24].

1.7.1 Waste cooking oil as wastage

In general, polar material content can be easily measured and so, it is used as a measure of oil degradation. When frying oil contains more than 25% TPM, it is generally considered as Waste cooking oil (WCO). According to TPM value in WCO significantly differs based on the type of oil.

1.7.2 Negative impact of waste cooking oil

When food items, prepared using WCO, are consumed, it causes many health hazards. Author concluded that long-term consumption of cooking oil that is repeatedly heated, results in hepatic dysfunction. Previously, author reported increase in blood pressure, increase in total cholesterol, and vascular inflammation as the consequences of prolonged consumption of repeatedly-heated oil. Owing to the health risks associated with consumption of WCO and environmental effects owing to the disposal of WCO, various research efforts have been initiated to recycle or repurpose WCO. WCO can also be used as a feedstock for producing biofuels such as biodiesel. WCO is an economic feedstock for biodiesel production [24].

1.7.3 Recycle of waste cooking oil as a biofuel

Increased energy consumption and the depletion of petroleum reserves have pushed up oil prices globally. The diminishing petroleum reserves are a problem inherent in this type of fossil energy. One alternative energy source that has the potential to be developed in Indonesia is biodiesel. Used cooking oil or used cooking oil is a potential raw material for making biodiesel.

1.8 Metallic nanoparticles

Metallic nanoparticles have fascinated scientist for over a century and are now heavily utilized in biomedical sciences and engineering. They are a focus of interest because of their huge potential in nanotechnology. Today these materials can be synthesized and modified with various chemical functional groups which allow them to be conjugated with antibodies, ligands, and drugs of interest and thus opening a wide range of potential applications in biotechnology, magnetic separation, and pre-concentration of target analyses, targeted drug delivery, and drug delivery and more importantly diagnostic imaging and vehicles as a fuel additive.

Nanotechnology refers to the branch of science and engineering dedicated to materials, having dimensions in the order of 100th of nm or less. The term being new, but has been widely used for the development of more efficient technology. In recent years, nanotechnology has been embraced by industrial sectors due to its applications in the field of biotechnology, magnetic separation targeted drug delivery, and as fuel additives in mechanical engineering. Consequently, with wide range of applications available, these particles have potential to

make a significant impact to the society. As the field of nanotechnology advanced, novel nanomaterials become apparent having different properties as compared to their larger counterparts. This difference in the physiochemical properties of nanomaterials can be attributed to their high surface-to-volume ratio. Due to these unique properties, they make excellent candidate as fuel additives in petroleum oils [25].

1.8.1 Importance of nanoparticles as fuel additives

In the quest to enhance engine performance and characteristics, researchers have introduced nanoparticles as additives in biodiesel. The unique high surface-to-volume ratio of nanoparticles provides several advantages over biodiesel without nanoparticles. These benefits include improved fuel atomization, increased fuel interaction with oxygen, reduced ignition delay, enhanced evaporation, better air-fuel mixing, lowered cylinder pressure, and a reduced heat release rate, as depicted in Figure 1.7. Research findings indicate that introducing nanoparticles into biodiesel results in heightened brake thermal efficiency, decreased brake-specific fuel consumption (BSFC), diminished NO_X emissions, and improved overall emission characteristics, including reductions in hydrocarbons (HC), carbon monoxide (CO), and carbon dioxide (CO_2). The utilization of fuel additives can alter various fuel properties like density, sulphur content, and volatility, consequently influencing fuel emissions.

- Researchers have explored the viability of enhancing combustion characteristics by incorporating nanoparticle additives into liquid fuels as a supplementary energy carrier. The feasibility of utilizing modified fuels containing metal oxides such as Cu, Fe, Ce, Pt, B, Al, and Co has been investigated in diesel engines and biodiesel fuel blends.
- Nanoparticles addition improves fuel droplet propagation and injected fuel dispersion. Adding nanoparticles create smaller droplets, lower fuel viscosity and expose to higher effective fuel surface.
- The main reason for this power increase can be attributed to the produced additional energy inside the cylinder by increasing the surface to the volume ratio of nanoparticles, and thereby enhancing the heat transfer.
- The addition of nanoparticles aids in fuel droplet propagation and injected fuel dispersion. Nano sized particles possess reactive surfaces which aids in reactivity as a potential catalyst. Fuel air mixing and combustion characteristics improvements were shown due to the presence of nanoparticles.
- Shorter ignition delay of nanoparticles leads to the reduction of premixed burn fraction of combustion, reduction of cylinder combustion temperature and NOx emissions.
- This accelerates the combustion process with minimum thermal break down of the hydrocarbon compounds. The presence of lower active radicals led to a decrease in the potential of thermal NOx formation [26–30].

1.9 Response surface methodology

In general, all RSM problems use either one or the mixture of the both of these models. In each model, the levels of each factor are independent of the levels of other factors. When the levels of each factor are not independent then a mixture model is appropriate for designing an RMS model. RSM model obtained the optimum combinations of input variables at which maximum or minimum responses of problem obtained. Response surface methodology used the following sets to obtain the optimum results:

- Decision on independent variables and possible responses
- Selection of experimental strategy design
- Execution of experiments
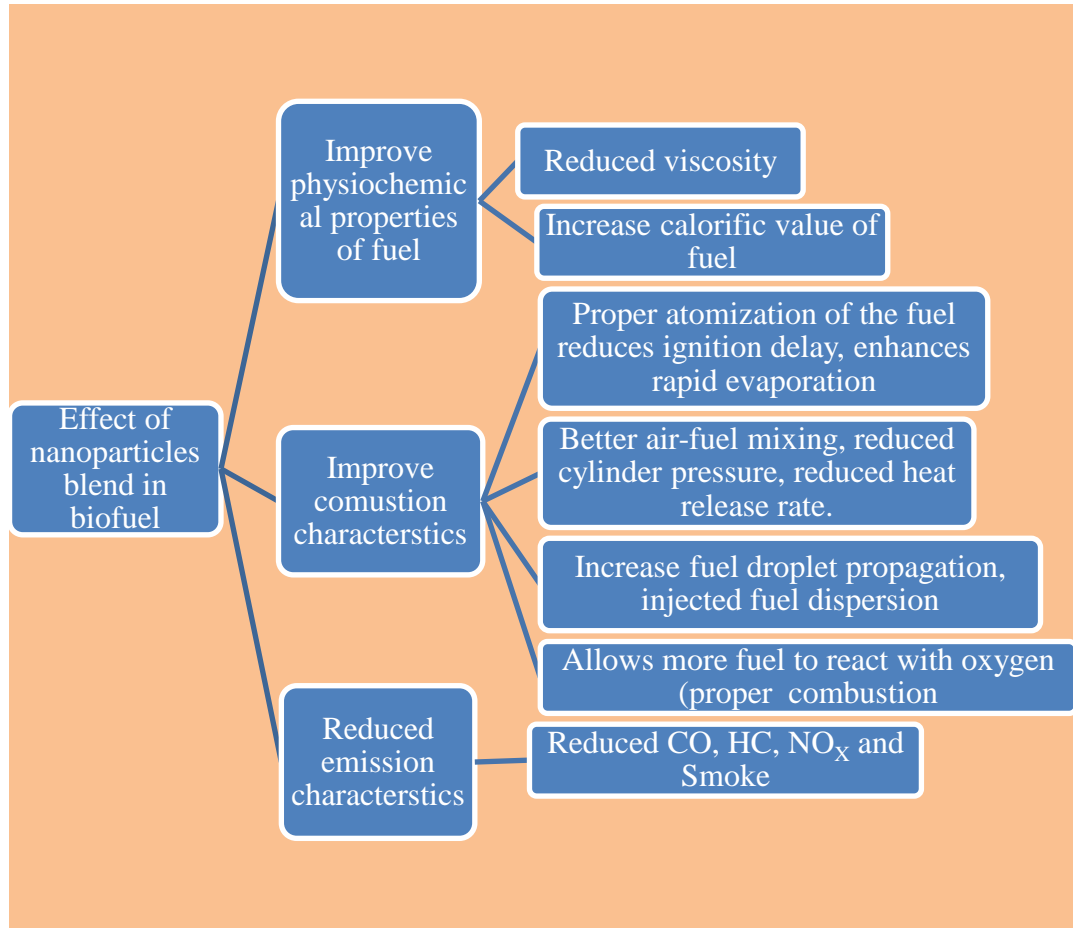
Fig.1.7 Impact of nanoparticles on combustion, emission and performance of diesel engine

- Fitting the model equation
- Verification of model (ANOVA)
- Determination of optimal condition

1.9.1 Decision on independent variables and possible responses

     In response surface methodology (RSM), the selection of independent variables and the range of their values are important factors that can greatly influence the quality of the response surface model and the resulting analysis. The selection of the most important parameters and their ranges from a range of prospective applications constitutes the first stage of the RSM. There are a number of boundaries; therefore, it's important to pick the most valuables that will have the impact on the process. Therefore, screening investigations should be used. The declaration of the extent of the boundaries has to be made in the subsequent phase. A well specified range of variables enhances the probability of optimum response identification.

1.9.2 Selection of experimental strategy design
      Choose an appropriate experimental design to gather data for building the response surface model. Common designs include factorial designs, central composite designs, and Box-Behnken designs. The design should allow for estimation of main effects, interaction effects, and curvature. A central composite design is a widely used experimental design which is commonly used in response surface methodology. It is used to build a for second order (quadratic) model for the optimization of process outcomes without needing to use a complete three-level factorial experiment. Central composite design is also used to determine the regression model equations and operating conditions from the appropriate experiments.
A Box-Wilson Central Composite Design, commonly called 'a central composite design, contains an imbedded factorial or fractional factorial design with centre points that is augmented with a group of 'star points' that allow estimation of curvature [31].
Central composite design uses the central points, extreme (corner) points and either faces points or extended points. Central point is used to detect the curvature in the process outcomes; they contribute to the estimation of the coefficients of quadratic terms. Axial points are also used to estimate the coefficients of quadratic terms, while factorial points are used mainly to estimate the coefficients of linear terms and two-way interactions. Central composite design consists the following.

> - If the number of independent variables each in two levels is k, the points of factorial experiments are 2^k if the number of independent variable(k) are 2 and 3 then factorial point will be 4 and 8. Factorial points are also called the vertices of cube.
> - If there are k factors. Central cubic design requires the 2k axial points which are also known as star points. To determine the local axial point it is necessary to identify the α value in CCD design. A value determine the design shape, it may face centered, rotatable and orthogonal. Axial points (also called star points) are points located at a given distance α from the design center in each direction on each axis to allow estimation of curvature. While the choice of α depends on the type of design, a common value is $\alpha= (2K)^{1/4}$. Axial points are 4 and 6 with α=1.414 and 1.682 for K=2 and 3 designs, respectively. The axial points are usually outside the cube, but they could be inside the cube (for α<1) or on the cube (for α=1). A special type of CCD with α=1 is the face-centered design where the axial points are at the center of each face of the factorial space. Position of α value determines the quality of the design.
> - Center point designs should include enough replication, often at the center points, to allow checking the accuracy of the model (lack of fit). The default number of center points is 5 and 6 for K=2 and 3 designs, respectively.

The sum of factorial points, axial points, and center points (if the number of repeats at a central point is n) determines the total number of experimental runs.
<div align="center">The total number of experiments = 2k +2k+n [32].</div>

1.9.3 Execution of experiments After selections the appropriate factors, levels and model of design, experiments are performed according to selected parameter. Process outcomes are recorded for further analysis.

1.9.4 Fitting the model equation
To calculate and analyse the results from response surface methodology, a polynomial equation needs to be implemented to study the correlation between dependent variable and independent variable.

1.9.5 Verification of model (ANOVA)

The ANOVA test is the initial step in analyzing factors that affect a given data set. Once the test is finished, an analyst performs additional testing on the methodical factors that measurably contribute to the data set's inconsistency. The analyst utilizes the ANOVA test results in an f-test to generate additional data that aligns with the proposed regression models. The ANOVA test allows a comparison of more than two groups at the same time to determine whether a relationship exists between them. The result of the ANOVA formula, the F statistic (also called the F-ratio), allows for the analysis of multiple groups of data to determine the variability between samples and within samples. If no real difference exists between the tested groups, which is called the null hypothesis, the result of the ANOVA's F-ratio statistic will be close to 1. The distribution of all possible values of the F statistic is the F-distribution. This is actually a group of distribution functions, with two characteristic numbers, called the numerator degrees of freedom and the denominator degrees of freedom.

1.9.6 Determination of optimal condition

Optimization of single response model can be done by calculation. The first derivative is calculated and any zero in the test range is identified. In the next step the value of second derivative is calculated to determine the possibility to presence of a saddle point. If both the second and first derivative is zero, then the presence of local extreme must be avoided by graphing the model. When examining the different answers, it may be desirable to optimize two or more values at same time. The desirability function finds out the most suitable condition for the two or more system responses. The method takes the objective function D(X), called the desirability function and converts the estimate response into a cale free value (d) called the desirability. It ranges zero to one (at least the most desirable in each case). The factors settings with the highest overall desirability are considered to be the most optimal parameter conditions. The desirability equation can be changed y applying weights. Numerical methods are often useful to optimize the desirability function. The desirability functions were used to find the optimal parameters for the performance and emissions properties of the waste cooking biodiesel. To find the optimal combinations of factors, a CCD consisting of four factors (mixture of blend mix, load, CR, IP) was used at each of 5 levels. Response surface optimizations were achieved using the desirability function [32].

The present study investigates the diesel engine performance and emissions fuelled by waste cooking biodiesel with nanoparticles. The recycled and processed used cooking oils serve as raw materials used in the production of biodiesel. However, one of the important aspects of waste cooking oil, that is, utilization of wastage of edible oil, has not been given more attention. Waste cooking oil has been used as a supporting biofuel with diesel within the current study, which inspires the recycling of waste cooking oil. Therefore, waste cooking oil of various edible oils has been selected for investigation. It was found out from literature that blend of nanoparticles in biodiesel works as a boost. That's why metallic nanoparticles have been selected to blend in waste cooking biodiesel in different proportion. Researchers usually want to know the performance and emission behaviour of C.I. engine at various engine variables such as compression ratio, injection pressure, load and different blend proportions of nanoparticle, biodiesel with diesel. This can be achieved by conducting experiments at different present variables, but it is time consuming and need huge resources. Another way to test the engine performance and behaviour of engine is by developing suitable model for

simulation. This is sometimes very difficult to make simulating model because of complex nature of process involved in engine.

As a response surface methodology is best used for determining optimize parameter of engine variables and different blend proportions. Early study shows that RSM is suitable for curvilar nature of responses with respect to independent variables. In the present study response surface methodology have been used to make a mathematical model and predict the performance and emission response on different engine input variables. Moreover, desirability approach has been applied for optimize engine input variables for the performance and emission behaviour on research diesel engine.

Organization of thesis

First chapter

Introduction

The contents of the chapter justify the basis for which this area has been chosen in the present research work. It begins with the importance of energy and proper balance between energy and environment. This chapter discusses the general overview of the concept of the world energy scenario and in the India context. The search for a renewable alternative fuel to alleviate the energy and environment problems is the focuses of this chapter. The significant roles played by internal combustion engines in this context, justifies the significance of adopting biodiesel as an environmentally friendly fuel. Explain the potential benefits associated with the use of nanoparticles as fuel additives. In this chapter a brief introduction of response surface mythology was discussed as a multi optimization tool for optimizing input variables.

Second chapter

Literature Review

The chapter covers an exhaustive review of literature on production of biofuel and its physiochemical properties. Furthermore, review the existing literature on the effects of different type's biofuel fuel and its physiochemical properties on engine performance and emissions characteristics such as particulate matter, nitrogen oxides, and carbon monoxide. The chapter also enumerated the significant effects of nanoparticle blend as a fuel additive with biodiesel on the engine performance, emissions and combustion properties. This led the formulation of some well-defined objectives and the routes towards achieving them. Consequently, an in-depth and comprehensive literature review was conducted to identify the trends in the existing research and to outline the literature short comings.

Third chapter

Methodology and system development

Fourth chapter includes the biofuel production and experimental setup and procedure. This chapter discusses detailed materials used in the research. It also explains the production techniques employed for the waste cooking oil, the different blends formulation with nanoparticles and detailed physio-chemical properties characterization of developed various blend. It contains the selection methodology for the conversion of waste cooking oil via transesterification in to biodiesel. It also contains the methodology of nanoparticle dispersion in various ratios with waste cooking oil.

It also describes about the XRD and SEM technique used to find properties of metallic nanoparticles. It also describes the engine system developed and its specifications for the evaluation of the engine properties and selection of proper instruments and equipment components, on which the completion of the research work depends. This includes the layout

of the entire experimental set up with required instrumentation for the measurement of performance and emission parameters during dynamic operating conditions. Third chapter included the research gap, objectives and methodology.

Fourth chapter

Results and discussion

This section depicts the significant finding of the exploration work. For instance, variety in thermal brake efficiency (BTE), BSFC, and engine emanations, for example, CO, HC, and NO_X of different created fuel tests.

Engine performance analysis: Present and analyse the data related to engine performance parameters, like BTE, and BSFC for the different created appropriate blends. Further, a comparative investigation of engine performance and emissions was discussed for various combinations of nanoparticles and B20.

Discharges emissions: Present and analyse the emissions data for the various types of the blend, focusing on the concentrations of particulate matter, nitrogen oxides, carbon monoxide, and other relevant pollutants.

Statistical analysis: this section likewise incorporates the utilization of RSM for the various input engine parameter strategies to recognize the appropriate engine input parameter at which the engine produces maximum output. This part incorporates the Understanding of results and conversation of the trial discoveries from your experimental study, comparing them with the existing literature and any theoretical expectations. Further, this part enlights the detailed analysis of the mechanisms which give an itemized examination of the components through which waste cooking biodiesel, nano biofuel, and engine parameters impact engine execution and outflows.

Fifth chapter

Conclusion

The significant conclusions drawn from the present experimental investigations, is being explained in this chapter.

- ➢ Conversion of waste cooking oil into biofuel via transesterification process.
- ➢ Impact of nano-additive on physiochemical properties of biofuel.
- ➢ Impact of nanoparticle as a fuel additive on engine performance and emission characteristics.
- ➢ Comparative assessment of various types of blends such as B20, D100, nanobiofuel on engine performance and emissions.
- ➢ Finding the optimum engine results with the help of suitable response surface methodology.

References

Include a comprehensive list of all the references cited throughout your thesis following a specified citation style (IEEE).

CHAPTER 2
LITERATURE REVIEW

Overview

In an era where concerns about environmental degradation and the finite nature of fossil fuels drive the pursuit of cleaner and more efficient energy alternatives, the synergistic use of nanoparticles as fuel additives with biofuels has emerged as a promising avenue. This chapter investigates the biofuel production from various types of feedstocks and the impact of biofuel on engine performance and emissions. Further, this chapter aims to explore the impact of the addition of nanoparticles into biofuels, focusing on their effects on engine performance and emissions

2.0 Introduction

Biofuel is a type of fuel derived from organic materials, primarily plants and plant-derived substances. Renewable energy sources can be used as an alternative to traditional fossil fuels, such as coal, oil, and natural gas. The properties of biofuels, such as higher viscosity, lower calorific value, and higher nitrogen oxide emissions compared to traditional diesel fuels, can pose technical challenges for engine performance and emissions. Nanoparticles, due to their unique physio-chemical properties, have the potential to address some of these limitations by acting as catalysts, combustion enhancers, and emission reduction agents. Their high surface area to volume ratio, along with the ability to manipulate their surface characteristics, opens up new possibilities for fine-tuning combustion processes and optimizing fuel-burning efficiency. The review will critically examine findings related to engine performance parameters such as combustion stability, ignition delay, and thermal efficiency. Moreover, the intricate interplay between nanoparticles and emissions reduction will be a central focus, considering pollutants such as nitrogen oxides (NOx), particulate matter (PM), and unburned hydrocarbons. In this chapter exhaustive and systemic literature review has been carried out as follows.

1. Biofuel production from diverse feedstock sources.
2. Effect of biofuel composition on physiochemical properties of biofuel.
3. Impact of biodiesel blends on compression Ignition (C.I.) engine performance.
4. Impact of nanoparticle addition with biodiesel on compression Ignition (C.I.) engine performance.
5. Computational analysis to optimize parameters affecting the performance and emission characteristics of diesel engines.

2.0 Production of biodiesel

Biofuels can be used in diesel engines, there are challenges associated with directly using them without any modifications. Diesel engines are designed to run on conventional diesel fuel, which has specific properties. Biofuels, such as biodiesel, may have different

physicochemical properties, such as higher viscosity, lower energy content, and different combustion characteristics. This can affect engine performance, efficiency, and emissions. Biofuels, particularly biodiesel, may have higher cloud points and poor cold-weather performance compared to traditional diesel fuel. This can lead to issues like fuel gelling or filter plugging in colder temperatures, affecting engine operation.

To address these challenges, various techniques are employed to produce biofuels, for example, pyrolisis and micro emulsion, dilution, thermal splitting, and so forth.

Each technique has its own advantages and disadvantages as well as its own specifically convenient feedstock character. Favourable circumstances and deficiency of various biofuel techniques are given in table 2.0 underneath.

Table 2.0 Advantage and disadvantage of biofuel production technology

Technique	Pyrolysis process
Advantages	• Very simple, eco- friendly process, Lower processing cost, less waste , integration of reaction and separation process, fast reaction rate [33, 34, 35, 36].
Disadvantages	• Need high temperature (600-700°C), required distillation apparatus. • Gasoline contain sulphur, carbon residues means less pure comparatively. Produce low material value (heating value) fuel due to reaction occurred in absence of oxygen, incomplete volatility, and instability [33, 34, 35, 36].
Technique	Micro emulsion process
Advantages	• Then chemical process is simple, the viscosity is reduced, the cetane number is increases, and the biofuel spray characteristics are better [37, 38, 39, 40, 41].
Disadvantages	• Injector stuck needle, carbon deposit formation and incomplete combustion [41].
Technique	Dilution process
Advantages	• Simple process, reduced viscosity, density [42]. • Ethanol quantity to diesel fuel may improve brake thermal efficiency, brake torque and braking power, while reducing the brake specific fuel consumption on other side [43].
Disadvantages	• Remove oil deterioration and incomplete combustion [37, 38]. Poor combustion produces carbon oxides and particles [33].
Technique	Reactive distillation process
Advantages	• Higher conversion rate, increase reaction selectivity, decreases energy consumption, elimination of solvents and azeotropes voids in the separation process [44]. • RD posses an enhanced performance on the biodiesel production, 3 times faster than conventional batch reactors [45,46]. • Reaction and separation process take place simultaneously in a single column, thus intensifying the mass transfer and simplifying the process flow sheet and operation [47].

	• Beneficial for the high free fatty acid biofuel. Less use of methanol and easily separation of by-products [47].
Disadvantages	• High required amount of energy. Mass transfer depends on catalyst performance. • Costly setup, less simple than transesterification process. Less efficient for low free fatty acids [33,47].
Technique	Microwave technology
Advantages	• Less reaction time, less amount of heat loss [33] • Rapid and uniform heating for organic and inorganic materials, time and work space savings; precise and controlled processing; selective heating; reduced processing time; improved quality and properties [48–54]. • Considered to be the preferred method for green chemistry, the choice is enhanced due to several advantages, such as reduced energy consumption, significant reduction in reaction time, solvent requirements, and improved conversions with less by-product formation. Short reaction time, cleaner reaction products, and reduced separation-purification times are the key observations reported by many researchers [55].
Disadvantages	• It is not suitable for feedstock with solids. The requirement separation from the end product. Conversion depends upon catalyst performance [33]. • Biodiesel process is sensitive to change in temperature of heat that why controlled heating required. Besides it, effective transfer of microwave energy into work area with fewer losses to the reactor walls and environment, compatibility of the process with rest of the process pipeline which includes biodiesel product separation and purification [55].
Technique	Super critical method
Advantages	• Catalyst free reaction, high speed of reaction conversion, highly conversion supercritical transesterification reduces the pre-treatment and operating costs [57]. High yield, very short reaction time and biodiesel purification and recovery are very easy [57, 58, 59].
Disadvantages	• The high amount of energy consumes. The process takes place at a critical temperature. • Using high quantity of water to wash of biofuel. • Required high temperature and pressure [58, 59].
Technique	Transesterification Process [60,61,62]
Advantages	• Highly conversion, rapid reaction rate, can be used with a suitable catalyst. It can be commercially used.
Disadvantages	• Catalyst selection depends on the type of feedstock.

2.1.1 Transesterification process

The transesterification is demonstrating to be a superior method to produce biofuels. Usually, in the transesterification process, crude feedstock of biofuel and alcohol are mixed in a beaker with suitable molar ratio in presence of appropriate catalyst. The entire process is pivoted at a specific rpm to keeping the temperature in the range of 60-70°c throughout. Triglycerides transform into mono alcohol ester and glycerol during the transesterification process. Glycerol is a by-product which is separated from the mono alcohol ester (biofuel). Glycerol may be commercially used in the pharmacy industry, food. It popularly used in the cosmetic industry as these types by the product is a value-added medium [61, 62]. Mono alcohol ester symbolizes biofuel which has viscosity one-third of the base oil. Mono liquor ester signifies the free unsaturated fat contains in biofuel. It is critical to take note that unsaturated fat structure doesn't modify during that cycle [63, 64]. To improve the transesterification process rate different kinds of catalysts are being used; they may be homogenous, heterogeneous, enzymes and nanoparticles. These catalysts accelerate the reaction rate in the mixing tank of the transit increase process [65]. Catalysts have a significant impact on the production because they are natural bases that require downstream post-treatment. An aforementioned sensitivity of the transesterification reaction under what might be termed as standard conditions towards moisture, free-fatty acid content, mass transfer limitations, and other factors has caused significant research effort towards developing other process systems [66, 67]. Transesterification process is shown in fig. no 2.0.
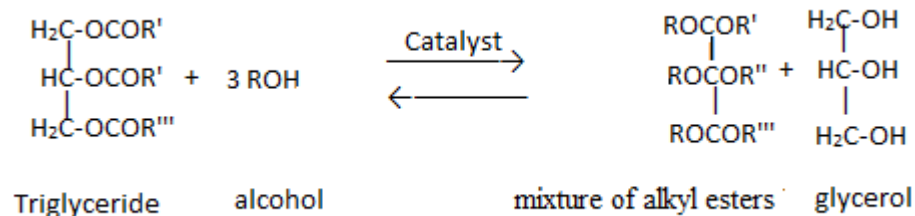
Fig. 2.0 Transesterification process

Catalytic have the major impact on the transesterification process. Catalytic activity accelerates the oil extraction process which endorses the increment in yielding of the product. Catalyst utilized in transesterification is generally categorized into four types which are given below.

        (i)   **Heterogeneous catalyst transesterification process**
        (ii)   **Homogenous catalyst transesterification process**
        (iii)   **Enzymes catalyst transesterification process**
        (iv)   **Homogenous catalyst transesterification process**

2.1.1.1 Homogenous catalyst

The transesterification process primarily utilizes homogeneous catalysts, which are known for their simplicity and speedy completion of the production reaction. Despite these advantages, homogeneous catalysts face significant limitations. They lack reusability, are challenging to separate from the final product, and their separation necessitates additional equipment and time. The purification process involving homogeneous catalysts generates a substantial amount of wastewater [68]. These catalysts are categorized into acid and base

catalysts, such as H_2SO_4, HCL, CH_3ONa, $AlCl_3$, $ZnCl_2$, NaOH, KOH, CH_3ONa, among others.
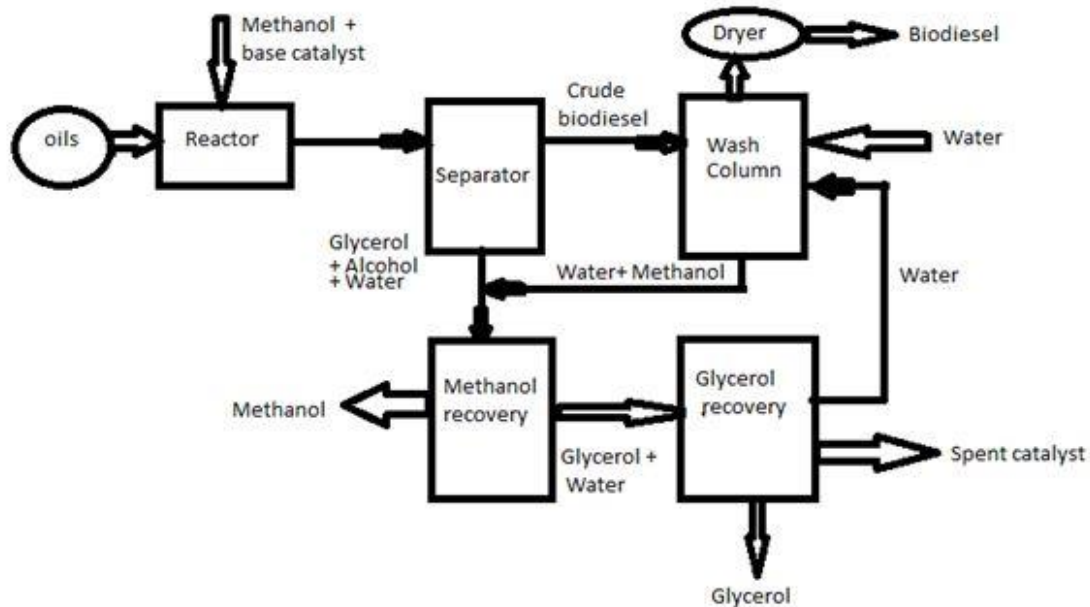
Fig. 2.1 Commercially biofuel production process

2.1.1.1.1 Homogenous base catalyst

Alkaline catalysts play a crucial role in the transesterification process for biodiesel production. They are known for being cost-effective, efficient, highly reactive, and effective under mild operating conditions. When alkaline catalysts are employed, the free unsaturated fats in the feedstock, along with the water content, promote esterification and saponification reactions. However, saponification can lead to a reduction in the overall biodiesel yield [69]. The alkaline catalyst induces the saponification process by reacting with higher free fatty acids (FFA). This occurs when the hydroxide ion of the base catalyst interacts with the FFA, leading to the saponification process. Consequently, the saponification process diminishes the catalyst's effectiveness, thereby reducing biofuel production. Typically, base catalysts are predominantly employed for feedstock with FFA levels below 1%, highlighting the importance of selecting appropriate catalysts based on feedstock characteristics [70,71,72,73]. Alkaline catalysts exhibit higher reactivity compared to acid catalysts, making them widely employed commercially. In investigations using basic catalysts like NaOH and KOH at 60°C, a methanol-to-oil ratio of 6:1, and catalyst concentrations at 0.35%, 1.3%, and 0.5% biodiesel yields for palm oil, fish oil, and sunflower oil were reported at 92%, 96%, and 98.4%, respectively [74,75,76]. The hydroxide group present in alkaline catalysts contributes to the formation of soaps through triglyceride saponification, and alkaline oxides are particularly effective, yielding over 98%. Alkaline catalysts demonstrate efficiency by completing reactions in less time with lower molar concentrations. For instance, the use of bone catalyst (calcite at 900°C, 2h) and KOH at 60°C, with methanol-to-oil ratios of 21:1, 20:1, and 6:1, and catalyst concentrations at 18%, 18%, and 1%, resulted in biodiesel production rates of 96%, 94%, and 90% for rapeseed, peanut, and waste cooking oil, respectively. Notably, NaOH, KOH, and CH_3ONa are commonly utilized for biofuel production from various feed

stocks, including soybean, pongamia pinnata, sunflower, and palm oil. However, when these catalysts were used at a catalytic load weight of 1%, and 0.35%, biodiesel production decreased from 92%, 96% to 99%, indicating the undesirable formation of soap products due to saponification. In the context of base catalysts, the nucleophile (OH-) group attacks the heavy triglyceride carbon chain in biofuel. On the other hand, acid catalysts involve protons in the carbon matrix of triglycerides. When dealing with biofuels with higher fatty acid content, a multi-step process is needed to break down triglycerides. The first and second steps involve the production of tetrahedral intermediates, which are then broken down into glycol ions and fatty acids. The final step is the recovery of proton transfer catalysts [77-84].

$$FFA + OH^-(RO^-) \xrightarrow{\text{Catalyst}} Soap + H_2O \ (ROHL)$$
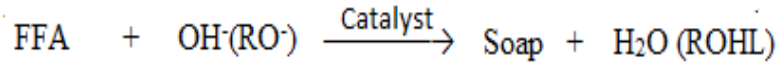
Fig.2.2 Saponification process when FFA reacts with hydroxide ion and form soap

Table 2.1 Analysis of homogeneous base catalyst used for biofuel yielding

Source	Catalyst	M/O Ratio	Reaction Environment			
			Reaction Time (Mint)	Concentration (%w/w)	Temp (°C)	Yield (%)
Pongamia pinnata [82]	KOH	10:1	90	1	105	92
Soybean oil [83]	NaOH	6:1	180	1	60	97.89
Palm oil [74]	NaOH	6:1	180	0.35	60	92
Palm oil [76,77]	CH$_3$ONa	10:1	60	0.125	70	99
Sunflower oil [75]	KOH	6:1	120	1.3	60	98.4
Rapeseed oil [80]	Bone catalyst (calcined at 900 °C, 2 h)	21:1	240	18	60	96
Waste cooking oil [81]	KOH	6.18:1	Day	1	66.5	90
Peanut oil [80]	Bone catalyst (calcined at 900 °C,2 h)	20:1	240	18	60	94
Fish oil [76,77]	KOH	6:1	60	0.5	32	96

2.1.1.1.2 Homogenous acid catalyst

When oil possesses a substantial amount of Free Fatty Acids (FFA), homogeneous acid catalysts are commonly used to transform raw materials into biodiesel. The use of acid catalysts addresses the issue of saponification processes, preventing the formation of soap and streamlining downstream processes. This, in turn, enhances the overall biodiesel production and reduces associated costs. Consequently, homogeneous acid catalysts enable the utilization of feedstocks such as Jatropha curcas, Pongamia pinnata, Palm oil, and Sunflower oil, which may have higher FFA content (above 2%), in the second generation of oil [85,86]. The acid catalysts effectively convert the feedstock into biodiesel by concurrently undergoing esterification of FFA and transesterification of triglycerides, as illustrated in Figure 2.3 [87].

$$R\text{-}COOH + R_4OH \underset{\longleftarrow}{\overset{\text{Catalyst}}{\longrightarrow}} H_2O + R\text{-}COOH_2CR_4$$

FFA   Alcohol   Water   Ester
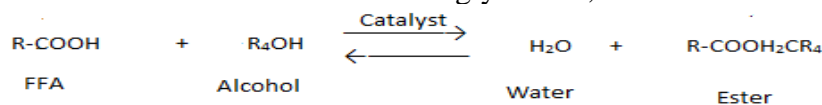
Fig. 2.3 Esterification processes

The presence of water content poses a significant challenge for acid catalyst reactions. Moisture quality can lead to catalyst deactivation due to the polar carbon-oxygen interaction in the raw material. Additionally, the transesterification reaction with an acid catalyst is prone to corrosive actions. For homogeneous acid catalysts in transesterification reactions, high alcohol-oil ratios, molar ratios, elevated acid catalyst concentrations, and extended reaction times are often required. For instance, Chlorella pyrenoidosa may necessitate a Methanol-to-oil ratio of 40:1 in the presence of H_2SO_4 catalyst. However, the required molar ratio in transesterification reactions varies depending on the specific feedstock [88-91]. Vegetable oil by-products, for example, might require a Methanol-to-oil ratio of 6:1 and a 1% catalytic loading in the presence of H_2SO_4 catalyst. Sulphuric acid, along with other acid catalysts such as HCl and CH_4O_3S, is utilized for transesterification reactions in the production of biofuel from various feed stocks like Chlorella pyrenoidosa, palm oil, sunflower oil, and jatropha oil. When these catalysts are used with catalytic load weights of 0.5%, 0.1%, 2.5%, and 1.4%, biodiesel production may decrease from 92.5%, 90%, 88% to 95.2%, and 88% [92-95]. Researchers have explored the direct esterification process of Free Fatty Acids (FFA) in newly prepared oil composed of 50% sunflower oil and 50% soybean oil. Different types of acid catalysts were tested, and their effects were found to be in the order of H_2SO_4 > HCl > $AlCl_3$ > $FeSO_4$ > $SnCl-H_2O$. Under optimal conditions, a 96.6% FFA conversion rate can be achieved with a 6:1 methanol molar concentration, 60°C induction, 2.5% w/w H_2SO_4 catalytic loading, 300 rpm mixing speed, and a 60-minute reaction time [96].

Table 2.2. Analysis of homogeneous acid catalyst used for biofuel yielding

Source	Catalyst	M/O Ratio	Reaction Environment			Yield (%)
			Reaction Time (Mint)	Concentra tion (%)	Temp (°C)	
Chlorella pyrenoidosa oil [92]	H_2SO_4	40:1	180	0.5	120	92.5
Palm oil [76,77]	H_2SO_4	3:1	60	1	130	90
Vegetable oil by product [93]	H_2SO_4	6:1	50	1	180	90.4
Sunflower oil [76,77]	HCl	6:1	180	2.5	60	88
Sunflower oil [94]	HCl	Methanol	60	1.85	100	95.2
Palm oil [76,77]	CH_4O_3S	3:1	60	1	130	90
Jatropha oil [95]	H_2SO_4	0.28	88	1.4	60	88

2.1.1.2. Heterogeneous catalyst

Biodiesel production is well suited to heterogeneous solid catalysts that are robust and easy to commercialize. Their notable advantage lies in the ease with which they can be separated from the mixture and efficiently reused. These catalysts can be categorized into acids and base catalysts [97].

2.1.1.2.1 Heterogeneous base catalyst

Heterogeneous catalysts offer a promising alternative for specific and suitable feed stocks in the transesterification process. Heterogeneous catalysts present a more sustainable option compared to the aforementioned homogeneous catalysts [98]. Despite the energy-intensive post-processing treatment required for homogeneous catalyst removal from the end product, heterogeneous catalysts eliminate the need for washing and purification, leading to increased yield [99,100]. For instance, the transesterification of rapeseed oil necessitates a

Methanol-to-oil ratio of 20:1 in the presence of bone catalyst (18 wt%), completing the reaction in 4 hours at 60°C with a yield exceeding 95% [101]. While homogeneous catalysts often diffuse into the glycerine layer, compromising glycerine quality and catalyst repeatability, heterogeneous catalysts do require more rigorous operational conditions, including higher temperatures, pressures, and alcohol-to-oil molar ratios. However, they face challenges such as poisoning and leaching over time. Solid basic catalysts, with strong basic sites, are widely utilized, as demonstrated in the transesterification of soybean oil with a Methanol-to-oil ratio of 24:1 in the presence of rice husk catalyst (4 wt%), completing the reaction in 3 hours at 65°C with a yield above 99% [102]. Similarly, solid basic catalysts are applied to palm olein oil, vegetable oil, and waste frying oil, requiring Methanol-to-oil ratios of 15:1, 16.8:1, 6.03:1, respectively, with eggshells (10 wt%), asphalt (0.2 wt%), and snail shells (2 wt%) as catalysts. The transesterification reactions for each biofuel are completed in 2 hours, 4.5 hours, and 7 hours at temperatures of 65°C, 220°C, and 60°C, respectively, with yields exceeding 95% [104,105,106]. Different metal oxides such as MgO, CaO, SrO, and BaO serve as basic catalysts for the transesterification response [103]. MgO, functioning as a strong base catalyst, is initially weak and less soluble in alcohol, but its strength increases with higher calcinations temperatures at 873K [107].

2.1.1.2.2 Heterogeneous acid catalyst

While homogenous catalysts offer various advantages in the transesterification reaction, the complexity and expense of separating and recovering catalysts become significant challenges, particularly when the catalyst completely diffuses with the final product. In contrast, solid acid catalysts prove to be superior to both homogenous acid and base catalysts due to their ease of separation from the final product, enhancing repeatability and facilitating solid catalyst recovery. This effectively reduces processing costs [110]. To address these challenges, heterogeneous solid catalysts find application in the transesterification process. Some acidic catalysts include zeolites, VOPO$_4$, destined metal oxides, and heteropoly acids. Essential catalysts encompass dolomite, hydroxides, slick metals, blended oxides, loaded and supported basic and antacid earth components, and oxides. Strong oxides can be reused with or without recovery, and heteropoly acids and their derivatives are particularly efficient for the transesterification response due to their water tolerance. Sulfate metal oxides are commonly employed catalysts in transesterification reactions. For example, ZrO$_2$ is used as a supported catalyst with the sulfated metal oxides group in the transesterification process of waste cooking oil, where SO$_4$- / ZrO$_2$ (3 wt %) serves as the catalyst. With an alcohol-to-oil molar ratio of 9:1 and a reaction temperature of 120°C, the biofuel yields reach 94% in 4 hours, demonstrating oxidation and reduction reactions on the catalyst's surface [111].

Table 2.3. Analysis of heterogeneous base catalyst used for biofuel yielding

Source	Catalyst	M/O Ratio	Reaction Environment			Yield (%)
			Reaction Time (Mint)	Concentration (wt %)	Temp (°C)	
Rapeseed oil [101]	Bone	20:1	**240**	**18**	**60**	>95
Soybean [109]	K_2CO_3 with MgO	6:1	2	0.7	70	99.5%
Sunflower oil [109]	CaO	4:1	45	1.3	75	80
Soybean oil [102]	Rice husk	24:1	180	4	65	99.5
Soybean oil [112]	KI/Mg-Al mixed with metal oxides	20:1	8	5	70	>90
Palm oil [108,109]	CaO/Al_2O_3	12.14:1	5	5	465	98.64
Palm olein oil [104]	Egg shells	15:1	120	10	60	95
Jatropha oil [108,109]	Mg-Al hydrotalcite	4:1	1.5	1	45	95.2
Vegetable oil [105]	Asphalt	16.8:1	270	0.2	220	94.8
Waste frying oil [106]	Snail shells	6.03:1	420	2	60	99.58
Waste cooking oil [108,109]	BaO	6:1	2	0.75	73.6	95
Sunflower [108,109]	CaO	13:1	90	0.1	60	91
Mesua ferrea oil [108, 109]	ZnO nano-particle	9:1	108	2.5	60	98.3

For various feedstocks such as rapeseed oil, neem oil, and waste vegetable oil, the transesterification process requires specific conditions. For instance, in the presence of titanium-doped amorphous zirconia (11 wt %), sulfated zirconia (2 wt %), and carbon-based solid acid catalyst (0.2 wt %), the Methanol-to-oil ratios range from 40:1 to 16.8:1. The transesterification reactions are completed in 2 to 5 hours at temperatures of 245°C and 220°C, yielding above 90% for each biofuel [112,113].

Table 2.4 Analysis of heterogeneous acid catalyst used for biofuel yielding

Source	Catalyst	M/O Ratio	Reaction Environment			Yield (%)
			Reaction Time (Hr)	Concentration (wt%)	Temp (°C)	
Soybean oil [77]	ETS-10 Zeolite	6:1	24	0.03	120	94.5
WCO [70]	SO_4^{2-} / ZrO_2	9:1	4 hr	3	120	94
Rapeseed oil,[111]	Titanium-doped amorphous zirconia	40:1	-	11	245	65
Neem oil [112]	Sulfated zirconia	9:1	2	2	-	95
Oleic acid[108,109]	SO_4^{2-}/ZrO_2	40:1	12	0.5	60	90
WCO [105]	Carbon-based solid acid catalyst	16.8:1	4.5	0.2	220	94.8
Sunflower oil [76,77]	Fly ash Na-X Zeolite	6:1	8	3	65	83.5
Rapeseed oil [76,77]	ST-DVB (cation exchange resin)	15:1	-	10	100	97.8
Jatropha oil [76,77]	SO_4/TiO_2	20:1	3	4	90	97
RBD palm oil [76,77]	Natural zeolite	7:1	4	3	60	95

From the exhaustive survey of production process, some major finding was obtained which are given below. They can be difficult to separate from the reaction mixture, which can result in catalyst contamination and environmental concerns.

- ➢ Homogenous catalyst can be difficult to separate from the reaction mixture, which can result in catalyst contamination and environmental concerns. Homogenous catalyst may consume with product. That why separation of catalyst is difficult and required the large amount of water for purification process.
- ➢ Most edible oil contains the high percentage of free fatty acid. Saponification problem occurred which affect the yielding of product. To reduce the saponification problem two step transesterification process required. Two step transesterification process required large amount of energy. Various types of nonedible biofuel feedstock possess the freer fatty acids which required the two-step transesterification process
- ➢ Basic catalyst generally produced the saponification process due to contain –OH group. Saponification can occur if the FFA content in the oil is more than 2 wt%. Saponification will decrease the biodiesel yield and cause problem during product purification. Acid catalyst may be used but it takes long time in transesterifaction reaction.
- ➢ It was observed that molar ratio, catalyst, feed stock and operating parameter impact the biofuel extraction process. It is difficult to select those which types of catalyst and molar ratio is best for a selected feedstock. That why optimization of the process parameter is necessary for the large-scale production process.

2.2 Impact of biofuel composition on physio- chemical properties of biofuel

Biofuels, derived from renewable biological sources, have garnered significant attention as a sustainable alternative to conventional fossil fuels. One of the key components in the composition of many biofuels is fatty acids, which are found in various feedstocks. These fatty acids can be broadly categorized into two types: saturated and unsaturated [114,115]. Saturated fatty acids have carbon chains that consist of single bonds between carbon atoms and are "saturated" with hydrogen atoms. SFAs do not contain any double bonds. They tend to have linear or straight molecular structures. SFAs are commonly found in animal fats and some vegetable oils. Saturated fatty acids include:

- Palmitic Acid (C16:0): A 16-carbon fatty acid with no double bonds.
- Stearic Acid (C18:0): An 18-carbon fatty acid with no double bonds.
- Myristic Acid (C14:0): A 14-carbon fatty acid with no double bonds.
- Butyric Acid (C4:0): A short-chain fatty acid with no double bonds [116,118].

Unsaturated fatty acids contain one or more double bonds between carbon atoms in their carbon chains. UFAs are generally liquid at room temperature. They are further categorized into monounsaturated and polyunsaturated fatty acids based on the number of double bonds present. Monounsaturated Fatty Acids (MUFAs) consists one double bond in their carbon chains such as oleic acid. Oleic Acid (C18:1, Δ9): An 18-carbon fatty acid with a single double bond at the 9th carbon-carbon position from the methyl end. Polyunsaturated Fatty Acids (PUFAs) have multiple double bonds in their carbon chains such as omega -3 fatty acids, and omega -3 fatty acids. In the omega-3 Fatty acid first double bond is located at the third carbon-carbon position from the methyl end (omega end). Examples include alpha-linolenic acid (ALA), eicosapentaenoic acid (EPA), and docosahexaenoic acid (DHA). In the omega-6 Fatty Acids first double bond is located at the sixth carbon-carbon position from the

methyl end (omega end). Examples include linoleic acid (LA) and arachidonic acid (AA) [119]. The detailed free fatty acid compositions of various types of feedstocks are given in table no 2.5.

The molecular structure of biofuel chains, specifically the arrangement of carbon atoms and the presence of functional groups, has a significant impact on the physical, chemical, and combustion properties of the biofuel. The molecular structures of diesel, biofuels (triglycerides), and different types of FAME are shown in Figure 2.2 [117].

Table 2.5 The fatty Acids composition of various types of biofuels [117]

Biofuel oil/Fatty acids	Lauric (12:0)	Myristic (14:0)	Palmitic (C16:0)	Stearic (18:0)	Oleic (18:1)	Linoleic (18:2)	Linolenic (18:3)
Sunflower			5-8	2-6	15-40	30-70	
Rapeseed			1-3	0-1	10-15	12-15	8-12
Soybean			6-10	2-5	20-30	50-60	5-11
Peanut			8-9	2-3	50-65	20-30	
Olive			9-10	2-3	72-85	10-12	0-1
Palm oil		0.5-2	39-48	3-6	36-44	9-12	
Coconut	45-53	16-21	7-10	2-4	5-10	1-2.5	
Sesame			13	4	53	30	
Linseed			4-7	2-4	25-40	35-40	25-60
Jatropha		14.1-15.3	0-13		34.5-46	14.1-15	0-0.3
Karanja			4-8	2.4-8.6	44.5-72	11-18	
Pongamia		11.65			51.5	11.65	
Stillingia	0.4	0.1	7.5	2.3	16.7	31.5	41.5
Waste cooking			8.5	3.1	21.2	55.2	5.9
Tallow		23.3	19.3	42.4	2.9	0.9	2.9

Diesel fuel ($C_{12}H_{26}$)　　　　　　　　　　Methyl sterate ($C_{19}H_{98}O_2$)
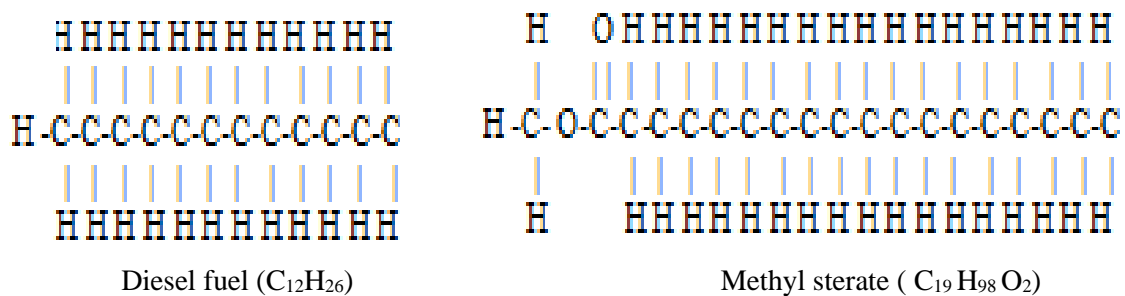
Fig.2.4. Molecular structure of biofuel

Biofuel composition feathers influences the biofuel properties such as the density, flash point, pour point, viscosity, density, surface tension, iodine value, compressibility, cetane number etc. These properties play a crucial role in determining the overall suitability of biofuels for various applications. Here's an overview of how the molecular structure of biofuel chains affects their properties [117].
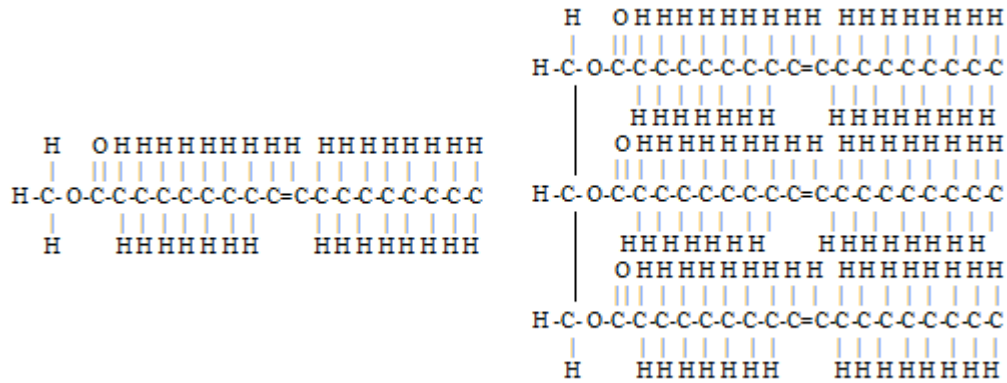
Triglyceride ($C_{19}H_{96}O_2$)   Triglyceride ($C_{51}H_{92}O_6$)

Fig.2.4. Molecular structure of biofuel

2.2.1 Viscosity

The length and complexity of the carbon chain in biofuels influence their viscosity, which is the measure of a fluid's resistance to flow. Longer carbon chains and greater molecular complexity generally result in higher viscosity. Additionally, Viscosity depends upon the spatial structure of molecule of biofuel i.e., either it is geometric isomers of unsaturated fats contrasting in the direction of the double bond of the structure or they are geometric isomers of fatty acids varying in the direction of the double bonds. The cis double bond produces 30.00 degrees of bending in the structure of the fatty acid chain, so the unsaturated fat chain is not properly arranged. Due to improper packing, the intermolecular forces decrease the resulting viscosity. The Trans double bond has a compact intermolecular bound similar to the saturated fatty acids [120]. As a result, biofuel which has the trans configuration of the double bond has a higher kinematic viscosity. Effects of double bond position, configuration, and chain length on fatty acid motion viscosity as shown in Table 2.6 [120,121].

2.2.2 Cetane Numbe

The cetane number is a measure of a fuel's ignition quality. Higher cetane numbers indicate better ignition characteristics. Thus, branching in the chain and increasing the unsaturation decreases the cetane number. It was seen that CN is high in the straight saturated long-chain in comparison to the unsaturated and branched-chain.

Table2.6 length of chain and position of double bond in biofuel molecular structure

Length of Chain and (=) bond position	Position of Double bond	
	Cis	Trans
14.0:1.0; Δ9	2.7	-
16.0:1.0; Δ9	3.7	-
18.0:1.0; Δ6	4.6	5.5
18.0:1.0; Δ9	4.5	5.9
18.0:1.0; Δ11	4.3	5.4
18.0:2.0; Δ9-12	3.6	5.3

Double bond position plays a major role in CN. When a double bond is in position at one end rather than the middle, then CN will be higher. CN has a nonlinear relationship with the ignition delay. If the CN is high, the ignition delay will be short vice versa. CN affects the ignition delay, calorific value, and related to combustion properties [120,121,122].

2.2.3 Cold flow

The flow of biodiesel at low temperatures is the major problem. At low-temperature solids and crystals rapidly grow which can plug the fuel and filter lines. The cold flow described by the cloud point. Cloud point is the temperature at which fatty acid in the fuel becomes cloudy due to the formation of crystal and solidification of crystals. When more temperature decreases, more solid forms, and materials reach the pour point. The pour point is the lowest temperature at which it can be flow. It was seen by the researcher that saturates fatty acids have a higher melting then the unsaturated fatty acid. It can say that saturated fatty acids have higher CP and PP. However, the cloud point and pour point are lower for the branched esters. The cloud point of isopropyl soyate was given as -9°C and that of 2 butyls soyate as -12°C [120,121,122].

2.2.4 Oxidation Stability

Oxidation stability means stability towards the moisture and microbial growth. The oxidation process is a very complex phenomenon, it starts when hydro peroxides formed with the subsequent secondary reactions and formed aldehydes, carboxylic acids, ketones, and polymers, etc. it was seen by the researcher presence of double bond in the fatty acid composition is responsible for the auto-oxidation. Auto oxidation rates depend upon the position and the number of double bonds such as the allylic position of the double bond is susceptible to auto-oxidation but bis-allylic are more prone to oxidation. So, auto-oxidation increases with increase the unsaturation. Algae oils are more susceptible to auto-oxidation [120,121,122].

2.2.5 Density

The density of biofuel increases with increasing unsaturation i.e. for the long-saturated chains, the density of biofuel found less in comparison to the unsaturated fatty acids chain. Viscosity and density are correlated with each other. Higher density and viscosity fuel have a higher bulk modulus and less compressibility. When fuel injected into the injection system biofuel creates higher pressure waves due to higher bulk modulus comparatively. Due to which the injection valve opens before the opening time and affects the ignition delay time. Ignition delay time affects the combustion of fuel inside the combustion chamber. As this type of biofuel composition, directly and indirectly, influences the performance and emission of the diesel engine [120,121,122]. Comparisons of physio-chemical properties of various biofuels are given in table no 2.7.

Table.2.7. Comparison of Physio-Chemical Properties of Different Types of Biodiesel [121]

S.N	Fuel	Flash point	Kinematic viscosity	Density kg/m3	Calorific value (j/kg)	Cetane number
1	Sunflower oil	-	4.9	880	45.3	49
2	Rapeseed oil	-	4.10	881	45	49
6	Soyabean oil	-	4.08	885	40	49
7	Peanut oil	-	4.42	883	40.1	54
	POM2O	71.5	2.82	835	41.5	
10.	POME	-	4.1	875	38.75	60.4

11.	Sesame oil	-	5.34	875	38.36	55.84
12.	Jatropha oil	-	4.78	863	42	63
16.	CMT corn methyl ester	-	3.6	840	39	45
17.	Karanja oil			875	38.3	
18.	WCOME30		4.41	852	44	53
19	Mahua methyl ester (MME)	136	4.90	869	40	56

2.3 Effect of biodiesel blend on C.I. engine

This study seeks to delve into the multifaceted interactions between biofuel blends and C.I. engines, investigating the influence of different operating parameters on combustion efficiency, emissions, and overall engine performance. By comprehensively examining the intricate relationships between biofuels and C.I. engines, this research aims to contribute valuable insights that can inform the development of sustainable and efficient renewable energy systems. The engine performance and emissions of biofuels are intricately linked to their physio-chemical properties and molecular structure. Biofuels typically exhibit molecular structures containing O_2 molecular double bonds, which are shorter than single bonds. This characteristic reduces compressibility and increases bulk modulus, resulting in an earlier injection time, decreased heat transfer rate, and elevated combustion flame temperature [123]. Additionally, biofuels are characterized by higher viscosity, which contributes to challenges in atomization and fuel dispersion, ultimately leading to suboptimal combustion for biodiesel. Despite biodiesel having a higher cetane number and oxygen content, conducive to improved combustion, its lower calorific value is a key factor contributing to diminished engine performance. Investigations into the impact of Jatropha biofuel on emissions and performance characteristics revealed noteworthy findings. The utilization of Jatropha biodiesel demonstrated a reduction in CO, CO_2, and HC emissions, along with an increase in NO_X levels compared to conventional diesel [124]. Furthermore, when contrasted with diesel fuel, the use of Jatropha biodiesel resulted in a decreased brake thermal efficiency (BTE) in diesel engines. This phenomenon is attributed to the higher viscosity and lower calorific value inherent in Jatropha biodiesel [124, 125]. The performance of the diesel engine increased with the increase of the amount of JOME in the diesel. This is due to the high cetane number of JOME Biodiesel. BTE of JOME 20 increased by 11% compared to D100. BSFC decreased with the increasing amount of JOME in biodiesel compared to D100 due to the high cetane number and high oxygen content in the molecular structure of JOME. Since oxygen molecules promotes complete combustion, JOME20's carbon mono oxide, HC, and smoke levels are lower in comparison to D100 [126]. BTE of the engine increased for the various proportion of Jatropha ethyl ester with butanol in the diesel. The BSFC slowly decreased as the quantity of butanol increased in biodiesel. Butanol possesses more oxygen molecules. Therefore, when the butanol content in the JEE and diesel blend expanded, the CO and HC emissions reduced [127]. Shirneshan observed an increase in NOx emissions and a reduction in hydrocarbon (HC) and carbon monoxide (CO) emissions in a multi-cylinder, four-stroke, and compression-ignition (C.I.) engine when utilizing waste cooking oil as fuel. Additionally, due to the fuel's higher viscosity and lower calorific value (CV), there was an increase in brake-specific fuel consumption (BSFC) and a decrease in brake thermal efficiency (BTE). Noteworthy reductions in CO, HC, and particulate matter (PM) emissions were observed, accompanied by

an increase in NOx emissions [128]. In another experimental investigation involving four-stroke diesel engines fuelled by waste palm oil methyl ester (WPOME) and coconut oil methyl ester (COME), there were significant reductions in CO, HC, and smoke opacity by 14.29%, 9.52%, 86.89%, and 72.68%, 67.65%, 47.96%, respectively, for both oils. However, a slight increment in NOx emissions was observed [129]. Biodiesel is produced from tallow oil and blended in different ratios (B10, B20 and B30) with diesel and used as an engine fuel to compare combustion and performance characteristics e.g., in-cylinder pressure, rate of pressure rise, mean gas temperature, HRR, brake power, SFC, BTE and torque. The experimental results showed that engine responses support the use of biodiesel and its blends as fuel as the difference between maximum brake power values of diesel and B30 is 1.7%. However, SFC was higher in the case of biodiesel blends because of its lower heating value relative to diesel [130]. Further, with biodiesel, the diesel engine produced reduced brake thermal efficiency and increased brake-specific fuel consumption. Furthermore, the use of plant-based biofuels reduced HC, CO, and CO_2 as advantages as well as increased NO_X emission levels as one of the main disadvantages [131, 132]. In a diesel engine experiment, B100 biodiesel demonstrated a notable reduction of 43.75% in CO and 25.98% in HC emissions, yet it exhibited an increase in NOx emissions [133]. The use of Karanja biodiesel led to a 3-5% decrease in Brake Thermal Efficiency (BTE), with higher CO_2 and NOx emissions, while showing milder effects on Unburned Hydrocarbons (UHC) and CO emissions [134]. When employing coconut oil biodiesel and its blends, there was a decrease in torque and Brake Power (BP), accompanied by a slight increase in Brake Specific Fuel Consumption (BSFC) compared to conventional diesel fuel. Additionally, NOx and CO_2 emissions were higher for biodiesel, whereas CO and HC emissions were lower. Interestingly, elevating the proportion of coconut biodiesel blend by approximately 30% resulted in an enhancement of BP, while reducing the biodiesel percentage led to a decline in BP [135]. Some of exhaustive literature reviews are given below in tabulated form.

Table 2.8. Impact of biodiesel on engine performance and emissions

S. N	Materials & Test condition	Key Finding	Source
1.	• Waste cooking-oil biodiesel blends B10, B20, and B30. Four-stroke single-cylinder diesel engine (maximum power 5.775 kW). Constant engine Speed (1500 rpm), Working under varying load conditions 1, 2, 3, and 4 kW.	• BTE and specific fuel consumption of waste cooking oil biodiesel blends were found to be lower than pure diesel fuel. In comparison to diesel fuel, waste cooking oil biodiesel mixes emit lesser CO and HC. The amount of biodiesel fuel in the blends increases with an increase in NO_X emissions.	Abed,K. A., et al. (2018) [136]

2.	• Four-stroke single-cylinder diesel engine. The engine speed is 1500 rpm working under varying load conditions no load, 25% load, 50% load, and 75% load.	• The BTE of waste cooking oil biodiesel mixes was lower than that of pure diesel fuel, and the specific fuel consumption was higher. Waste cooking oil biodiesel blends emit less CO and HC emissions than diesel fuel. As NO_X outflows increment, biodiesel fuel content expands in the mixes.	Adhike savan, C., et al. (2022) [137]
3.	• Single cylinder, engine having a peak power varying the engine load at constant speed	• The engine's BTE with a 5% neem oil blend was slightly higher than pure diesel across all loads, indicating improved combustion attributed to dissolved oxygen. However, as the neem oil percentage increased, the BSFE decreased significantly at higher loads, likely due to increased fuel viscosity impeding proper combustion. The BSF was found to be the lowest for the 5% neem oil blend at all loads. Subsequently, with an increase in neem oil concentration, the full-load BSFC became lower at part loads and higher at full loads compared to neat diesel. Smoke opacity for the 5% blend was comparable to the baseline diesel data but increased noticeably at higher neem oil blends. As the percentage of neem oil in the fuel increased, the exhaust temperature exhibited a downward trend, indicating a relatively improved tendency for NO_X emission.	R. C. Singh., R. Gautam et al. (2012) [138]
4.	• DF80+B20 WCO, DF70+ B30WCO, DF60+B40WCO, and DF50+B50WCO. Single cylinder, Varying load and constant speed.	• The experimental results show that DF80+B20WCO, DF70+B30WCO, DF60+B40WCO, and DF50+B50WCO decrease engine efficiency, CO, and UHC while increasing specific energy consumption. For the corresponding compression ratios of 16.5, 17.5, and 18.5, BTE of DF80+B20WCO was greater than that of DF70+B30WCO, DF60+B40WCO, and DF50+B50WCO for all engine loads. Additionally, when WCO biodiesel is blended with diesel fuel, the BSFC for C.R. rises at all engine loads.	Rajak, et al. (2022) [139]
5.	• Review paper	• Due to waste cooking oil's higher viscosity than diesel fuel, engines consume more fuel specifically for the brakes, and their thermal efficiency is reduced. There has been a noticeable decrease in CO, HC, PM, and smoke emissions; nevertheless, NO_X and CO_2	Singh, D., et al. (2022) [140]

		emissions have increased because of the oxygenating properties of biodiesel.	
6.	• Blends of used cooking oil, two distinct waste cooking oils and metallic nanoparticle. Experiment was conducted on single cylinder CRDI engine at varying load condition	• Waste Cooking oil biodiesel blends have a lower thermal efficiency than diesel. There is larger specific fuel consumption for biodiesel blend than for diesel fuel. Diesel oil has lower CO_2 emissions than biodiesel blends made from used cooking oil. Blends of biodiesel had lower CO, smoke opacity, and HC emissions than diesel fuel. Diesel fuel has lower NOx emissions than biodiesel mixtures.	S. Bhan, et al. (2018) [141]
8.	• Four-cylinder, four-stroke engine WCOME's B10, B20, B30, B40, and B50 blends of diesel fuel. Load rates between 1800 and 2400 rpm.	• WCOME content cannot be maintained at a level high enough owing to a lack of sources. In terms of smoke and NOx emissions, blends with WCOME concentration performed much better than diesel fuel. This advantage grew as WCOME percentage did. The B10 blend, however, had the same benefit in terms of CO and THC emissions.	Ulusoy, Y., et al. (2017) [142]
9.	• Diesel engine with a single cylinder, four strokes, direct injection, and air cooling. Electronic tachometer was used to measure the output shaft's speed (N) in rpm. A dynamometer (1200 N) was mounted at the engine output shaft to measure the braking force, and the braking torque of the engine.	• In comparison to pure diesel, the BTE of DWB10D90 and DWB20D80 increased, but DWB30D70 and DW40BD60 showed a decrement In comparison to the baseline data, the values of BSFC for DWB10D90 and DWB20D80 decreased respectively. As a result, the performance of the engine using the fuels DWB10D90 and DWB20D80 was better than that of the engine using the fuels DWB30D70, DWB40D60, and DWB50D50. The variation of CO, NO_X, O_2, and CO_2 emission was measured in relation to diesel and mixed fuels. As the percentage of WCO biodiesel blends in diesel grew, CO and O_2 emissions fell, while CO_2 and NO_X emissions rose as a result of the excessive oxygen content and higher cetane number of biodiesel blends.	Mahmo od, T.et al. (2022) [143]
10.	• The effect of noncircular orifices was assessed to analyse the atomization and air-fuel mixing of fuel and their impact on performance and emissions.	• Increasing the swirl of air within the combustion chamber has the potential to boost the performance of a diesel engine with alternate fuels (AFs). A notable enhancement of 3–11% in heat transfer within the combustion chamber was noted with increased swirl.	] P. Yadav., et al. (2021) [144]

From the exhaustive literature review it was found out that biofuels can be blended with diesel oil to develop biodiesel blends, which have a range of effects on diesel engines. Enhancing engine performance and reducing NOx emissions represent significant challenges in the context of biofuels. Therefore, there has been extensive research into the combustion characteristics of biodiesel with the aim of improving engine performance and minimizing NOx emissions. The addition of nanoparticles as fuel additives holds potential for improving fuel properties and addressing existing limitations, presenting an avenue for further advancements in this area [145].

2.4. Impact of nanoparticle addition with biodiesel in diesel engine

Nanoparticles can be used as an additive with biodiesel to improve its properties and performance. Various types of chemical analysis have been tested by adding the various types of nanoparticles in different ratio with biofuel to improve the physio- chemical properties of biodiesel. Apart from that nanoparticles addition with biodiesel improved the performance and emissions of biodiesel by improving the physio-chemical properties. Extensive studies and experiments have been conducted to improve the engine performance, combustion and emission characteristics fuelled by nanobiodiesel by changing the various engine operating parameter.

On the contrary, the incorporation of nanoparticles into biodiesel has been shown to enhance its physicochemical properties. This enhancement is evidenced by the reduction in fuel viscosity, leading to improved fuel atomization, dispersion, and mixing. These improvements contribute to enhanced combustion characteristics, resulting in better engine performance, as measured by parameters such as Brake Thermal Efficiency (BTE) and Brake Specific Fuel Consumption (BSFC). Furthermore, the heightened surface-to-volume ratio of nanoparticles introduces additional reaction surfaces within the air-fuel mixture. This, in turn, accelerates combustion, facilitates rapid flame propagation, ensures proper fuel dispersion, enables early absorption of latent heat of vaporization, promotes swift heat transfer in the air-fuel mixture, and contributes to the early fracture of thermal hydrogen compounds [146]. The experimentation involved a four-stroke, direct injection, air-cooled engine operating at 2000rpm speed under varying load conditions. Three different fuel blends (B30+ 50 Al_2O_3, B30+ 50 ZnO, and B30+ 50 MgO) were utilized in Compression Ignition (C.I.) engines. The results indicated that the minimum Brake Specific Fuel Consumption (BSFC) was observed at 176 kg/kWh for B30-50MgO, and there was a notable 47% increase in Brake Thermal Efficiency (BTE) for the fuel blend B30+50MgO under full load conditions. The addition of nanoparticles led to an augmentation in the calorific value of the fuel, consequently boosting brake power. These nanoparticles served as oxygenated catalysts, enhancing combustion efficiency and thereby reducing fuel consumption [147]. The enhanced fuel characteristics contributed to improved volatility, turbulence ratio, and fuel dispersion within the combustion chamber. This, in turn, improved thermo-chemical combustion characteristics, resulting in reduced ignition delay, cylinder pressure, and heat transfer. Consequently, there was a decrease in emissions of carbon monoxide (CO), nitrogen oxides (NO_X), and hydrocarbons (HC).

Three varieties of nanoparticles—such as CNT, titanium oxides, and Al_2O_3—in different nanoparticle sizes (25, 50, and 100 ppm) were combined with B20 Jatropha biodiesel blend for experimentation. Results demonstrated that blending jatropha biodiesel with Al_2O_3, particularly J20Al100, led to the highest improvement in Brake Thermal Efficiency (BTE) at 6.5%. Conversely, the combination of jatropha biodiesel with CNT, like J20C50, exhibited a

reduction of 35% in CO emissions and 52% in NO_X emissions [30]. The introduction of Al2O3 nanoparticles into biodiesel blend JB20D increased the heating value, subsequently enhancing the self-ignition temperature. This improvement in self-ignition temperature directly correlates with a shortened ignition delay period, resulting in improved engine power. The addition of Al_2O_3 was observed to increase the oxygen content in the charge, supporting the ignition of the air-fuel mixture and ensuring proper combustion within the combustion chamber. Al_2O_3's higher thermal conductivity contributed to an increased fuel evaporation rate, thereby reducing ignition delay and enhancing overall engine performance [65]. The inclusion of graphene oxide (GO) nanoparticles in diesel/biodiesel blends led to a reduction in Unburned Hydrocarbons (UHC), CO, and Brake Specific Fuel Consumption (BSFC), but an increase in NOx emissions [148]. Examining nanoparticle size, an increased CuO size was found to improve diesel engine performance and emission characteristics. The experiment included three blend types: BD100CuO20, BD100CuO10, and BD100. CuO with a particle size of 20 nm increased BTE by 0.9% over BD100 and 0.2% over BD100CuO10. The lower kinematic viscosity of BD100CuO20 resulted in reduced droplet size, enhancing atomization, dispersion, mixing, and combustion of the fuel, thereby lowering BSFC and CO emissions. BD100CuO20 exhibited smaller HC and NO_X emissions compared to BD100CuO10 and BD100 due to increased nanoparticle size, promoting greater contact between fuel and air, and lower HC emissions. The larger size accelerated the evaporation rate, reducing ignition delay. The overall reduction in BSFC, CO, HC, Smoke, NO_X emissions, and higher BTE supported the positive impact of nanoparticle addition in biodiesel for diesel engines [149]. At 75% engine load, experimental results revealed that J20Al100 exhibited the lowest BSFC compared to diesel and other tested fuels [150, 63, 151]. The Tafel extrapolation method indicated a decrease in erosion rate with the addition of Al_2O_3 nanoparticles. Furthermore, the pitting corrosion resistance improved based on the results of the erosion test using potentiodynamic cyclic polarization. The utilization of Al_2O_3 as nanoparticles in biodiesel was considered safe for the engine combustion chamber and its components [152]. Some of exhaustive literature related to impact of nanoparticle as fuel additive on engine performance and emissions are given below in tabulated form.

Table 2.9 Tabular form of literature Review

S.N	Materials & Test condition	Key finding	Source
1.	• Jatropha biodiesel blend (J20) with nano-additives (CNT, TiO_2, and Al_2O_3) in different proportions. Four-stroke single-cylinder diesel engine (maximum power 5.775 kW) was working under varying load conditions and constant Speed (1500 rpm).	• In comparison to J20, J20Al100 produced lower specific fuel consumption and improved thermal efficiency. Compared to all other fuels, Jatropha biodiesel (J20C50) with nanoparticle addition resulted in the highest CO emission decline. When compared to all other fuels, J20C50 can reduce NOx discharges. When compared to diesel oil, jatropha biodiesel with nanoparticle (J20T25) had a maximum reduction in HC emissions.	M.S. Gad, et al. (2020) [30]
2.	• Waste cooking + diesel oil + aluminum oxide	• In comparison to other blends, B30 blend has the greatest peak pressure, measuring 7.17 MPa under	A.M. Abdallah

	(Al$_2$O$_3$), magnesium oxide (MgO), and Zinc oxide (ZnO). Diesel engine was working under varying load condition constant speed (1500 rpm).	full load. It was discovered that the specific fuel is reduced to 176 g/kWh by the addition of nanoparticles 50 MgO in B30 blend. Nonetheless, 50 Al$_2$O$_3$ added to D100 demonstrated the maximum rate of heat transmission. Maximum BTE for the B30-50 MgO blend is 27%, while the lower NOx emission concentrations for the D100-50 Al$_2$O$_3$ blend and 246 ppm for CO emission are both recorded at 339 ppm.	, et al. (2020) [147]
4.	• Graphene oxide + primrose + Tree of heaven + Camelina. All experiments were conducted at peak load and constant speed (2100 rpm).	• Reduction in UHC, CO, and BSFC but increased NOx increased was realized with all graphene oxide (GO) nanoparticles addition in diesel/biodiesel blends. The results indicated that the amount of saturated fatty acid of Evening primrose is higher than the fruit of the Tree of heaven and the Camelina seed. Therefore, the oxidative stability of Evening primrose seed is much higher, and it can be maintained over a longer period. The oil content of the fruit of Tree of heaven is higher than the Evening primrose seed and the Camelina seed. The results indicated that the amount of saturated fatty acid of Evening primrose is higher than the fruit of the Tree of heaven and the Camelina seed. Therefore, the oxidative stability of Evening primrose seed is much higher, and it can be maintained over a longer period.	S.S. Hoseini ,et al. (2020) [148]
5.	• Waste cooking oil mixed with mineral diesel (20:80) is used along with cerium oxide (CeO$_2$) nanoparticles as additives. The engine is running at several fuel injection pressures (180, 210 and 240 bar) and with a nanoparticle CeO$_2$ concentration of 80 ppm.	• Cerium oxide nanoparticles added to B20 at a 24MPa injection pressure decreased the ignition delay by 25% compared to B20. High injection pressure causes optimal fuel atomization and dispersion inside the combustion chamber. Due to cerium oxide's high surface-to-volume ratio, which increases heat transmission between air and fuel droplets, the ignition delay is reduced. The inclusion of nanoparticles raised BTE by 2.5%, lowered BSEC by 3.1%, and reduced hydrocarbon by 20% at high pressure compared to B20.In comparison to clean B20 operation, improved combustion and lower emissions result from the combined effects of greater injection pressure and the inclusion of metallic nanoparticles.	Shiva Kumar, et al. (2019)[153]
6.	• Pongamia biodiesel + titanium oxide. The engine was working under various load conditions and at a speed	• Due to the increased surface to volume proportion and improved rate of fuel and air mixing in the combustion chamber, TiO$_2$ nanoparticles significantly reduced NOx and smoke emissions when compared to biodiesel fuel, by up to 3.8% and 2.7%,	Devaraj Rangaba shiam, et al. (2019)

	1500 rpm.	respectively. TiO$_2$ nano additive is used to lessen the viscosity of biodiesel. A reduced viscosity results in smaller droplet size, faster evaporation, and less CO emissions. TiO$_2$100PBD100 is lower than PBD100 in all conditions according to the BSFC for TiO$_2$50PBD100. With an increase in TiO$_2$ nanoadditive (50, 100 ppm), BSFC fell. TiO$_2$ nano additive was increased in the PBD100, which had better BTE. TiO$_2$ nano additive improves BTE and the oxidation process.	[154]
7.	• JB20D blend with Al$_2$O$_3$ nano particle additives. The diesel engine was working under various load condition and at constant speed1500.	• With the addition of Al$_2$O$_3$, engine performance testing revealed a striking gain in brake thermal efficiency of up to 15% and a reduction in BSFC of up to 12%. As Al$_2$O$_3$ was added to JB20D, the emissions of NOx, CO, UHC, and smoke opacity were all dramatically reduced as compared to JB20D by up to 70%, 80%, 60%, and 35%, respectively.	Ahmed , et al. (2018) [65]
8.	• Calophyllm nophyllm biodiesel blend with diesel and Al$_2$O$_3$ nanoparticles with exhaust gas recirculation. Single cylinder, four stroke diesel engine 5.2 kW (Kirloskar) was working under varying load condition constant speed 1500 rpm.	• The brake thermal efficiency of CIB20ANP40 fuel shows an increase of 5.04% and 7.7% compared to CIB20 and CIB20ANP40 + 20% EGR fuels, respectively. The brake-specific fuel consumption decreases by 11.5% and 17.85% when alumina nanoparticles are added to CIB20, compared to CIB20 alone. The exhaust gas temperature is lower for the combined effect of alumina nanoparticles and EGR in CIB20 fuel, as opposed to other fuel samples. CO emissions are reduced by 6.09% with the addition of alumina nanoparticles to CIB20. Nanoparticles in CIB20 also lead to a decrease in HC emissions compared to CIB20 alone. The addition of alumina nanoparticles to CIB20 results in a 7.76% reduction in NOx emissions. Furthermore, the combined effect of alumina nanoparticles and a 20% EGR in CIB20ANP40 fuel exhibits a substantial reduction in NOx emissions by 36.84%, 31.53%, and 17.67% when compared to CIB20, CIB20ANP40, and CIB20 + 20% EGR fuel samples, respectively.	Praveen , et al. (2018) [155]
9.	• Copper oxide nano particle + pongamia methyl ester. Kirloskar Diesel engine was working under varying load condition, and constant speed (1500 rpm).	• The experimental results provides a constructive result of 4.01% increase in BTE, a reduction of around 1.0% in BSFC and a reduction of around 12.8% in smoke emission and 9.8% reduction in NOx emission for the blend B20CuO100.	Varathar ajuPeru mala, et al.(2018) [156]

10.	• Three types of nanoparticle aluminum oxide, carbon nano tubes and silicon oxide blend with pure diesel 1800 rpm engine speed, engine loads of 0%, 25%, 50%, 75% and 100%.	• CNT blends improved BSFC by as much as 19.85% due to its higher calorific value. CNT blends show highest improvement in BTE (compared to DF) of 18.8% for DC50 due to shorter ignition delay thus promoting more complete combustion. Al_2O_3 and SiO_2 blends show 1.76 times reduction in HC emissions due to shorter ignition delay but negatively affect NOx (produce 0.59 and 4.29 times more for Al_2O_3 and SiO_2 blends) due to higher HRR and narrower combustion period. CNT blends improved by 4.48% overall in NOx emissions but results in an increase in carbon emissions, such as CO, CO_2 and HC.	Ang F. Chena, et al. (2018)[1 57]
11.	• Calophyllm inophyll methyl ester blended zinc oxide and titanium dioxide nanoparticles. CI engine was working under At various load conditions and at constant engine speed.	• In comparison to CIME fuel, CIME nano emulsions increase brake thermal efficiency by 5–17% at maximum braking power. Comparing CIME nano emulsions to biodiesel and diesel fuel, significant reductions in CO, smoke, and HC emissions were observed. Furthermore, compared to pure Calophyllm biodiesel, the NOx was modestly decreased for all CIME nano emulsions.	Nanthag opal K, et al. (2017) [158]
13.	• Rice bran oil (RBO) [80% diesel + 20% biodiesel + (CeO_2)]. CI engine has a bore of 87.5 mm and a stroke of 110 mm. CI engine was working under various load conditions.	• Addition of CeO_2 in B20 shows the improvement in BTE. Additionally, CeO_2 mixes in B20 shows decline in oxides of nitrogen, carbon mono oxide and hydrocarbons emissions in compare B20.	Karthike yan et al.(2016) [159]
14.	• Neat BD, Canola BD emulsion fuel, and alumina nanoparticle blended Canola emulsion fuels.CI engine Speed 1500 rpm 220 bar injection pressure compression ratio of 17.5, Loading system Eddy current dynamometer Tested at various load conditions	• Improvement in the brake thermal efficiency (BTE) for the alumina blended Canola emulsion fuels compared with that of neat Canola BD and Canola BD emulsion fuel. The use of a nano particle blended BD fuel reduced the hydrocarbon (HC) and carbon monoxide (CO) emissions but increased oxides of nitrogen (NOx). The smoke emission was reduced by 50% with the use of the nano particle blended emulsion fuel.	A.Anbar asu , et al. (2016) [160]

15.	• Cerium zirconium oxide nanoparticle + diesel. The load test was carried out on a 5 hp four stroke, water cooled, single cylinder diesel engine at constant speed.	• Performance studies shows 31% reduction in exhaust smoke and 3% enhancement in brake thermal efficiency of diesel engine for a nanoparticle concentration of 17.5 ppm	Ajin C. Sajeevan, et al. (2016)[161]
16.	• Mahua seeds pure biofuel TiO_2 nano particle. One thousand eight hundred revolutions per minute constant speed, various load conditions.	• When TiO_2 nanoparticles (200 ppm) are added to mahua biodiesel, the resulting reductions in carbon monoxide, hydrocarbon, nitrogen oxide, and smoke emissions are, respectively, 9.3, 5.8, 6.6, and 2.7% when compared to neat mahua biodiesel. NOx emissions for BD100T100 and BD100T200 are significantly reduced by the addition of TiO_2 nanoparticles to BD100.	Amith Kishore Pandian, et al. (2017) [162]
17.	• Nanometal oxide blended Mahua biodiesel. CRDI diesel engine at different loading conditions and constant speed.	• As a result of the inclusion of nanoparticles, the peak pressure and heat release rate has increased significantly. A further reduction in SFC and an increase in BTE were made for the nano biodiesel mix. The addition of nanoparticles significantly reduced NOx, CO, UHC, and soot emissions.	Aalam CS, et al.(2015) [27]
18.	• Jatropha biodiesel alumina and Cerium oxide nanoparticles are blended separately. Diesel engine was working under under load conditions and constant speed of 1500 rpm.	• Percentage reduction of NO emission by 9 %, Smoke opacity by 17 %, and unburned hydrocarbon by 33 % and carbon monoxide by 20 % are observed along with percentage reduction of NO emission by 7 %, Smoke opacity by 20 % and unburned hydrocarbon by 28 % and carbon monoxide by 20 % for cerium oxide blended test fuel. 5 % improvement in brake thermal efficiency is observed for both the test fuel.	Prabu Arockias amy, et al. (2015) [63]
19.	• Karanja biodiesel + nanoparticle blends (CRDI). Engine was working under varying load and constant speed condition.	• Number of larger size particulates in the engine exhaust reduced significantly with increasing fuel injection pressure for all test fuels. Advancing SOI timings resulted in lower particulate number concentration for all test fuels. KOME10 showed emission of lowest total particulate numbers. Particulate number concentration increased with further increase of biodiesel content in the test fuel.	Avinash Kumar Agarwal, et al. (2014) [163]
20.	• Nanobiofuel (Review paper)	• This study investigates the impact of dispersing various nanoparticles on improving performance and reducing emissions in a compression ignition (CI) engine using diesel-biodiesel blends. The study indicates that metallic and carbon nanotube (CNT) nano-additives exhibit positive effects on emission reduction and engine performance enhancement. Particularly, titanium dioxide (TiO_2) additives prove	M. E. M. Soudagar et al. [164]

		to be more effective in boosting engine power. The introduction of metallic nanoparticles results in a shortened ignition delay period, increased calorific value, and elevated oxidation rates, contributing to a more thorough and cleaner combustion process.	
21.	• Jojoba methyl ester and diesel fuel blended with alumina nanoparticles. A single cylinder diesel engine was working under varying load condition and constant speed 1500rpm and injection pressure 175 bar.	• BSFC is reduced by about 6%. Efficiency is increased up to 7%, and all engine emissions have been reduced (NOx about 70%, CO about 75 %,Smoke opacity about 5% and UHC about 55 %) compared with the corresponding values obtained when only a blended fuel of 20% biodiesel is used.	Ali M.A. et al. (2014) [165]
22.	• Zizipus jujube methyl ester blended fuel (ZJME25) blended with aluminum oxide nanoparticles. Four stroke, single cylinder, air cooled and common rail direct injection (CRDI) speed of 1500 rpm and a standard injection pressure of 220 bar under varying load condition.	• The specific fuel consumption is higher for the ZJME25 than neat diesel at the entire load and it has reduced with a raise in the dosing level of AONP. The brake thermal efficiency of neat diesel is higher than ZJME25 blend at all the loads and a small improvement is observed with the AONP with ZJME25. The CO emission decreases with the use of AONP in ZJME25.The addition of AONP decreases the HC emissions when comparing with neat diesel and ZJME25 blend. The NOx emission is lower for the neat diesel than the ZJME25. The NOx emission was found to be slightly increased with the addition of AONP with biodiesel blends.	C. Syed Aalam , et al. (2015) [166]
23.	• Study, Jatropha oil methyl and ethyl ester (JOME & JOEE) with diesel single cylinder, vertical, naturally aspirated, air cooled, direct injection engine speed 1500.	• The results suggest that BTE was higher for both JOME and JOEE blends and CO, HC and smoke opacity were lower as compared to diesel fuel. NOx was found to be increasing for both JOME and JOEE.	Gautam, , et al. (2013)[1 167]
23.	• Ricinuscommunis biodiesel (RCME20), diesel (80%), and their blends with strontium-zinc oxide nanoparticle The CRDI engine 1000 bar injection pressure, 23.5°BTDC injection timing and constant speed.	• The engine characteristics such as BTE, HRR and cylinder pressure increased by 20.83%, 24.35% and 9.55%, and BSFC, ID, CD, smoke, CO, HC and CO_2 reduced by 20.07%, 20.64%, 14.5%, 27.90%, 47.63%, 26.81%, and 34.9%, while slight increase in NOx for all nanofuel blends was observed.	Soudagar , et al. (2020) [168]

24	• Calophyllum Inophyllum seed oil BCM20, 20 ppm Cerium Oxide,20 ppm MWCNT	• BTE is increased for BCM20 when compared with B20 and diesel respectively. It is observed that the fuel consumption and emissions such as NO, CO and smoke are decreased for BCM20 and BCM40 blends	C.H.Harsha , et al.(2020) [169]
25.	• Ethyl ester Kusum oil (Vegetable oil) and butanol blended with diesel as a fuel. *as* B5KOEE95,B10KOEE90 ,B15KOEE85 and B20KOEE80. Single cylinder, four strokes, speed 1500 rpm under varying load condition.	• At full load conditions B5KOEE95, B10KOEE90, B15KOEE85 and B20KOEE80 showed an increment in BTE and were found to be 26.67%, 27.45%, 29.67% and 29.00% respectively whilst that of diesel is 29.87%. Addition of butanol resulted in improvement of BTE of various blends which can be easily viewed at higher loads. CO emissions, HC emissions were found to be less in comparison to diesel and CO_2 emissions and smoke opacity were slightly increased. NOx emissions were lower for KOEEB blends. At full loads, Diesel showed NOx emissions which were found to be 11% higher than the KOEEB blends. This may be due to the quenching effect of butanol. At partial loads, NOx emissions were comparable for all the blends of KOEEB.	Vishal Singh, , et al. [170]

In conclusion, the utilization of metallic nanoparticles as fuel additives presents a promising avenue for enhancing engine performance and reducing emissions. Through an extensive review of the literature, it becomes evident that these nanoparticles offer multifaceted benefits, including improved combustion efficiency, enhanced thermal conductivity, and reduced pollutant emissions. The studies reviewed demonstrate that the incorporation of metallic nanoparticles into fuels leads to finer atomization, increased surface area, and more homogeneous mixing, resulting in more efficient combustion processes.

Furthermore, the catalytic properties of metallic nanoparticles have been shown to facilitate the cleaner and complete combustion. The reviewed literature also underscores the need for comprehensive investigations into the optimal nanoparticle types, sizes, and concentrations for different fuel formulations in order to achieve the desired performance and emissions outcomes.

However, the literature reviewed reveals that there is limited application of metallic nanoparticles in different concentration as a fuel additive with waste cooking biofuel at different engine operating parameter. The proposed study investigates the impact of metallic nanoparticles in different concentration as fuel additives with waste cooking biofuel on performance, and emissions of diesel engines at various engine operating parameter.

2.5 Computational study for optimization of parameter affecting performance and emissions behaviour of diesel engine

Diesel performance may be optimized through the adjusting of engine parameters (injection pressure, compression ratio, speed, and load) using Response Surface Methodology (RSM). RSM provided the valuable insights into the intricate relationship between various engine variables and their impact on engine responses. Some exhaustive literature reviews

related to impact of variation in engine parameter on engine performance and emissions are given beneath.

Various optimization methodologies are used to model and analyse the system using the test results. RSM is one of the most remarkable research method techniques to anticipate and optimize system parameters with the least number of trials [171, 172]. RSM optimization is used to optimize engine operating parameters such as combustion temperature, ignition delay time, and combustion pressure that promote the reduction of NOx and another particulate without changing the BTE [173]. The researcher analysed to optimisation the multiple injection system configurations of an HSDI diesel engine using the RSM optimization technique [174]. RSM was used to find out the significant influence of engine operating parameters and injection timing on BTE, BSFC, and emission [175]. An algorithm was planned and incorporated to predict the optimum condition of diesel engine performance. The scientist's objective is to advance a control system that can administer and adjust split injection parameter that forces changes in working parameter [176]. The researcher worked on RSM and power fit laws. The researcher examines the information to understand the complex ignition process of IC engines which is affected by cylinder pressure, temperature, combustion duration, fuel dispersion, swirl ration, fuel penetration, and the air-fuel ratio [177]. RSM was used to find out the relations between engine operating parameters (fuel injection timing, engine speed, engine load, and oxygen volume fraction) and engine BTE, BSFC, and BP [178]. A central composite design (CCD) in RSM was used to design and analyze the experiments. CCD is a type of design that allows for the estimation of both linear and quadratic effects of the independent variables on the response variable, which in this case are the performance and emission characteristics of the diesel engine. The study optimized three parameters, including the ratio of biodiesel in the blend, the ratio of alumina nanoparticles as an additive, and the engine load. The authors used RSM to develop a quadratic model that relates the three parameters to the engine performance and emission characteristics, such as brake thermal efficiency, brake specific fuel consumption, carbon monoxide emissions, and nitrogen oxide emissions. Author used the model to identify the optimum conditions for achieving the best engine performance and emission characteristics [179]. In the multi-objective optimization of diesel engine performance, vibration and emission parameters employing blends of biodiesel, hydrogen and cerium oxide nanoparticles with the aid of response surface methodology approach, the authors used a central composite design (CCD) of response surface methodology (RSM) to optimize the engine performance, vibration, and emission parameters of a diesel engine running on blends of biodiesel, hydrogen, and cerium oxide nanoparticles. The authors optimized engine performance and emission parameter such as nitrogen oxide (NOx), hydrocarbon (HC), carbon monoxide (CO), and smoke opacity [180]. A response surface methodology (RSM) approach was used to study the effect of optimized input parameters on a CRDI diesel engine running with a waste frying oil methyl ester-diesel blend fuel with ZnO nanoparticles. The RSM design used in the study was a central composite design (CCD), which is a commonly used design for RSM experiments. The input parameters that were optimized in the study were the engine speed (X1), fuel injection pressure (X2), and blending ratio of waste frying oil methyl ester and diesel (X3). The response parameters that were optimized were engine torque (Y1), specific fuel consumption (Y2), and exhaust gas temperature (Y3). For engine torque (Y1), the maximum value was found to be 247.31 Nm at an engine speed of 2375 rpm, fuel injection pressure of 1396 bar, and blending ratio of 14.56% waste frying oil methyl ester and 85.44% diesel. For specific

fuel consumption (Y2), the minimum value was found to be 0.253 kg/kWh at an engine speed of 2000 rpm, fuel injection pressure of 1000 bar, and blending ratio of 17.08% waste frying oil methyl ester and 82.92% diesel. For exhaust gas temperature (Y3), the minimum value was found to be 279.67 °C at an engine speed of 2000 rpm, fuel injection pressure of 1000 bar, and blending ratio of 17.08% waste frying oil methyl ester and 82.92% diesel [173]. In the paper "Collective effect of ternary nano fuel blends on the diesel engine performance and emissions characteristics", the Response Surface Methodology (RSM) was used for the experimental design. The authors optimized three parameters: the injection timing (IT), the compression ratio (CR), and the percentage of the ternary fuel blend (TFB) in the diesel fuel. The response parameters that were optimized were the brake thermal efficiency (BTE), the oxides of nitrogen (NOx) emissions, and the smoke opacity (SO). The RSM was used to develop a second-order polynomial equation for each response parameter using a central composite design (CCD) of experiments. For BTE, the maximum value of 41.14% was achieved at an injection timing of 21.5 degrees before top dead centre (BTDC), a compression ratio of 18.5, and a TFB percentage of 5%. For NOx emissions, the minimum value of 195.6 ppm was achieved at an injection timing of 22.5 degrees BTDC, a compression ratio of 17.5, and a TFB percentage of 5%. For SO, the minimum value of 14.06% was achieved at an injection timing of 20.5 degrees BTDC, a compression ratio of 17.5, and a TFB percentage of 5% [181]. The authors optimized three parameters: the engine load (EL), the CuO nanoparticles concentration in the fuel, and the injection pressure (IP). The response parameters that were optimized were the brake thermal efficiency (BTE), the oxides of nitrogen (NOx) emissions, and the smoke opacity (SO). The RSM was used to develop a second-order polynomial equation for each response parameter using a central composite design (CCD) of experiments. The optimized values for the response parameters were as follows: For BTE: the maximum value of 33.59% was achieved at an engine load of 70%, a CuO nanoparticles concentration of 0.05 wt%, and an injection pressure of 250 bar. For NOx emissions: the minimum value of 501 ppm was achieved at an engine load of 100%, a CuO nanoparticles concentration of 0.1 wt%, and an injection pressure of 250 bar. For SO: the minimum value of 3.6% was achieved at an engine load of 70%, a CuO nanoparticles concentration of 0.05 wt%, and an injection pressure of 250 bar [182]. The authors optimized three parameters: the injection pressure (IP), the injection timing (IT), and the percentage of nickel oxide (NiO) dosed in the Azadirachta indica methyl ester (AIME) fuel. The response parameters that were optimized were the brake thermal efficiency (BTE), the oxides of nitrogen (NOx) emissions, and the smoke opacity (SO). The RSM was used to develop a second-order polynomial equation for each response parameter using a central composite design (CCD) of experiments. The optimized values for the response parameters were as follows: For BTE: the maximum value of 30.56% was achieved at an injection pressure of 240 bar, an injection timing of 20 degrees before top dead center (BTDC), and a NiO dosing percentage of 0.5%. For NOx emissions: the minimum value of 580 ppm was achieved at an injection pressure of 200 bar, an injection timing of 15 degrees BTDC, and a NiO dosing percentage of 0.5%. For SO: the minimum value of 22.32% was achieved at an injection pressure of 220 bar, an injection timing of 20 degrees BTDC, and a NiO dosing percentage of 0.5% [183]. The authors optimized three parameters: the engine speed (ES), the hemp seed oil biodiesel (HSOBD) blend ratio, and the concentration of nano-TiO_2 in the fuel. The response parameters that were optimized were the brake thermal efficiency (BTE), the oxides of nitrogen (NOx) emissions, and the smoke opacity (SO). The RSM was used to develop a second-order polynomial equation for each response parameter

using a central composite design (CCD) of experiments. The optimized values for the response parameters were as follows: For BTE: the maximum value of 35.25% was achieved at an engine speed of 2200 rpm, an HSOBD blend ratio of 20%, and a nano-TiO_2 concentration of 50 ppm. For NOx emissions: the minimum value of 391.51 ppm was achieved at an engine speed of 1500 rpm, an HSOBD blend ratio of 20%, and a nano-TiO_2 concentration of 50 ppm. For SO: the minimum value of 0.28 m^-1 was achieved at an engine speed of 2200 rpm, an HSOBD blend ratio of 20%, and a nano-TiO_2 concentration of 50 ppm [184].

The design used in this paper is an experimental design. The researchers conducted experiments on a single-cylinder diesel engine using various blends of ethanol, biodiesel, and diesel fuel with the addition of nano-biochar to investigate the effects on engine performance and exhaust emissions characteristics. The parameters that were optimized in this study were the blend ratio of ethanol-biodiesel-diesel and the amount of nano-biochar added to the fuel blend. The researchers used a response surface methodology (RSM) to optimize the engine performance and exhaust emissions. The values of the optimized parameters are not provided in the abstract, but they can be found in the full article [185].

The optimization of variables was executed using the desirability method within the Response Surface Methodology (RSM), aiming to maximize engine performance and CO_2 while minimizing emissions, particularly hydrocarbons (HC). Following the RSM modelling, the optimized engine settings for input factors were determined as follows: diesel/linseed blend ratio of 8.10%, Fuel Injection Pressure (FIP) of 600 bar, EGR of 4.667%, and engine load of 9.33 kg. With these constant values, the optimized output parameters, including torque, Brake Thermal Efficiency (BTE), Brake Mean Effective Pressure (BMEP), mechanical efficiency, HC, and CO_2, were found to be 20.04 Nm, 26.035%, 3.474 bar, 52.503%, 28.14 ppm, and 7.319 % vol, respectively. The predicted values were experimentally validated, and the errors in the predicted values were observed to be within a limited range [186].

Throughout the literature review, it became evident that the utilization of Response Surface Methodology offers a systematic and effective approach for optimizing engine performance. Additionally, RSM analyse the significant impact of input variables (engine parameters) on output responses (engine performance). This enables the identification of optimal parameter settings that lead to improved efficiency, reduced emissions, enhanced power output, and overall better engine operation.

2.6. RESEARCH GAPS

On the through scrutiny of the published work on the nanoparticle biofuel blending used for engine performance and emission characteristics, the following observations have been made:

- It has been observed that the limited work has been done for combustion and emission characteristics of suitable nanoparticle blended biofuel.
- There are more efforts needed to achieve the optimal engine performance for suitable nanoparticle blended biofuel.
- There is a less evidence about the optimum addition of suitable NPs in particular biodiesel feed stocks. While numerous studies have explored the synergies of metallic nanoparticles (NPs), the incorporation of organic NPs in conjunction with metallic and/or carbon nanotube (CNT) NPs in diesel/biodiesel fuel remains unexplored and warrants further investigation.
- It is investigated that that there is a limited study about comparative analysis of emission, combustion and performance of engine for various NPs fuel blends for optimization of engine parameter.
- Although some work has been done with various metallic and their oxides nanoparticle blend with biofuel, additional efforts are needed in achieve the desired optimum engine performance and emission Characteristics.
- An in-depth investigation is required to thoroughly examine the stability, thermal conductivity, and shelf life of nanoparticles (NPs) in relation to liquid fuels.
- The exploration of organic NPs as nano-additives in diesel/biodiesel fuels is currently less extensive compared to metallic, non-metallic, and carbon nanotube (CNT) NPs. There is additional potential for research into the impact of nanoparticles on exhaust emissions.
- There is no more information available for injection pressure effect on penetration of fluid spray, dispersion of fuel, mass transfer, evaporation and heat transfer rate of molecule of fuel and air.
- There is a lack of research evidence towards the improvement in free fatty composition of biofuel with suitable catalyst and nanoparticles additives. Biofuel free fatty acids composition directly related to biofuel properties.

2.7. PROBLEM STATEMENT

The extensive literature review has revealed a research gap, highlighting that incorporating metallic nanoparticles as fuel additives in biodiesel enhances engine performance and reduces emission characteristics. With the increasing demand for sustainable energy sources, attention has shifted towards the use of waste cooking biodiesel. However, challenges persist in terms of combustion efficiency, emissions, and engine performance. This research aims to explore how the addition of nanoparticles as fuel additives influences the engine performance and emission characteristics of waste cooking biodiesel in internal combustion engines. By addressing these challenges, the study aims to provide valuable insights for improving the viability and environmental sustainability of waste cooking biodiesel as a potential alternative fuel. This research focuses on evaluating the impact of adding metallic nanoparticles as fuel additives to waste cooking biodiesel.

2.8. OBJECTIVES OF THE STUDY

The present investigation aims to improve engine performance, combustion and also reduce harmful emissions for nanoparticles blended biodiesel engine. Following objectives has been identified for proposed research:

- To identify and select waste cooking oil and metallic nanoparticle for desired novel blending.
- To develop novel biofuel blend with selected waste cooking oil feedstock and metallic nanoparticle.

- To conduct chemical analysis of selected biodiesel blend and characterize the physio-chemical property of selected blend.

- Design of experiment by the selected various parameter of diesel engine using a suitable optimization technique.

- Experimental investigation of novel biofuel for performance and emission characteristics   on CI engine.

CHAPTER 3
METHODOLOGY AND SYSTEM DEVELOPMENT

Overview

This chapter delineates the systematic approach undertaken for the development of the system and methodology for producing biodiesel, nano-biodiesel and evaluating engine performance and emissions. It commences with the selection of the waste cooking oil for biodiesel production and the selection of Al_2O_3 nanoparticles as a fuel additive in combination with the developed waste cooking biodiesel. The chapter also details the estimation of physico-chemical properties for the developed blends. Subsequently, this chapter discusses the experimental engine configuration, encompassing engine type, specifications, and any modifications made for the testing process. Finally, the chapter introduces the response surface methodology (RSM) employed for optimization of engine responses at selected input parameters.

3.0 Introduction

This chapter provides a concise summary of the research steps that are addressed in the problem statement. Fig 3.1 includes a visual representation of the problem statement in the form of a flow chart. The study encompasses both chemical and physical aspects of the materials involved, with a primary focus on evaluating engine performance and emissions. Waste cooking oil selected as the source material for biofuel, and the transesterification process is employed to convert it into biofuel. This chapter extensively describes the transesterification process and the laboratory facilities at DTU used to analyze the biofuel chemically. Additionally, it discusses the selection and physicochemical characteristics Al_2O_3 and CeO_2 metallic nanoparticles, including morphology analysis using X-ray diffraction (XRD) and scanning electron microscopy (SEM). The chapter also provides details about the ultrasonic sonicator used for homogeneously blending metallic nanoparticles and used cooking oil biodiesel. Experimental work involving VCR CRDI (Variable Compression Ratio Common Rail Direct Injection) engines is thoroughly explained, covering engine specifications and modifications for testing. Furthermore, Response Surface Methodology (RSM) is applied to optimize engine responses under different engine parameters and the relevant data analysis and processing software is introduced.

3.1 Waste cooking as feedstock

3.1.1 Collection of waste cooking oil

Waste cooking oil obtained from various restaurants and cafeterias in Greater Noida, Uttar Pradesh, as a precursor to biofuel production. Subsequently, chemical analysis is performed in the laboratory by instrument to check the quality of waste cooking oil.

3.2 Extraction of biofuel from waste cooking oil

Transesterification process was used to convert vegetable oil into biofuel. Due to its simplicity and inexpensive cost, the transesterification technique has gained widespread acceptance. The following steps were taken to complete the entire process of creating biodiesel from used cooking oil. Flow chart of preparation of biodiesel from waste cooking oil was shown in figure no 3.2.
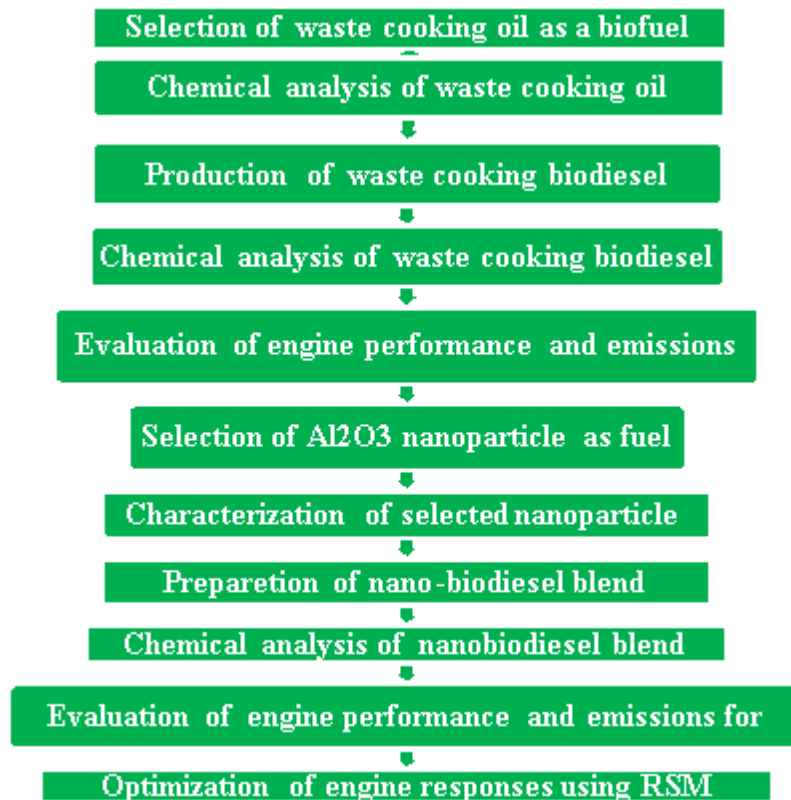
Fig. 3.1 Flow chart of research methodology

- Pretreatment of waste cooking oil
- Transesterification process
- Separation of biofuel and glycerin
- Water washing process
- Drying

3.2.1 Pre-treatment of waste cooking oil
3.2.1.1 Filtration of waste cooking oil

Filtering waste cooking oil before using it to prepare biofuel is very important. Waste cooking oil may contain solid particles such as food crumbs or burnt bits that can clog the fuel lines and nozzles of the biofuel production equipment. These particles can also reduce the efficiency of the production process and may cause damage to the equipment. Filtering waste cooking oil before using it to produce biofuel is important for ensuring a high-quality and

efficient production process, as well as for preventing equipment damage. Waste cooking oil was filtered before preheating of waste cooking oil.

3.2.1.2 Preheating of waste cooking oil

Preheating waste cooking oil before preparing biofuel from it serves a few important purposes.

Reducing viscosity: Waste cooking oil is often thick and viscous. Preheating the oil reduces its viscosity, making it suitable to use with I.C. engine.
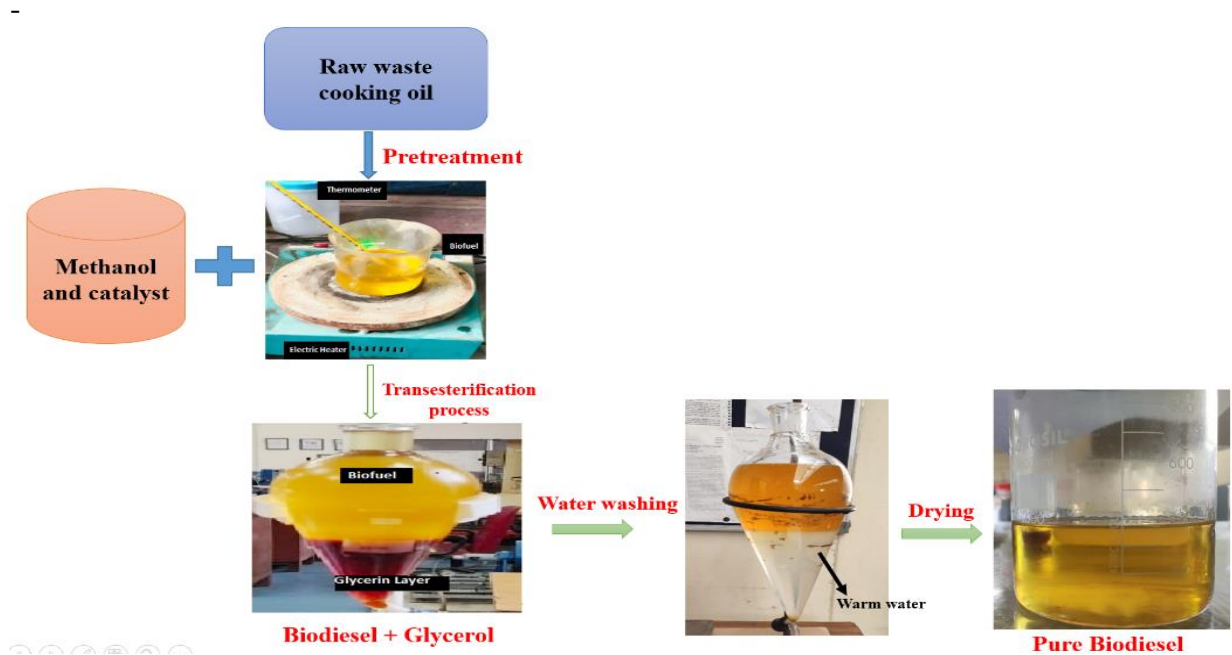
Fig 3.2 Flow diagram of preparation of biodiesel

Removing moisture: Preheating the waste cooking oil helps to drive off any moisture that may be present in the oil. Moisture in the oil can cause the oil to foam or splatter during processing, which can be dangerous and may also reduce the quality of the resulting biofuel. Before transesterification, raw WCO is heated in a beaker up to 100°C to remove moisture, and then it is cooled to 60°C as shown in Fig.No.3.3.

Fig. 3.3 Preheating of waste cooking oil

3.2.2 Transesterification process

Transesterification is a chemical process used to convert waste cooking oil into biodiesel. After pre-treated of the waste cooking oil, WCO and CH_3OH was mixed in the molar ratio of 6.5:1 in presence of KOH (potassium hydroxide) (1%w/w). The catalyst helps to facilitate the chemical reaction that will convert the oil into biodiesel. The mixture of waste cooking oil, catalyst, and methanol is heated to 60^oC-70^oC and stirred at 400rpm for several hours. During the reaction, the catalyst helps to break the ester bonds in the oil, freeing the fatty acids and allowing them to react with the methanol to form biodiesel. The whole process was left for 2 hours to settle down. The transesterification process has shown in fig no 3.4.
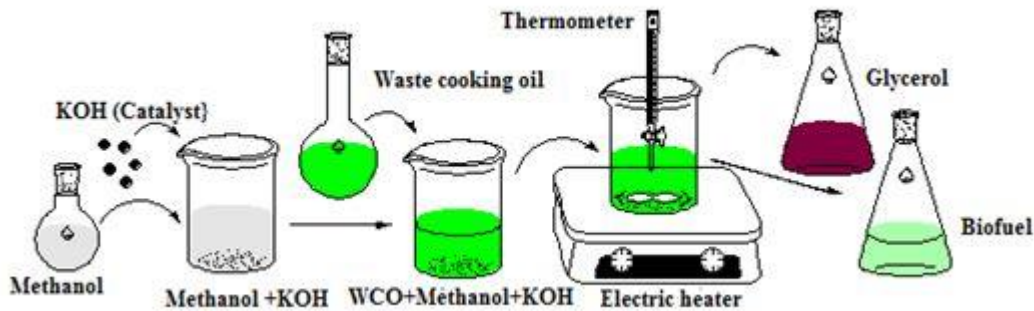
Fig 3.4. Transesterification process

3.2.3 Separation of glycerin from biofuel

After transesterification reaction, the mixture of waste cooking biodiesel and glycerine is allowed to settle for several hours. During this time, the glycerine and other by products settle to the bottom of the container. The remaining mixture of glycerine and by products is then separated from the biodiesel. This was done using a method of sedimentation as shown in figure 3.5.
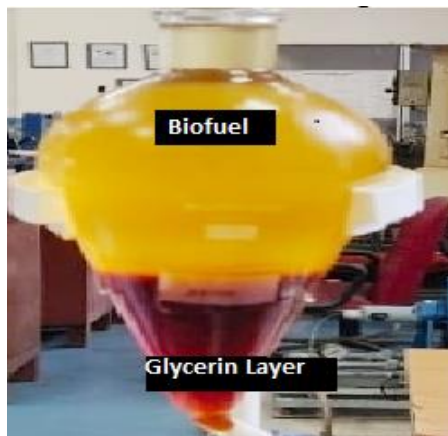
Fig. 3.5 Sedimentation of glycerine

3.2.4 Water washing and drying

Washing and drying are important steps in the transesterification process used to purify the biodiesel. The purpose of washing is to remove any remaining impurities or catalysts from the biodiesel, while the purpose of drying is to remove any remaining moisture. *Washing:* After the transesterification process, the glycerine was separated from the waste cooking biodiesel, after that the waste cooking biodiesel was typically washed with water to

remove any remaining impurities or catalysts. In this step, 80-90ºC of heated water is poured into the biodiesel and stirring the mixture for several minutes as shown in fig. no 3.6. *Separation:* After the stirring the biofuel, the mixture is allowed to settle so that the water and any remaining impurities can separate from the biodiesel. In this process a heavy fat residual would be carried away by heated water due to high density and settle down as shown in fig no.3.7. The water and impurities are then drained off, leaving the washed biodiesel behind.
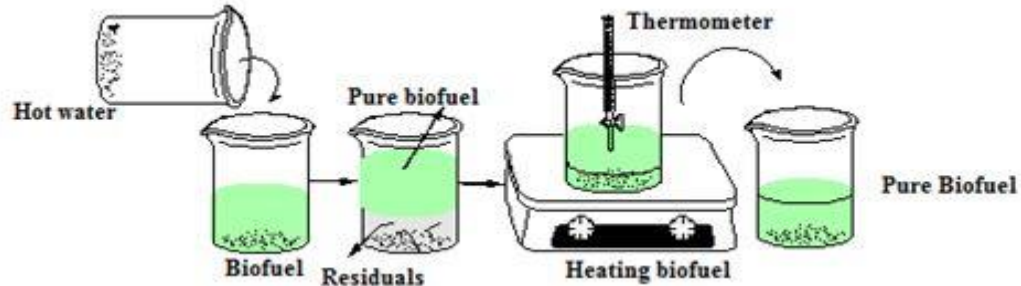
Fig. 3.6 Water washing and drying process

Drying: After washing, the biodiesel is typically dried to remove any remaining moisture. This can be done by heating the biodiesel to a temperature of around 70-100°C and stirring the mixture for several hours. The heat helps to evaporate any remaining water in the biodiesel, while the stirring helps to ensure that the biodiesel is evenly dried. Washing and drying are important steps in the transesterification process, as they help to ensure that the resulting biodiesel is of high quality and free from any impurities or moisture that could impact its performance or stability.

3.3 Evaluation of physio-chemical properties of waste cooking biodiesel

The study contributes to the evaluation of crucial physico-chemical properties of waste cooking oil and its methyl ester, following the ASTM D 6751 standard. These properties encompass density, viscosity, distillation point, cold filter plugging point (CFPP), calorific value, moisture content, oxidation stability, carbon residue, flash point, copper strip corrosion, among others. The discussion includes specific properties and the equipment utilized for measurement, along with their respective manufacturers.
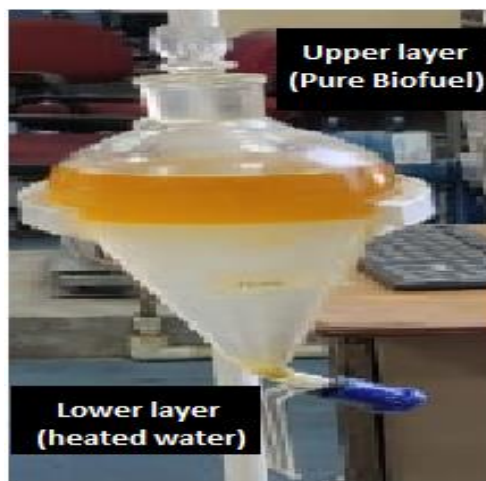
Fig. 3.7 Water washing process

3.3.1. Density

The density of developed nanobiodiesel blends was determined using the "Antan Par Density Meter," Model DMA 4500, as illustrated in Plate 3.1. This study involves measuring the specific gravity of test fuel samples at a temperature of 150°C, following ASTM D-4052 standards. The instrument operates based on the U-tube oscillation principle, commonly employed for measuring the density of liquids and gases by assessing the frequency of oscillation. Frequency measurement is accomplished using a spring-mass system. Prior to the measurement, the test fuel pipeline was cleaned by injecting 10 ml of toluene. Subsequently, a 10 ml sample was introduced into the instrument port. The procedure was replicated five times using a single pilot fuel, and the final value was determined as the average of these repetitions.

3.3.2. Kinematic viscosity

The determination of kinematic viscosity was conducted using a viscometer, as depicted in Plate 3.2. Analyzing viscosity and its variation across a temperature range provides valuable insights into the suitability of waste cooking oil biodiesel as a fuel lubricant. Viscosity measurements were performed on various biodiesels and nanobiodiesels at different temperature intervals. The "Petrotest Viscometer" was employed in accordance with ASTM D-445 standards at a temperature of 40°C. The sample, along with its calculated parameters, was passed through a capillary tube, and the time taken for the fuel to move from the lower to upper level marks in the capillary tube was recorded. Subsequently, the kinematic viscosity was determined by multiplying the time duration by the capillary constant, as expressed in Equation 3.1:

$$\nu = k * t \tag{3.1}$$

where, ν, k, and t represents kinematic viscosity (mm^2/sec); capillary constant (mm^2/sec^2); (k= 0.005565 mm2/sec2) and time (in second) respectively.

3.3.3. Calorific Value

Calorific value is defined as the quantity of heat produced by the combustion of a unit mass of fuel under specific conditions in a calorimeter. The high heating value represents the total heat generated during the combustion reaction of oxygen with carbon and hydrogen, forming carbon oxides and steam. The condensed steam releases additional heat in kJ/kg. Calorific value measurements were conducted in accordance with ASTM D240.0 standards, utilizing an isothermal bulb calorimeter. In this process, fuel combustion occurs at constant volume within an adiabatic water tank in the presence of oxygen. The fuel sample is ignited, leading to combustion in a bomb calorimeter. The resulting temperature rise in the thermocouple is measured, and the calorific value of the test sample is subsequently calculated. The laboratory equipment used for calorific value measurement was the "Parr Model 6100EF," and Plate 3.3 illustrates the measuring device employed in the laboratory.

3.3.4. Flash Point

The flash point is defined as the minimum temperature at which a combustible mixture is formed by the vaporization of oil, as air combines with oil droplets and produces a flash. The determination of flash point was conducted using the Pensky-Martens flash point apparatus, and the flash point value was calculated in accordance

with ASTM D93 standards for the test fuel, as depicted in Plate 3.4. The fuel sample underwent heating until a small pilot flame in a test cup, introduced through the upper cover, reached a steady temperature. The recorded flash point values were 130°C and 120°C, measured by ASTM D-6751 and EN-14214, respectively.

Plate 3.1: Density meter
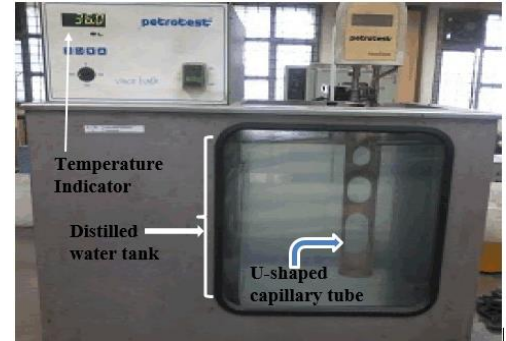
Plate 3.2: Viscometer
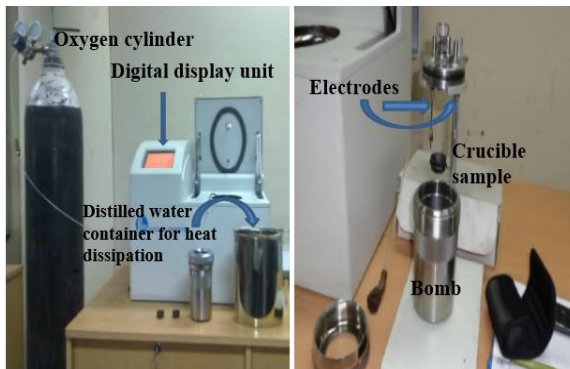
Plate 3.3: Bomb calorimeter

Plate 3.4: Flash point tester

3.3.5. Cetane Number

The Cetane Number (CN) serves as an indicator of the ignition quality of diesel engine fuel, representing the ignitibility quality in Compression Ignition (CI) engines for petroleum diesel or diesel-like fuels. The current investigation determined the cetane index in accordance with ASTM D4737 standards. The cetane index measurement involved distillation and the construction of a density curve for various fuel samples. Plate 3.5 displays the equipment utilized to obtain the distillation temperature. The autoignition values of different biodiesels and their blends are provided through the correlation (3.2) below.

$ECI = 45.2 + [0.131 + (0.901)(X)][BT645] + (0.0892)(BT345) + [(BT345)8 - (BT745)8](107X + 60X8) + [0.0523 - (0.420)(X)][BT745] + [0.00049]$ (3.2). Here, D stands for density, and BT10, 50 and 90 for Boiling/ Recovery temperature to get 10%, 50% and 90% distilled fuel respectively. Z= D-0.85

3.3.6. The saponification value

The saponification value is a measure of the average molecular weight of the ester compounds in the biofuel, particularly biodiesel. It is expressed as milligrams of potassium hydroxide (KOH) required to saponify one gram of the biodiesel. This value is useful for assessing the quality and properties of the biofuel. During this process, Weigh

accurately around 2-5 grams of the biofuel sample using the weighing balance. Record the exact weight.

Plate 3.5: Distillation setup

Transfer the weighed sample to a glass beaker or Erlenmeyer flask. Add a few drops of phenolphthalein indicator solution to the beaker containing the sample. This indicator will change color during the titration process. After that KOH Solution of 0.1 N IS prepared for titration process. Place the beaker or flask with the biofuel sample on a magnetic stirrer or use a glass rod to stir the sample. Slowly add the KOH solution from the burette into the biofuel sample while continuously stirring. Continue adding KOH solution drop by drop until the pink color of the phenolphthalein indicator becomes permanent. This indicates that the saponification reaction is complete.Note the initial and final readings of the burette to calculate the volume of KOH solution used in the titration. Calculate the saponification value using the formula:

Saponification Value (mg KOH/g) = (Volume of KOH used in mL) × (KOH concentration in N) × (Equivalent weight of biodiesel)

The equivalent weight of biodiesel is the molecular weight of the biodiesel divided by the number of ester groups.

3.3.7. The acid value

The acid value of a biofuel measures the amount of acidic compounds, typically free fatty acids, in the biofuel. A high acid value can indicate poor quality or storage issues. Collect a representative sample of the biofuel to be analyzed. Ensure that the sample is well-mixed and represents the entire batch.If necessary, extract the acidic components from the biofuel using an appropriate solvent (e.g., ethanol or isopropanol). To do this, mix the biofuel with the solvent and stir. Allow the acidic components to dissolve into the solvent phase. Weigh accurately around 2-5 grams of the sample using an analytical balance. Record the exact weight. Add a few drops of phenolphthalein indicator solution to the weighed sample. This will change color during the titration process. After that KOH Solution of 0.1 N IS preparted for titration process. Place the beaker or flask with the biofuel sample on a magnetic stirrer or use a glass rod to stir the sample.Slowly add the

standardized KOH solution from the burette into the biofuel sample while continuously stirring. The addition of KOH will neutralize the acidic components in the sample. Continue adding KOH solution drop by drop until the pink color of the phenolphthalein indicator becomes permanent. This indicates that the acid in the sample has been neutralized.Note the initial and final readings of the burette to calculate the volume of KOH solution used in the titration. Calculate the acid value (in mg KOH/g) using the formula:

Acid Value (mg KOH/g) = (Volume of KOH used in mL) × (KOH concentration in N) × (1000) / Sample weight in grams

3.4. Cold Flow Properties

Properties that impact diesel engine performance at low temperatures can pose challenges such as engine starting issues, white smoke emissions, filter plugging, and injector clogging. The fuel's performance in cold weather is typically characterized by parameters such as cold point (CP), pour point (PP), and cold filter plugging point (CFPP).

3.4.1. Cold Point & Pour Point

The pour point is the lowest temperature at which wax in the fuel crystallizes, resulting in a cloudy appearance. Additionally, the pour point represents the minimum temperature at which the liquid fuel loses its flow characteristics. The determination of pour point and cloud point was carried out in accordance with ASTM D97 and D2500 standards, respectively. The process involved placing a test tube filled with the test fuel, sealed with a rubber cork, into a hole above the refrigerator. The cork had an opening at its center to accommodate an RTD temperature sensor, providing the sample's temperature. Subsequently, the test tube was removed, and at each temperature drop of 3°C, visual observations were made to assess pour point and cloud point formation, as illustrated in Plate 3.6.
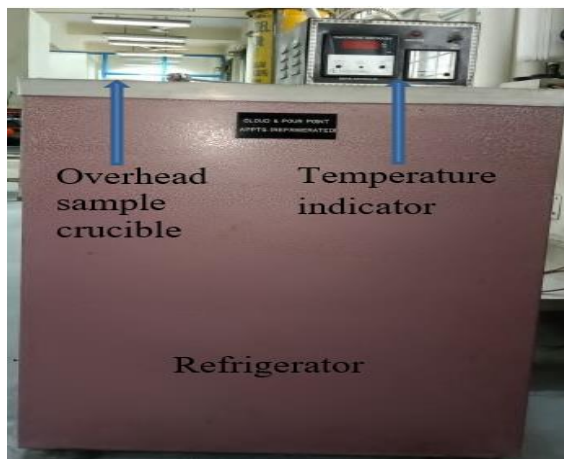
Plate 3.6. Cloud point and Pour point Apparatus

Plate 3.7. Cold filter plugging point apparatus

3.4.2. Cold Filter Plugging Point (CFPP)

The cold filter plugging point of fuel is situated between the pour point and cloud point. It marks the temperature at which the test fuel begins to gel, impacting its ability to flow through a standard fuel filter within a specified duration. The assessment of this fuel property was conducted using Linetronic Technologies, as depicted in Plate 3.7, and follows the ASTM

D6371 standards for estimating the cold filter plugging point of biodiesel and diesel blends. In the initial step, the bath temperature is lowered to -34°C. Once the temperature reaches the specified range, a measured quantity of fuel is drawn through a vacuum-supported mechanism into a capillary tube. Subsequently, the temperature of the fuel sample is allowed to decrease within the bath. The duration of one minute, during which the fuel column achieves a nearly steady state within the standardized filter of 10 microns, is taken as the cold filter plugging point (CFPP) of the fuel.

3.5 Preparation of biodiesel blend

New developed supporting biodiesel sample (B20) was prepared. B20 is the mixture of 20% waste cooking methyl ester and 80% diesel.The physiochemical properties of B20 was tested as discussed above.

3.6 Selection of metallic nanoparticle as fuel additives

Aluminum oxide nanoparticles and cerium oxide nanoparticles are selected as fuel additives in biofuels to improve engine performance and reduce emissions.

Aluminum oxide nanoparticles:

It is also known as alumina, which has a high surface area to volume ratio and are very stable at high temperatures. When added to biofuels, they act as a catalyst, improving the combustion efficiency of the fuel; improve engine performance and reducing emissions such as carbon monoxide carbon di oxide, and unburned hydrocarbons. Additionally, alumina nanoparticles assist to prevent engine deposits and wear by reducing friction between the engine components.

Cerium oxide nanoparticles:

it also known as ceria, and another popular fuel additive for biofuels. Ceria nanoparticles have more oxygen, which helps to promote more complete combustion of the fuel. This leads to reduced emissions of harmful pollutants such as nitrogen oxides and particulate matter. Ceria nanoparticles acts as a catalyst to improve the oxidation of carbon monoxide and other pollutants.

The uses of aluminum oxide and cerium oxide nanoparticles as fuel additives in biofuels improves the fuel efficiency of engines and reduce harmful emissions, making them a promising option for sustainable transportation. That why, in this study, Nanoparticle Al_2O_3 and CeO_2 were selected for experimental investigations. Alumina nanopowder was acquired from D54, Site4, Surajpur, Greater Noida, UP-201308, as illustrated in figure 3.8. CeO2 was procured from mincometsal simplified solutions located in Konena Agrahara, Bangalore-560017, as depicted in figure 3.9. Both types of nanoparticles exhibit favorable physicochemical properties, which are detailed in table 3.1.

Table 3.1. Physical and chemical properties of cerium oxide and aluminum oxide

Al_2O_3		CeO_2	
Form	Power	Form	Power
Colour	White	Colour	Light yellow
Order	Order less	Order	Order less
Melting point	2072°C	Melting point	Not determined
Boiling range	2500-3000°C	Boiling range	Not determined
True density	3.9 g/cm^3	True density	6.5 g/cm^3

Morphology	Spherical	Morphology	Not determined
Crystallographic structure	Rhombohedra	Crystallographic structure	Not determined
Molecular weight	121.96 g/mol	Molecular weight	172.118 g/mol
Molecular formula	Al_2O_3	Molecular formula	CeO_2
Average particle size	10-20 nm	Average particle size	10-30 nm
Bulk density	$1.5g/cm^3$	Bulk density	$1.3g/cm^3$
Purity	99.9%	Purity	99.9%
SSA	120-140 m^2/g	SSA	40-45 m^2/g
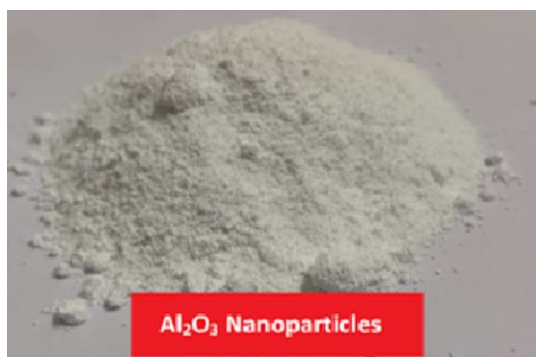
Fig. 3.8. Al_2O_3 Nanoparticles   Fig. 3.9. CeO_2 Nanoparticles

3.7 Purpose of XRD and SEM of nanoparticles

3.7.1 **XRD**

    X-ray diffraction (XRD) is commonly used for characterizing nanoparticles because it can provide information about their crystal structure and phase composition. The crystalline structure of a material determines many of its physical and chemical properties, and this is particularly important for nanoparticles, where the surface-to-volume ratio is high and surface effects can dominate their properties. When X-rays are directed at a sample, they interact with the electrons in the atoms of the sample and are diffracted in specific patterns that are related to the arrangement of the atoms in the sample. The resulting X-ray diffraction pattern provides information about the crystal structure, crystal lattice spacing, and the orientation of the crystal planes within the sample. For nanoparticles, the XRD pattern can help to determine their size, shape, crystal structure, and the presence of impurities. It can also provide information about the degree of crystalline, which can affect the physical and chemical properties of the nanoparticles. XRD is a valuable tool for analyzing nanoparticles and can provide important information for understanding their properties and potential applications

3.7.2 SEM

    Scanning electron microscopy (SEM) is a useful tool for characterizing nanoparticles because it can provide high-resolution images of their size, morphology, and surface features. SEM works by scanning a beam of electrons over the surface of a sample, which causes the electrons to interact with the surface and emit secondary electrons. These electrons are detected and used to create an image of the sample. Nanoparticles have a high surface-to-volume ratio, which means that their properties and behaviour can be strongly influenced by surface effects. SEM can provide detailed information about the surface features of nanoparticles, such as surface roughness, surface area, and the presence of defects, which can affect their reactivity, stability, and other properties. In addition, SEM can also be used to

determine the size distribution of nanoparticles, as well as their aggregation state and distribution within a sample. SEM can be used to analyze both individual nanoparticles and bulk samples containing a large number of nanoparticles. For individual nanoparticles, SEM can provide information about their size, shape, and surface features, while for bulk samples; SEM can provide information about the overall distribution and arrangement of the nanoparticles within the sample. SEM is a valuable tool for characterizing nanoparticles, as it can provide high-resolution images and information about their surface features, size distribution, and aggregation state, which can be important for understanding their properties and potential applications.

3.8. Morphology testing of metallic nanoparticles

Nanoparticles Al_2O_3 and CeO_2 morphology was tested by XRD and SEM in DTU. The XRD and SEM image of both nanoparticles (Al_2O_3 and CeO_2) was shown in fig. 3.10, fig. 3.11, fig. 3.12, and fig.3.13. Al_2O_3 TEM image was also shown in fig no. 3.14. The mean size of nanoparticles Al_2O_3 and CeO_2 varies from 10-20 nm for Al_2O_3 and 10-30 for CeO_2. XRD and SEM is the preferred method for direct determination of size composition, crystal structure, sample purity, morphology, and unit dimension analysis of nanoparticle samples. XRD and SEM images pointed out that the purchased Al_2O_3 and CeO_2 are good nanoparticles to use with biodiesel.
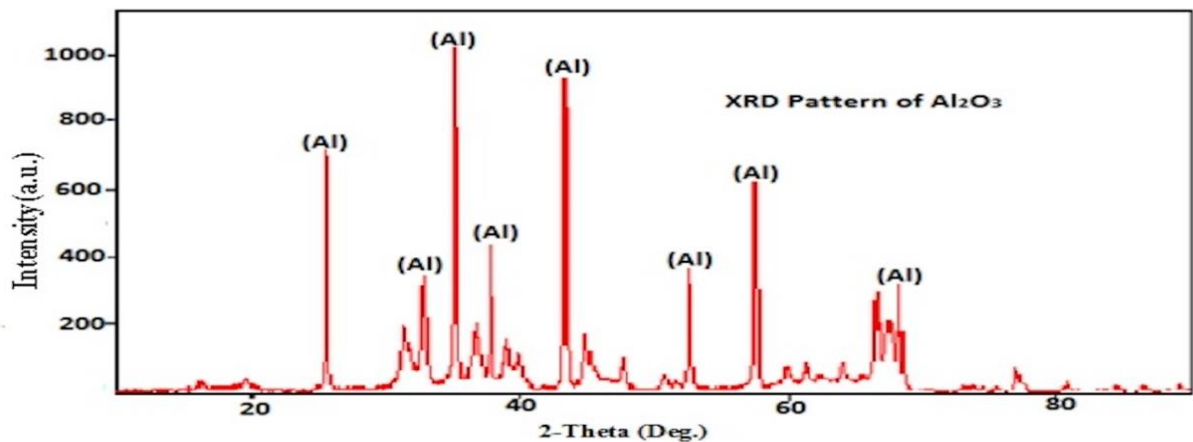
Fig. 3.10. Al_2O_3 Nanoparticles XRD analysis
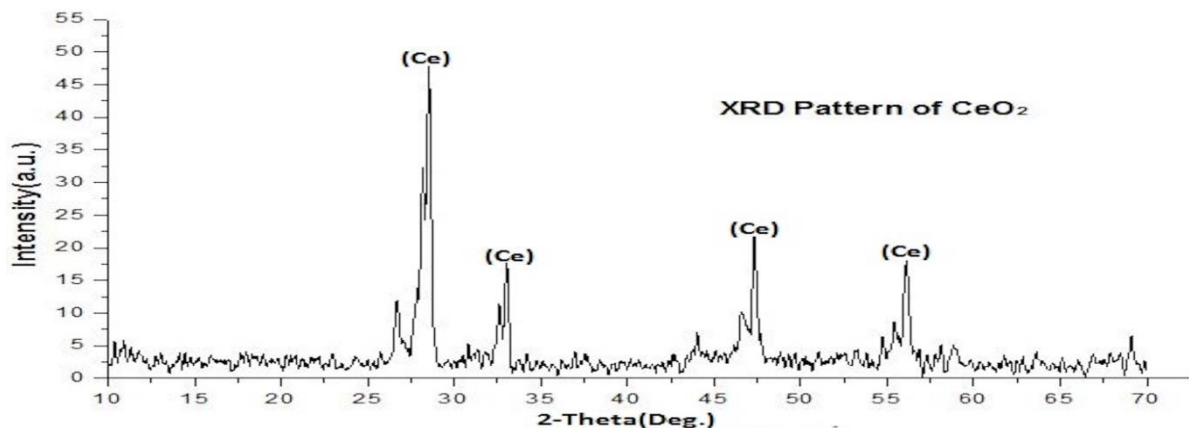
Fig. 3.11. CeO$_2$ Nanoparticles XRD analysis
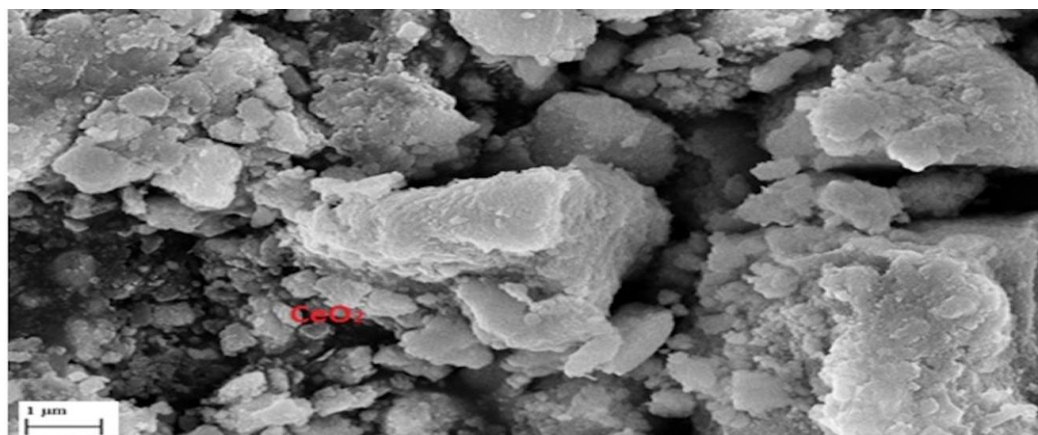
Fig. 3.12. CeO$_2$ Nanoparticles SEM analysis
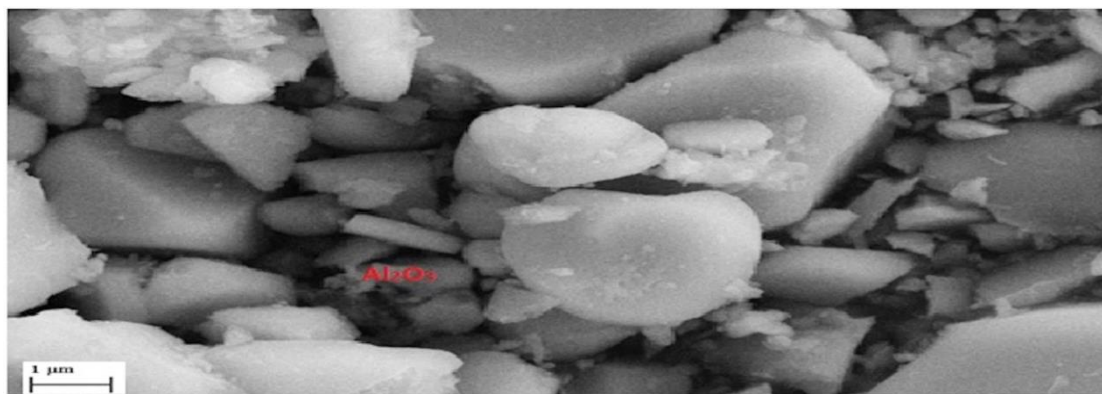
Fig. 3.13. Al$_2$O$_3$ Nanoparticles SEM analysis
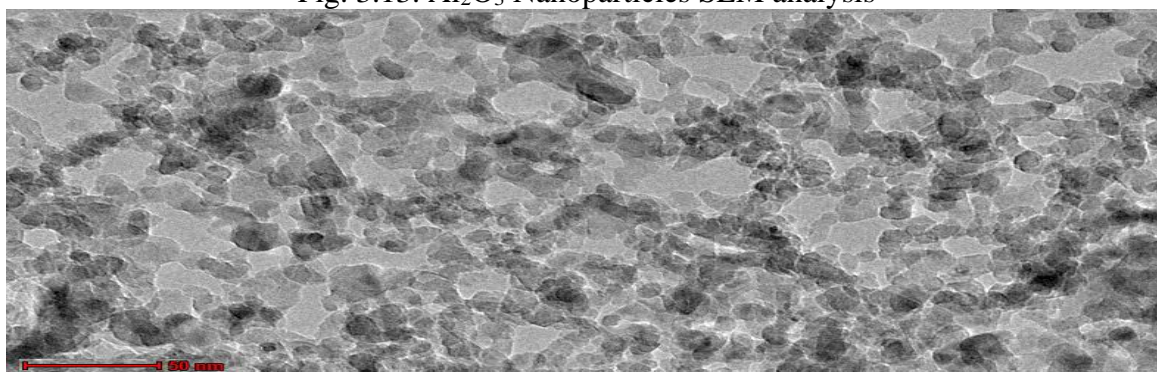
Fig. 3.14. TEM analysis of Al$_2$O$_3$

3.9. Nano-biofuel blend preparation and stability test

In this experimental investigation, Al$_2$O$_3$ nanoparticles were individually incorporated into B20 biofuel (a blend of waste cooking oil and diesel) at concentrations of 25 ppm, 50 ppm, 75 ppm, and 100 ppm for every 1 kg of biodiesel fuel. The mixing process involved an ultrasonicator operating at a frequency of 40 kHz and 160 watts for 30 minutes. The ultrasonicator effectively prevented nanoparticle agglomeration. High-frequency ultrasonication was then employed for one hour to ensure the complete dissolution of

homogeneous nanoparticles in the mixture, as illustrated in Figure 3.15. The newly developed nano-additive fuels were denoted as B20+25 PPM (Al_2O_3), B20+50 PPM (Al_2O_3), B20+75 PPM (Al_2O_3), and B20+100 PPM (Al_2O_3). Furthermore, CeO_2 nanoparticles were also blended with waste cooking biodiesel at concentrations of 50 ppm and 100 ppm using the same ultrasonication process. The newly developed nanobiofuel samples were designated as B20+50 PPM (CeO_2) and B20+100 PPM (CeO_2). Subsequently, the physiochemical properties of the developed samples were tested.

In this experimental study, Al_2O_3 were added in various ratios separately into supporting biodiesel B20. Each nanoparticle is weighted to a mass fraction of 100ppm. The nanoparticle is added in different ratios such as be 25mg, 50mg,75mg and 100mg for 1 kg diesel fuel in that order. Subsequently, each sample fuel was dispersed by ultrasonicator at a frequency of 40 kHz and 300W for 30 minutes. Ultrasonicators prevent the agglomeration of the nanoparticle **by** utilizing high pulsating frequency otherwise nanoparticles clustered collectively to shape a micro molecule and begin to the residue. Surfactants help to stabilize nanoparticles in the biodiesel blend by forming a layer around them. Surfactant treatment can enhance nanofluid stability by reducing particle-particle interactions and improving colloidal stability. This prevents the nanoparticles from agglomerating or settling out of the mixture, ensuring a uniform dispersion. Span-80 (Sorbitan monooleate) surfacnt was used to in developed blend to prevent agglomeration.

Evaluating stability and sedimentation zeta potential test was used for all developed blends after three days of preparation of blends. It was found that zeta potential is more than 25 Mv for all blends means that this electrostatic volt is enough to avoid agglomeration of nanoparticles. This analysis indicates that blend maintains the homogeneity overt the time for 72 hours.

Temperature Stability:

Temperature stability assesses the ability of nanofluids to maintain particle dispersion and prevent agglomeration over a range of temperatures encountered during storage or application. Nanofluid stability can be affected by temperature variations due to changes in fluid viscosity, surface tension, and Brownian motion of nanoparticles. Stability testing was done for all blends at room temperature. These blends was prepared for the testing of engine performance that why threr was no need to change the temperature for various blends. Ultransoncator, surfactant and zeta potential test all were performed at room tempreaure. There was no role to change the stability by varying temperature.

Concentration Stability:

Concentration stability refers to the ability of nanofluids to maintain particle dispersion at various nanoparticle concentrations within the base fluid. Zeta potential test was used to different concentration of nanoparticle blend in biodiesel. There was variation in electro potential reading for different blend.   Typically, when nanoparticles are added to a fluid, the zeta potential is increased as the concentration of nanoparticles increases. However, beyond a certain concentration, it was found that zeta potential was decreased for 75ppm and 100ppm nanoparticle concentration in biodiesel.

3.10. Experiment setup and test procedure

The experimentation was conducted on a Kirloskar AVI, Variable Compression Ratio (VCR), 4-stroke single-cylinder Common Rail Direct Injection (CRDI) diesel engine. Detailed specifications of the diesel engine are provided in table number 3.2. Eddy current

dynamometers with a maximum power of 7.5 kW were employed for loading the engine, and AVL gas analyzer was used for calculating engine emissions.
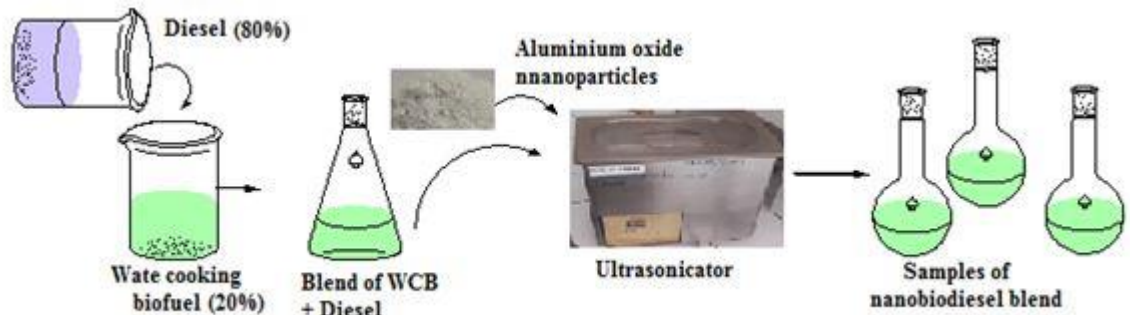
Fig. 3.15. Homogenously mixing of nanoparticle with biofuel

Combustion characteristics were computed using a data acquisition system interfaced with a dual-core processor. The experimental setup is illustrated in figures 3.16 and 3.17. The engine's rated power is 3.5 kW. Initially, diesel fuel was used to run the engine, and the results obtained for diesel served as reference data for the current experiment. The engine was subsequently fueled with newly developed nano biofuel blends. To measure air flow rate, a standard orifice meter was utilized, fitted to the airbox. The pressure differentiation between two sides of the orifice was determined using a U-tube manometer. Temperature at various points in the experimental setup was measured using a type K thermocouple. Fuel flow rate was gauged using a burette equipped with a stopcock and a two-way valve.

3.10.1 Fuel injection pump

The fuel injection pump in a biodiesel engine plays a critical role in delivering the right amount of fuel to the engine at the right time. Biodiesel is a renewable fuel made from vegetable oils, animal fats, or recycled greases, and it has different properties compared to petroleum diesel fuel. Therefore, the fuel injection pump used in a biodiesel engine is designed to work with these properties and to optimize the engine's performance**.** The fuel injection pump is responsible for delivering biodiesel from the fuel tank to the engine's combustion chamber. The pump pressurizes the fuel to a very high level, typically in the range of 1000 to 3000 bar, and then injects it into the combustion chamber at the right time and in the right amount.

Table 3.2 Engine specifications

Engine model	VCR (Diesel engine) 4 stroke
Fuel Injection	Common rail direct injection
Cylinder diameter	87.5mm
length of Connecting rod	234mm
Stroke length	110mm
Engine Power @ 1500 RPM	3.5kw
Orifice diameter	20mm

length of Dynamometer arm	185mm
Power	3.5kw
Compression Ratio Variation	12:1 to 22:1
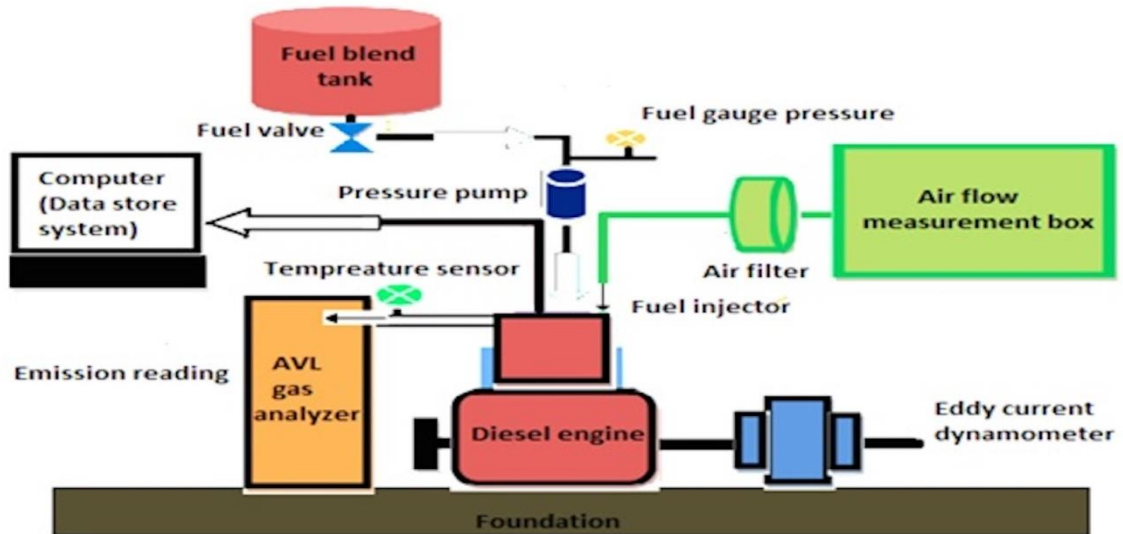
Fig. .3.16 Block diagram according to biofuel engine setup in DTU lab
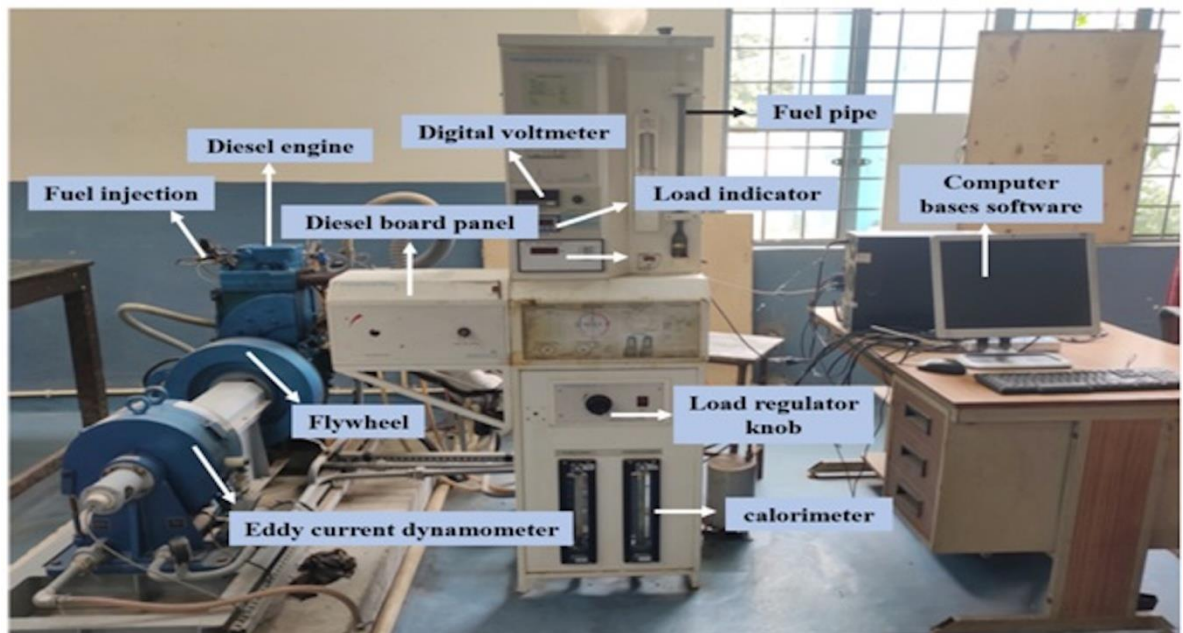
Fig. No 3.17 Pictorial view of biofuel engine setup

The pump needs to be precise, reliable, and durable to ensure that the engine runs smoothly and efficiently. One of the challenges with using biodiesel is that it has a higher viscosity compared to petroleum diesel, which can affect the fuel injection system's performance. Therefore, the fuel injection pump used in biodiesel engines may need to be specially designed or modified to handle the higher viscosity fuel. In this study MICO BOSCH fuel injection pump was used is shown in fig 3.18. The fuel injection pump injects the fuel in CRDI VCR single cylinder injection pump. The camshaft mechanism is used for injecting high pressure fuel in a diesel engine.

Fig. 3.18. Fuel injection pump

3.10.2 Measurement system

There are several measurement devices that can be used in biodiesel single cylinder engines, each with its own specific function. Here are some of the most commonly used measurement devices:

Load cell: A load cell is a device that measures the force applied to it. It can be used in biodiesel single cylinder engines to measure the torque and power output of the engine.

Thermocouple: A thermocouple is a temperature sensor that consists of two wires made from different metals. It can be used in biodiesel single cylinder engines to measure the temperature of the engine coolant, exhaust gas, and other engine components.

Pressure transducer: A pressure transducer is a device that converts pressure into an electrical signal. It can be used in biodiesel single cylinder engines to measure the pressure inside the combustion chamber, intake manifold, and exhaust system.

Fuel flow meter: A fuel flow meter is a device that measures the flow rate of fuel. It can be used in biodiesel single cylinder engines to measure the amount of fuel consumed by the engine.

Emission analyzer: An emission analyzer is a device that measures the concentration of pollutants in the exhaust gas. It can be used in biodiesel single cylinder engines to measure the emissions of carbon monoxide, hydrocarbons, and nitrogen oxides.

These measurement devices are essential tools for researchers and engineers working on biodiesel single cylinder engines, as they provide critical information about the engine's performance and emissions.

3.10.2.1 Load measurement system

3.10.2.1.1Eddy current dynamometer

An eddy current dynamometer is a type of dynamometer that is commonly used to measure the power output of diesel engines. In this study eddy current dynameters is used which is shown in fig 3.19. The dynamometer works by creating an electromagnetic field, which induces eddy currents in a conductive rotor. As the rotor spins, the eddy currents generate a resistance to the motion of the rotor, which in turn generates a torque that can be measured. In the case of diesel engines, the eddy current dynamometer is typically used to measure the engine's power output and torque characteristics.

Load cells, on the other hand, are devices that measure force or weight by sensing the deformation of a mechanical element, such as a strain gauge, when a load is applied. To measure the load of a single cylinder biodiesel engine using an eddy current dynamometer and a load cell, the load cell would typically be installed between the engine and the dynamometer. The loading unit would then be connected to the eddy current dynamometer, which would apply the electromagnetic field to the cylinder and measure the resulting torque and power. The load cell would measure the force or weight of the engine as it operates, which would be transmitted to a data acquisition system or controller that would collect and process the measurements. The connection between the eddy current dynamometer and the loading unit would typically be made through a coupling or adapter that allows the dynamometer to be attached to the engine. The load cell would be connected to the engine or engine mount, and the electrical signals from both the load cell and the dynamometer would be fed to the data acquisition system. The data acquisition system would then compute the torque, power, and load measurements and provide real-time feedback on the performance of the engine. The crank angle sensor and water coolant serve different functions in an eddy current dynamometer of a diesel engine. The crank angle sensor is a sensor that measures the position of the engine's crankshaft. It provides information to the engine control unit (ECU) about the engine's speed and position, which is essential for proper fuel injection timing and ignition timing. In an eddy current dynamometer, the crank angle sensor is used to measure the engine's speed and torque output, which is then used to calculate the power output of the engine. On the other hand, the water coolant is used to regulate the temperature of the engine during testing. Diesel engines generate a lot of heat during operation, and this heat can damage the engine if it is not properly dissipated. In an eddy current dynamometer, the water coolant is circulated through the engine to absorb heat and carry it away from the engine. By regulating the engine's temperature, the water coolant ensures that the engine operates within safe temperature limits during testing. In summary, the crank angle sensor is used to measure the engine's speed and torque output, while the water coolant is used to regulate the engine's temperature during testing. Both are essential components of an eddy current dynamometer used for testing diesel engines.

Fig no. 3.19 Eddy current dynamometer

3.10.2.2 Load cell

Load cells are electronic transducers that convert mechanical force or weight into an electrical signal. Load cells typically consist of a metal body, a strain gauge, and electrical connections as shown in fig. 3.20. The metal body is designed to deform when subjected to a load, and the strain gauge is attached to the metal body to measure the deformation. When a load is applied to the load cell, the metal body deforms, and the strain gauge experiences a change in resistance proportional to the deformation. This change in resistance is very small, typically on the order of a few micro-ohms, so a Wheatstone bridge circuit is used to amplify the signal. The Wheatstone bridge circuit consists of four resistors, including the strain gauge, arranged in a bridge configuration. A voltage is applied across the bridge, and the output voltage is measured across the strain gauge. When a load is applied, the change in resistance of the strain gauge causes an imbalance in the Wheatstone bridge circuit, resulting in a change in the output voltage. The output voltage is then converted into an electronic signal using an amplifier and filtering circuitry.

Load cells convert mechanical force or weight into an electrical signal by using a metal body that deforms under load, a strain gauge that measures the deformation, and a Wheatstone bridge circuit that amplifies and measures the change in resistance of the strain gauge. The resulting electrical signal is then amplified and filtered to provide an accurate and reliable measurement of the load applied to the load cell.

Fig. 3.20 Load cell figure

3.10.2.3 Loading unit

A loading unit consists of an electric actuator that applies a load to the engine, and a control system that regulates the load based on the engine's speed and torque output. The current study's loading unit picture shown in fig. 3.21. The control system typically includes sensors to measure the engine speed and torque, as well as a controller that adjusts the load applied to the engine based on these measurements. When a diesel engine is connected to a dynamometer and loading unit, the engine's output torque is measured by the dynamometer. The loading unit applies a load to the engine, simulating the resistance that the engine experienced this load. The control system adjusts the load applied by the loading unit to match the engine's speed and torque output. As the engine runs, the dynamometer measures its speed and torque output, and the loading unit applies a load that matches the engine's power output. Power output of the engine to be accurately measured, and various performance parameters are analyzed, such as specific fuel consumption, brake thermal efficiency, and emissions. A loading unit works with a dynamometer to simulate the engine load. The loading unit applies a load to the engine, while the dynamometer measures the engine's speed and torque output.

Together, they provide an accurate measurement of the engine's power output and performance characteristics.

Fig.3.21 Engine panel box

3.10.3 Data acquisition system

In a diesel engine, there are various parameters that can be measured to monitor the engine's performance and diagnose any issues that may arise. To measure these parameters, a data acquisition system is used as shown in fig 3.22. The basic operation of a data acquisition system in a diesel engine involves the following steps:

Sensor placement: The first step in a data acquisition system is to place the sensors in the appropriate locations on the engine. There are various sensors used in a diesel engine, such as pressure sensors, temperature sensors, and flow sensors. These sensors are typically attached to the engine block or other components using bolts or other fasteners.

Signal conditioning: Once the sensors are in place, the signals they produce need to be conditioned before they can be measured. This involves amplifying and filtering the signals to remove any noise or interference that may be present. Signal conditioning can be done using analog or digital signal processing techniques.

Data conversion: After the signals are conditioned, they need to be converted into a digital format so that they can be processed by a computer. This is done using an analog-to-digital converter (ADC) that samples the analog signals and converts them into a series of digital values.

Data processing: Once the signals are in digital format, they can be processed by a computer or microcontroller. The processing can involve simple calculations, such as averaging or peak detection, or more complex algorithms, such as FFT (Fast Fourier Transform) analysis or digital filtering.

Data storage: The processed data can be stored in various formats, such as a database, a spreadsheet, or a log file. The data can be used for various purposes, such as real-time monitoring of the engine performance, diagnostics, or trend analysis.

Data visualization: Finally, the data can be displayed graphically using various visualization tools, such as charts, graphs, or gauges. This allows the user to quickly and easily interpret the data and identify any issues or trends in the engine's performance.

A data acquisition system in a diesel engine is a complex system that involves various sensors, signal conditioning, data conversion, processing, storage, and visualization. The system is designed to provide accurate, reliable, and timely data to monitor the engine's performance and diagnose any issues that may arise.

Fig.3.22 Sensor interface circuit

3.10.4 Exhaust gas analyzer

The function of an exhaust gas analyzer is to measure and analyze the composition of the exhaust gases produced by an engine. Specifically, an exhaust gas analyzer is used to measure the concentrations of various gases in the exhaust stream, including carbon monoxide (CO), carbon dioxide (CO2), nitrogen oxides (NOx), and hydrocarbons (HC).

The exhaust gas analyzer typically consists of a probe that is inserted into the exhaust stream of the engine, which then captures a sample of the exhaust gases. The pictorial view of exhaust gas analyzer is shown in fig. no.3.23 and specification of gas analyzer is shown in table no 3.3. The sample is then analyzed by the analyzer, which typically uses a series of sensors and detectors to measure the concentration of each gas. Finally, an exhaust gas analyzer can be used to optimize engine performance by identifying areas where emissions can be reduced without compromising engine efficiency or power output. This can help engine manufacturers to design more efficient and environmentally-friendly engines.

Fig. 3.23 Exhaust gas analyzer

Table 3.3. Specification of exhaust gas analyzer

Description	Measurement range	Accuracy
CO (% volume)	0-10	0.01
CO_2 (% volume)	0-20	0.1
NO_X (ppm)	0-5000	1
HC (% volume)	0-2000	1
Oil temperature (°c)	-30 to 125	1
Lambda	0-0.9999	0.01

3.11. Engine software (IC engine soft version 9.0)

IC engine software is an analysis software tool for analyzing engine data. It provides the following tests.

a) Performance against load/speed for constant/ variable speed engines.

b) Combustion analysis.

IC engine software serves most of your IC engine testing application need including analysis, data logging and reporting. One can access all the functionality through the IC engine soft menu. The buttons on the IC engine soft control panel give you easy access to various function of test and display. IC engine soft is configurable for any engine and enables the study of different parameters of engine related to combustion and performance for evaluation which are follows.

Combustion data:

- Cylinder pressure reference value
- TDC value
- Polytrophic index
- Indicated mean effective pressure
- Indicated power
- Cylinder volume
- Log pressure and log volume
- Rate of pressure rise
- Net heat release rate
- Start of combustion and end of combustion
- Cumulative heat release
- Mass fraction burned
- MFB 5%, MFB 10%, MFB 50% & MFB 90%
- Means gas temperature
- Fuel line pressure
- Respective average cycle data
- MAX values and corresponding angles

Performance data:

- Brake power(BP)
- Frictional power
- Torque
- Brake mean effective pressure
- Frictional mean effective pressure
- Brake thermal efficiency
- Indicated thermal efficiency
- Frictional thermal efficiency
- Mechanical efficiency
- Volumetric efficiency

- Air flow
- Fuel flow
- Brake specific fuel consumption

- Air fuel ratio
- Heat equivalent to brake poer
- Heat in jacket cooling water
- Heat in exhaust gas

This software provides the various grapes at different operating conditions. By default IC engine soft operates in offline mode. To run IC engine soft in online mode, switch ON the mode and measurement. Starting measurement access the interface. The interface includes a communication driver. Communication interface will select USB port automatically. On requires signals are scanned during the calculation, processed and displayed in the form of graph and tablets. The results and graphs report can be generated. Figure 3.24 exhibit the display of IC engine software version 9.0.
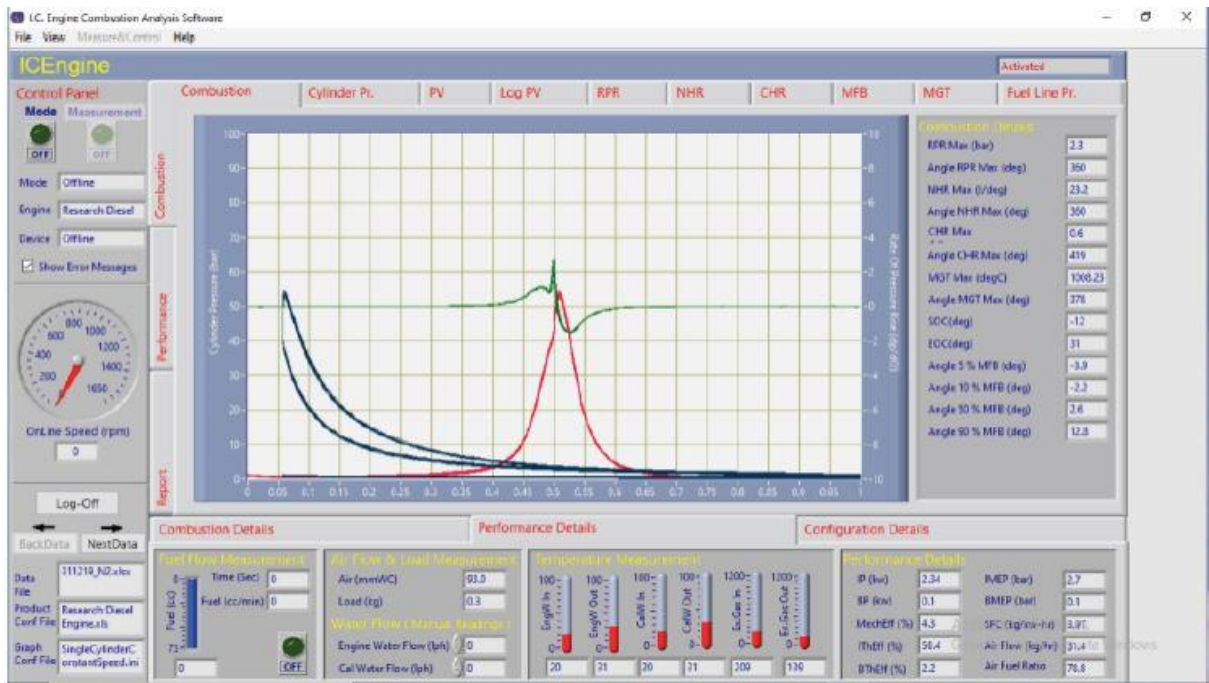
Fig. 3.24 Interface of IC engine soft 9.0

3.12. Procedure of testing

In the present investigation experiments have been carried out for at on VCR CRDI diesel engine at constant speed 1500rpm and constant injection timing 23º bTDC for the combined blends of waste cooking oil and metallic nanoparticles. Input parameters such as compression ratio, injection pressure and engine loads are varied for different develop blends. Details of the variable and fixed parameter are given in table 3.4. Results were evaluated by measuring performance and emission characteristics as given in the table 3.5. Initially, the diesel engine test system runs on a standard 10 minutes. The nanobiodiesel blend was cautionary blended before it was required by engines on the appraisal system. Then the necessary nanobiodiesel blends were poured into the fuel tank. Efficiency and emissions parameters were checked three times, and the analysis was recorded to calculate the average reading.

Table no. 3.4 Variable & fixed-parameters of engine trail

Variable parameters				Fixed-parameters	
Tertiary blend	**Load (Kg)**	**Fuel Injection Pressure(bar)**	**Compression ratio**	**Injection timing**	**Engine speed (rpm)**
Diesel, B20, B20+25 Al_2O_3, B20+50 Al_2O_3, B20+75 Al_2O_3, B20+100 Al_2O_3, B20+50 CeO_2, B20+100 CeO_2	0-12	500-700	17-19	23º b TDC	1500

Table no. 3.5 Evaluated parameters during engine trail

S.N.	Performance parameters	Emission parameters
1	Brake thermal efficiency	Hydrocarbon (HC)
2	Brake specific fuel consumption	Nitrogen oxide (NO_X)
3	-	Carbon mono oxide (CO)

3.13. Uncertainty analysis

The analysis of experimental uncertainty involves the examination and evaluation of uncertainties within an experimental investigation. The uncertainties associated with measured values may arise from errors in measuring instruments, human errors during the measurement of experimental data and computational processes, and can be subtly influenced by environmental factors [187]. The experimental procedure inherently introduces various potential sources of uncertainty that pertain to all measurements. These uncertainties may stem from environmental conditions, the imprecise selection of instruments, the ambient state of the laboratory, engine instrument calibration, adjustments and modifications to the engine setup, operating conditions, and manual calibration of readings [188]. In the context of engine experiments, individual uncertainties related to Brake Thermal Efficiency (BTE), Specific Fuel Consumption (SFC), chamber pressure, heat release rate, and harmful emissions are incorporated into Equation (3.3) to quantify the overall uncertainty. In this analytical review, each experimental test is conducted three times, and their mean values are considered. The error bar (I) diagram is employed with a confidence level (alpha=0.05) in the "Results and Discussion" section. The percentage uncertainty of measured parameters is detailed in Table 3.6. For the experimental study, the uncertainty of the measured parameter was determined using a specific equation.

$$\frac{U_y}{y} = \sqrt[2]{\left(\frac{1}{y}\frac{\partial y}{\partial x_1}\right)^2 + \left(\frac{1}{y}\frac{\partial y}{\partial x_2}\right)^2 + \left(\frac{1}{y}\frac{\partial y}{\partial x_3}\right)^2 + \dots \left(\frac{1}{y}\frac{\partial y}{\partial x_n}\right)^2}$$

(3.3)

Where 'y' is a particular factor, U_y denotes the degree of uncertainty, x_i denotes parameter.

Total error (%) = ± [(0.5)^2 + (0.55)^2 + (0.28)^2 + (0.47)^2 + (0.23)^2 + (0.45)^2 + (0.6)^2]$^{1/2}$

Total uncertainty (%) = ±1.211%.

The examination of uncertainty (error) might be estimated utilizing Eq (3.3). The consequence of all error (%) was ±1.211%, for example serenely inside the permitted edge.

Table 3.6. Range, accuracy, and uncertainty of measuring instruments

Parameters	Uncertainty (%)	Accuracy (±)
BTE	±0.5	-
BSFC	±0.55	-
Pmax	±0.28	± 0.25 bar
HRR	±0.47	-
CO emission	±0.23	±0.01 vol %
NOx emission	±0.6	±15 ppm
UHC emission	±0.45	±20 ppm

3.14. Response surface methodology

Response surface models are developed using regression analysis, fitting mathematical equations to the experimental data. These models elucidate the relationships between the response variables and the independent factors, allowing for insights into engine behaviour and performance.

3.14.1 First-order model design

A first-order model is the simplest approximation of the response surface and assumes a linear relationship between the response variable and the independent variables. It is suitable when there is little to no curvature or interaction between factors in the response surface. The first-order model can be expressed as given in equation no 3.4:

$$Y = b0 + b1*X1 + b2*X2 + ... + bk*Xk \qquad (3.4)$$

where Y is the response variable, X1, X2, ..., Xk are the independent variables (factors), and b0, b1, b2, ..., bk are the coefficients to be estimated.

- Exploratory Research:

In exploratory research, the goal is to understand the relationship between the response and variables. The 2k factorial method is mentioned, which is a common experimental design used to explore these relationships. Fractional replication is discussed as a way to reduce the number of experiments while still obtaining information about the uncertainty of experimental errors.

Methods for Dealing with Lack of Fit:

Lack of fit refers to situations where the first-order model does not adequately describe the relationship between the response and variables.

The methods mentioned for dealing with lack of fit include repeating the experiment, using prior research with known error variation, and applying a series of checks at different stages of experimentation.

- Linear Equation and Coefficients:

The linear equation mentioned, k(x), includes (k+1) coefficients of regression that need to be determined. The choice of an experimental design should provide enough information to estimate these coefficients with sufficient precision.

- Exploration and Transformation:

If there is no lack of fit and sufficient precision in the first-order model, the direction of the steepest ascent is determined, and exploration continues. Transformation of variables and responses may be considered to improve model fit. Careful blocking and expanding the size of the experimental design can also increase precision.

- Second-Order Design:

If satisfactory fit and precision cannot be achieved with the first-order model, then second-order designs (e.g., central composite designs) may be considered. Second-order designs allow for the modeling of curvature and interactions in the response surface. Starting with a first-order model is a common approach, but more complex designs like second-order designs may be required when the response surface exhibits curvature or interactions that cannot be adequately captured by a linear model. The choice of experimental design and methods for addressing lack of fit depend on the specific research goals and constraints.

3.14.2 Second-Order Model design

A second-order model is a more complex model that takes into account not only the linear effects of the factors but also the quadratic effects and interactions between factors. It is used when there is curvature or non-linearity in the response surface and when interactions between factors need to be considered. The second-order model can be expressed as:

Y = b0 + b1*X1 + b2*X2 + ... + bk*Xk + b11*X1^2 + b22*X2^2 + ... + bkk*Xk^2 + b12*X1*X2 + ... + b1k*X1*Xk + b2k*X2*Xk   (3.5)

Here, in addition to the linear terms (b1, b2, ..., bk), you have quadratic terms (b11, b22, ..., bkk) representing the curvature effects and interaction terms (b12, b1k, b2k) representing the interactions between factors.

The choice between a first-order and second-order model depends on the complexity of the system being studied and the available data. In many cases, starting with a first-order model is a good initial step, and if the response surface appears to be nonlinear or if interactions are suspected, you can then move to a second-order model to better capture the system's behaviour. It's important to note that the coefficients (b0, b1, b2, ..., bk) and (b11, b22, ..., bkk, b12, b1k, b2k) in both models need to be estimated from experimental data using techniques like least squares regression. Once the models are developed, they can be used for optimization and prediction within the studied parameter space.

3.14.3 Factorial Designs and Limitations

To test the coefficients of regression in a second-order model, it's common to use factorial designs, specifically 3k factorial designs when each factor has at least three separate levels. The main drawback of full 3k factorial designs is that they can become large and require a large number of experiments as the number of factors (k) increases.

3.14.4 Box and Wilson's Central Composite Design

To address the limitations of full factorial designs, Box and Wilson introduced the central composite design (CCD). CCD includes a set of "star" or "composite" treatments in addition to the factorial points. These treatments, as described in your text, allow for the exploration of the response surface within a limited number of experiments. The parameter alpha controls the distance of the axial points from the center, impacting the design's orthogonality and precision in estimating coefficients.

3.14.5 Determining Factor Levels for Optimization

Before conducting experiments, it's crucial to select which variables to include and to choose the range for each variable. This is often based on prior knowledge, preliminary studies, or domain expertise. Factors that have a significant impact on the response should be considered, while those with little influence may be excluded. The range of each factor should cover the expected variability in practice and should be chosen carefully to explore the response surface adequately.

Overall, RSM is a systematic approach to optimizing processes or systems by modeling and analyzing the relationship between factors and a response variable. Second-order models and central composite designs are valuable tools in this process, allowing researchers to efficiently explore and understand the response surface while minimizing the number of experiments required. Careful selection of factors and their ranges is essential for successful experimentation and optimization

3.14.6 Methods of steepest ascent

In response surface methodology (RSM), the ascent and descent steepest method is used to optimize a response function by finding the maximum or minimum value of the function within a specified region. The method is commonly applied to fit a second-order polynomial model to experimental data in order to approximate the relationship between the input variables and the response variable.

- Box and Wilson's Method:

Box and Wilson introduced the method of steepest ascent/descent as a systematic approach to optimizing a response function. The method involves a sequence of experiments, each prepared based on the results of the preceding ones.

The first experiment has two primary objectives:

(i) Fit a linear equation to approximate the response function.
(ii) Ensure that the linear approximation remains valid within the experimental error limits.

The 2k factorial or fractional factorial designs are often used for this purpose in the first experiment.

- Moving the Testing Area:

After the first experiment is complete, the testing area is transferred to another range of input variables (x's) to maximize the expected increase in the response. The direction of the move is determined by finding the steepest ascent path.

- Steepest Ascent Path:

The steepest ascent path is the direction along which the response function increases most rapidly. It is typically perpendicular to the contours of the response surface and often follows the line through the center of the region of interest.

- Response Surface Model:

The response surface model is typically a polynomial model that can capture linear, quadratic, and interaction effects. The model is expressed as you mentioned: $Y = b_0 + \sum b_i X_i + \sum b_{ij} X_i X_j + \varepsilon$, where b_i and b_{ij} are the coefficients.

Continued Exploration: Depending on the results of the experiments, there are two possible scenarios for further exploration: If the linear equation still seems to be a good fit but all b_i coefficients are small, it suggests a plateau approach, where the response is not changing significantly.

If the linear approximation is inappropriate, indicating curvature in the response surface, second-order designs (e.g., central composite designs) are used to explore the region more thoroughly.

The method of steepest ascent is a systematic approach to optimizing a response function by moving along the steepest path in a region of interest. It starts with a linear approximation and may transition to second-order designs if needed to capture curvature effects. This method helps in efficiently finding optimal conditions for a process or system while minimizing the number of experiments required

3.14.7 Canonical Correlation Analysis

In CCA, one typically seeks a stationary point in the response surface, which is a point where the correlation between the canonical variables reaches an extreme (maximum or minimum). Characterizing the stationary point involves determining whether it is a maximum, a minimum, or a saddle point.

Contour Plot and Canonical Study:

Contour plots of the response surface are often used to visualize the relationships between the variables.

For more detailed analysis, a canonical study may be conducted, especially when there are very few variables. This study involves a deeper examination of the canonical equation.

- Canonical Equation:

The canonical equation is a mathematical representation that transforms the original variables into a new set of coordinates. This transformation often involves shifting the center of the old coordinates to the solution surface and rotating the axes to obtain symmetry. The canonical equation typically contains only quadratic effects, as linear and cross-product terms are deleted through this transformation.

- Canonical Varieties:

The canonical equation allows for the calculation of canonical varieties, which are the linear combinations of the original variables. These canonical varieties are used to measure the correlation between the two sets of variables.

Interpreting Relationships:

Researchers analyze the canonical equation and associated coefficients to interpret the relationships between the original variables. This analysis helps in understanding the strength and direction of the relationships between the canonical varieties.

CHAPTER FOUR
RESULTS AND DISCUSSION

Overview

This chapter presents a thorough examination of the research findings, commencing with a concise elucidation of the rheological properties of waste cooking biodiesel and nanobiodeisel. Subsequently, engine performance was scrutinized under various load conditions and constant speeds for both waste cooking biodiesel and nanobiodiesel. A comparative analysis was conducted on engine performance and emissions at different load conditions and constant speeds, exploring the impact of two types of nanoparticles—cerium oxide and aluminium oxide—when separately introduced into diesel and biodiesel. The chapter further explores the intricate process of optimizing engine responses by manipulating carefully selected input parameters. Rigorous experiments were conducted on a VCR CRDI diesel engine to evaluate its performance and emission characteristics. These experiments involved operating the engine at different input parameter fuelled with various fuels, including conventional diesel fuel, selected diesel/biodiesel blends, and nano-biodiesel blends. The chapter concludes with the validation of the optimized engine responses through a comprehensive set of experimental tests.

4.1. Physico-chemical properties

In this section, chemical analysis of the physico-chemical properties of waste cooking oil, waste cooking biodiesel, and their blends with metallic nanoparticles is

presented. The methods employed for this analysis have been detailed in the preceding section, and the testing procedures adhere to the established ASTM standards.

4.1.1. Density

Density serves as crucial characteristic providing valuable insights into the suitability of fuels for use in diesel engines. It's essential to recognize that density is closely linked to key parameters like heating value and cetane number, all of which directly influence the engine's power output [189]. The diesel fuel standards of EN 590 and ASTM D1298 specify density ranges of 820-845 kg/m³ and 820-860 kg/m³, respectively. The Anton par density meter, a recognized tool for liquid density measurement, is employed to determine the density of test fuels. Table 4.1 presents the density values of various test fuels, including Diesel, waste cooking oil (WCO), waste cooking biodiesel, and their blends with metallic nanoparticles. The findings indicate that used palm oil and used sunflower oil have the highest density, while diesel oil exhibits the lowest density among the tested fuels. Additionally, it's important to note that the process of transesterification, used in producing biodiesel from waste cooking oil, results in a reduction in the density of the waste cooking oil

4.1.2. Kinematic viscosity

Kinematic viscosity plays a crucial role in spray atomization and the fuel injection system, directly impacting combustion, engine performance, and emissions. This property is, however, susceptible to temperature variations.

Poor atomization of spray jets can lead to increased carbon deposits and soot formation in diesel engines. According to EN 590 and ASTM D445 standards for diesel fuel in compression ignition engines, the recommended kinematic viscosity range is 2 – 4.5cSt.

Table 4.1 Density of various types of develop fuels

Oil	D100	Unused palm oil	Used palm oil	Unused Sunflower oil	Used sunflower oil	Used Palm biofuel	Used Sunflower biofuel	B20	B20+25PPM (Al_2O_3)	B20+50PPM (Al_2O_3)	B20+75PPM (Al_2O_3)	B20+100PPM (Al_2O_3)	B20+50 PPM (CeO_2)	B20+100PPM (CeO_2)
Density (kg/m^3)	0.8107	0.8965	0.9003	0.9061	0.950	0.8599	0.8677	0.8159	0.8203	0.8303	0.8403	0.8777	0.8274	0.8304

Table 4.2 illustrates the kinematic viscosity of various test fuel samples. Sunflower oil and palm oil, before being used in cooking, have kinematic viscosities of 31.217 mm^2/s and 36.562 mm^2/s, respectively. After cooking, the kinematic viscosities of used palm oil and sunflower oil increase to 41.043 mm^2/s and 32.508 mm^2/s, respectively. The higher kinematic viscosity of used cooking oil makes it incompatible with diesel engines, prompting the adoption of the transesterification process to reduce oil viscosity. Following transesterification, the kinematic viscosity of used palm oil, sunflower oil and B20 becomes 4.4579 mm^2/s, 4.3019 mm^2/s and 2.4696 mm^2/s, respectively. Subsequently, nanoparticles are introduced as fuel additives in biofuel to enhance engine performance. The kinematic viscosity after nanoparticle addition for various blends (B20+25Al_2O_3, B20+50Al_2O_3, B20+75Al2O3, and B20+100Al_2O_3) are recorded as 2.6574, 2.6876, 2.7146, and 2.8765 mm2/s, respectively. The data indicates that blending with diesel can reduce kinematic viscosity due to the oxygen content. A study by Manchanda et al. further supports this, demonstrating that the presence of oxygen in fuel leads to increased viscosity [190].

4.1.3. Saponification, acid value and flash point

The saponification value is a measure of the average molecular weight of the esters in the biofuel. ASTM D5558 is used to determine the saponification value of biodiesel and other ester-based biofuels. Typical saponification values for biodiesel range from 185 to 205 mg KOH/g (milligrams of potassium hydroxide per gram of biodiesel). ASTM D664 is a common standard for determining the acid value of biodiesel and other biofuels. The acid

value measures the acidity of the biofuel, which can indicate the presence of free fatty acids and other acidic impurities. Typical acid values for biodiesel should be less than 0.5 mg KOH/g. ASTM D93 is commonly used to determine the flash point of biofuels, including biodiesel. The flash point is the lowest temperature at which the vapor above the biofuel can ignite in the presence of an open flame or spark. The flash point of biodiesel is typically above 130°C (266°F), which is higher than many petroleum-based diesel fuels

Table 4.2 Viscosity of various types of fuels

Oil	D100	Unused palm oil	Used palm oil	Unused Sunflower oil	Used sunflower oil	Used Palm biofuel	Used Sunflower biofuel	B20	B20+25PPM (Al_2O_3)	B20+50PPM (Al_2O_3)	B20+75PPM (Al_2O_3)	B20+100PPM (Al_2O_3)	B20+50 PPM (CeO_2)	B20+100PPM (CeO_2)
Dynamic viscosity (kg/m^3) at 40°C	1.8845	32.777	36.952	28.252	29.441	3.8322	3.7329	2.0149	2.1800	2.2004	2.2317	2.3665		
Kinematic viscosity (mm^2/s)	2.3244	36.562	41.043	31.217	32.508	4.4579	4.3019	2.4696	2.6574	2.6876	2.7146	2.8765	2.5877	2.6913

. The flash point of fuel is measured through Anton par density meter. The saponification value, acid value and flash point of test fuels such as diesel, WCO, WCO biodiesel and its blend with metallic nanoparticle are shown in table no 4.3. This is observed that used palm oil and used sunflower oil showed the highest saponification value, acid value and flash point. Further, it was seen that transesterification of waste cooking oils decreased the saponification value, acid value and flash point.

Table 4.3 Acid value, saponification value and flash point of fuel

Oil	Unused palm oil	Used palm oil	Unused Sunflower oil	Used sunflower oil	Used Palm biofuel	Used Sunflower biofuel
Acid no. (mg KOH/g oil)	3.79	28.12	0.1903	2.12	0.344	0.396
Saponification value (mgKOH/g)	199.3	246	190.5	218	180.4	168
Flash point	195	260	307	312	>100	>100

4.1.4. Calorific value

The bomb calorimeter stands as a well-established and precise method for determining the calorific value of diverse fuels, encompassing biofuels, fossil fuels, and other combustible materials. In this research, the calorific value is assessed using a bomb calorimeter, offering crucial insights into the energy content and combustion characteristics of various fuel sources. The ASTM standard employed for measuring the calorific value, also known as heating value or energy content, is ASTM D4809. This standard is applicable to a range of fuels, including biofuels, and ensures standardized measurement practices. The calorific value of biofuels can vary based on their composition and source. As per ASTM D4809, the calorific value of B20 is determined to be 40365 kJ/kg. Notably, the addition of metallic nanoparticle Al_2O_3 into biodiesel results in an enhancement of its calorific value. For B20 blended with different proportions of Al_2O_3 (B20+25Al_2O_3, B20+50Al_2O_3, B20+75Al_2O_3, and B20+100Al_2O_3), the calorific values are measured at approximately 40603 kJ/kg, 40752 kJ/kg, 40958 kJ/kg, and 41202 kJ/kg, respectively which is given in table no 4.4. It is essential to recognize that these values are approximations and may vary due to factors such as the specific feedstock used in biofuel production and the methods employed in its processing.

Table 4.4 Calorific value of various types of fuels

Oil	D100	Unused palm oil	Used palm oil	Unused Sunflower oil	Used sunflower oil	Used Palm biofuel	Used Sunflower biofuel	B20	B20+25PPM (Al_2O_3)	B20+50PPM (Al_2O_3)	B20+75PPM (Al_2O_3)	B20+100PPM (Al_2O_3)	B20+50 PPM (CeO_2)	B20+100PPM (CeO_2)
High calorific value(kJ/kg)	42875	38642	39847	38.8	39.76	40509	40.02	40365	40503	40752	40958	41202	40585	40773

4.2 Impact of waste cooking biodiesel on engine performance and emissions characteristics

4.2.1 Engine Performance characteristics

This study investigates the influence of waste cooking biodiesel on the performance and emissions of a single-cylinder diesel engine. Waste cooking biodiesel B20 (comprising 10% WCPM, 10% WCSM, and 80% diesel) was utilized alongside diesel fuel in a single-cylinder CRDI engine to assess both engine performance and emissions. The engine parameters, including compression ratio, injection pressure (60 Mpa), and injection angle (30 degrees), were kept constant during the experiments. The overall uncertainty of the experiment was 1.211%. Tests were conducted at various engine loads (3, 6, 9, 12 kg) and a constant speed of 1500 rpm.

4.2.1.1 Specific fuel consumption

Specific fuel consumption (SFC), defined as the fuel consumed per unit time to produce mechanical power on the engine shaft, was a focal point of the analysis.

The Specific Fuel Consumption (SFC) is a measure of the fuel consumption rate of an engine, typically expressed in units like grams per kilowatt-hour (g/kWh) or kilograms per hour per kilowatt (kg/h/kW). It indicates how much fuel the engine consumes to produce a certain amount of power.

SFC can calculate by using one of the following formulas:

For SFC in units of g/kWh:

SFC= Fuel Flow Rate (g/s) × 3600/ Power Output (kW)

For SFC in units of kg/h/kW:

SFC= Fuel Flow Rate (kg/h)/Power Output (kW)

SFC is influenced by fuel properties such as viscosity, density, calorific value, and cetane number. Higher viscosity, lower calorific value, and increased density can impact combustion behavior, affecting atomization, air-fuel mixing, dispersion, swirl ratio, and penetration, thus influencing engine performance. The findings revealed that B20 exhibited higher brake-specific fuel consumption (BSFC) compared to diesel across various load conditions. This difference may be attributed to the lower calorific value and higher viscosity of B20. The study observed a gradual decrease in SFC as the load increased, as depicted in Figure 4.1. This trend could be explained by the elevated heat transfer and friction loss to the combustion chamber at low engine loads [191]. Conversely, at higher loads, engine power increased, leading to improved thermal efficiency and combustion quality, resulting in lower SFC.
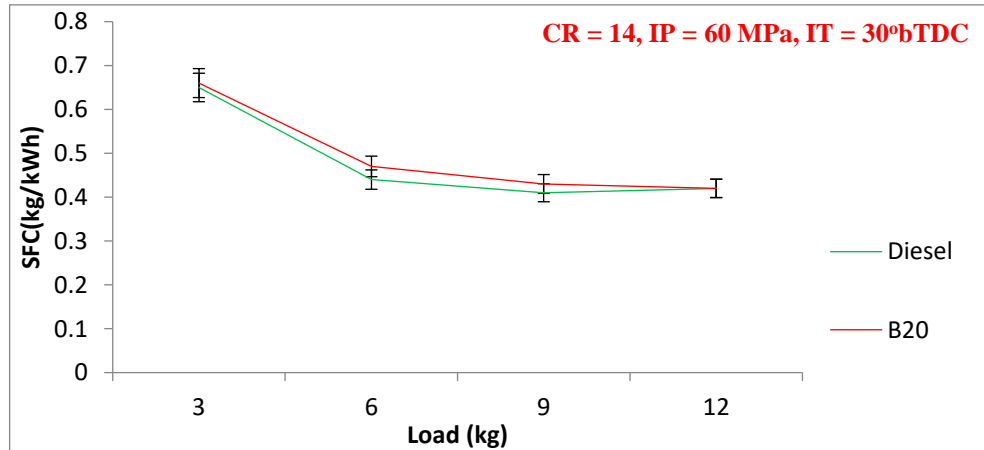
Fig. 4.1 Variation of SFC with respect to load

4.2.1.2 Brake thermal efficiency

Brake thermal efficiency (BTE) was employed to assess the engine's capability to convert the chemical energy of fuel into useful work. Figure 4.2 illustrates a gradual increase in BTE with the rising load, indicating improved efficiency. This is attributed to the reduction in heat loss and the addition of power as the load increases. In comparison to diesel, B20 exhibited lower BTE, a consequence of its lower calorific value and higher viscosity. The elevated viscosity of B20 contributes to inadequate fuel atomization and suboptimal air-fuel mixing, leading to imperfect combustion. This reduced efficiency may result from an ineffective conversion of fuel energy into useful work. This discrepancy in BTE between B20 and diesel can be reasonably explained by these factors [192].

4.2.2 Engine emissions
4.2.2.1 Carbon mono oxide

When the combustion cycle lacks sufficient oxygen and the fuel-air mixture contains an excess of fuel for engine combustion, carbon monoxide (CO) is produced. Insufficient oxygen for converting carbon to carbon dioxide (CO_2) results in unburned fuel and the formation of CO.
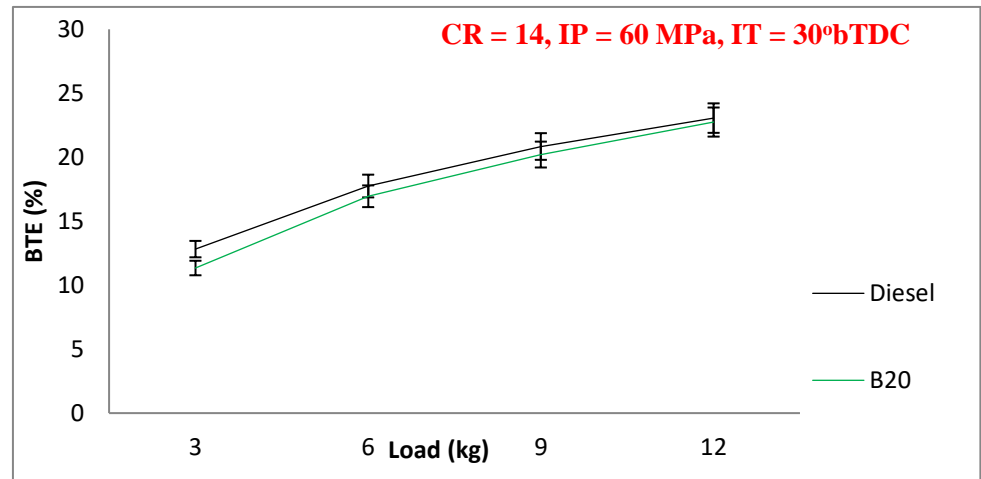
Fig. 4.2 Variation of BTE with respect to load

The primary factors contributing to carbon monoxide production include poor mixture, locally rich conditions, incomplete combustion, and insufficient oxygen. Harmful emissions, including CO, CO_2, hydrocarbons (HC), nitrogen oxides (NOx), smoke opacity, and particulate matter (PM), are emitted by internal combustion engines [193]. The introduction of biodiesel blends into diesel has been observed to decrease harmful emissions such as CO, HC, and PM [194,195]. CO emissions exhibited a reduction with increasing engine load for all fuel samples, as depicted in Figure 4.3. Notably, B20 demonstrated a significant decrease in CO emissions compared to diesel across all engine loads. The molecular structure of biofuels, containing oxygen molecules (WCO with a 13.6% weight O_2 content), contributes to complete combustion at higher temperatures.

4.2.2.2 Hydrocarbon emissions

Increased hydrocarbon (HC) emissions arise from the incomplete combustion of fuel particles. Biodiesel, in contrast to regular diesel fuel, exhibits higher oxygen content and lower carbon and hydrogen content, leading to reduced HC emissions, as illustrated in Figure 4.4. HC emissions showed an upward trend with the increase in engine load. At higher loads, a greater mass of fuel is injected into the combustion chamber, resulting in a rich air-fuel mixture. In a rich mixture, more fuel comes into contact with heated air, reducing the evaporation rate of fuel droplets. This phenomenon implies insufficient oxygen for combustion, contributing to the observed increase in HC emissions [196].
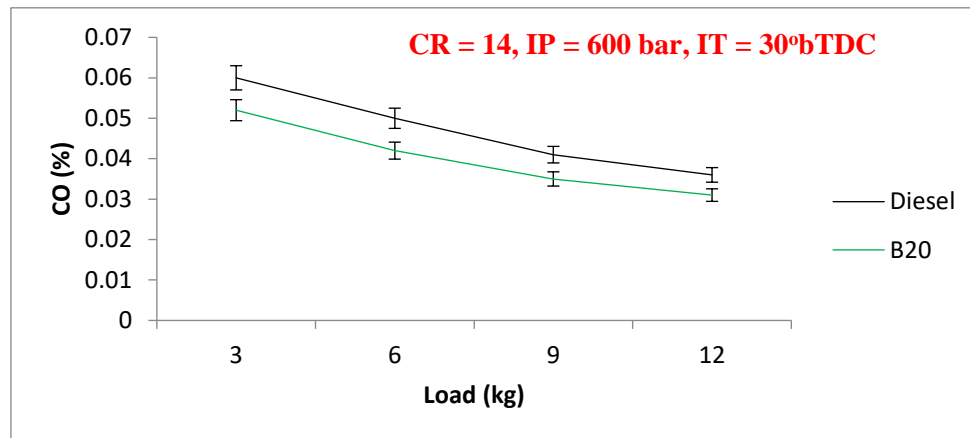
Fig. 4.3 Variation of CO with respect to load

4.2.2.3 Nitrogen oxide emissions

Temperature and high activation energy play crucial roles in the generation of nitrogen oxides (NOx) during fuel combustion. The elevated temperature leads to high activation energy, converting atmospheric nitrogen into nitrogen oxides. Generally, the increased oxygen content in biodiesel results in elevated temperatures during combustion, contributing to significant NOx production.
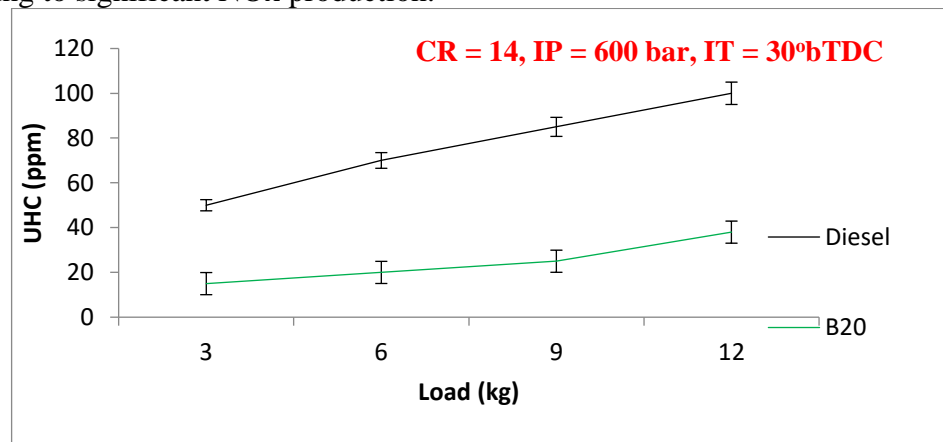
Fig. 4.4 Variation of UHC with respect to load

Figure 4.5 illustrates a gradual increase in NOx emissions with rising engine load for all tested fuels. At higher loads, a greater quantity of fuel is injected into the cylinder, leading to higher combustion flame temperatures, where NOx is produced. Notably, B20 exhibits higher NOx emissions than D100 under full load conditions, attributed to its increased oxygen content, supporting complete combustion at higher temperatures.

4.3. Impact of metallic naoparticles as fuel additives on engine performance and emissions

4.3.1 Engine performance

Different ratios of metallic nanoparticles (Al_2O_3) were introduced to waste cooking biodiesel (B20) to enhance both engine performance and emissions. Novel nanobiodiesel blends, namely B20+25Al_2O_3, B20+50Al_2O_3, and B20+100Al_2O_3, were formulated and utilized in a single-cylinder CRDI engine to assess their impact on engine performance and emissions. The engine parameters, including compression ratio, injection pressure (60 Mpa), and injection

angle (30 degrees), were kept constant. Experimental trials were conducted at various engine loads (3, 6, 9, 12 kg) with a constant engine speed of 1500 rpm.
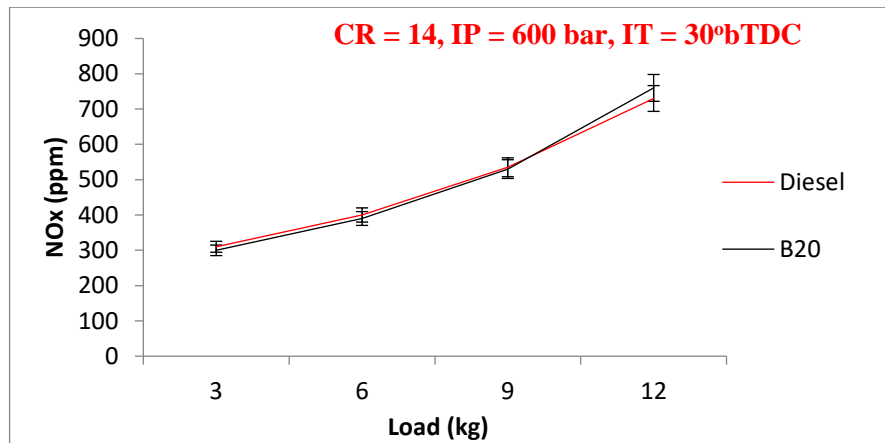
Fig. 4.5 Variation of NO$_X$ with respect to load

4.3.1.1 SFC

In an attempt to improve the physical and chemical characteristics of fuel and consequently decrease brake-specific fuel consumption (BSFC), different concentrations of Al_2O_3 nanoparticles were integrated into B20. The specific fuel consumption (SFC) for $B20+25Al_2O_3$, $B20+50Al_2O_3$, and $B20+100Al_2O_3$ was observed to be lower than that of both diesel and B20. With an increase in nanoparticle concentration in the biofuel, there was a noticeable elevation in calorific value and a reduction in ignition delay, leading to decreased SFC. The introduction of nanoparticles exposes a more reactive surface area to the air-fuel mixture, promoting faster heat transfer and accelerating the evaporation rate of the mixture. This results in the mixture reaching auto-ignition temperature sooner, thereby reducing the ignition delay period. Shorter ignition delays contribute to increased engine output for the same fuel consumption, as the combustion gases are utilized more effectively during the engine's exhaust stroke. Among the blends, B20+100Al2O3 exhibited the highest calorific value and the shortest ignition delay, leading to the lowest SFC at all engine loads. The addition of 100Al2O3 to B20 resulted in a significant 20.93% reduction in SFC at maximum load compared to B20, as illustrated in Figure 4.6.
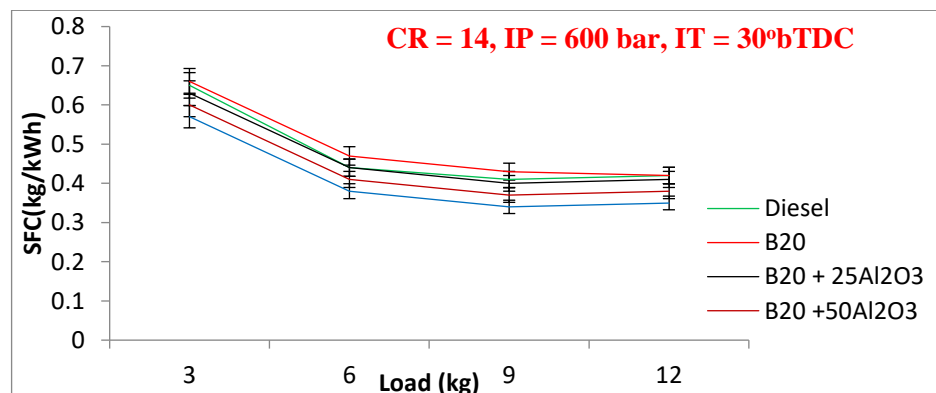
Fig. 4.6 Variation of SFC with respect to load for nanobiodiesel

4.3.1.2 BTE

The improvement in Brake Thermal Efficiency (BTE) became evident with the escalating concentration of nanoparticles in biofuel, as illustrated in Figure 4.7. The augmentation of nanoparticle concentration further enhances fuel properties, a pivotal factor in evaluating air-fuel mixing ratio, air-fuel dispersion, fuel penetration, and the ignition process. The modification of fuel properties through the addition of nanoparticles emerges as the optimal approach for enhancing engine performance without necessitating alterations to the engine design. The thermodynamics of the combustion process, engine performance, and emission characteristics were evaluated, focusing on various features such as kinematic viscosity, heating value, flash point, density, and cetane number [197].

The dispersion of Al_2O_3 metallic nanoparticles in diesel methanol mix contributes to improved engine performance due to increased conductivity, a higher surface-to-volume ratio, oxygen augmentation, and catalytic activity. Experimental assessments demonstrated a notable 3.6% increase in Brake Thermal Efficiency (BTE) for fuel containing 100 ppm Al_2O_3 nanoparticles [197]. Additionally, nano molecules, characterized by a high surface-to-volume ratio, actively participate in air-fuel blending [198], thereby accelerating the evaporation rate of the mixture, enhancing fuel droplet propagation, and promoting the dispersion of the air-fuel mixture. The incorporation of nanoparticles aims to achieve more efficient combustion and enhanced conversion of fuel energy. The heightened surface-to-volume ratio of nanoparticles leads to increased heat transfer, a primary factor contributing to the rise in power and additional energy produced within the cylinder. Nano additions also reduce ignition time and fuel combustion, resulting in elevated cylinder peak pressure and rapid heat release [199, 63,200]. The incorporation of CERIA nanoparticles into waste cooking oil (B20+CERIA45) resulted in a notable enhancement in Brake Thermal Efficiency (BTE), with a significant increase of 10.5% compared to the base diesel fuel under full engine load conditions. This improvement is attributed to the catalytic behaviour of nanoparticles, influencing the thermodynamics of the ignition process and ultimately impacting engine performance and emissions [201, 202]. Al_2O_3 nanoparticles exhibit high thermal conductivity and an elevated surface-to-volume ratio, leading to improvements in air-fuel mixing, dispersion, fuel penetration, evaporation rate, combustion temperature, and pressure. The alteration of combustion characteristics, including reduced ignition delay, contributes to heightened engine performance. The B20+$Al_2O_3$100 blend demonstrates the highest BTE across all load conditions compared to D100 and B20. Notably, there were recorded gains of 3.56%, 7.51%, and 13.53% in BTE for fuel additives containing Al_2O_3 nanoparticles, such as B20+25Al_2O_3, B20+50Al_2O_3, and B20+100Al_2O_3, when compared to B20 under full load conditions and 1500 rpm. The addition of Al_2O_3 improves the calorific value of the new fuel blends. The combined effects of high thermal conductivity and surface-to-volume ratio contribute to the overall enhancement of air-fuel mixing, dispersion, fuel penetration, evaporation rate, and combustion temperature and pressure. This leads to improved combustion characteristics, reduced ignition delay, and increased engine performance. Incorporating Al2O3 nanoparticles into fuel formulations or as additives in engine lubricants has been proposed to improve combustion efficiency and reduce frictional losses, thereby enhancing fuel economy. However, the incorporation of Al2O3 nanoparticles into biodiesel formulations offers a promising solution to this challenge.
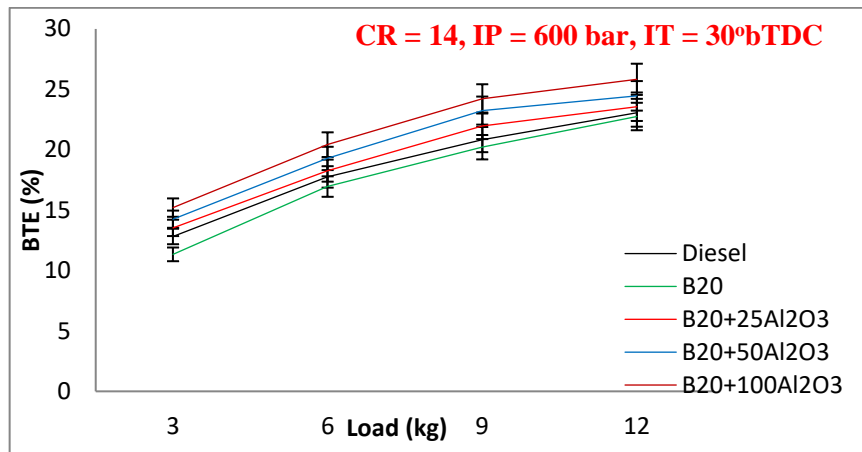
Fig. 4.7 Variation of BTE with respect to load for nanobiodiesel

By dispersing finely dispersed aluminium oxide nanoparticles within the biodiesel matrix, the overall calorific value of the fuel can be significantly enhanced. This increase in calorific value results from the higher energy content provided by the nanoparticles, thereby boosting the overall energy output during combustion.ne of the remarkable characteristics of Al2O3 nanoparticles is their ability to act as oxygen carriers due to the presence of oxygen vacancies on their surface. When introduced into biodiesel, these nanoparticles effectively increase the oxygen content of the fuel. The additional oxygen molecules supplied by the nanoparticles play a crucial role in supporting the combustion process within the engine. During combustion, the presence of oxygen facilitates more complete fuel oxidation, leading to improved combustion efficiency and reduced emissions of unburned hydrocarbons and particulate matter [63,199].

4.3.2 Emission characteristics

4.3.2.1 Carbon monoxide emission

The researcher conducted an analysis on the influence of Al_2O_3 nanoparticles as a diesel fuel additive, focusing on various aspects such as fuel atomization, air-fuel mixing, flame propagation, fuel spray, swirl ratio, fuel dispersion, fuel penetration, and ignition flame characteristics. Experimental evaluations demonstrated that the incorporation of Alumina nanoparticles may increase fuel penetration length, enhance flame propagation, and influence the thermodynamics of combustion, ultimately promoting complete combustion and reducing harmful emissions like CO [202]. B20+100Al$_2$O$_3$ exhibited the lowest CO emissions across all engine loads. The utilization of Al_2O_3 nanoparticles in combination with a diesel-biodiesel blend led to a reduction in CO emissions. The introduction of nanoparticles in biofuel improved fuel combustion characteristics, resulting in decreased harmful CO emissions due to the effective oxidation of fuel by nanoparticles. These findings align with the conclusions of the referenced study [202]. The expansive surface area of Al_2O_3 enhances chemical reactivity, thereby reducing ignition delay and improving combustion. As a result, there is a reduction in carbon monoxide (CO) emissions. Furthermore, nanoparticles exhibit the capability to convert CO to CO_2 through their potent redox-active properties, contributing to the decline in CO emissions from the tested fuels [26, 203]. The reductions in CO emissions are recorded as 3.22%, 4.83%, and 8.06% for B20+25Al$_2$O$_3$, B20+50Al$_2$O$_3$, and B20+100Al$_2$O$_3$ fuels, respectively, at full load compared to B20, as depicted in Figure 4.8. Notably, the maximum

reduction in CO emissions, approximately 20.8%, was observed for B20+Al$_2$O$_3$100 compared to diesel under full load conditions, supporting the findings in the existing literature.
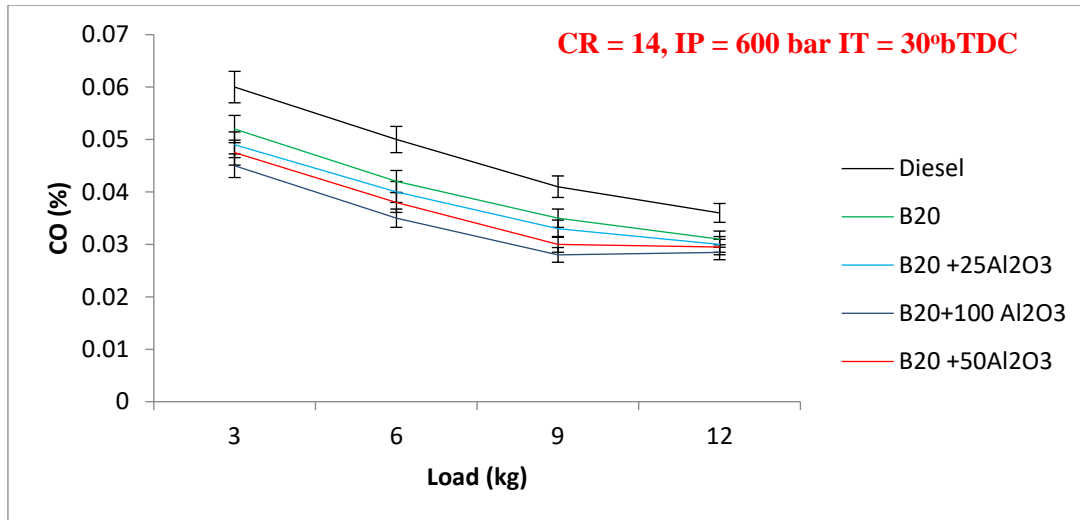
Fig. 4.8 Variation of SFC with respect to load for nanobiodiesel

4.3.2.2 Hydrocarbon emissions

The incorporation of nanoparticle additives into gasoline blends has proven to be effective in significantly reducing hydrocarbon (HC) emissions. Nanoparticles function as catalysts, augmenting the oxidation of hydrocarbons and facilitating complete combustion. The secondary atomization induced by Nano additives expedites HC oxidation, leading to a noticeable reduction in HC emissions. The diminished size of nanoparticles contributes to improved fuel atomization in fuel injectors. Additionally, the presence of nanoparticles promotes higher fuel-air blending rates, optimizing combustion and ultimately reducing HC emissions [204]. The dispersion of nanoparticles in the fuel enhances fuel atomization and spray characteristics, facilitating proper air-fuel blending, accelerating the rate of air-fuel heat transfer, and improving combustion. This, in turn, results in decreased HC emissions [205]. CeO2 nanoparticles, in particular, serve as oxidation agents, expediting the oxidation process within the charge and consequently reducing harmful emissions such as CO and HC, as well as smoke opacity [206].

As for Al$_2$O$_3$ metallic nanoparticles, their higher surface-to-volume ratio contributes to effective atomization, air-fuel mixing, and dispersion within the combustion process. They act as oxygen donors, promoting complete combustion within the combustion chamber. Complete combustion is crucial for minimizing HC emissions. Interestingly, at a higher load, diesel emits 62% more HC compared to B20. However, B20+Al$_2$O$_3$100 produce approximately 28.94% more emissions than B20 under full load conditions. The predicted average HC emissions for all conditions are 11.8%, 22.36%, and 28.94% higher for B20+25Al$_2$O$_3$, B20+50Al$_2$O$_3$, and B20+100Al$_2$O$_3$, respectively, compared to B20 at full load, as illustrated in figure 4.9.
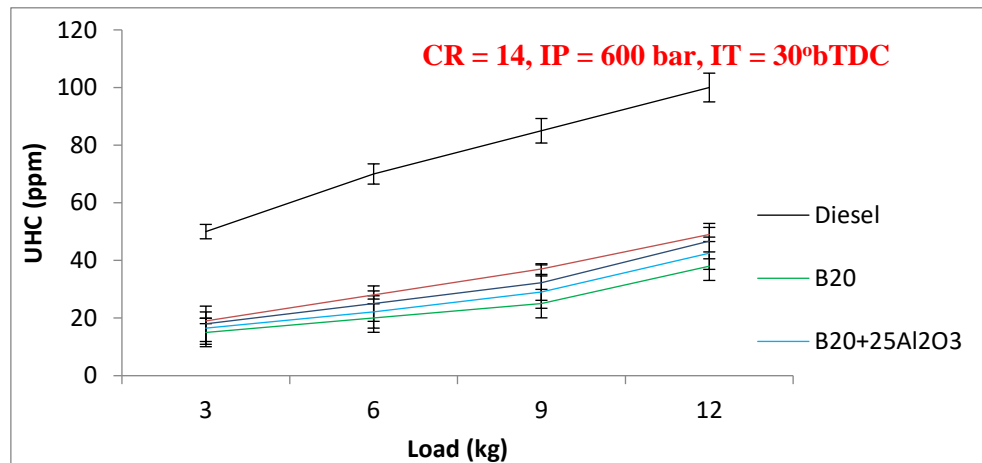
Fig. 4.9 Variation of UHC with respect to load for nano-biodiesel

4.3.2.3 Nitrogen oxide emissions

Figure 4.10 illustrates the highest observed increase in NOx emissions, reaching up to 13.63% for B20+100Al$_2$O$_3$ compared to B20 at full engine load. The generation of NOx emissions is significantly influenced by the combustion flame temperature, which is heightened due to the increased ignition reaction rate. Interestingly, higher temperatures were associated with reduced HC and CO emissions [207].

The rise in NOx emissions is attributed to the inclusion of Al$_2$O$_3$ and CuO nanoparticles as fuel additives. Nanoparticles serve as oxygenated additives, contributing to improved ignition and elevated temperatures. However, as the dosage of nanoparticles increases, NOx emissions decrease due to the positive impact of oxygenated additives on combustion enhancement. The addition of nano-metal oxide particles acts as an oxygen catalyst, promoting complete combustion. This results in high peak pressure and maximum heat release rate during combustion. The shorter ignitions delays of nanoparticles lead to a lower premixed burn percentage, decreased cylinder combustion temperature, and ultimately lower NOx emissions [208, 30]. Regarding the optimal concentration of Al$_2$O$_3$ additive in biofuel, the addition of 100 ppm of Al$_2$O$_3$ in waste cooking biodiesel demonstrates maximum engine performance, improved combustion characteristics, and reduced emissions
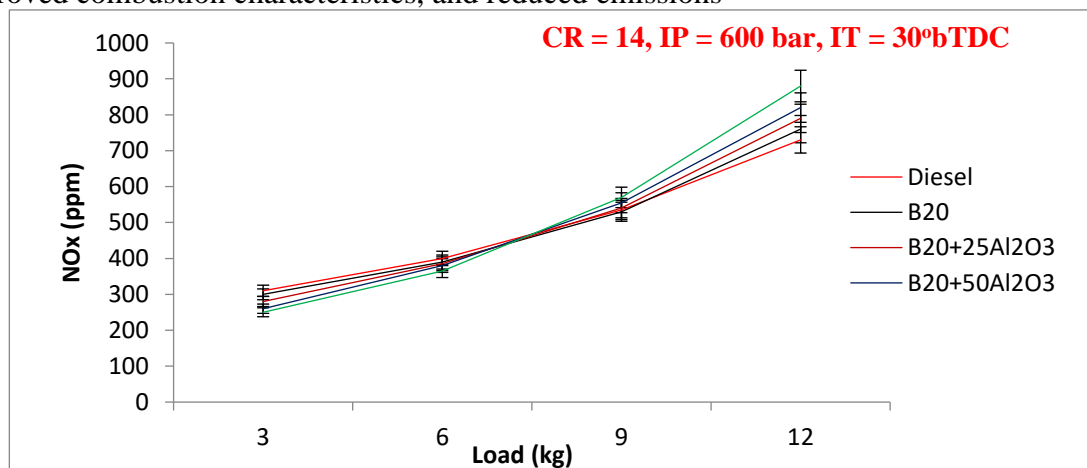
Fig. 4.10 Variation of NOx with respect to load for nanobiodiesel

4.4. Comparative study of Impact of adding two nanoparticles (Al₂O₃ and CeO₂) to waste cooking biodiesel on engine performance, combustion and emissions characteristics

The purpose of this experimental study is to compare the emission, combustion, and performance parameters of a CRDI diesel engine fuelled by B20 blend with two distinct metal-based nanoparticles cerium oxide (CeO_2) and aluminium oxide (Al_2O_3). The mass fraction of 50 ppm, 100 ppm Al_2O_3, and CeO_2 were separately blended into B20 (waste cooking methyl ester) biofuel. The engine compression ratio, injection pressure, and injection angle were 14, 60Mpa, and 30º respectively. Experiments were conducted at various engine loads (3, 6,9,12 kg) and a constant engine speed of 1500rpm.

4.4.1 Engine performance

4.4.1.1 SFC

In Fig. 4.11, it is evident that the Specific Fuel Consumption (SFC) of the engine decreases with increasing load for all developed fuel blends. This can be attributed to lower heat transfer and friction loss at elevated loads [209], leading to enhanced engine power. The SFC values for different fuel blends (Diesel, B20, B20+50 Al_2O_3, B20+100 Al_2O_3, B20+50 CeO_2, and B20+100 CeO_2) at peak load are 0.346, 0.371, 0.32, 0.334, 0.344, and 0.353 kg/kW-hr, respectively, as depicted in Fig. 4.11. Notably, the SFC of diesel engines using nano fuel is lower than that of pure diesel and B20. Furthermore, the SFC for B20+50 Al_2O_3 exhibits a maximum decrease of 13.74% compared to B20 at peak load. The addition of nanoparticles into biofuel promotes effective air-fuel dispersion and enhances the heat transfer rate, resulting in rapid fuel evaporation and thorough combustion [210]. This accelerated evaporation leads to early combustion within the same combustion period, thereby reducing both physical and chemical delay times. The shortened ignition times contribute to increased thrust exerted by combustion gases on pistons, consequently boosting engine torque. Additionally, the dispersion of nanoparticles in biofuel contributes to an elevated calorific value, enabling the production of more power for the same fuel quantity. These crucial factors collectively contribute to the observed decrease in specific fuel consumption (SFC) for biofuels with nanoparticle additives [211]. In contrast, the B20 fuel blend, lacking a heat transfer accelerator and having a lower calorific value, experiences increased ignition delay, resulting in an elevated SFC for B20.
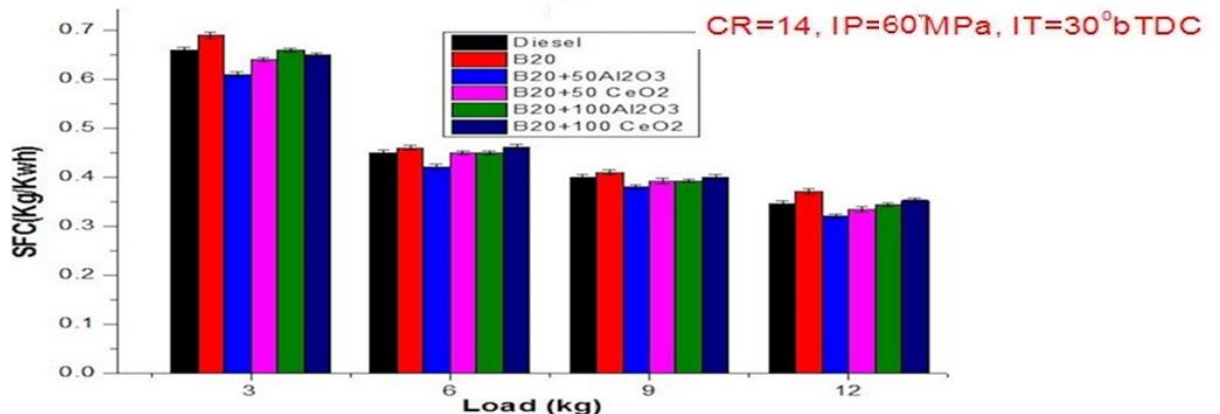

Fig. 4.11 Impact on SFC of diesel engine by adding with Al_2O_3 and CeO_2 as fuel additive to B20 under various load conditions

4.4.1.2 Brake thermal efficiency

BTE represents the engine's ability to convert the chemical energy of fuel into useful work. Figure 4.12 illustrates the BTE for Diesel, B20, B20+50 Al_2O_3, B20+100 Al_2O_3, B20+50 CeO_2, and B20+100 CeO_2. The BTE of the engine consistently increased with the elevation of engine load across all fuel blends. This can be reasonably attributed to the favorable heat mass fuel properties contributing to increase in-cylinder pressure and temperature at higher loads [30]. Moreover, the introduction of nanoparticles in biofuel results in a notable enhancement in BTE. As shown in Figure 4.12, the nano blend B20+50 Al_2O_3 exhibits an 11.39% higher BTE than B20 at peak load. A similar trend was observed by Afzal et al. [212], who conducted experiments with silver nanoparticles in diesel/biodiesel blend fuel in CI engines. Nanoparticles in biodiesel, with their high surface-to-volume ratios, contribute to improved atomization, swirl ratio, and fuel scattering patterns, leading to accelerated heat transfer. This enhanced heat transfer causes the fuel to vaporize earlier, resulting in a shorter ignition delay, higher temperatures, and pressures in the cylinders. Consequently, during a power stroke, the full chemical energy of the fuel is effectively converted into mechanical energy, leading to significant improvements in BTE [213]. Additionally, nanoparticles added to biofuel contribute to a higher calorific value, where fuels with higher calorific values generate more power for the same quantity of fuel. This could explain why B20 exhibits the lowest BTE, while B20+50 Al_2O_3 has the highest BTE.
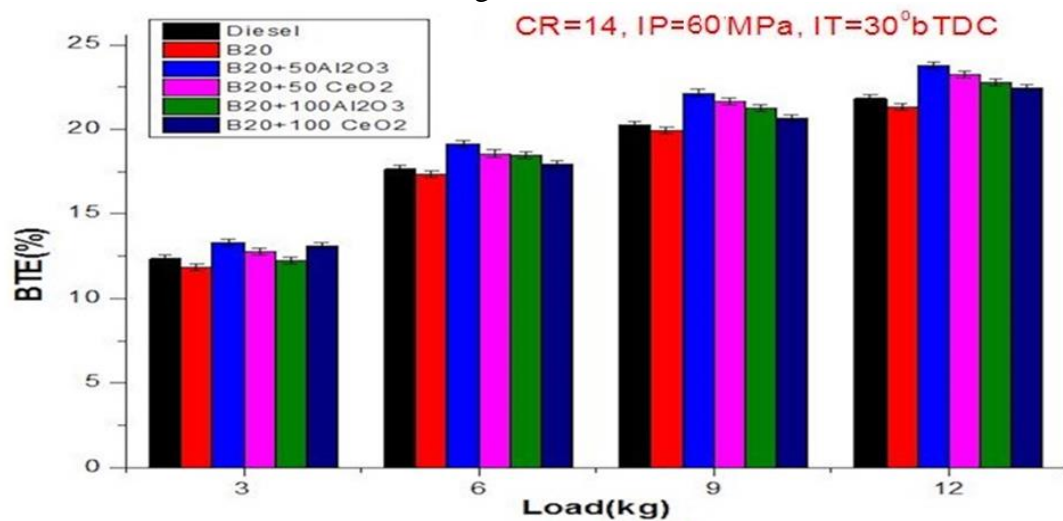
Fig. 4.12 Impact on BTE of diesel engine by adding with Al_2O_3 and CeO_2 as fuel additive to B20 under various load conditions

4.4.2. Combustion characteristics

4.4.2.1 Cylinder pressure

The dissimilarity in the cylinder pressure in opposition to the crank angle was traced and plotted for diesel, B20, B20 +50 Al_2O_3, B20 +100 Al_2O_3, B20 +50 CeO_2, and B20 +100 CeO_2 in Fig 4.13. A significant increment in upsides of cylinder pressure was acquired from the burning of B20 +50 Al_2O_3, B20 +100 Al_2O_3, B20 +50 CeO_2, and B20 +50 CeO_2 than ignition of B20. Fig 4.13 revealed that pressure values for the blends B20+50 Al_2O_3 and B20+50 CeO_2 are 18.41% and 16.55% higher than B20 at 4° crank angle after TDC. The optimum pressure of blend B20 +50 Al_2O_3 is 16.77% higher than B20 at a 4° crank angle after TDC.

Nanoparticles addition with B20 increased the cylinder pressure. This might have been a direct result of the larger surface area to volume proportion, and excellent thermal conductivity of nanoparticles. Also, the benefit of nanoparticles came about in expanding the reactivity with the charge, improved atomization, short ignition lag, accelerating evaporation rate, and rapid propagation of flame which advanced the better ignition process [214]. A shorter ignition delay impacts the burning duration which prompts ascribes of ignition. The addition of nanoparticles in biofuel had effects on their properties like lowering the viscosity, incrementing the CN, and further developing heat release rate, which prompts pre-ignition and lessens the duration of ignition delay lag. Shorter ignition delay is liable for more heat energy stored in the premixed stage; fuel accumulation is more in the premixed stage, coming about in rapid burning and thusly increasing the pressure of the cylinder and heat transfer rate [201].
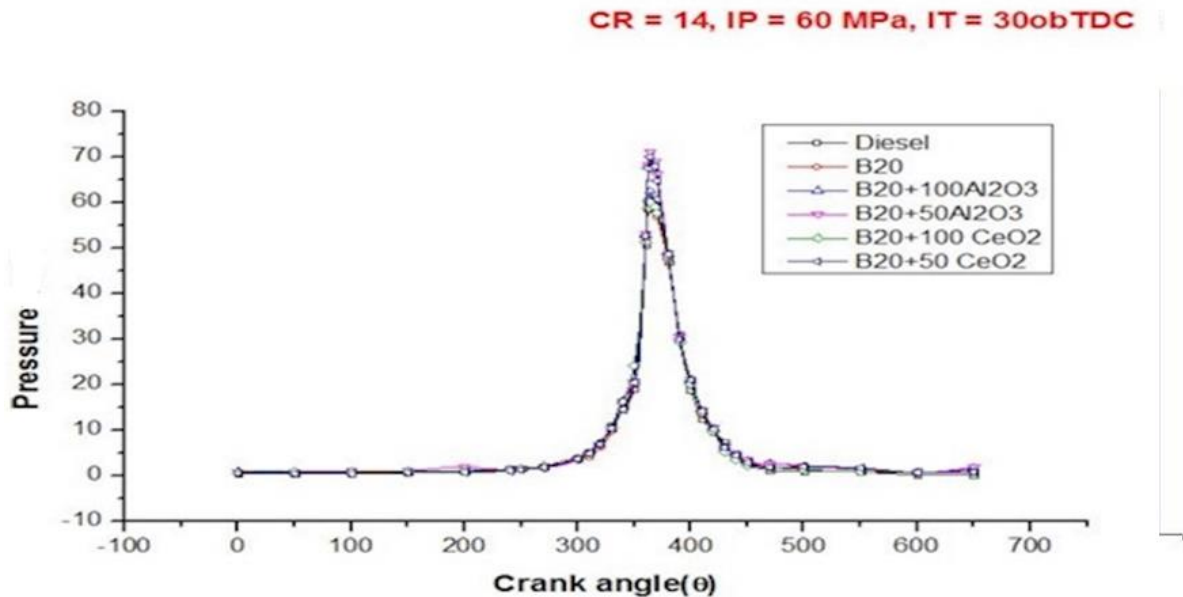
Fig. 4.13 Impact on cylinder pressure of diesel engine by adding with Al_2O_3 and CeO_2 as fuel additive to B20 under various load conditions

Nanoparticles, particularly metal oxides like Al2O3, exhibit catalytic properties that can enhance combustion efficiency and reduce emissions. The catalytic activity of nanoparticles promotes the oxidation of fuel molecules and facilitates the conversion of harmful pollutants into less toxic species. For example, Al2O3 nanoparticles have been shown to catalyze the oxidation of carbon monoxide (CO), hydrocarbons (HC), and particulate matter (PM) in diesel exhaust. Additionally, nanoparticles can influence combustion kinetics by lowering activation energy barriers, thereby accelerating combustion processes and promoting more complete fuel oxidation. Nanoparticles possess high surface-to-volume ratios, allowing them to interact extensively with the surrounding fuel and air molecules during combustion. These surface interactions can affect combustion kinetics, flame stability, and pollutant formation pathways. For instance, Al2O3 nanoparticles dispersed in fuel blends can enhance air-fuel mixing, promote uniform flame propagation, and mitigate flame quenching effects, leading to more efficient combustion and reduced emissions of nitrogen oxides (NOx) and particulate matter [3]. Moreover, nanoparticles can act as sites for adsorption and desorption processes, influencing the concentration of reactive species and intermediate radicals involved in

combustion reactions. Nanoparticles incorporated into engine components or thermal barrier coatings can modify heat transfer characteristics and thermal management within the combustion chamber. By altering surface temperatures and heat fluxes, nanoparticles can influence ignition processes, combustion stability, and pollutant formation mechanisms. For example, Al2O3-based thermal barrier coatings applied to piston crowns or cylinder heads can reduce heat losses to the coolant and cylinder walls, thereby increasing combustion chamber temperatures and promoting more efficient combustion. The size, morphology, and dispersion of nanoparticles play critical roles in determining their impact on combustion and emissions. Nanoparticles with smaller sizes and higher surface areas exhibit greater reactivity and catalytic activity, leading to more pronounced effects on combustion performance. Moreover, the uniform dispersion of nanoparticles within the fuel or combustion chamber is essential for ensuring consistent interactions with reactants and optimal utilization of their catalytic properties [63,199,200,211, 212].

4.4.2.2 Heat release rate

The addition of nanoparticles enhanced the heat transfer rate of the air-fuel mixture. Biodiesel with nanoparticles has shown a slight improvement in heat release rate over B20 as shown in Fig. 4.14. Nanoparticles have a greater surface area; they result in a higher air-fuel evaporation rate, causing an early auto-ignition temperature of the fuel. The early auto-ignition temperature of the air-fuel mixture reduces the ignition delay. A shorter ignition delay is desirable for better heat transfer. Besides it, Nan particle's higher thermal conductivity makes them an excellent heat transfer accelerator. Adding nanoparticles to the fuel blend catalytically affects the combustion process. That's why B20+50 Al_2O_3 has a higher HRR than biodiesel [215]. The evaporation rate of the fuel is enhanced by the superior thermal conductivity of Al_2O_3, which builds the cylinder pressure and ROHR [216]. The variation in the heat release rate in opposition to the crank angle was estimated and depicted in Fig. 4.14. Significant increases in values of heat release rate were acquired from the ignition of B20 +50 Al_2O_3, B20 +100 Al_2O_3, B20 +50 CeO_2, and B20 +50 CeO_2 than the ignition of B20. Figure 13 revealed that B20 indicated a lower heat release rate than diesel. Less HRR is the result of the less heating value of the fuel blend. Inferior heating value fuel delivers less heat energy during combustion [217]. The HRR for B20 +50 Al_2O_3, B20 +100 Al_2O_3, B20 +50 CeO_2 and B20 +100 CeO_2 is marginally higher in compare to diesel fuel at high load.

CeO$_2$ and Al$_2$O$_3$ nanoparticles have higher surface region-to-volume proportion and higher thermal conductivity which brings about upgraded burning, lesser ignition delay times, and more prominent HRR [218]. Adding CeO_2 and Al_2O_3 nanoparticles enhanced the heat transfer of the air-fuel mixture, resulting in faster fuel evaporation and dispersion. Additionally, the dispersion of CeO_2 and Al_2O_3 nanoparticles enhanced the thermal conductivity of fuel. The result is the less physical and chemical delay for nanoparticle dispersion. That's why, combustion is initiated earlier, and substantial amounts of energy accumulate in the premixed combustion mixture, increasing the heat release rate described in the figure 5.14.

Fig. 4.14 Impact on heat release rate of diesel engine by adding with Al_2O_3 and CeO_2 as fuel additive to B20 under various load conditions

The energy balance equations which are provided below can be used to determine the heat release rate.

$$\frac{dQ}{d\theta} = \left(1 + \frac{C_V}{R}\right) P \frac{dV}{d\theta} + \left(\frac{C_V}{R}\right) V \frac{dP}{d\theta} \qquad (5.1)$$

$$\frac{dQ}{dt} = \left(1 + \frac{C_V}{R}\right) P \frac{dV}{dt} + \left(\frac{C_V}{R}\right) V \frac{dP}{dt} \qquad (5.2)$$

$$\frac{dQ}{d\theta} = \frac{\gamma}{\gamma - 1} P \frac{dV}{d\theta} + \frac{1}{\gamma - 1} V \frac{dP}{d\theta} \qquad (5.3)$$

dQ/dt = Net heat transfer rate with respect to time, dQ/dθ = Net heat transfer rate with respect to crank angle, R=Gas constant, P= gas pressure=volume, C_V specific heat at constant volume.

4.4.3 Emission characteristics

4.4.3.1 Carbon monoxide emission

Carbon mono oxide emission is exhausted from diesel engines due to incomplete combustion of the air-fuel mixture. Incomplete combustion occurred due to insufficient oxygen for converting CO into CO_2. The addition of nanoparticles in biodiesel acts as an oxygen donor to complete combustion. Due to the instability of Al_2O_3 at higher temperatures, Al_2O_3 decomposed in Al_2O and O and offer oxygen to good combustion as shown in equation no 5.4 [64].

$$Al_2O_3 \rightarrow Al_2O + 2O \qquad (5.4)$$
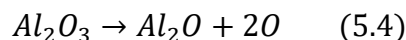
In the context of CeO_2, the Addition of CeO_2 nanoparticles in biodiesel reduced the CO emissions because CeO_2 has the ability to oxidize the CO into CO_2 as shown in equation no.5.5 [219].

$$2CeO_2 + CO \rightarrow Ce_2O_3 + CO_2 \qquad (5.5)$$
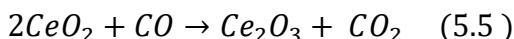
Nanoparticle does not act only as oxygen donor but even accelerates the evaporation rate resulting in shortening the duration of the ignition lag. Less ignition delay ensured better ignition characteristics which in turn less CO. Subsequently, metal-oxide Nanoparticles work on the level of air-fuel blending, good injection spray, and enhance fuel properties, these variables support uniform burning which endues to complete ignition [30]. Besides it, the

harmful emissions are based on several factors like air-fuel ratio, cylinder temperature, injection pressure, fuel quality, engine load, and design of piston. Fig. 4.15 depicts the CO emissions decreased with the increase of engine load. Figure 4.15 revealed that B20+50 Al_2O_3 has 15.06% lower CO emissions than B20 at peak load. At full load, the CO of Diesel, B20 +50 Al_2O_3, B20 +100 Al_2O_3, B20 +50 CeO_2 and B20 +100 CeO_2 are 0.036, 0.0312, 0.028, 0.0265, 0.03 and 0.029 respectively [220].

Additionally, Fig.5.15 revealed that CO emissions produced less biodiesel than pure diesel. Because biofuel sub-atomic construction contains O_2 particles and higher cetane number which endues developed combustion at a higher temperature [221].

4.4.3.2 Hydrocarbon emissions

The HC emissions are caused by partially burned fuel fragments that are not completely combusted or evaporated. HC emissions concerning load are indicated in fig 4.16. The graph depicted the significant impact of engine load on emissions. Fuel is injected into the combustion chamber at a high rate at a high load, resulting in a rich fuel-air mixture. Rich air-fuel mixtures have more fuel contact with heated air, resulting in reduced evaporation rates of fuel droplets, and combinations of the blend exude more HC [222].
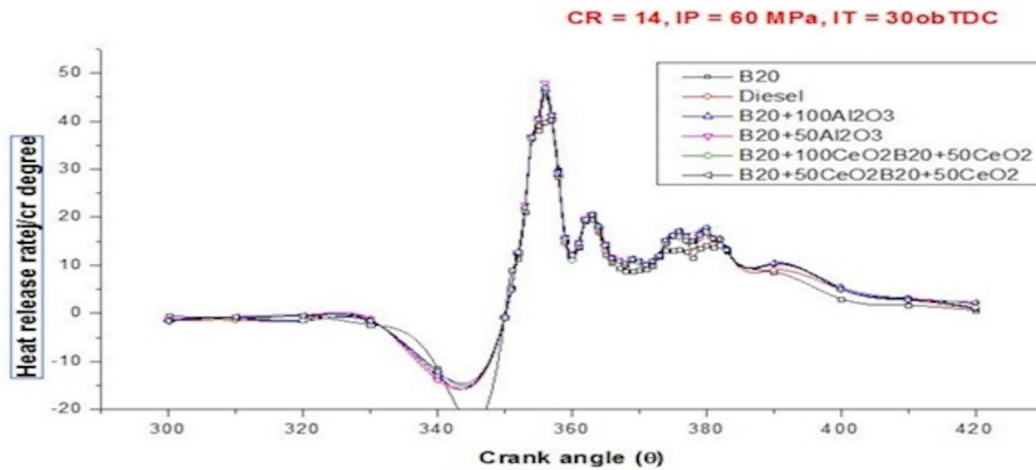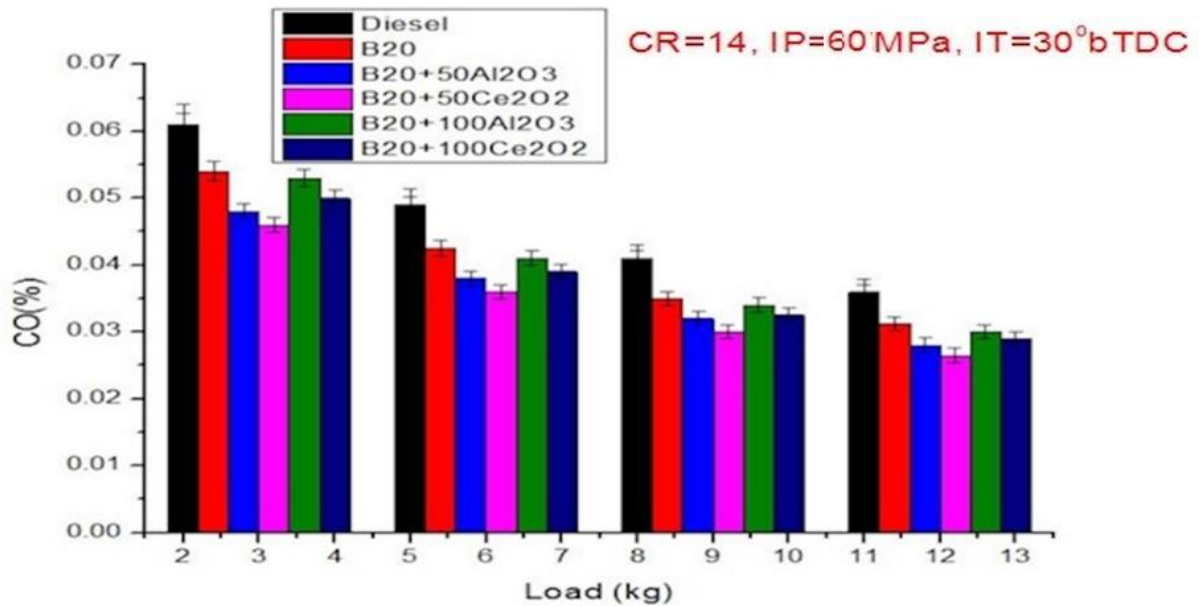

Fig. 4.15 Impact on CO of diesel engine by adding with Al_2O_3 and CeO_2 as fuel additive to B20 under various load conditions

The existence of nanoparticles in fuel improved the ignition, which thusly decline HC emissions. Nanopartcile's ability to act as an oxygenated additive stimulates combustion efficiency, resulting in a substantial reduction in HC emissions [201]. The addition of oxygen content in biofuel emphasized the reason for reduced emissions. The process of oxygen delivery facilitated by cerium oxide results in decreased emissions of unburned hydrocarbons (UHC), soot, and carbon monoxide (CO), as illustrated in Equation 5.6 [223].

$$(2x + y)CeO_2 + C_X H_Y = \left[\frac{1}{2}(2x + y)\right] Ce_2O_3 + \frac{x}{2}CO_2 + \frac{Y}{2}H_2O \qquad (5.6)$$
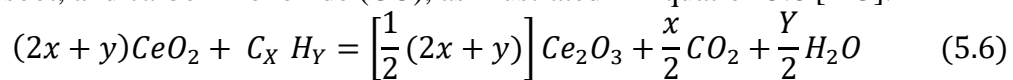
Nanoparticles, which occupy higher surface regions and act as energy exciters to ignite the carbon particles that are exposed on the chamber walls and speed up the ignition process, are the significant factor contributing to the lessening of HC released into the atmosphere [224].

Further, the higher thermal conductivity of nanoparticles endorses rapid acceleration in evaporation rate due to enhancing the heat transfer rate of the air-fuel mixture. The fuel attained auto-ignition temperature rapidly resulting in complete combustion of fuel for the same elapsed ignition time. Figure 5.16 revealed that at a higher load diesel emits 51.16 % higher HC level in comparison to B20. B20+50 CeO_2 produced 50 % lower emissions than diesel at peak load conditions. The average HC emissions is 86,42,44.3,43, 46.5 and 45ppm for the Diesel, B20 +50 Al_2O_3, B20 +100 Al_2O_3, B20 +50 CeO_2 and B20 +100 CeO_2 respectively. A similar trend was observed by Krishnakumar et al., [225] with blend fuel mixed with graphene nanoparticles.
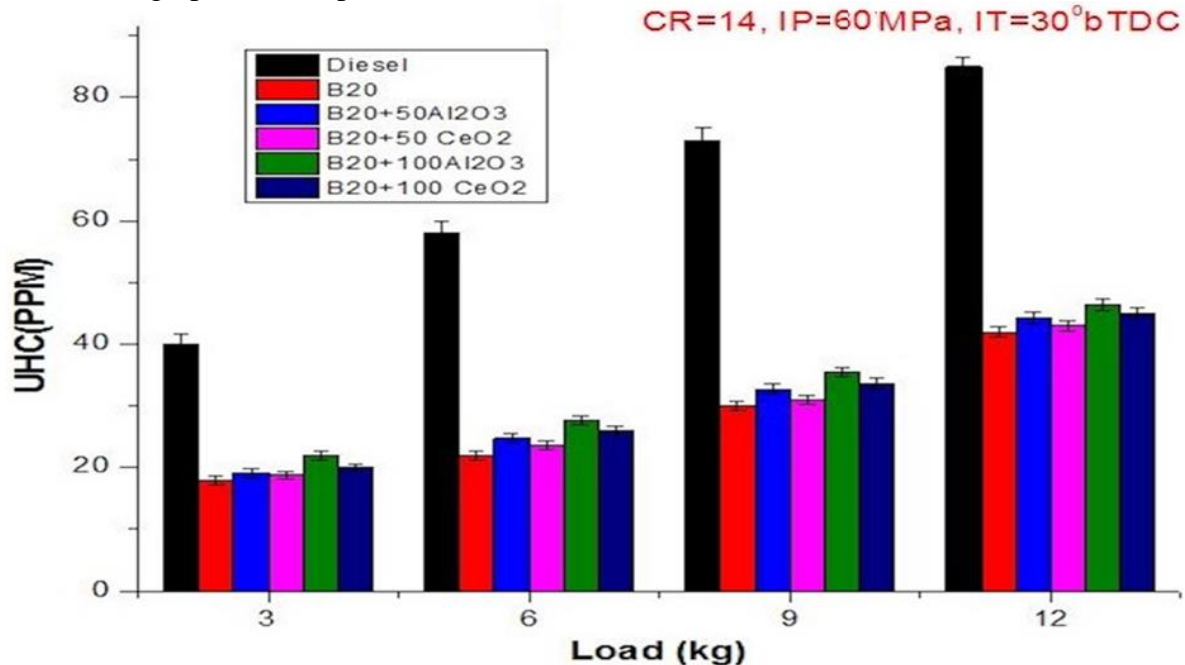
Fig. 4.16 Impact on UHC of diesel engine by adding with Al_2O_3 and CeO_2 as fuel additive to B20 under various load conditions

4.4.3.3 Nitrogen oxide emissions

Oxides of nitrogen are extremely hazardous to human health. To maintain a clean and secure environment, it is preferable to reduce NOx emissions. The reasonable aspects to generate NOx emissions may be oxygenated fuel, a shorter ignition delay, and a high in-cylinder temperature. Unmodified biofuels exhibit an increase in NOx emissions of diesel engines caused by more biofuel quantity in the biodiesel blends. Biofuel's inherent oxygenate properties induce combustion at a high flame temperature, resulting in higher NO_X [226]. Noticeably, the Use of waste cooking biofuel instead of diesel caused the brake thermal efficiency to decrease along with other pollutants including CO, CO_2, and HC, though at the same time it increased brake-specific fuel consumption and nitrogen oxide emissions. Further, previous reports have shown that using metallic nanoparticles as fuel additives induces higher combustion flame temperature. The expansion of metal oxide-based nanoparticles into fuel leads to complete ignition since nanoparticles act as an oxygen-donor impetus in the combustion chamber [26]. The present study reveals that B20 has higher NOx emissions than D100 and nano additive fuel blends. The quantity of oxygen in the biofuel causes the fuel to

burn at high temperatures, creating more NOx because the nitrogen oxides are produced at a higher temperature. Figure 4.17 reveals that NOx emissions increased with increases in engine load for all tested fuel blends. Fig 4.17 uncovered that a maximum decrease in NOx emissions up to 18.29 % at a higher load for B20+50 CeO_2 is seen in contrast with B20. Afzal et al. [227] showed a similar trend of NOx with silver nano additives. In the context of CeO_2 nanoparticles in biodiesel have the ability to break oxides of nitrogen into nitrogen gas resulting in the reduction of NOx which is illustrated in equation no 5.7 [228],

$$Ce_2O_3 + NO \rightarrow 2CeO_2 + N_2 \qquad (5.7)$$
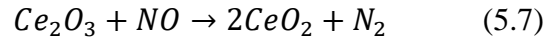
Besides it, the addition of nanoparticles promotes complete burning, as it goes about as oxygen impetus due to which heat release rate and high peak pressure of combustion increased. As a result, the ignition delay is reduced; reduced ignition delay shortens the period of pre-burn fractionation of ignition, which in turn reduces cylinder temperature and nitrogen oxides. Nanoparticle blend accelerates the combustion; Nanoparticle interacts with unburned hydrocarbons and accelerates the minimum time of thermal breakdown of the unburned hydrocarbon molecules without the need for additional energy. The presence of lower active radials prompted a diminishing in the capability of NOx development [26].
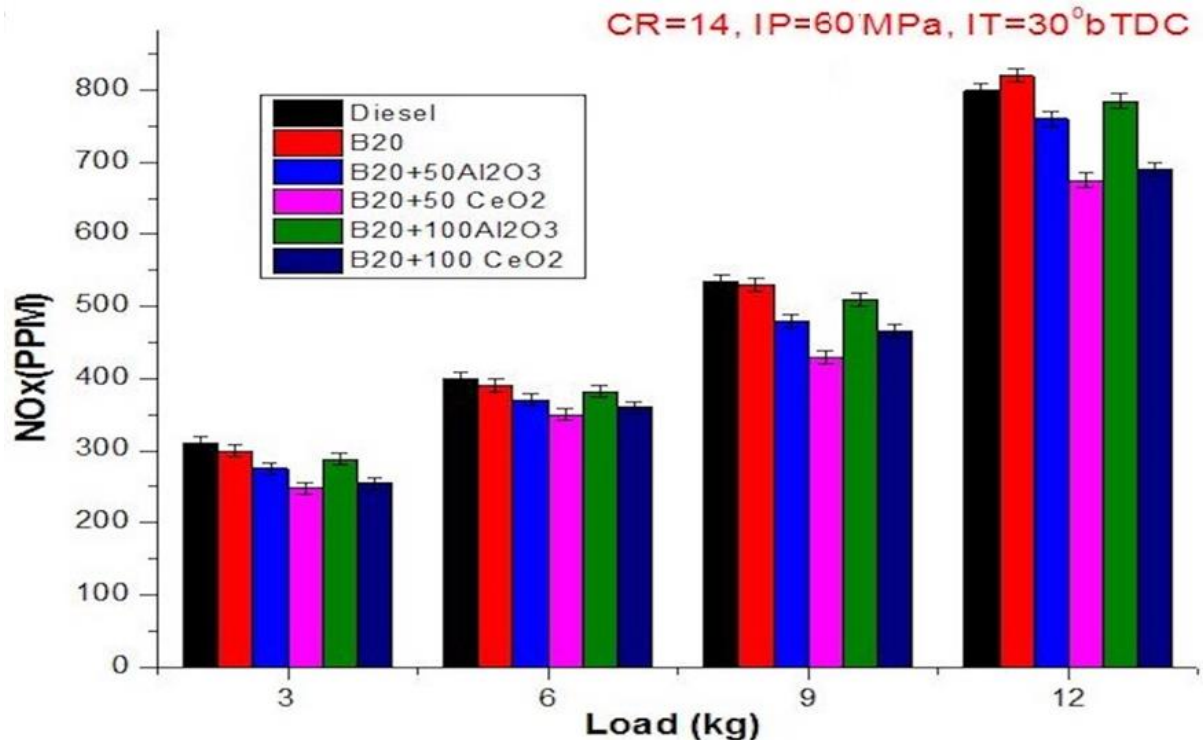
Fig. 4.17 Impact on NO_X of diesel engine by adding with Al_2O_3 and CeO_2 as fuel additive to B20 under various load conditions

4.5 Optimization of engine responses at various engine input parameters

4.5.1 Experimental design

For further exploration, a recently developed waste cooking biodiesel (B20) containing nanoparticles (Al_2O_3) underwent testing to optimize the response of a CRDI single-cylinder four-stroke VCR engine across different input parameters. The nanoparticle content in waste cooking oil was systematically altered to investigate the influence of various nano-

biodiesel blends on both engine performance and emissions. Key engine parameters, such as injection pressure (IP), load, compression ratio (CR), and load, were systematically varied to analyse their effects on engine performance and emissions. All experiments were conducted at a constant speed of 1200 rpm and an injection timing of 23 before top dead centre (23b°TDC). Response Surface Methodology (RSM) stands as a robust statistical technique employed for the optimization and modelling of intricate processes. It delves into the relationships among various input parameters, such as injection pressure (IP), load, compression ratio (CR), and nanoparticle concentration, and engine responses, encompassing brake thermal efficiency (BTE), specific fuel consumption (SFC), carbon dioxide (CO), hydrocarbon (HC), and nitrogen oxide (NO_X) emissions. The central composite rotational design (CCRD) is utilized to determine the optimal values of input parameters and their interactions. The experimental array for the CCRD design is presented in Table 4.5, effectively optimizing the nonlinear system.

The CCRD involves a full factorial design with all combinations of factors at five levels: -2, -1, Canter 0, +1, and +2. MINITAB software is employed for developing the RSM model. Given the intricate nature of combustion in an internal combustion engine, which entails non-linear correlations among variables, numerical models are essential to predict the behaviour of input parameters and responses. In this optimization method, a higher-order polynomial equation is employed as a numerical model to capture the nonlinear relationship between inputs and responses. The equation incorporates all interaction parameters to ascertain the responses, with a second-order polynomial model being indicated by the equation provided below.

$$Y = b_o + \sum b_i X_i + \sum b_{ij} X_i X_j \qquad (i, j = 1, 2, 3 \ldots \ldots k)$$

Y= output responses, X_i= input variable, X_j= input variable, b_i = constant, b_j = constant

Table no. 4.5 Input variables and levels selected for the CCRD

Input parameters	Symbol	Coded Levels				
		-2	-1	0	1	2
Fuel	Ppm	B20 (0)	B20+0.25Al$_2$O$_3$ (25)	B20+0.5Al$_2$O$_3$ (50)	B20+0.75Al$_2$O$_3$ (75)	B20+1Al$_2$O$_3$ (100)
Load	Kg	0	3	6	9	12
IP	Bar	500	550	600	650	700
CR	-	17	17.5	18	18.5	19

Table 4.6 Experimental design for optimization of responses of diesel engine

Exp. Run	Input 1	Input 2	Input 3	Input 4	Exp. Run	Input 1	Input 2	Input 3	Input 4
1	1	1	1	1	16	1	1	-1	-1
2	0	0	0	0	17	-1	1	1	1
3	0	0	0	0	18	-2	0	0	0
4	0	0	2	0	19	-1	1	1	-1
5	1	-1	1	-1	20	0	-2	0	0

6	-1	-1	1	-1	21	0	2	0	0
7	1	1	1	-1	22	-1	-1	1	1
8	-1	-1	-1	1	23	0	0	0	0
9	-1	-1	1	-1	24	0	0	0	0
10	0	0	0	-2	25	1	-1	-1	1
11	0	0	0	0	26	1	1	-1	1
12	0	0	-2	0	27	1	-1	1	1
13	-1	1	-1	1	28	-1	1	-1	-1
14	0	0	0	0	29	0	0	0	0

Table 4.5 presents the levels of various input variables, both in coded and uncoded forms. The engine tests were systematically carried out in adherence to the 30 experiments detailed in Table 4.6, with Table 4.7 providing an overview of the corresponding response variables related to performance and emission characteristics. After conducting engine trials and analysing the tabulated results depicting engine responses, it is evident that the maximum brake thermal efficiency and the minimum brake specific fuel consumption have been identified. Furthermore, the tabulated results for emission responses, encompassing hydrocarbons (HC), carbon monoxide (CO), carbon dioxide (CO_2), and nitrogen oxides (NO_X), have been computed.

4.5.2 Experimental results on the basis of experimental design run

Figures 4.18 and 4.19 present the variations in Specific Fuel Consumption (SFC) and Brake Thermal Efficiency (BTE) with respect to load. In Figure 4.18, it is observed that the BTE of the $B20+50Al_2O_3$ blend effectively increases, while SFC decreases with rising loads, maintaining injection pressure (IP) and compression ratio (CR) constant at 600 bar and 18, respectively.
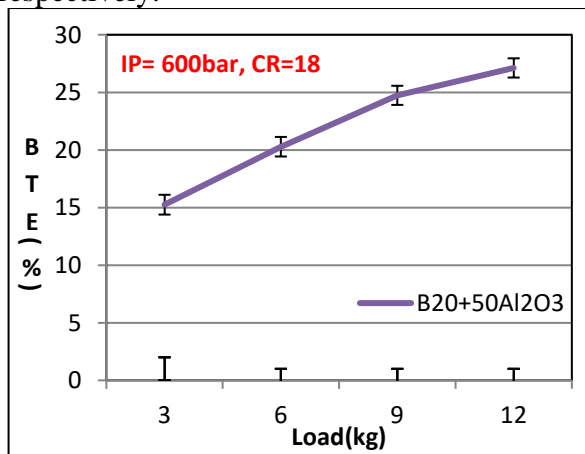
Fig 4.18. Variation of BTE with respect to load   Fig 4.19. Variation of SFC with respect to load
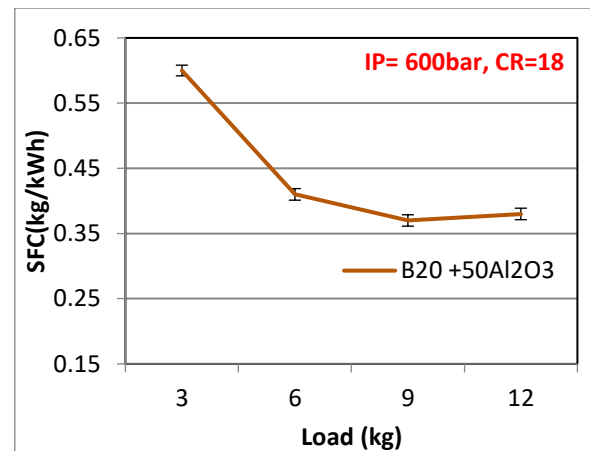
Higher loads in the engine result in elevated temperatures and pressures, reducing heat losses to the surroundings. This indicates a more efficient conversion of the energy released during combustion into useful work rather than dissipating as waste heat [229]. For the ($B20+50Al_2O_3$) blend, the SFC of the diesel engine decreases with increasing load when IP=600 bar and CR=18 are held constant.
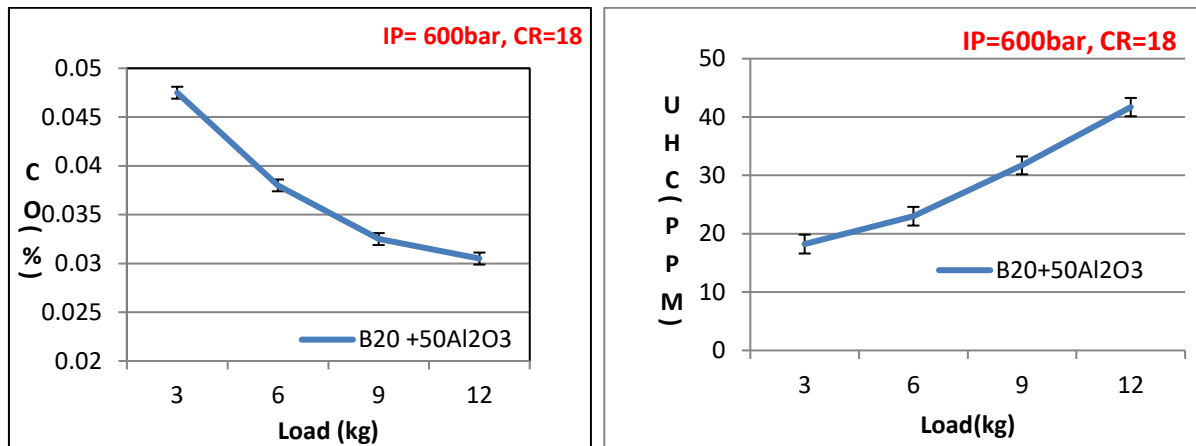
The Brake Specific Fuel Consumption (BSFC) shows a decreasing trend with an increase in load for all tested fuels. Higher loads lead to increased combustion pressures and more robust mechanical operation, reducing internal friction losses due to improved lubrication and more efficient mechanical interactions, ultimately contributing to improve BSFC [229]. Figures 4.20 and 4.21 illustrate the variation of carbon monoxide (CO) and unburned hydrocarbons (UHC) concerning load, with IP and CR held constant at 600 bar and 18, respectively. CO emissions decrease with an increase in load for the B20+50Al$_2$O$_3$ blend, indicating that operating at higher loads brings the engine closer to its design point, optimizing combustion processes. Improved mixing of the air-fuel mixture and higher combustion temperatures and pressures lead to more complete combustion and reduced CO emissions [165]. On the other hand, Fig 4.21 shows an increase in the concentration of unburned hydrocarbons with engine load for the B20+50Al$_2$O$_3$ blend. Fig 4.22 depicts that the nitrogen oxide emissions of the B20+50Al$_2$O$_3$ blend increase with respect to load from zero to 12 kg. Higher engine loads intensify the combustion process, elevating temperatures within the combustion chamber. The heightened temperatures promote the formation of nitrogen oxides (NOx) through the reaction between nitrogen and oxygen from the air. NOx formation is temperature-sensitive, and the increased temperatures at higher loads contribute to elevated NOx emissions [230]. Fig 4.24. Variation of SFC with respect to IP   Fig 4.25 Variation of UHC with respect to IP

Figure 4.23 illustrates that the Brake Thermal Efficiency (BTE) for the B20+75Al$_2$O$_3$ blend increases concerning injection pressure, while load and compression ratio (CR) are maintained at 3 kg and 17.5, respectively. As the injection pressure rises, there is an enhancement in brake thermal efficiency (BTE). Elevated injection pressures contribute to the finer breakdown of fuel into droplets, facilitating better mixing of fuel with air within the combustion chamber. This finer atomization ensures a more homogeneous fuel-air mixture, promoting more efficient and complete combustion. . Higher injection pressure can also lead to shorter ignition delay periods, which is the time

between the start of fuel injection and the actual ignition of the fuel. A shorter ignition delay results in combustion starting sooner after fuel injection, leading to more complete combustion and less fuel wastage [231]. The consequence of this situation is depicted in Figure 4.24, where Brake Specific Fuel Consumption (BSFC) decreases with increasing injection pressure for B20+75Al$_2$O$_3$. This indicates that the engine can generate the same amount of power or thrust with less fuel, resulting in lower Specific Fuel Consumption.
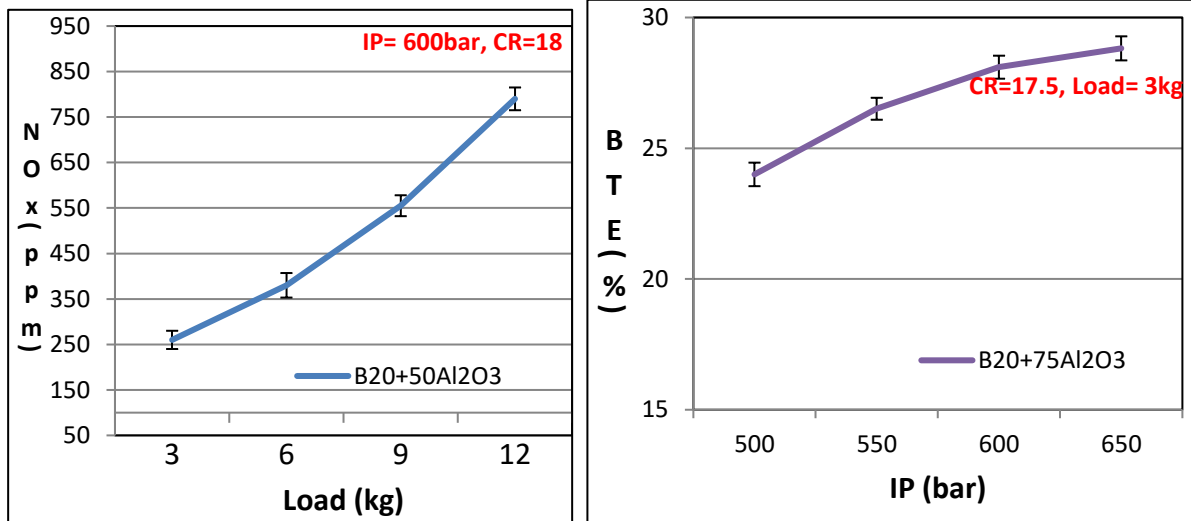
Fig 4.22.Variation of NOx with respect to load Fig 4.23. Variation of BTE with respect to load
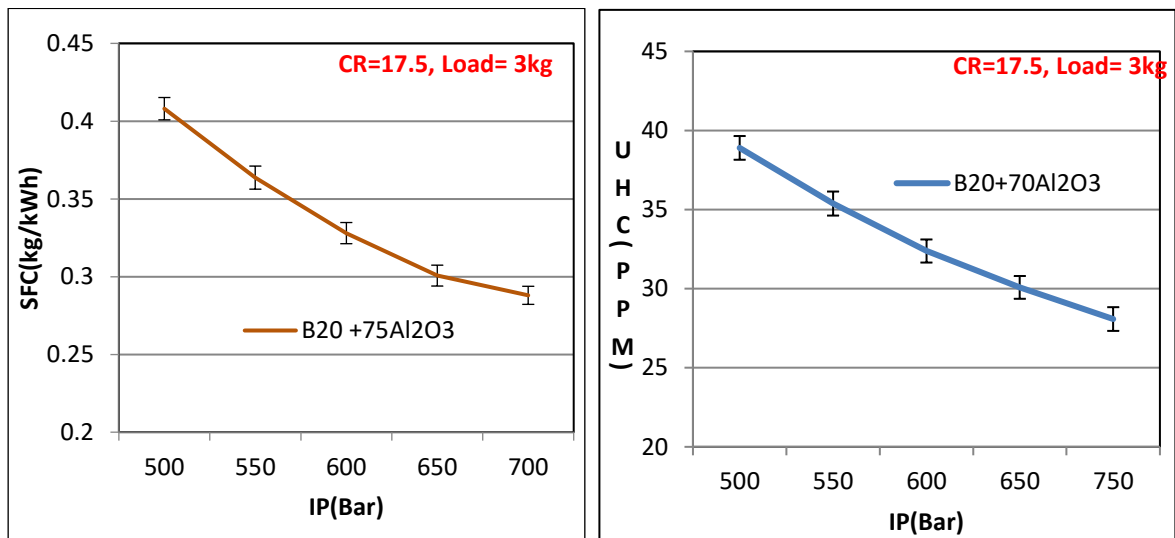
When fuel and air are more thoroughly mixed, the occurrence of pockets with rich or lean fuel concentrations, which can lead to incomplete combustion and the formation of unburned hydrocarbons (UHCs), is reduced. Figure 4.25 demonstrates that the UHC levels in the B20+75Al$_2$O$_3$ blends decrease with increasing injection pressure when the compression ratio (CR) and load are held constant at 17.5 and 3 kg, respectively. With an increase in injection pressure, the droplet size of the fuel decreases. Higher injection pressure enhances fuel atomization, breaking it down into finer droplets. These smaller fuel droplets exhibit more effective mixing with air in the combustion chamber [232]. Improved combustion efficiency results in less unburned or partially burned fuel in the exhaust gases. Carbon monoxide (CO) is a byproduct of incomplete combustion, so more thorough combustion leads to reduced CO emissions.
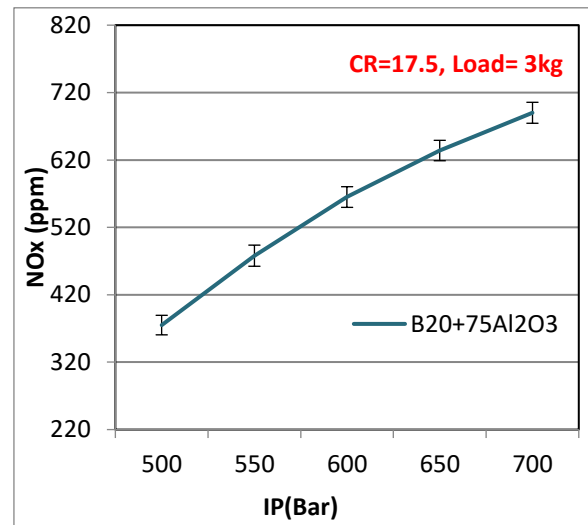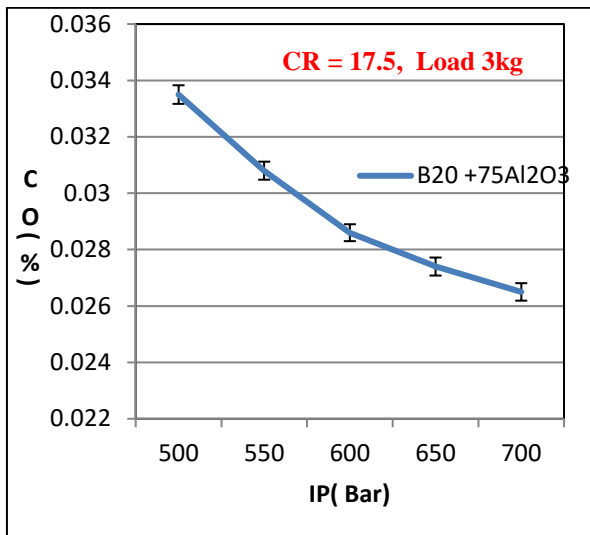
Fig 4.26. Variation of CO with respect to lP

Fig 4.27. Variation of NOx with respect to IP

This effect is evident in Figure 4.26, where CO emissions decrease with increasing injection pressure, while CR and load are held constant at 17.5 and 3 kg, respectively. Higher injection pressure fosters better fuel and air mixing, resulting in increased oxygen availability within the combustion chamber. While this is advantageous for combustion efficiency, it can also lead to higher concentrations of oxygen radicals [233]. Elevated oxygen availability and faster combustion rates due to increased pressure contribute to rising combustion temperatures. Higher temperatures, in turn, promote the formation of nitrogen oxides, as depicted in Figure 4.27.

Fig 4.28 . Variation of BTE with respect to CR
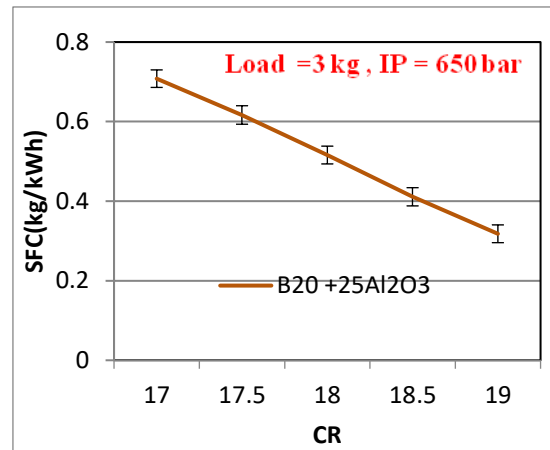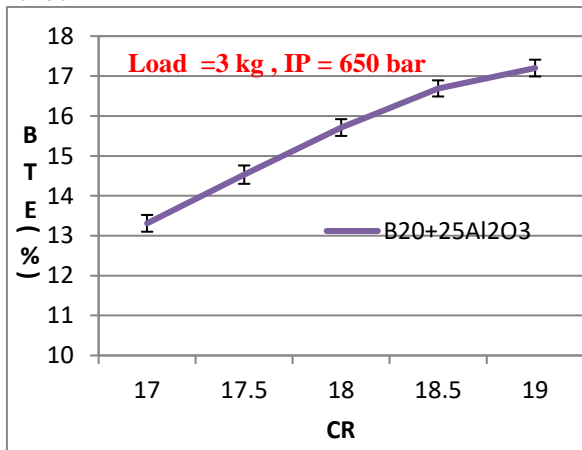
Fig 4.29. Variation of SFC with respect to CR

Figures 4.28 and 4.29 illustrate the variation in Brake Thermal Efficiency (BTE) and Specific Fuel Consumption (SFC) concerning Compression Ratio (CR) when Injection Pressure (IP) and load were kept constant at 650 bar and 3 kg for the fuel blend $B20+25Al_2O_3$. The higher compression ratio contributes to elevated combustion temperatures and pressures during the power stroke. This heightened pressure and temperature during combustion lead to extracting more work from each unit of fuel, resulting in increased power output for the same fuel consumption [234]. This increase is evident in the elevated Brake Thermal Efficiency.

As previously mentioned, the higher compression ratio enables more energy to be extracted from the same quantity of fuel. Consequently, for a given power output, the engine burns less fuel, resulting in lower Specific Fuel Consumption.
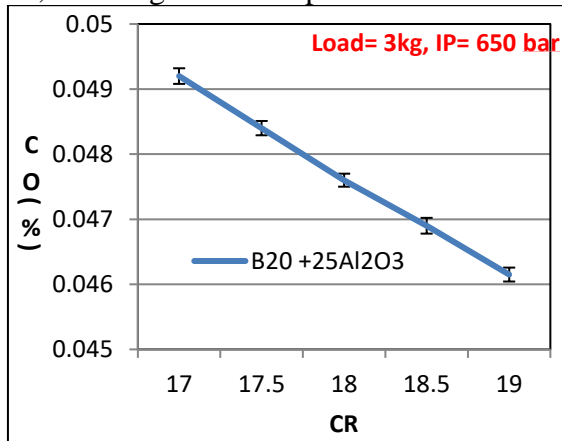
Fig. 4.30 Variation of CO with respect to CR   Fig 4.31 Variation of CO with respect to CR
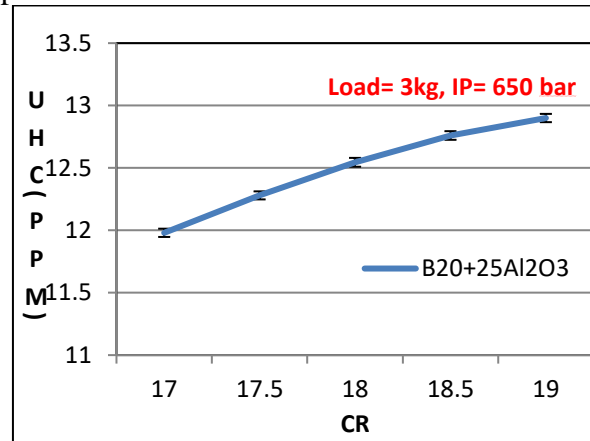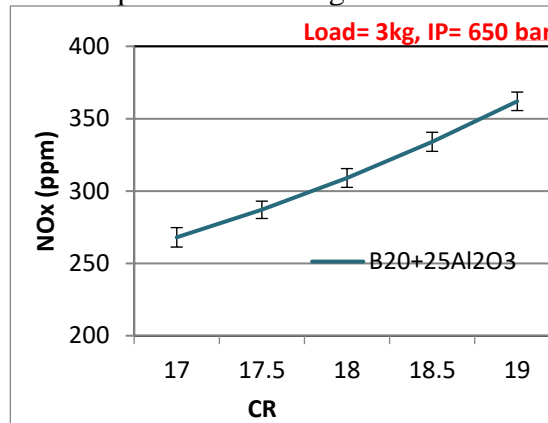
Fig. 4.32 Variation of NOx with respect to CR

As evident from Figure 4.30, carbon monoxide (CO) emissions exhibit a gradual decrease with an increase in compression ratio for B20+25Al$_2$O$_3$, with injection pressure (IP) and load held constant at 650 bar and 3 kg, respectively. Higher compression ratios contribute to a more efficient combustion process. When the air-fuel mixture undergoes higher compression before ignition, it becomes more homogeneous and uniformly mixed [235]. This results in a more complete combustion of the fuel, leaving fewer unburned or partially burned hydrocarbons (which contribute to CO emissions) in the exhaust gases. Figure 4.31 shows an increase in unburned hydrocarbon (UHC) emissions with the increment in compression ratio for B20+25Al$_2$O$_3$. In certain operating conditions, higher compression ratios can lead to leaner air-fuel mixtures, where there is more air relative to fuel. Lean mixtures may promote partial combustion, resulting in higher UHC emissions. Under lean conditions, there might not be sufficient fuel present for complete combustion, leading to the release of unburned hydrocarbons into the exhaust. It is noteworthy that the higher in-cylinder temperature, along with the additional oxygen content in biodiesel fuel blends, enhances the combustion process rate and the oxidation of UHC emissions. Figure 4.32 indicates higher nitrogen oxide (NOx) production with increasing compression ratio, attributed to higher combustion temperatures.

As compression ratio rises, combustion temperatures increase, promoting the formation of nitrogen oxides.

Table 4.7 Experimental design for optimization of the performance and emission characteristics of diesel engine

Exp. Run	Input 1	Input 2	Input 3	Input 4	BTE (%)	SFC (kg/kWh)	CO (%)	HC (ppm)	NOx (ppm)
1	1	1	1	1	26.09	0.311	0.0259	30.56	641
2	0	0	0	0	20.28	0.41	0.038	23	380
3	0	0	0	0	20.28	0.41	0.038	23	380
4	0	0	2	0	20.62	0.381	0.0255	19.7	505
5	1	-1	1	-1	15.02	0.5697	0.0449	15.78	302
6	-1	-1	1	-1	13.53	0.6197	0.0484	12.28	287
7	1	1	1	-1	25.82	0.3107	0.0274	30.08	594
8	-1	-1	-1	1	13.64	0.6351	0.0501	16.06	218
9	-1	-1	1	-1	13.52	0.6197	0.0484	12.28	287
10	0	0	0	-2	20.02	0.4268	0.0395	22.52	340
11	0	0	0	0	20.28	0.41	0.038	23	380
12	0	0	-2	0	19.12	0.437	0.0408	25.80	292
13	-1	1	-1	1	23.59	0.4051	0.0326	30.36	498
14	0	0	0	0	20.28	0.41	0.038	23	380
15	0	0	0	2	20.42	0.3905	0.0365	23.52	428
16	1	1	-1	-1	25.51	0.3637	0.0306	33.38	478
17	-1	1	1	1	23.82	0.3719	0.0294	27.06	604
18	-2	0	0	0	16.95	0.47	0.0419	20.08	355
19	-1	1	1	-1	23.59	0.3897	0.0309	26.58	567
20	0	-2	0	0	0.10	0.57	0.0551	9.43	155
21	0	2	0	0	27.12	0.38	0.0305	41.7	790
22	-1	-1	1	1	13.89	0.411	0.0469	12.76	334
23	0	0	0	0	20.28	0.41	0.038	23	380
24	0	0	0	0	20.28	0.41	0.038	23	380
25	1	-1	-1	1	14.62	0.5851	0.0466	19.56	233
26	1	1	-1	1	25.82	0.3451	0.0291	33.82	525
27	1	-1	1	1	15.33	0.5511	0.0434	16.26	349
28	-1	1	-1	-1	23.21	0.4237	0.0344	29.88	450
29	0	0	0	0	20.28	0.41	0.038	23	380
30	1	-1	-1	-1	14.62	0.6037	0.0481	19.08	186

4.5.3 Analysis of variance (ANOVA) of response surface model

To statistically assess the results of the developed model, Analysis of Variance (ANOVA) was employed to determine the significance of each input's influence on the responses. ANOVA quantifies the variability in the response variable that can be attributed to each individual input and their interactions, assessing whether the model adequately represents the data and whether the model's assumptions are met. The results of the ANOVA for the conducted experiments are presented in Tables 4.8 and 4.9, including degrees of freedom, sum of squares, mean sum of squares, F-values, and P-values corresponding to combined blends, load, compression ratio, and injection pressure. The model exhibits a p-value < 0.01, indicating its statistical significance. All models show a probability value (p-value) of less than 0.01, affirming their statistical significance according to ANOVA. The model F-values

for Specific Fuel Consumption (SFC), Brake Thermal Efficiency (BTE), carbon monoxide (CO), hydrocarbons (HC), and nitrogen oxides (NOx) are 5.72, 53.03, 25.03, 213.92, and 390.07, respectively. The investigation reveals that load and nanoparticles (p-value < 0.01) have a significant impact on SFC. The P-value and F-value serve as crucial metrics to evaluate the validity of the provided model and experimental variables.

Table 4.8 Analysis of variance for SFC and BTE

		SFC (kg/kWh)		BTE (%)	
Source	DF	F- value	p-value	F- value	p-value
Model	14	5.72	0.001	53.03	0.000
Linear	4	0.88	0.497	0.83	0.524
Fuel	1	0.78	0.391	0.42	0.528
Load (kg)	1	1.53	0.234	2.42	0.140
IP(bar)	1	0.45	0.513	0.23	0.636
CR	1	0.37	0.554	0.37	0.554
Square	4	1.54	0.237	14.23	0.000
Fuel*Fuel	1	0.57	0.461	0.03	0.865
Load (kg)*Load (kg)	1	5.60	0.031	53.08	0.000
IP(bar)*IP(bar)	1	0.54	0.475	0.14	0.710
CR*CR	1	0.52	0.480	0.65	0.431
2-Way Interaction	6	0.84	0.559	0.28	0.937
Fuel*Load (kg)	1	1.31	0.269	0.22	0.643
Fuel*IP(bar)	1	0.11	0.747	0.30	0.592
Fuel*CR	1	0.81	0.383	0.21	0.654
Load (kg)*IP(bar)	1	0.11	0.742	0.58	0.457
Load (kg)*CR	1	0.82	0.379	0.11	0.749
IP(bar)*CR	1	1.34	0.263	0.42	0.527
Error	16				
Lack-of-Fit	9	295477.24	0.000	295477.24	0.000
Pure Error	7				
Total	30				

Table 4.9 Analysis of variance for CO, HC, and NOx emission

		CO (%)		HC (ppm)		NOx (ppm)	
Source	DF	F- value	p-value	F-value	p-value	F-value	p-value
Model	14	25.30	0.000	213.92	0.000	390.07	0.000
Linear	4	0.58	0.680	0.14	0.963	0.19	0.938
Fuel	1	0.04	0.834	0.05	0.825	0.05	0.830
Load (kg)	1	0.38	0.545	0.49	0.492	0.62	0.443
IP(bar)	1	0.90	0.356	0.01	0.914	0.00	0.969
CR	1	0.29	0.601	0.10	0.753	0.01	0.943
Square	4	5.01	0.008	7.03	0.002	35.73	0.000
Fuel*Fuel	1	0.46	0.505	4.60	0.048	2.44	0.138
Load (kg)*Load (kg)	1	11.61	0.004	19.77	0.000	132.86	0.000
IP(bar)*IP(bar)	1	5.54	0.0302	0.67	0.426	4.13	0.059
CR*CR	1	0.29	0.595	0.10	0.759	0.03	0.867
2-Way Interaction	6	0.01	1.000	0.00	1.000	0.43	0.850

Fuel*Load (kg)	1	0.01	0.944	0.00	0.974	1.91	0.186
Fuel*IP(bar)	1	0.02	0.933	0.00	0.983	0.02	0.904
Fuel*CR	1	0.02	0.944	0.00	0.974	0.05	0.822
Load (kg)*IP(bar)	1	0.02	0.882	0.00	0.983	0.08	0.780
Load (kg)*CR	1	0.01	0.895	0.00	0.974	0.03	0.854
IP(bar)*CR	1	0.01	0.933	0.00	0.983	0.11	0.746
Error	16						
Lack-of-Fit	9						
Pure Error	7						
Total	30						

Similarly, the ANOVA results indicate that the R^2 values for Specific Fuel Consumption (SFC), Brake Thermal Efficiency (BTE), carbon monoxide (CO), hydrocarbons (HC), and nitrogen oxides (NOx) are 93.34%, 97.89%, 95.68%, 99.47%, and 99.71%, respectively, as illustrated in Table 4.10. The observed R^2 values are close to 1, underscoring the accuracy and adequacy of the model. R^2 values serve as a measure of the success of the modeling process.

Additionally, there is reasonable agreement between the Adjusted R^2 (Adj. R^2) value and the Predicted R^2 (Pred. R^2) value. A higher R^2 is always desirable for the best fitting of the model. As the R^2 values approach unity, the model fits the experimental data more effectively. In the selected second-order model, the coefficient of R^2 for performance and emission responses exceeds 95. This suggests the suitability of the second-order model for the present study. The value of R^2 (adj) is also above 95%, indicating the significance of the model for the present study.

Table 4.10 Model summary of input parameters

Coefficient of determination	Value				
	SFC	**BTE**	**CO**	**HC**	**NOx**
R^2	93.34%	97.89%	95.68%	99.47%	99.71%
Adjusted R^2	88.76 %	96.04 %	91.90 %	99.00 %	99.45 %
predicted R^2	83.04%	86.94%	73.89%	96.73%	98.22%

In this research, equations have been formulated to model and predict the performance and emission responses of a research diesel engine, considering a blend of nanobiofuel, compression ratios, injection pressures, and loads. Regression analysis has been employed to derive the following response models.

SEC (kg/kWh) = 5.9 - 0.498 Fuel - 0.232 Load (kg) + 0.0078 IP (bar) - 0.73 CR + 0.0076 Fuel*Fuel + 0.00265 Load (kg)*Load (kg) + 0.000003 IP (bar)*IP(bar) + 0.0292 CR*CR - 0.00535 Fuel*Load (kg) + 0.000094 Fuel*IP (bar)   + 0.0252 Fuel*CR + 0.000032 Load (kg)*IP (bar) + 0.00846 Load (kg)*CR - 0.000664 IP (bar)*CR .

BTE(%)   =   123   + 7.4 Fuel   + 5.91 Load (kg)   + 0.114 IP(bar)   - 18.5 CR   - 0.035 Fuel*Fuel   - 0.1653 Load (kg)*Load (kg)   + 0.000031 IP(bar)*IP(bar)   + 0.659 CR*CR   + 0.0447 Fuel*Load (kg)   -

0.00317 Fuel*IP(bar)   - 0.259 Fuel*CR   - 0.00147 Load (kg)*IP(bar)   - 0.061 Load (kg)*CR   - 0.0075 IP(bar)*CR

***CO(%)** = 0.252 - 0.0050 Fuel - 0.00482 Load (kg) + 0.000460 IP(bar) - 0.0335 CR - 0.000285 Fuel*Fuel + 0.000159 Load (kg)*Load (kg)   - 0.000000 IP(bar)*IP(bar)   + 0.00091 CR*CR + 0.000017 Fuel*Load (kg) - 0.000001 Fuel*IP(bar) + 0.00017 Fuel*CR - 0.000001 Load (kg)*IP(bar) + 0.000033 Load (kg)*CR - 0.000002 IP(bar)*CR*

***HC   (ppm)**   =   -47   + 1.68 Fuel   + 1.75 Load (kg)   + 0.017 IP(bar)   + 6.4 CR   - 0.287 Fuel*Fuel + 0.0661 Load (kg)*Load (kg)   - 0.000044 IP(bar)*IP(bar)   - 0.167 CR*CR   - 0.0021 Fuel*Load (kg) + 0.00008 Fuel*IP(bar)   - 0.012 Fuel*CR+ 0.00003 Load (kg)*IP(bar)   - 0.004 Load (kg)*CR + 0.00017 IP(bar)*CR*

***NOx(ppm)**   =   -761   - 24 Fuel   + 28.5 Load (kg)   - 0.09 IP(bar)   + 21 CR   - 3.04 Fuel*Fuel + 2.495 Load (kg)*Load (kg)   + 0.001583 IP(bar)*IP(bar)   + 1.33 CR*CR   + 1.248 Fuel*Load (kg) + 0.0068 Fuel*IP(bar) + 1.24 Fuel*CR - 0.0052 Load (kg)*IP(bar) - 0.34 Load (kg)*CR - 0.036 IP(bar)*CR*

The input variables encompass fuel, load, injection pressure, and compression ratio, representing the nanoparticle content in biodiesel, engine load, injection pressure, and compression ratio. An analysis of variance, F-ratio test, and P-value test were carried out, and the outcomes are condensed in Table 4.11 through Table 4.20.

Table 4.11 Analysis of variance for SFC

Source	DF	Adj SS	Adj MS	F- value	p- value
Model	14	0.232120	0.016580	5.72	0.001
Linear	4	0.010	0.002	0.88	0.497
Fuel	1	0.00225	0.00225	0.78	0.391
Load (kg)	1	0.00443	0.0044	1.53	0.234
IP(bar)	1	0.001296	0.001296	0.45	0.513
CR	1	0.000686	0.000686	0.37	0.554
Square	4	0.017909	0.004477	1.54	0.237
Fuel*Fuel	1	0.001658	0.001658	0.57	0.461
Load (kg)*Load (kg	1	0.016241	0.01624	5.60	0.031
IP(bar)*IP(bar)	1	0.001552	0.001552	0.54	0.475
CR*CR	1	0.001515	0.001515	0.52	0.480
2-Way Interaction	6	0.014579	0.002430	0.84	0.559
Fuel*Load (kg)	1	0.003799	0.003799	1.31	0.269
Fuel*IP(bar)	1	0.000312	0.000312	0.11	0.747
Fuel*CR	1	0.002337	0.002337	0.81	0.383
Load (kg)*IP(bar)	1	0.000325	0.000325	0.11	0.742
Load (kg)*CR	1	0.002375	0.002375	0.82	0.379
IP(bar)*CR	1	0.003895	0.003895	1.34	0.263
Error	16	0.046401	0.002900		
Lack-of-Fit	9	0.046401	0.005156	295477.24	0.000
Pure Error	7	0.0000	0.0000		
Total	30	0.278521			

Table 4.12 Model summary for SFC

Coefficient of determination	Value
R^2	93.34%
Adjusted R^2	88.76 %

predicted R^2	83.04%

Table 4.13 Analysis of variance for BTE

Source	DF	Adj SS	Adj MS	F- value	p- value
Model	14	881.329	62.9520	53.03	0.000
Linear	4	3.951	0.9871	0.83	0.524
Fuel	1	0.494	0.4943	0.42	0.528
Load (kg)	1	2.867	2.8673	2.42	0.140
IP(bar)	1	0.276	0.2764	0.23	0.636
CR	1	0.434	0.4338	0.37	0.554
Square	4	67.577	16.8941	14.23	0.000
Fuel*Fuel	1	0.035	0.0352	0.03	0.865
Load (kg)*Load (kg	1	63.021	63.0212	53.08	0.000
IP(bar)*IP(bar)	1	0.170	0.1703	0.14	0.710
CR*CR	1	0.774	0.7737	0.65	0.431
2-Way Interaction	6	2.009	0.3349	0.28	0.937
Fuel*Load (kg)	1	0.265	0.2649	0.22	0.643
Fuel*IP(bar)	1	0.355	0.3550	0.30	0.592
Fuel*CR	1	0.248	0.2483	0.21	0.654
Load (kg)*IP(bar)	1	0.690	0.6903	0.58	0.457
Load (kg)*CR	1	0.125	0.1255	0.11	0.749
IP(bar)*CR	1	0.495	0.4955	0.42	0.527
Error	16	18.995	1.1872		
Lack-of-Fit	9	18.995	2.1106	295477.24	0.000
Pure Error	7	0.0000	0.0000		
Total	30	900.324			

Table 4.14 Model summary for BTE

Coefficient of determination	Value
R^2	97.89%
Adjusted R^2	96.04 %
predicted R^2	86.94%

Table 4.15 Analysis of variance for CO emission

Source	DF	Adj SS	Adj MS	F- value	p- value
Model	14	0.001770	0.000126	25.30	0.000
Linear	4	0.000012	0.000003	0.58	0.680
Fuel	1	0.0000	0.00000	0.04	0.834
Load (kg)	1	0.000002	0.000002	0.38	0.545
IP(bar)	1	0.000005	0.000005	0.90	0.356
CR	1	0.000001	0.000001	0.29	0.601
Square	4	0.000100	0.000025	5.01	0.008
Fuel*Fuel	1	0.000002	0.000002	0.46	0.505
Load (kg)*Load (kg	1	0.000058	0.000058	11.61	0.004
IP(bar)*IP(bar)	1	0.000028	0.000028	5.54	0.0302
CR*CR	1	0.000001	0.000001	0.29	0.595
2-Way Interaction	6	0.00000	0.00000	0.01	1.000
Fuel*Load (kg)	1	0.00000	0.00000	0.01	0.944
Fuel*IP(bar)	1	0.00000	0.00000	0.02	0.933
Fuel*CR	1	0.00000	0.00000	0.02	0.944
Load (kg)*IP(bar)	1	0.00000	0.00000	0.02	0.882
Load (kg)*CR	1	0.00000	0.00000	0.01	0.895
IP(bar)*CR	1	0.00000	0.00000	0.01	0.933
Error	16	0.000080	0.000005		
Lack-of-Fit	9	0.000080	0.00009		

Pure Error	7	0.0000	0.0000		
Total	30	0.001850			

Table 4.16 Model summary for CO emission

Coefficient of determination	Value
R^2	95.68%
Adjusted R^2	91.90 %
predicted R^2	73.89%

Table 4.17 Analysis of variance for HC emission

Source	DF	Adj SS	Adj MS	F- value	p- value
Model	14	1524.95	108.925	213.92	0.000
Linear	4	0.29	0.073	0.14	0.963
Fuel	1	0.03	0.026	0.05	0.825
Load (kg)	1	0.25	0.252	0.49	0.492
IP(bar)	1	0.01	0.006	0.01	0.914
CR	1	0.05	0.052	0.10	0.753
Square	4	14.31	3.579	7.03	0.002
Fuel*Fuel	1	2.34	2.340	4.60	0.048
Load (kg)*Load (kg	1	10.07	10.067	19.77	0.000
IP(bar)*IP(bar)	1	0.034	0.339	0.67	0.426
CR*CR	1	0.05	0.049	0.10	0.759
2-Way Interaction	6	0.00	0.001	0.00	1.000
Fuel*Load (kg)	1	0.00	0.001	0.00	0.974
Fuel*IP(bar)	1	0.00	0.000	0.00	0.983
Fuel*CR	1	0.00	0.001	0.00	0.974
Load (kg)*IP(bar)	1	0.00	0.000	0.00	0.983
Load (kg)*CR	1	0.00	0.001	0.00	0.974
IP(bar)*CR	1	0.00	0.00	0.00	0.983
Error	16	8.15	0.509		
Lack-of-Fit	9	8.15	0.905		
Pure Error	7	0.00	0.00		
Total	30	1533.10			

Table 4.18 Model summary for HC emissions

Coefficient of determination	Value
R^2	99.47%
Adjusted R^2	99.00 %
predicted R^2	96.73%

Table 4.19 Analysis of variance for NOx emission

Source	DF	Adj SS	Adj MS	F- value	p- value
Model	14	590300	42164.3	390.07	0.000
Linear	4	84	20.9	0.19	0.938
Fuel	1	5	5.2	0.05	0.830
Load (kg)	1	67	66.8	0.62	0.443
IP(bar)	1	0	0.2	0.00	0.969
CR	1	1	0.6	0.01	0.943
Square	4	15451	3862.8	35.73	0.000
Fuel*Fuel	1	264	263.6	2.44	0.138
Load (kg)*Load (kg	1	14361	14361.3	132.86	0.000
IP(bar)*IP(bar)	1	446	446.0	4.13	0.059
CR*CR	1	3	3.1	0.03	0.867
2-Way Interaction	6	277	46.2	0.43	0.850
Fuel*Load (kg)	1	207	206.8	1.91	0.186
Fuel*IP(bar)	1	2	1.6	0.02	0.904

Fuel*CR	1	6	5.7	0.05	0.822
Load (kg)*IP(bar)	1	9	8.7	0.08	0.780
Load (kg)*CR	1	4	3.8	0.03	0.854
IP(bar)*CR	1	12	11.7	0.11	0.746
Error	16	1730	108.1		
Lack-of-Fit	9	1730	192.2		
Pure Error	7	0.00	0.00		
Total	30	592030			

Table 4.20 Model summary for NO_X emission

Coefficient of determination	Value
R^2	99.71%
Adjusted R^2	99.45 %
predicted R^2	98.22%

4.5.4 Response surface plot and contour plot of engine input variables

The optimization contour plots and surface plots is generated by MINITAB software. These graphs are graphical representation that depicts the relationship between two input variables and the response variable at same time while keeping the two input variables constant (hold values) at certain levels.

A contour plot of the engine response shows these hold values on the right-hand side. This contour illustrates the regions where the response is maximized or minimized and provides valuable insights into the interaction between the input variables. Additionally, the contours lines help identify the direction in which adjustments to the input variables should be made to achieve the desired response. Complementing the optimization contour is the three-dimensional diagram, which provides a more comprehensive view of the response surface. In this diagram, the two input variables are represented on the axes, while the response variable is shown as the height of the surface above the plane defined by the input variables. This 3D visualization allows for a deeper understanding of the intricate relationships and interactions between the variables.

4.5.4.1 Effect of engine input variables on Specific fuel consumption (SFC)

Specific Fuel Consumption (SFC) refers to the amount of fuel utilized per unit of time required to generate a specified engine output. It serves as a mathematical metric for assessing how efficiently an engine converts fuel into power. The contour and surface plot depicted in Figure 4.33 illustrate the influence of Al_2O_3 content in biodiesel and Compression Ratio (CR) on SFC, with fixed values for Injection Pressure (IP) at 600 bar and load at 6 kg. The dark red color in the contour zone indicates high nanoparticle (Al_2O_3) content and low engine SFC at elevated CR. As the concentration of nanoparticles (Al_2O_3) in biodiesel and CR increases, the color transitions to red.

The investigation revealed a decrease in Specific Fuel Consumption (SFC) with an increase in the Al_2O_3 ratio in the fuel. This is attributed to the expansion of nanoparticles, enhancing the ignition quality of the fuel through improvements in air-fuel blending, physicochemical properties (resulting in higher calorific value of the fuel), fuel dispersion, and heat transfer [236]. As the Compression Ratio (CR) increased, SFC decreased, likely due to improved combustion and lower heat losses. A slight decrease in SFC was observed at higher CR, with a nearly 30% reduction at full load when CR was increased from 17 to 19.
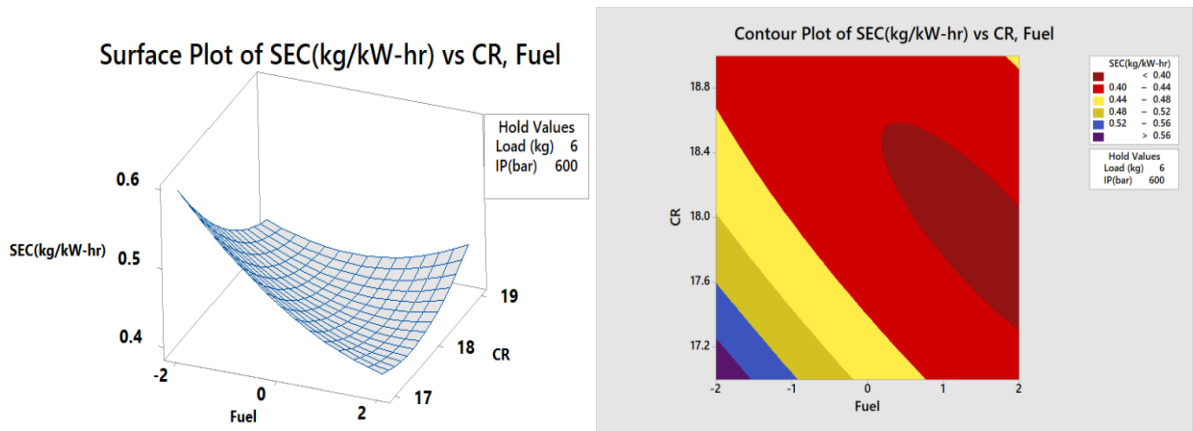
Fig. 4.33 Three dimensional plot depicts the impact of fuel and CR and their combined effect on the specific fuel consumption.
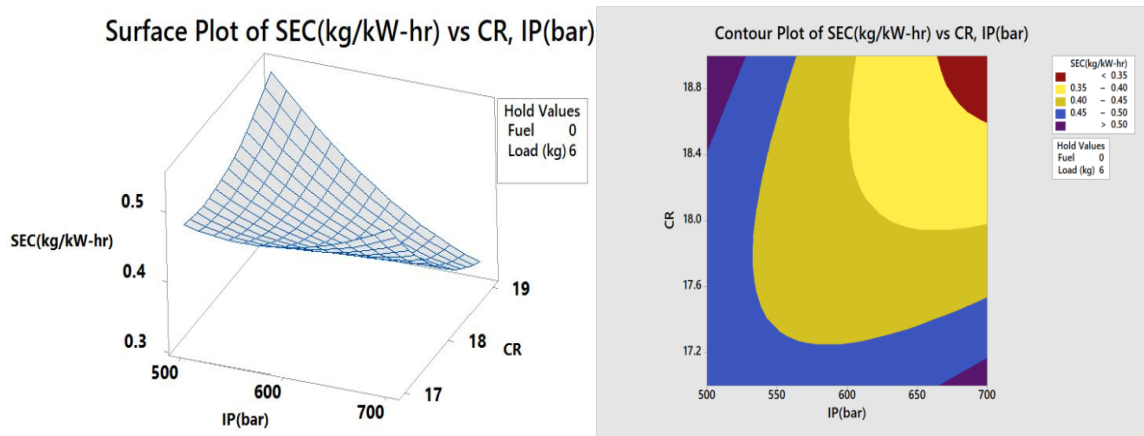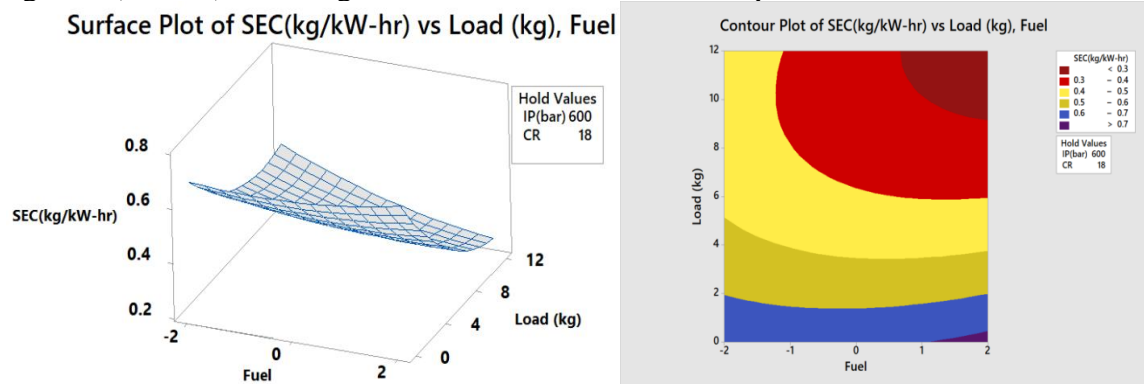

Fig. 4.34 Three dimensional plot depicts the impact of IP and CR and their combined effect on the specific fuel consumption.

The impact of increasing injection pressure and compression ratio on SFC is depicted in Figure 4.34, with load held at 6 kg and fuel addition at 0. At high CR, SFC decreases as injection pressure increases. This is attributed to the increased spray pressure and faster mixing time (air/fuel), resulting in a reduced amount of fuel required for combustion.
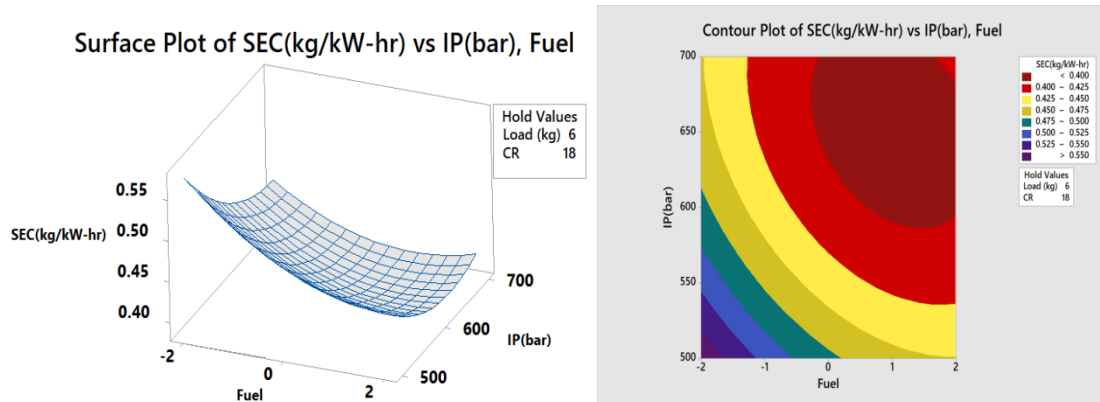

Fig. 4.35 Three dimensional plot depicts the impact of fuel and load and their combined effect on the specific fuel consumption.

The contour plot presented in Figure 4.35 illustrates the impact of load and nanoparticle ratio on specific fuel consumption. Notably, for the high load range, more pronounced variations in Specific Fuel Consumption (SFC) are observed compared to low loads, as depicted in the contour diagram [237]. Figure 4.36 displays the SFC trend with Injection Pressure (IP) and fuel concentration at a constant compression ratio and load. The contour diagram indicates that SFC decreases with an increased content of nanoparticles and injection pressure.

Fig. 4.36 Three dimensional plot depicts the impact of fuel and IP and their combined effect on the specific fuel consumption.

Higher injection pressure facilitates proper atomization, penetration, swirl ratio, dispersion, and mixing of fuel, accelerating combustion and consequently reducing ignition delay [238]. The SFC curve exhibits a slight increase and decrease at lower and higher IP, respectively, with an increasing content of nanoparticles, while parameters such as load (6 kg) and compression ratio (18) remain constant.

4.5.4.2 Effect of engine inputs variables on Brake thermal efficiency (BTE)

Brake Thermal Efficiency (BTE) is a specific parameter that assesses the engine's performance, representing the energy obtained by multiplying the lower heating value by the mass flow rate of injected fuel, known as fuel conversion efficiency. The contour and surface plot in Figure 4.37 illustrate the influence of nanoparticle content and Compression Ratio (CR) on BTE, with load held at 6 kg and Injection Pressure (IP) at 600 bar. The BTE curve exhibits an increase with the addition of nanoparticles in biofuel and an increase in compression ratio. The addition of nanoparticles signifies improved combustion and effective transfer of fuel energy to productive work. The increased surface-to-volume ratio of nanoparticles leads to better heat transmission, generating additional energy inside the cylinder. The findings indicate that BTE is enhanced by raising the compression ratio [239]. A higher compression ratio results in increased pressure and temperature in the cylinder, facilitating faster fuel evaporation and releasing more energy from the combustion of the same amount of fuel. This enhancement in combustion efficiency contributes to the observed increase in BTE [240]. Additionally, due to the high heating value of nanofuel, a higher nanoparticle content in the fuel leads to maximum brake thermal efficiency. Figure 4.38 illustrates the effect of Injection Pressure (IP) on BTE, showing an increment in BTE with increasing IP. Higher IP reduces the size of fuel droplets during injection, enabling faster fuel evaporation and better mixing with the surrounding air. This improvement in combustion efficiency contributes to the elevation of BTE [241].
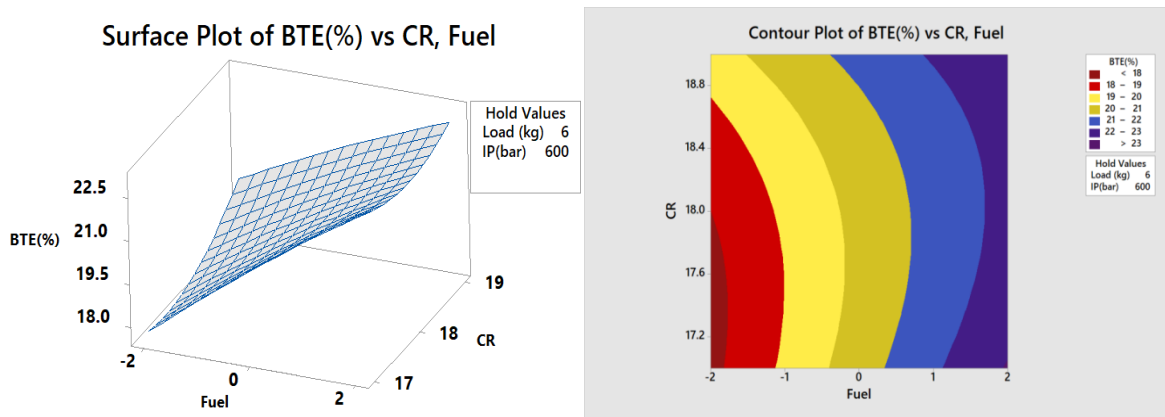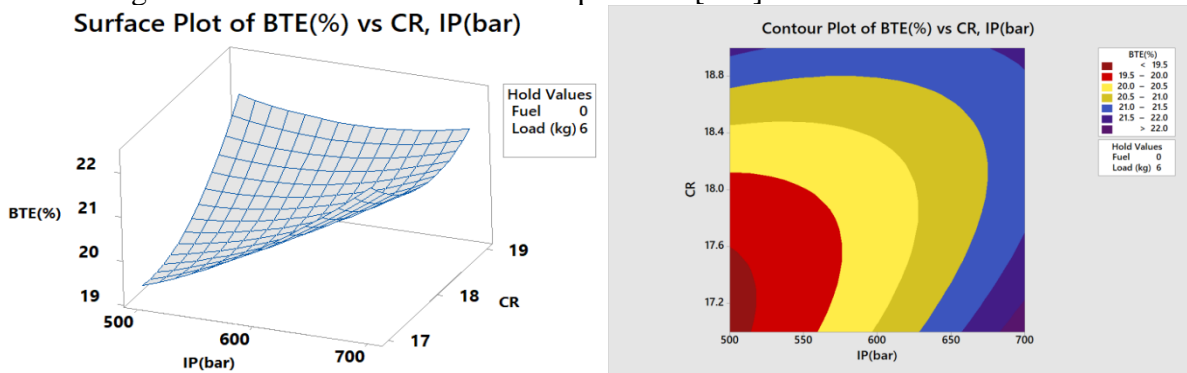
Fig. 4.37 Three dimensional plot depicts the impact of fuel and CR and their combined impact on the brake thermal efficiency.

The contour plot in Figure 4.39 illustrates the impact of load and nanofuel on Brake Thermal Efficiency (BTE) with Compression Ratio (CR) held at 18 and Injection Pressure (IP) at 600 bar. BTE of the engine is enhanced with increasing load and the content of metallic nanoparticles. The observed improvement in BTE with nanoparticle augmentation is attributed to the more complete combustion of the test fuel, facilitated by the high surface-to-volume ratio of nanoparticles [242].

Fig. 4.38 Three dimensional plot depicts the impact of IP and CR and their combined impact on the brake thermal efficiency.
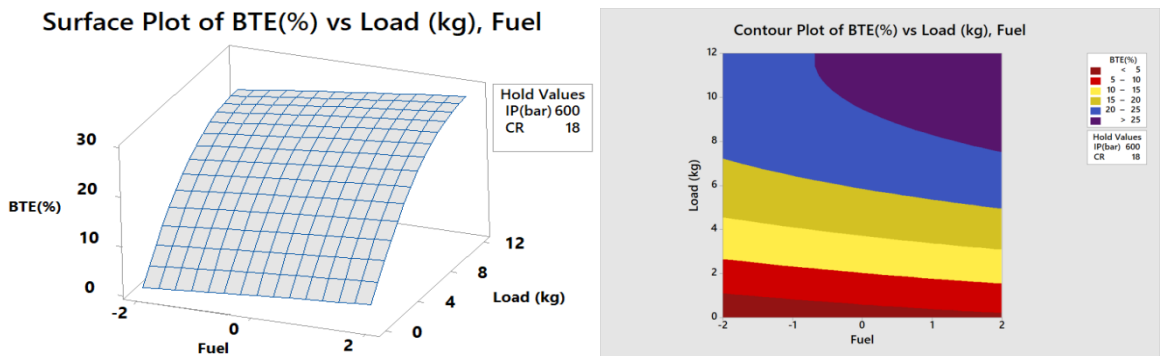

Fig. 4.39 Three dimensional plot depicts the impact of fuel and load and their combined impact on the brake thermal efficiency.
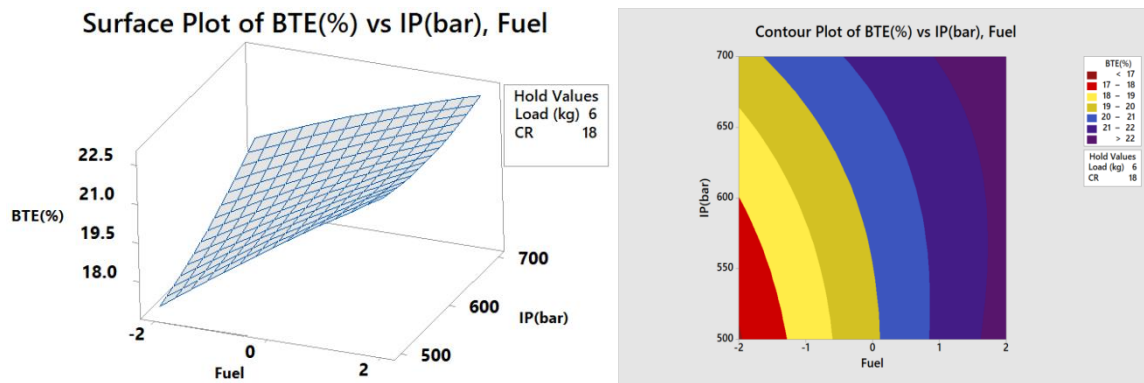
Fig. 4.40 Three dimensional plot depicts the impact of fuel and IP and their combined impact on the brake thermal efficiency.

Figure 4.40 depicts the increasing curve of BTE with increasing IP and nanofuel content. The enhancement in brake thermal efficiency with nanoparticles and increased IP is attributed to improved fuel atomization, dispersion, and mixing, contributing to more efficient combustion.

4.5.5 Emission characteristics

4.5.5.1 Effect of engine inputs variables on CO emissions

The main contributor to the generation of carbon monoxide is the partial combustion of fuel. Changes in carbon monoxide concerning Compression Ratio (CR) and nanofuel are depicted in Figure 4.41. The inclusion of nanoparticle content resulted in a reduction in carbon monoxide levels due to enhanced and more complete combustion. Metallic nanoparticles play a role as oxidation catalysts, converting carbon monoxide into CO_2 during combustion. Additionally, metallic nanoparticles induce the secondary atomization of fuel [243]. The contour diagram illustrates a decreasing trend in CO emissions with a higher content of nanoparticles at high CR.

The impact of CR and Injection Pressure (IP) is presented in the contour diagram in Figure 4.42. IP exhibits a more significant impact on CO emissions than CR, with a greater decrease observed with successive increases in IP. The higher injection pressure of fuel induces proper atomization, leading to improved air-fuel mixing, dispersion, penetration, and swirl ratio [244]. Notably, both IP and CR significantly influence CO emissions.
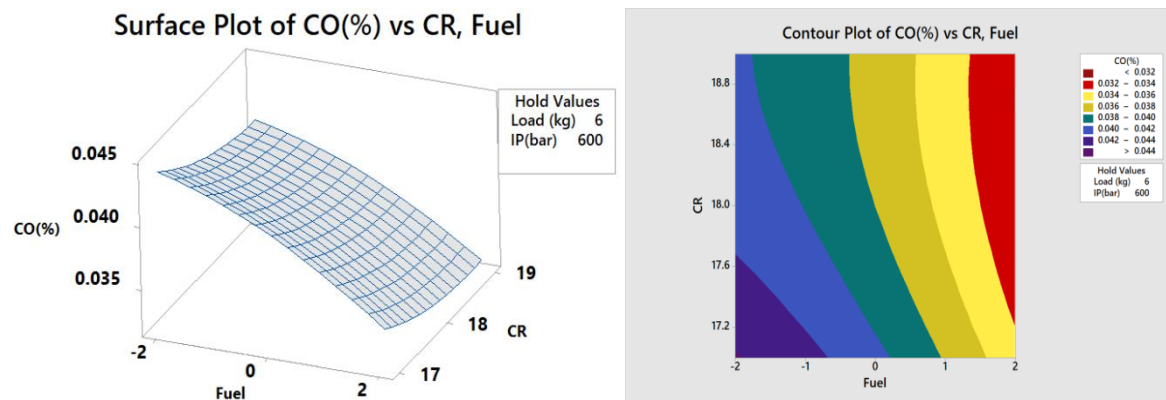

Fig. 4.41 Three dimensional plot depicts the impact of fuel and CR and their combined impact on the CO emissions
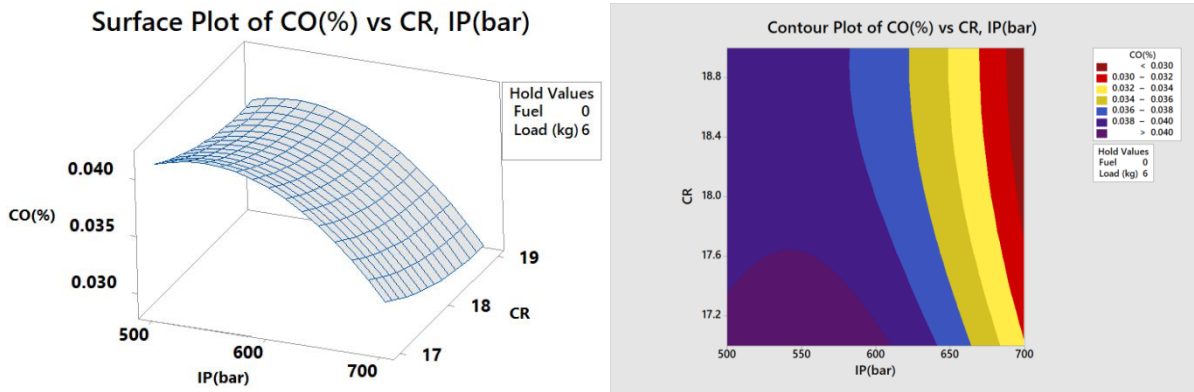
Fig. 4.42 Three dimensional plot depicts the impact of IP and CR and their combined impact on the CO emissions

CO emission diminishes with the addition of nanoparticles in B20. Combustion is suitably accomplished by increasing IP and nanoparticle ratios. The variation in CO utilizing load and Al_2O_3 content is displayed in Fig. 4.44. At higher load combustion temperature and pressure increase which enables the higher flame temperature of ignition, consequently supporting improved combustion [164].
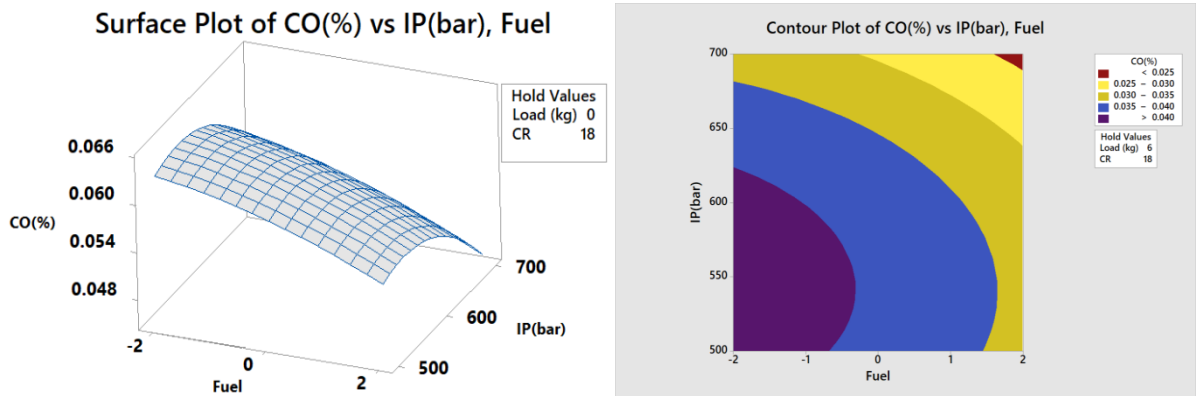

Fig. 4.43 Three dimensional plot depicts the impact of IP and fuel and their combined impact on the CO emissions
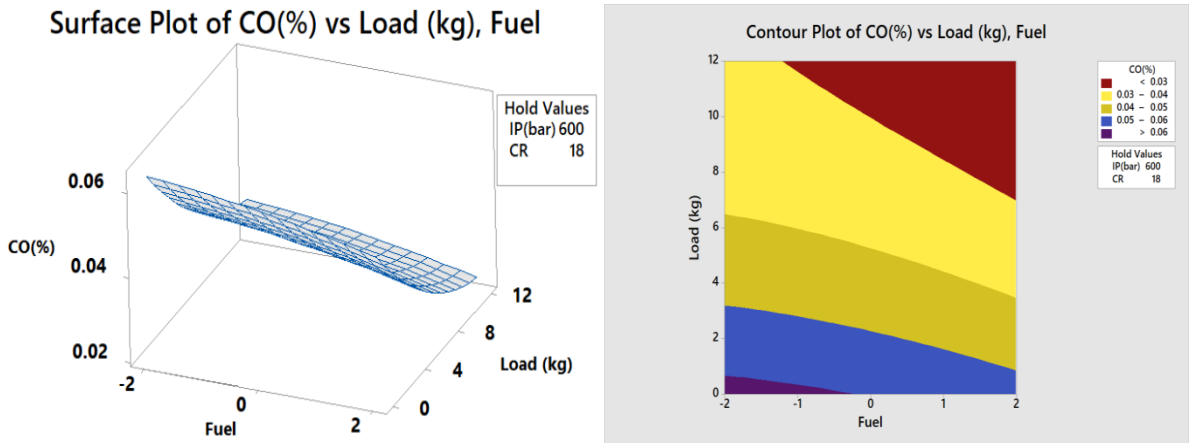

Fig. 4.44 Three dimensional plot depicts the impact of load and fuel and their combined impact on the CO emissions

4.5.5.2 Effect of engine input variables on HC emissions

The incomplete combustion of fuel particles leads to increased Hydrocarbon (HC) emissions. Figure 4.45 depicts HC emissions for different nanoparticle content in B20 and Compression Ratio (CR), with load held at 6 kg and Injection Pressure (IP) at 600 bar. It was observed that there is a slight increment in HC emissions with an increased ratio of nanoparticles. This is likely due to the unburned portion of the charge lingering because of the high specific heat capacity of nanoparticles. When using biodiesel as fuel, HC emissions were observed to be lower compared to other test fuels, possibly attributed to the good ignition of fuel, credited to the higher oxygen content in the biofuel molecular structure. Figure 4.46 illustrates the impact of engine load and nanoparticle ratio in biodiesel on HC emissions. The presence of nanoparticles in biodiesel led to a reduction in HC emissions, as they lowered the activation temperature of carbon and promoted ignition [245]. Concerning IP and CR, HC decreased, as increased IP resulted in proper atomization of fuel and reduced evaporation of fuel droplets, promoting better combustion. Similarly, a higher compression ratio decreased HC emissions due to increased in-cylinder temperature, pressure, and flame velocity [244, 245]. Figure 4.47 shows that higher CR and IP decreased HC emissions, with the possibility of increased HC levels due to flame quenching and deficient ignition resulting from the lower flame speed of fuel ignition [246]. Figure 4.48 depicts a decrease in HC emissions at high IP and CR. HC emissions with IP and fuel are displayed in Figure 4.48, with CR held at 18 and load at 6 kg. Unexpectedly, at higher IP, the highest nanoparticle ratio fuel ignition resulted in a decrease in HC levels. Notably, higher nanoparticle content in biodiesel at higher IP of the engine is a suitable parameter for decreasing HC emissions.
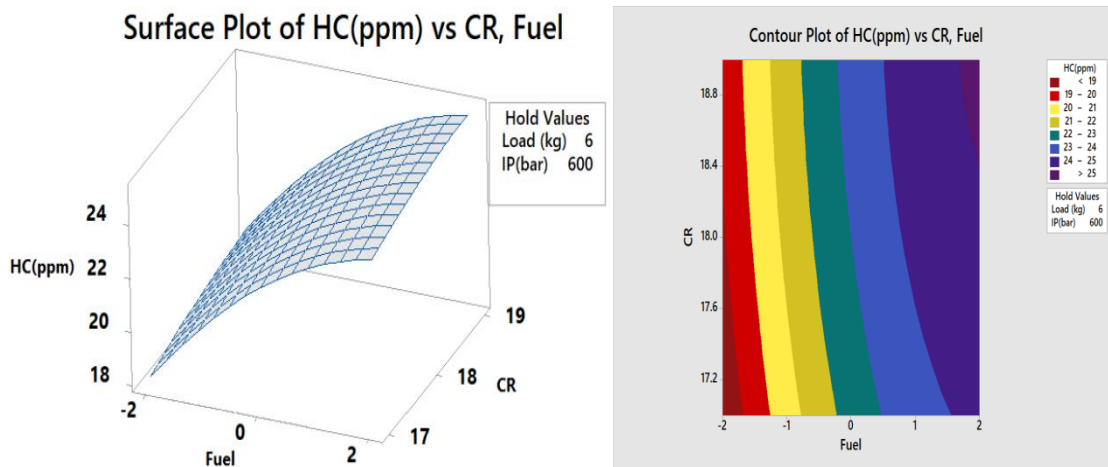

Fig. 4.45 Three dimensional plot depicts the impact of CR and fuel and their combined impact on the HC emissions
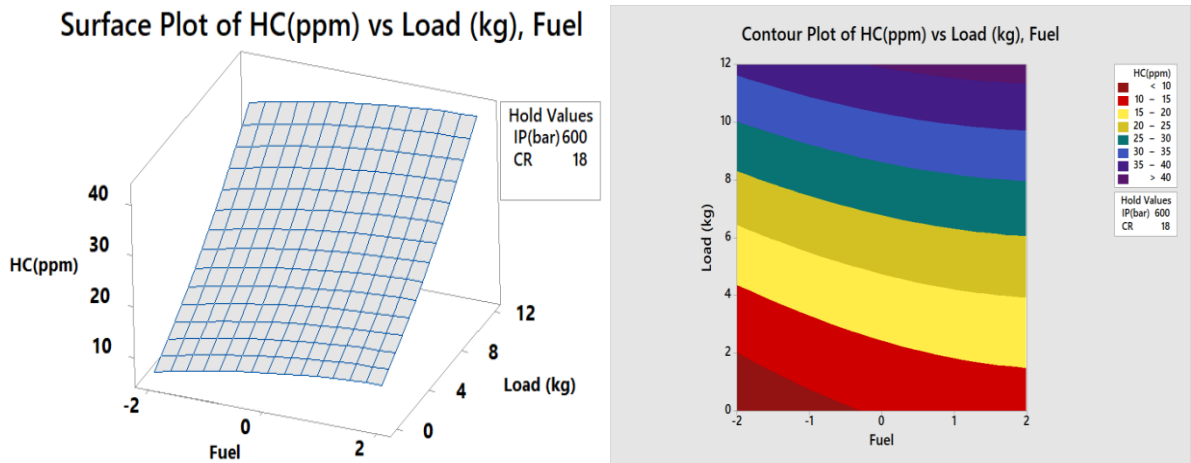
Fig. 4.46 Three dimensional plot depicts the impact of load and fuel and their combined impact on the HC emissions
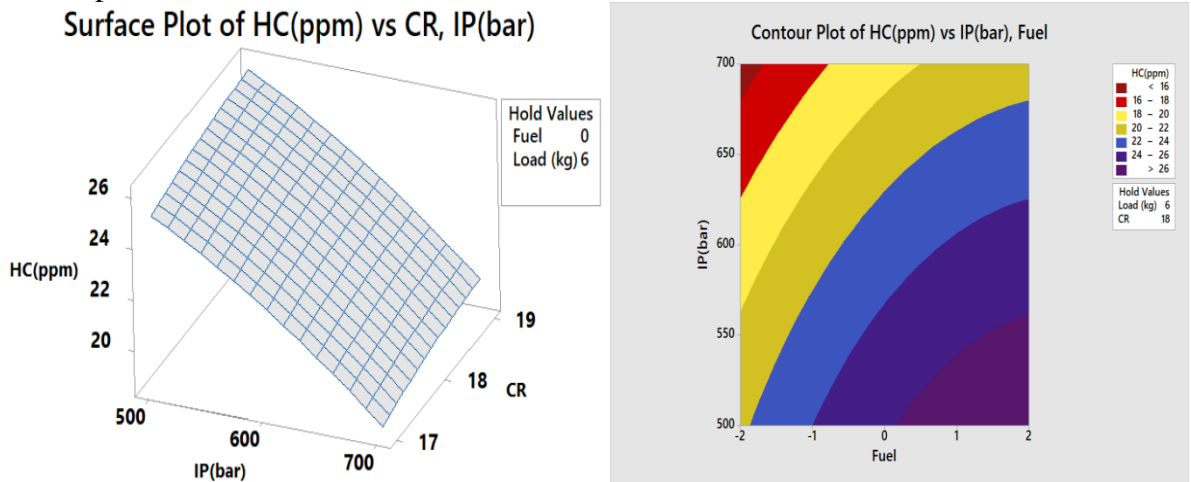

Fig. 4.47 Three dimensional plot depicts the impact of CR and IP and their combined impact on the HC emissions
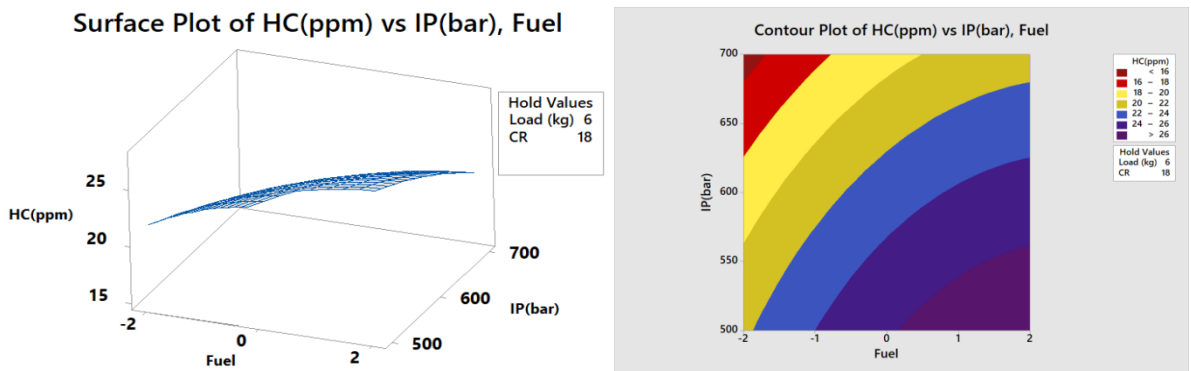

Fig. 4.48 Three dimensional plot depicts the impact of fuel and IP and their combined impact on the HC emissions.

4.5.5.3 NOx emissions

The enriched oxygen present in biodiesel contributes to high temperatures during combustion, leading to elevated Nitrogen Oxides (NOx) emissions. Figure 4.49 illustrates the emission of nitrogen oxides with nanobiofuel and Compression Ratio (CR). NOx shows a slight increment with an increase in nanoparticle concentration in biodiesel, attributed to metallic nanoparticles acting as an oxygen catalyst for combustion at higher temperatures. Additionally, higher cylinder pressure, temperature, and heat release rate contribute to increased NOx emissions [245]. The successive increase in NOx emission with CR could be attributed to the higher pressure and temperature of combustion in the cylinder . NOx emissions are enhanced at high CR when load is held at 6 kg and IP at 600 bar, as shown in Figure 4.50. The contour diagram indicates that NOx emissions increase with the increment in engine load and CR. Figure 4.51 demonstrates the variation of NOx emissions with nanofuel and load. Load has a more significant impact on NOx emissions than nanoparticle content in B20, as a higher quantity of fuel accumulates at high load inside the cylinder, resulting in a high-temperature flame of combustion. NOx is produced at higher temperatures [147]. The variation of NOx with different injection pressure and nanoparticle content in B20 is displayed in Figure 4.52. Fuel injection pressure increases NOx emissions more than nanoparticle concentration. This is because higher injection pressure induces complete combustion of better-atomized fuel with the same ignition delay, enabling ignition at higher temperatures [247]. NOx increased for the nano-alumina fuel blend compared to B20, as the increment in nanoparticle ratio encourages rapid premixed ignition and an increase in burning temperature, resulting in higher NOx emissions. The impact of oxygenated nanoparticles intensifies combustion and decreases the ignition lag.

Fig. 4.49 Three dimensional plot depicts the impact of fuel and CR and their combined impact on NOx emissions

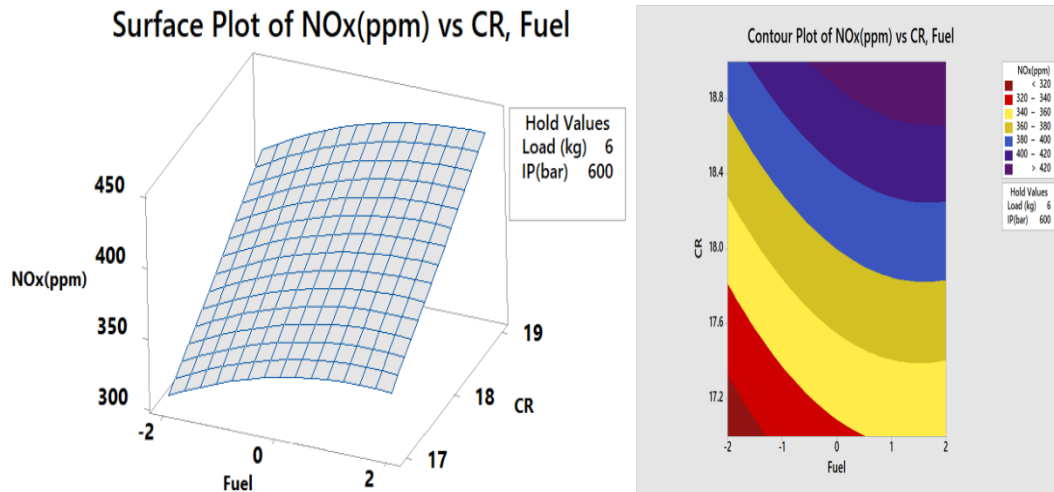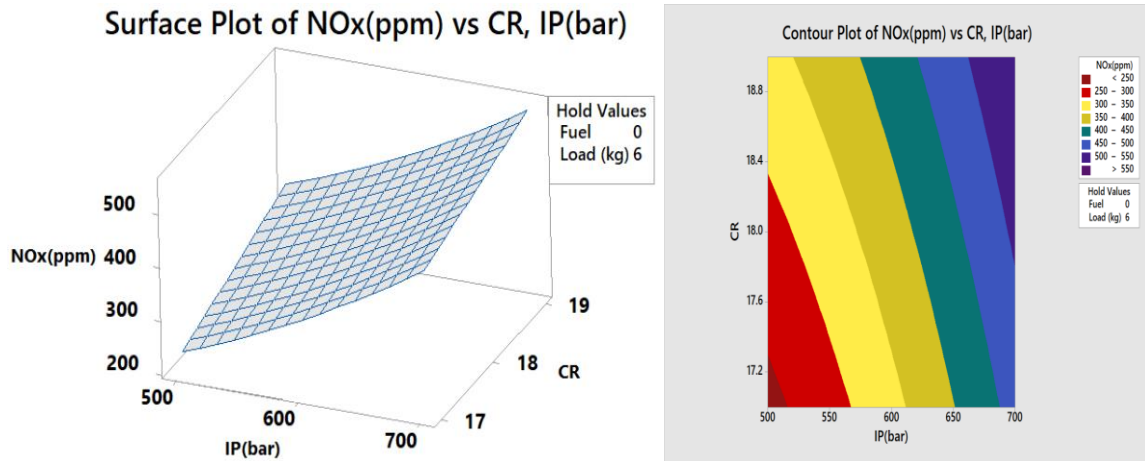Fig. 4.50 Three dimensional plot depicts the impact of IP and CR and their combined impact on NOx
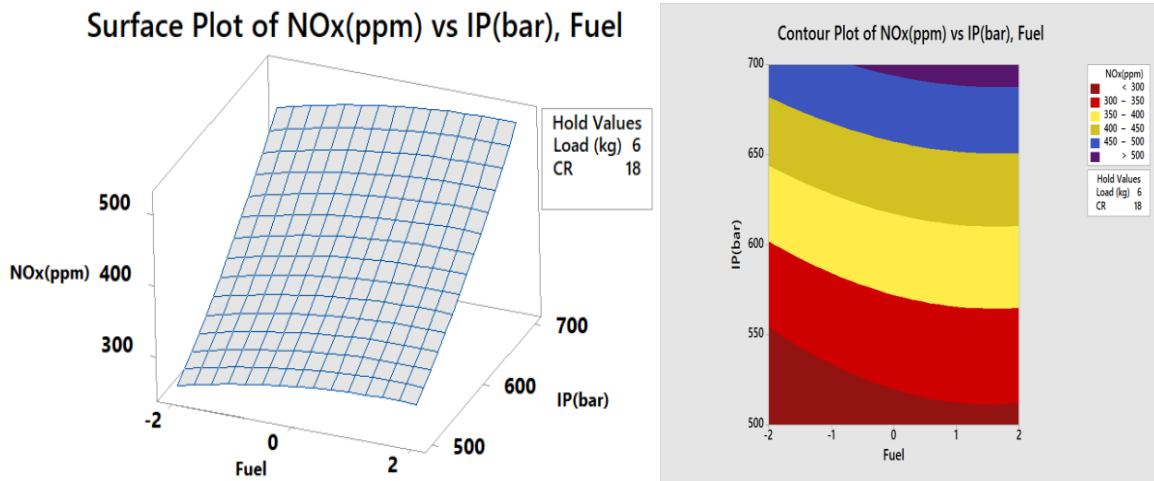

Fig. 4.51**:** Three dimensional plot depicts the impact of fuel and IP and their combined impact on NOx emissions
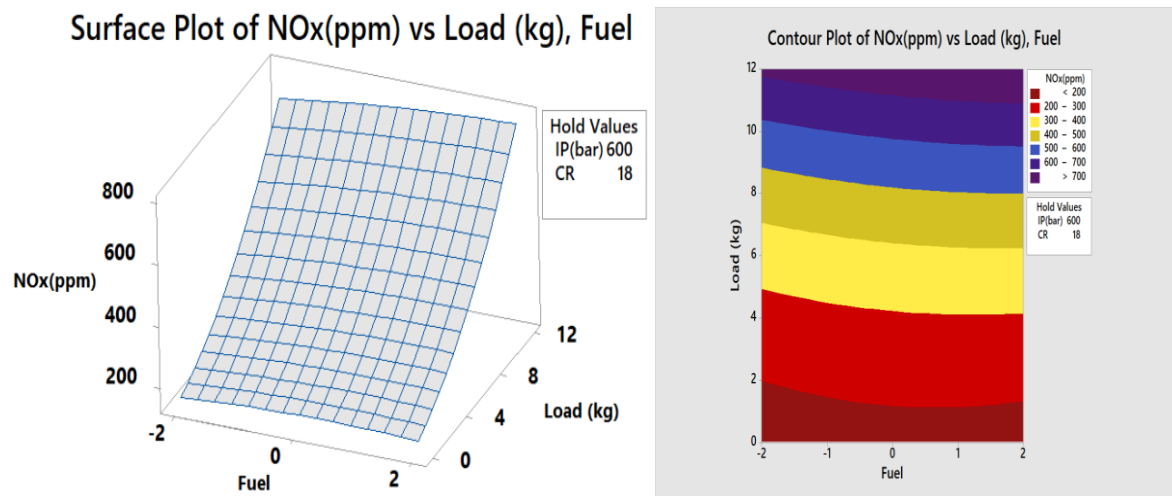

Fig.4.52 Three dimensional plot depicts the impact of fuel and load and their combined impact on NOx

4.5.6 Optimizing engine responses

The optimization of engine operating parameters in this study was carried out using the RSM optimizer in MINITAB17 software, which is a versatile multi-objective optimization tool. This software proved effective in achieving the optimization strategy successfully. The identification of input engine variables was crucial for optimizing multi-objective responses, including brake thermal efficiency, brake-specific fuel consumption, and emission components such as carbon monoxide (CO), hydrocarbon emissions (HC), and NO_X emissions. The response surface methodology technique, employing the desirability approach, was used to optimize engine performance and emissions for various input variables such as fuel, Injection Pressure (IP), Compression Ratio (CR), and load. The Desirability Approach provided a systematic and practical way to handle multi-response optimization issues. The primary goal of optimization in this study was to maximize Brake Thermal Efficiency (BTE) and minimize Specific Fuel Consumption (SFC) and engine emissions when fueled with nanofuel under various operating conditions. After RSM optimization, the target engine responses were set as follows: BTE at 23.60%, SFC at 0.3461 kg/kWh, CO at 0.0281%, HC at 25.3756 ppm, and NOx at 536.41 ppm. The optimized engine input settings were determined as 7.10 kg load, 18.50 CR, 656 bar fuel injection pressure, and a 1.10 fuel (B20) blend with Al_2O_3 nanoparticles, as illustrated in Figure 5.53. The composite desirability of the overall system was found to be 0.6775, falling within acceptable limits.
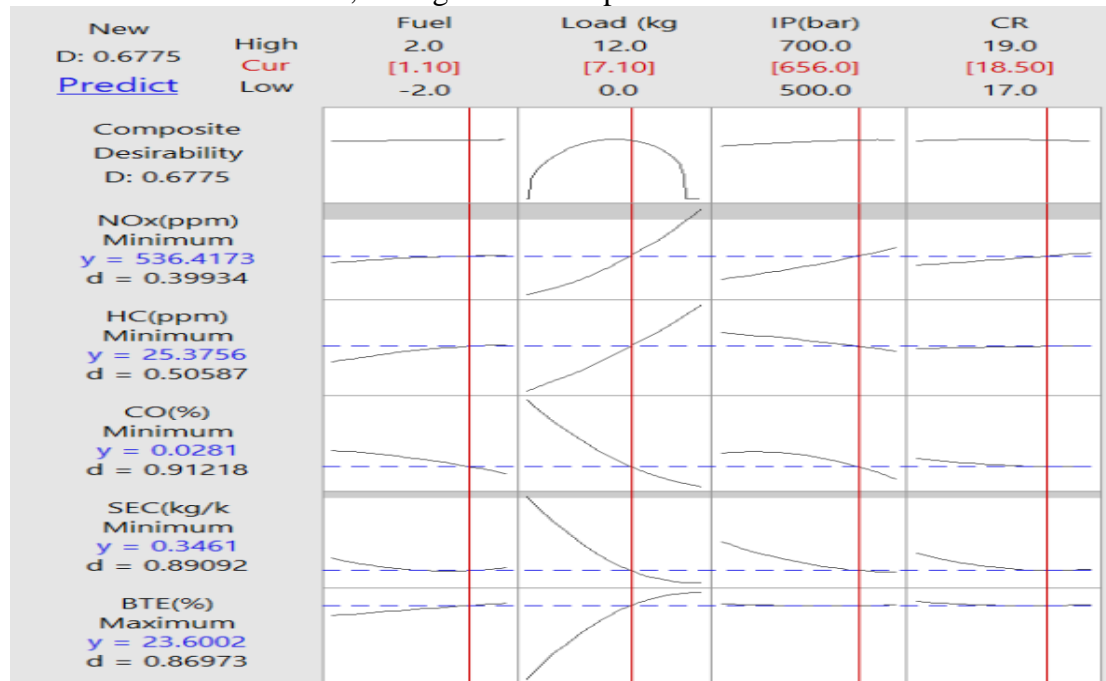
Fig. 4.53 Optimization of engine responses

4.5.7. Validation of optimization result with experimental results

The optimized results obtained through Response Surface Methodology (RSM) were validated through experimental trials on the engine. Engine tests were conducted using the optimal engine operating parameters determined by RSM, which included an Injection Pressure (IP) of 656 bar, Compression Ratio (CR) of 18.56, a load of 7.10 kg, and a fuel blend of 1.10. The engine performance and emissions, including Brake Thermal Efficiency (BTE),

Specific Fuel Consumption (SFC), carbon monoxide (CO), hydrocarbons (HC), and nitrogen oxides (NO_X), were measured and compared to the optimal RSM results as presented in Table 4.21.

The average error for the engine responses—BTE, SFC, CO, HC, and NO_X—was calculated as 2.9%, 1.04%, 6.04%, 1.5%, and 5.97%, respectively, using a standard method for error determination. These errors were found to be within an acceptable range, confirming the reliability and accuracy of the optimized results obtained through RSM.

Table 4.21 Comparative analysis of engine at optimised value

Best value under the RSM optimization method									
Optimization method	The best composition of the fuel	Engine operating parameter			Engine performance parameter		Engine emissions		
		IP (bar)	CR	Load (kg)	BTE (%)	SFC kJ/kg.hr	CO (%)	HC (ppm)	NOx (ppm)
RSM	1.10	656	18.50	7.10	23.60	0.3461	0.0281	25.37	536.41
The experimental result at the optimum parameter investigated by RSM									
Engine	Composition of fuel	IP (bar)	CR	Load (kg)	BTE (%)	SFC kJ/kg.hr	CO (%)	HC (ppm)	NO_X (ppm)
VCR CRDI engine	1.10	656	18.50	7.10	22.91	0.31	0.0267	24.98	504.34
Comparative analysis between optimization result and experimental result									
Engine responses	BTE (%)	SFC kJ/kg.hr		CO (%)		HC (ppm)		NOX (ppm)	
%Error	2.9	1.04		6.04		1.5		5.97	

The current study investigates the optimum engine input parameters for simultaneous performance and emission response. The optimum input parameters for optimising performance and emission behaviour are determined to be 1.10, 656bar, 18.50, and 7.10 for fuel, engine load, compression ratio, and fuel injection pressure.

CHAPTER 5
CONCLUSION AND FUTURE SCOPE

5.1 Conclusion

Biodiesel has proven to be a viable and sustainable alternative fuel for diesel engines. The compatibility of biodiesel with existing diesel engines is a significant advantage. Its chemical properties allow for a seamless integration into the existing infrastructure, requiring little to no modifications to diesel engines. Conventional vegetable oils have higher viscosity and density compared to petrodiesel, which can lead to challenges in atomization, combustion, and overall engine efficiency. the transesterification process stands as a crucial and transformative step in the production of biofuels, particularly biodiesel. This chemical reaction, where triglycerides from renewable sources like vegetable oils or animal fats react with an alcohol, such as methanol or ethanol, to yield biodiesel and glycerol, underscores the viability of sustainable alternatives to conventional fossil fuels. the viscosity reduction achieved via transesterification ensures that the resulting biodiesel physio-chemical properties are compatible to use into existing diesel infrastructure without requiring extensive engine modifications.

While vegetables are a source for a diesel engine but one of the primary concerns is the potential competition between using edible oils for food and for fuel. Using edible oils for biofuel could divert these resources away from the food supply chain, potentially leading to higher food prices and affecting vulnerable populations. Used cooking oil might be utilized as a biofuel due to it is a waste and does not impact consumable oil emergencies. In the present study waste cooking oil is converted into waste cooking biodiesel through transesterification process. After that its physio-chemical properties were checked that were lie in ASTM standards. Further, In the first stage of the current experimental study, waste cooking oil obtained from transesterification is mixed with diesel oil to prepare the B20 blend. B20 is a blend of 20% waste cooking methyl ester and 80% diesel. B20 is utilized as a fuel in a diesel engine to evaluate the engine performance and emissions. BTE and SFC are assessed for engine performance response. While HC, CO, CO_2, and NO_X emissions are evaluated for emission response. The engine input variables viz engine load are varied as 0-12kg. Throughout the experiment, the engine speed, fuel injection pressure, compression ratio, and injection timing are kept up at 1500 rpm, 14, 60 Mpa, and 30 ºbTDC. It was investigated from an experiment that B20 has slightly lower BTE and marginally higher SFC of diesel engines than pure diesel (D100) at all load conditions. In comparison to pure diesel, B20 also produced less emission of CO, CO_2, and UHC, except for NOx. That's why researchers are looking to investigate the technique to boost engine performance and reduce NO_X emissions for biodiesel.

Fuel modification by utilizing metallic nanoparticles as fuel additives with B20 may prove the best technique to boost engine performance and reduce emissions. Further, metallic nanoparticle Al_2O_3 was selected as a fuel additive to boost engine responses. With the use of an ultrasonicator, Al_2O_3 was blended homogenously in used cooking oil at various concentrations (25 ppm, 50 ppm, and 100 ppm) to create novel blends like $B20+25Al_2O_3$,

B20+50Al$_2$O$_3$, and B20+100Al$_2$O$_3$. The study assessed the performance and emissions of innovative fuel blends in a diesel engine operating at a constant speed of 1500 rpm, with fixed compression ratio (CR) at 14, injection pressure (IP) at 60 MPa, and injection timing (IT) at 30 degrees before top dead centre (^{o}bTDC).

The findings were compared to those obtained with conventional diesel oil and B20 biodiesel blend. The experimental analysis revealed that incorporating Al2O3 as a fuel additive in B20 biodiesel improved the engine performance and reduced emissions in the single-cylinder diesel engine. Based on the experimental findings, a summary of the results is provided.

- SFC of nanoparticles additives fuel (B20+100Al$_2$O$_3$) decreased and BTE increases significantly in contrast to B20 and pure diesel at all load conditions.
- CO, HC emissions with the addition of Al$_2$O$_3$ were decreased significantly. B20+100Al$_2$O$_3$ discharge lowest CO and HC emissions than B20, diesel and B20, diesel, B20+25Al$_2$O$_3$, and B20+50Al$_2$O$_3$ at all load conditions.
- However, there is a slight sustainable increment in oxides of nitrogen emissions of CI engine fuelled by B20+100Al$_2$O$_3$ than B20, diesel at high load condition.

Use of Al$_2$O$_3$ as a fuel additive with waste cooking oil improved the engine performance and engine emissions. These findings highlight the possibility of using a newly developed nanobiodiesel blend as an alternative renewable energy source.

In the next step Al$_2$O$_3$ and CeO$_2$ nanoparticle was used as fuel additives in B20 separately. Al$_2$O$_3$ and CeO$_2$ nanoparticle was mixed homogenously by ultrasonicator in B20 in different proportion (50ppm ,100ppm) to prepared new developed blends such as B20+50Al$_2$O$_3$, B20+50 CeO$_2$ B20+100Al$_2$O$_3$.and B20+100 CeO$_2$.. An engine of the CRDI VCR diesel type is fuelled by diesel, B20, B20+50Al$_2$O$_3$, B20+50 CeO$_2$ B20+100Al$_2$O$_3$.and B20+100 CeO$_2$. The engine compression ratio, injection pressure, and injection angle were 14, 60Mpa, and 30° respectively. Experiments were conducted at various engine loads (3, 6,9,12 kg) and a constant engine speed of 1500rpm. Results of an experimental investigation are listed below:

- In comparison to other blended fuels, B20+50 Al$_2$O$_3$ offer the highest BTE. The BTE of B20+50 Al$_2$O$_3$ has increased by 11.39% to B20 under peak loading conditions.
- At peak load, the SFC of nanoparticle additive fuel (B20+50 Al$_2$O$_3$) decreased by 13.74% compared to B20.
- It was observed that the cylinder pressure values for the blends B20+50 Al$_2$O$_3$ and B20+50 CeO$_2$ are 18.41% and 16.55% higher than B20 at 4° crank angle after TDC. The optimum pressure of blend B20 +50 Al$_2$O$_3$ is 16.77% higher than B20 at a 4° crank angle after TDC.
- Adding nanoparticles of Al$_2$O$_3$ and CeO$_2$ to biofuel increased the pressure in the cylinder. B20+50 Al$_2$O$_3$ has the highest peak pressure in comparison to B20 and diesel fuel. In addition, nanoparticles in B20 increased the heat release rate of the CI engine. Compared to other fuel samples, B20+50 Al$_2$O$_3$ has the highest heat release rate.
- Al$_2$O$_3$ and CeO$_2$ significantly reduced hydrocarbon and carbon monoxide emissions. B20+50 Al$_2$O$_3$ discharged the lowest CO and B20+50 CeO$_2$ produced the lowest HC emissions than other tested fuel samples.
- It was found that B20+50 Al$_2$O$_3$ has 15.06% lower CO emissions than B20 at peak load. At full load, the CO of Diesel, B20 +50 Al$_2$O$_3$, B20 +100 Al$_2$O$_3$, B20 +50 CeO$_2$ and B20 +100 CeO$_2$ are 0.036, 0.0312, 0.028, 0.0265, 0.03 and 0.029 respectively.

- B20+50 CeO$_2$ Produced 50 % lower emissions than diesel at peak load conditions. The average HC emissions is 86,42,44.3,43, 46.5 and 45ppm for the Diesel, B20 +50 Al$_2$O$_3$, B20 +100 Al$_2$O$_3$, B20 +50 CeO$_2$ and B20 +100 CeO$_2$ respectively.
- However, NOx emissions of the CI engine decreased slightly at the high load for B20+50 CeO$_2$ in comparison to other fuel blend.

Dispersion of Al$_2$O$_3$ and CeO$_2$ content in B20 improved the engine performance (BTE and SFC) and emissions significantly in compare to diesel and B20. An experimental result reveals that, Al$_2$O$_3$ addition in B20 impact significantly engine performance and emissions in compare to CeO$_2$ addition. Instead of it, addition of CeO$_2$ reduced slightly NO$_X$ emissions in compare to Al$_2$O$_3$. These outcomes support that Al2O3 nanopartcles is more effective to improve engine performance in compare to CeO$_2$ nanoparticles.

Further current study involved optimising CRDI single-cylinder four-stroke VCR engine responses under different input parameter. This study examines the impact of engine operating parameters IP, CR, load, and nanoparticle content in biodiesel on engine performance (BTE and SFC) and emissions (CO, HC, and NO$_X$). The responses of the CRDI VCR diesel engine are optimized to distinct engine input parameters using the response surface methodology. A numerical model was developed to analyze the engine BTE, BSFC, CO, HC, and NOx emissions. The analysis of variance and optimization results suggests that RSM is a powerful tool to optimize diesel engine responses at various input parameters. The results of the optimization study are given below:-

- R^2 values of BTE, SFC, CO, HC, and NO$_X$ emissions that have been determined are 97.89, 93.34, 95.68, 99.42, and 99.71%, separately. These values are within an acceptable range.
- The best input engine parameter found by RSM is 1.10 mixing of nanoparticles with B20, 18.50 CR, and 656 bar IP at an engine load of 7.10 kg load.
- In addition, The optimum value of BTE, SFC, CO, HC, and NO$_X$ is 23.60%, 0.3461kg/kWh, 0.0281%, 25.3756 ppm, and 536.41ppm, respectively at best-investigated engine inputs. This indicates that the model is statistically correct. Comparative analysis of RSM optimizes value and experimental trials show that errors are in an acceptable range.

Finally, it is determined that waste cooking biodiesel may be utilised as biodiesel in C.I. engines without any modifications and that waste cooking biodiesel can be utilized with Al2O3 as a fuel additive to improve engine responses.

5.2 Future scope

Nanoparticles, owing to their minute size and expansive surface area, manifest unique characteristics that hold potential to significantly influence various facets of biodiesel combustion and emissions within internal combustion engines. Drawing from insights gleaned in our ongoing experimental endeavours, several prospective future impacts of nanoparticles as fuel additives in biodiesel on engine performance and emissions emerge:

Exploration of Combined Blends: Incorporating combined blends of non-edible oils and waste cooking biodiesel is proposed as a strategy to enhance both performance and emissions behaviour.

Synergistic Use of Metallic Nanoparticles: Combining two metallic nanoparticles in varying ratios stands out as a promising avenue for augmenting engine performance.

Utilization of Organic Nanoparticles: Integration of organic nanoparticles into waste cooking biodiesel as fuel additives holds promise for mitigating nanoparticle emissions into the environment.

Composite Nanoparticle Additives: Utilizing a blend of organic nanoparticles alongside metallic and/or carbon nanotube nanoparticles could offer a viable means to enhance the performance of both diesel and biodiesel engines.

Diversified Experimental Parameters: While our current study employed a research diesel engine with a fixed injection timing of 23 ^{o}bTDC, future investigations should explore varying injection timings, angles, and nozzle diameters to comprehensively understand the influence of nanoparticles.

Integration of Computational Approaches: Employing computer-based and simulation-driven analyses holds potential for expanding our understanding and refining experimental findings.

Assessment of Long-Term Stability: A critical area for further exploration involves assessing the long-term stability of nanoparticles within fuel blends.

Nanoparticle Influence on Combustion Performance: Delving deeper into the role of nanoparticles in shaping combustion performance within diesel engines is essential for advancing our understanding.

Consideration of Manufacturing Costs and Risks: Research efforts should address the development of cost-effective manufacturing approaches for nanoparticles, alongside an exploration of the environmental and health risks associated with nanoparticle exposure.

By addressing these aspects, future research endeavours can unlock the full potential of nanoparticles as fuel additives in biodiesel, driving advancements in engine efficiency and emissions control while ensuring sustainable and safe implementation.

References

[1] U.S. Energy Information Administration, "Short-term energy outlook," 14 January 2019. Available: https://www.eia.gov/outlooks/steo/pdf/steo_full.pdf. (Accessed: 2018).

[2] L. Lyu and L. Fang, "A Study on EC Translation of BP Statistical Review of World Energy from the Perspective of Schema Theory," Journal of Linguistics and Communication Studies, vol. 2, no. 1, pp. 10-14, 2023.

[3] Renewable Energy Policy Network for the 21st Century, "Renewable Global Status Report," 12 February 2019. [Online]. Available: www.ren21.net. (Accessed: 2019).

[4] U.S. Energy Information Administration, "International Energy Outlook," 12 February 2019. Available: www.eia.

[5] N. Watts, M. Amann, S. Ayeb-Karlsson, K. Belesova, T. Bouley, M. Boykoff, and A. Costello, "The Lancet Countdown on health and climate change: from 25 years of inaction to a global transformation for public health," The Lancet, vol. 391, no. 10120, pp. 581-630, 2018.

[6] N. Watts, P. Gong, D. Campbell-Lendrum, A. Costello, and E. Robinson, "Health and climate change–Authors' reply," The Lancet, vol. 393, no. 10187, pp. 2197-2198, 2019.

[7] J. A. Leggett, "The United Nations framework convention on climate change, the Kyoto protocol, and the Paris agreement: a summary," UNFCC, New York, 2, 2019.

[8] P. Geng, E. Cao, Q. Tan, and L. Wei, "Effects of alternative fuels on the combustion characteristics and emission products from diesel engines: A review," Renewable and Sustainable Energy Reviews, vol. 71, pp. 523-, 2017.

[9] Li, F., Yi, B., Fu, W., Song, L., Liu, T., Hu, H., & Lin, Q. (2019). Experimental study on spray characteristics of long-chain alcohol-diesel fuels in a constant volume chamber. *Journal of the Energy Institute*, *92*(1), 94-107.

[10] Air pollution in India. (2022, December 3). In *Wikipedia*. https://en.wikipedia.org/wiki/Air pollution in India.

[11] H. Bakır, Ü. Ağbulut, A. E. Gürel, G. Yıldız, U. Güvenç, M. E. M. Soudagar, and A. Afzal, "Forecasting of future greenhouse gas emission trajectory for India using energy and economic indexes with various metaheuristic algorithms," Journal of Cleaner Production, vol. 360, p. 131946, 2022.

[12] A. Farooq, Jae J. Shafaghat, S-C. Jung, and Y-K. Park, "Enhanced stability of bio-oil and diesel fuel emulsion using Span 80 and Tween 60 emulsifiers," J Environ Manage, vol. 231, pp. 694–700, 2019.

[13] P. Friedlingstein et al., "Global carbon budget 2022," Earth System Science Data Discussions, 2022, pp. 1-159.

[14] C. Ngô and J. Natowitz, Our energy future: resources, alternatives and the environment. John Wiley & Sons, 2016.

[15] IEA, "Energy Technology Perspectives 2012," OECD Publishing, 2012.

[16] P. Gevorkian, Large-scale solar power systems: Construction and economics. Cambridge University Press, 2012.

[17] R. Gautam, Ansari, N. A. Thakur, P. Sharma, A. Singh, and Y. Singh, "Status of biofuel in India with production and performance characteristics: a review," International Journal of Ambient Energy, vol. 43, no. 1, pp. 61-77, 2022.

[18] R. D. Misra and M. S. Murthy, "Blending of additives with biodiesels to improve the cold flow properties, combustion and emission performance in a compression ignition engine: A review," Renewable and sustainable energy reviews, vol. 15, no. 5, pp. 2413-2422, 2011.

[19] M. Tariq, S. Ali, and N. Khalid, "Activity of homogeneous and heterogeneous catalysts, spectroscopic and chromatographic characterization of biodiesel: A review," Renewable and Sustainable Energy Reviews, vol. 16, no. 8, pp. 6303-6316, 2012.

[20] K. N. M. Zahri, A. Zulkharnain, S. Sabri, C. Gomez-Fuentes, and S. A. Ahmad, "Research trends of biodegradation of cooking oil in Antarctica from 2001 to 2021: A bibliometric analysis based on the Scopus database," International Journal of Environmental Research and Public Health, vol. 18, no. 4, p. 2050, 2021.

[21] E. G. Perkins and W. J. Visek, Eds., Dietary fats and health (No. 10). The American Oil Chemists Society, 1983.

[22] C. J. K. Henry and C. Chapman, Eds., The nutrition handbook for food processors. Elsevier, 2002.

[23] A. Kołakowska, Ed., Chemical and Functional Properties of Food Lipids. CRC Press, 2003.

[24] C. Adhikesavan, D. Ganesh, and V. C. Augustin, "Effect of quality of waste cooking oil on the properties of biodiesel, engine performance and emissions," Cleaner Chemical Engineering, vol. 4, p. 100070, 2022.

[25] V. V. Mody, R. Siwale, A. Singh, and H. R. Mody, "Introduction to metallic nanoparticles," Journal of Pharmacy and Bioallied Sciences, vol. 2, no. 4, p. 282, 2010.

[26] M. E. M. Soudagar et al., "The effect of nano-additives in diesel-biodiesel fuel blends: A comprehensive review on stability, engine performance, and emission characteristics," Energy Conversion and Management, vol. 178, pp. 146-177, 2018.

[27] C. S. Aalam and C. G. Saravanan, "Effects of nano metal oxide blended Mahua biodiesel on CRDI diesel engine," Ain Shams Engineering Journal, vol. 8, no. 4, pp. 689-696, 2017.

[28] M. H. U. Bhuiyan, R. Saidur, M. A. Amalina, R. M. Mostafizur, and A. K. M. S. Islam, "Effect of nanoparticles concentration and their sizes on surface tension of nanofluids," Procedia Engineering, vol. 105, pp. 431-437, 2015.

[29] S. Tanvir and L. Qiao, "Surface tension of nanofluid-type fuels containing suspended nanomaterials," Nanoscale Research Letters, vol. 7, pp. 1-10, 2012.

[30] M. S. Gad and S. Jayaraj, "A comparative study on the effect of nano-additives on the performance and emissions of a diesel engine run on Jatropha biodiesel," Fuel, vol. 267, p. 117168, 2020

[31] G. Gautam, N. Ansari, A. Sharma, and Y. Singh, "Development of the ethyl ester from jatropha oil through response surface methodology approach," Pollution, vol. 6, no. 1, pp. 135-147, 2020.

[32] M. N. Mahallati, "Advances in modelling saffron growth and development at different scales," in Saffron, Wood head Publishing, 2020, pp. 139-167.

[33] I. Ambat, V. Srivastava, and M. Sillanpää, "Recent advancement in biodiesel production methodologies using various feedstock: A review," Renewable and Sustainable Energy Reviews, vol. 90, pp. 356-369, 2018.

[34] R. French and S. Czernik, "Catalytic pyrolysis of biomass for biofuels production," Fuel Processing Technology, vol. 91, pp. 25–32, 2010.

[35] S. Singh and Dipti, "Biodiesel production through the use of different sources an characterization of oils and their esters as the substitute of diesel: a review," Renewable and Sustainable Energy Reviews, vol. 14, pp. 200–216, 2010.

[36] C. S. Singh, N. Kumar, and R. Gautam, "Thermal Cracking of Karanja de-oiled seed cake on Pyrolysis Reactor for producing Bio-oil with focus on its application in diesel Engine," in IOP Conference Series: Materials Science and Engineering, vol. 804, no. 1, April 2020, p. 012014. IOP Publishing.

[37] F. Ma and M. A. Hanna, "Biodiesel production: a review," Bioresource Technology, vol. 70, pp. 1–15, 1999.

[38] P. Mahanta and A. Shrivastava, "Technology development of bio-diesel as an energy alternative," Available from: http://newagepublishers.com/samplechapter/001305.pdf, 2004.

[39] A. Abbaszaadeh, B. Ghobadian, M. R. Omidkhah et al., "Current biodiesel production technologies: A comparative review," Energy Conversion and Management, vol. 63, pp. 138–148, 2012.

[40] A. Schwab, M. Bagby, and B. Freedman, "Preparation and properties of diesel fuels from vegetable oils," Fuel, vol. 66, pp. 1372–1378, 1987.

[41] W. Pairiawi, "Biodiesel production from Jatropha curcas: A review," Scientific Research Essays, vol. 5, pp. 1796–1808, 2010.

[42] A. Srivastava and R. Prasad, "Triglycerides-based diesel fuels," Renewable and Sustainable Energy Reviews, vol. 4, pp. 111–133, 2000.

[43] A. Bilgin, O. Durgun, and Z. Sahin, "The Effects of Diesel-Ethanol Blends on Diesel Engine Performance," Energy Sources, vol. 24, pp. 431–440, 2002.

[44] C. Mueanmas, K. Prasertsit, and C. Tongurai, "Feasibility study of reactive distillation column for transesterification of palm oils," International Journal of Chemical Engineering and Applications, vol. 1, no. 1, p. 77, 2010.

[45] A. A. Kiss, F. Omota, A. C. Dimian, and G. Rothenberg, "The heterogeneous advantage: biodiesel by catalytic reactive distillation," Topics in Catalysis, vol. 40, pp. 141-150, 2006.

[46] Y. S. Pradana, A. Hidayat, A. Prasetya, and A. Budiman, "Biodiesel production in a reactive distillation column catalyzed by heterogeneous potassium catalyst," Energy Procedia, vol. 143, pp. 742-747, 2017.

[47] R. J. Silva, I. C. Tschoeke, J. C. Melo et al., "Comparison between experimental and simulated results of biodiesel production by reactive distillation and energetic assessment," Brazilian Journal of Chemical Engineering, vol. 36, pp. 351-359, 2019.

[48] D. E. Clark and W. H. Sutton, "Microwave processing of materials," Annual Review of Materials Science, vol. 26, no. 1, pp. 299-331, 1996.

[49] S. Caddick and R. Fitzmaurice, "Microwave enhanced synthesis," Tetrahedron, vol. 65, no. 17, pp. 3325-3355, 2009.

[50] H. S. Ku, E. Siores, A. Taube, and J. A. Ball, "Productivity improvement through the use of industrial microwave technologies," Computers & Industrial Engineering, vol. 42, no. 2-4, pp. 281-290, 2002.

[51] A. De la Hoz, A. Diaz-Ortiz, and A. Moreno, "Microwaves in organic synthesis. Thermal and non-thermal microwave effects," Chemical Society Reviews, vol. 34, no. 2, pp. 164-178, 2005.

[52] B. A. Roberts and C. R. Strauss, "Toward rapid,"green", predictable microwave-assisted synthesis," Accounts of Chemical Research, vol. 38, no. 8, pp. 653-661, 2005.

[53] R. Varma, "Solvent-free organic syntheses. using supported reagents and microwave irradiation," Green chemistry, vol. 1, no. 1, pp. 43-55, 1999.

[54] R. J. Giguere, T. L. Bray, S. M. Duncan, and G. Majetich, "Application of commercial microwave ovens to organic synthesis," Tetrahedron letters, vol. 27, no. 41, pp. 4945-4948, 1986.

[55] V. G. Gude, P. Patil, E. Martinez-Guerra, S. Deng, and N. Nirmalakhandan, "Microwave energy potential for biodiesel production," Sustainable Chemical Processes, vol. 1, pp. 1-31, 2013.

[56] A. Demirbas, "Biodiesel from vegetable oils via transesterification in supercritical methanol," Energy conversion and management, vol. 43, no. 17, pp. 2349-2356, 2002.

[57] S. Karki, N. Sanjel, J. Poudel, J. H. Choi, and S. C. Oh, "Supercritical transesterification of waste vegetable oil: characteristic comparison of ethanol and methanol as solvents," Applied Sciences, vol. 7, no. 6, p. 632, 2017.

[58] Y. Alhassan, R. Gautam, N. Kumar, and I. M. Bugaje, "Non-Catalytic In-Situ Transesterification of Citrus Peel Waste into Biodiesel via Supercritical Technology: Optimization by Response Surface Methodology," 2014.

[59] C. S. Singh, N. Kumar, and R. Gautam, "Supercritical transesterification route for biodiesel production: Effect of parameters on yield and future perspectives," Environmental Progress & Sustainable Energy, vol. 40, no. 6, p. e13685, 2021.

[60] S. Hu, Y. Guan, Y. Wang, and H. Han, "Nano-magnetic catalyst KF/CaO–Fe3O4 for biodiesel production," Applied energy, vol. 88, no. 8, pp. 2685-2690, 2011.

[61] M. Naik, L. C. Meher, S. N. Naik, and L. M. Das, "Production of biodiesel from high free fatty acid Karanja (Pongamia pinnata) oil," Biomass and bioenergy, vol. 32, no. 4, pp. 354-357, 2008.

[62] R. Gautam, N. Kumar, H. S. Pali, and P. Kumar, "Experimental studies on the use of methyl and ethyl esters as an extender in a small capacity diesel engine," Biofuels, vol. 7, no. 6, pp. 637-646, 2016

[63] P. S. Yadav, Z. Said, R. Gautam, R. Raman, and H. Caliskan, "Novel investigation on atomization, performance, and emission characteristics of preheated jatropha oil methyl ester and ethyl ester," Energy, vol. 270, 126870, 2023.

[64] C. S. Aalam, C. G. Saravanan, and M. Kannan, "Experimental investigations on a CRDI system assisted diesel engine fuelled with aluminium oxide nanoparticles blended biodiesel," Alexandria engineering journal, vol. 54, no. 3, pp. 351-358, 2015.

[65] A. I. El-Seesy, A. M. Attia, and H. M. El-Batsh, "The effect of Aluminum oxide nanoparticles addition with Jojoba methyl ester-diesel fuel blend on a diesel engine performance, combustion and emission characteristics," Fuel, vol. 224, pp. 147-166, 2018.

[66] S. Gumus, H. Ozcan, M. Ozbey, and B. Topaloglu, "Aluminum oxide and copper oxide nanodiesel fuel properties and usage in a compression ignition engine," Fuel, vol. 163, pp. 80-87, 2016.

[67] R. Gautam, N. Ansari, A. Sharma, and Y. Singh, "Development of the ethyl ester from Jatropha oil through response surface methodology approach," Pollution, vol. 6, no. 1, pp. 135-147, 2020.

[68] G. Vicente, M. Martinez, and J. Aracil, "Optimization of integrated biodiesel production. Part I. A study of the biodiesel purity and yield," Bioresource technology, vol. 98, no. 9, pp. 1724-1733, 2007.

[69] M. K. Lam, K. T. Lee, and A. R. Mohamed, "Homogeneous, heterogeneous and enzymatic catalysis for transesterification of high free fatty acid oil (waste cooking oil) to biodiesel: a review," Biotechnology advances, vol. 28, no. 4, pp. 500-518, 2010.

[70] V. C. Eze, A. N. Phan, and A. P. Harvey, "A more robust model of the biodiesel reaction, allowing identification of process conditions for significantly enhanced rate and water tolerance," Bioresource technology, vol. 156, pp. 222-231, 2014.

[71] V. C. Eze, A. N. Phan, and A. P. Harvey, "Intensified one-step biodiesel production from high water and free fatty acid waste cooking oils," Fuel, vol. 220, pp. 567-574, 2018. https://doi.org/10.1016/J.FUEL.2018.02.050.

[72] P. S. Yadav and R. Gautam, "Numerical and experimental analysis on spray characteristics of biodiesel (waste cooking oil) using pressure swirl atomizer," Environmental Progress & Sustainable Energy, vol. 41, no. 3, e13761, 2022.

[73] P. K. Sahoo, L. M. Das, M. K. G. Babu, and S. N. Naik, "Biodiesel development from high acid value polanga seed oil and performance evaluation in a CI engine," Fuel, vol. 86, no. 3, pp. 448-454, 2007.

[74] V. R. Mamilla, M. V. Mallikarjun, and G. L. N. Rao, "Biodiesel production from palm oil by transesterification method," Int. J. Curr. Res, vol. 4, no. 8, pp. 83-88, 2012.

[75] G. Vicente, M. Martinez, and J. Aracil, "Optimisation of integrated biodiesel production. Part I. A study of the biodiesel purity and yield," Bioresource technology, vol. 98, no. 9, pp. 1724-1733, 2007.

[76] G. Baskar and R. Aiswarya, "Trends in catalytic production of biodiesel from various feedstocks," Renewable and sustainable energy reviews, vol. 57, pp. 496-504, 2016.

[77] K. Y. Wong, J. H. Ng, C. T. Chong, S. S. Lam, and W. T. Chong, "Biodiesel process intensification through catalytic enhancement and emerging reactor designs: A critical review," Renewable and Sustainable Energy Reviews, vol. 116, p. 109399, 2019.

[78] G. Vicente, M. Martınez, and J. Aracil, "Integrated biodiesel production: a comparison of different homogeneous catalysts systems," Bioresource technology, vol. 92, no. 3, pp. 297-305, 2004.

[79] N. Kondamudi, S. K. Mohapatra, and M. Misra, "Quintinite as a bifunctional heterogeneous catalyst for biodiesel synthesis," Applied Catalysis A: General, vol. 393, no. 1-2, pp. 36-43, 2011.

[80] A. A. Jazie, H. Pramanik, and A. S. K. Sinha, "Transesterification of peanut and rapeseed oils using waste of animal bone as cost effective catalyst," Mater Renew Sustain Energy, vol. 2, p. 11, 2013. https://doi.org/10.1007/s40243-013-0011-4.

[81] W. A. Kawentar and A. Budiman, "Synthesis of biodiesel from second-used cooking oil," Energy Procedia, vol. 32, pp. 190-199, 2013.

[82] S. K. Karmee and A. Chadha, "Preparation of biodiesel from crude oil of Pongamia pinnata," Bioresource technology, vol. 96, no. 13, pp. 1425-1429, 2005.

[83] E. Aransiola, E. Betiku, S. Layokun, and B. Solomon, "Production of biodiesel by transesterification of refined soybean oil," International Journal of Biological and Chemical Sciences, vol. 4, no. 2.

[84] A. K. Endalew, Y. Kiros, and R. Zanzi, "Inorganic heterogeneous catalysts for biodiesel production from vegetable oils," Biomass and bioenergy, vol. 35, no. 9, pp. 3787-3809, 2011.

[85] Y. T. Wang, Z. Fang, X. X. Yang, Y. T. Yang, J. Luo, K. Xu, and G. R. Bao, "One-step production of biodiesel from Jatropha oils with high acid value at low temperature by

magnetic acid-base amphoteric nanoparticles," Chemical Engineering Journal, vol. 348, pp. 929-939, 2018.

[86] K. V. Thiruvengadaravi, J. Nandagopal, P. Baskaralingam, V. Sathya Selva Bala, and S. Sivanesan, "Acid-catalyzed esterification of karanja (Pongamia pinnata) oil with high free fatty acids for biodiesel production," Fuel, vol. 98, pp. 1-4, 2012. https://doi.org/10.1016/J.FUEL.2012.02.047.

[87] S. N. Gebremariam and J. M. Marchetti, "Biodiesel production through sulfuric acid catalyzed transesterification of acidic oil: Techno economic feasibility of different process alternatives," Energy Conversion and Management, vol. 174, pp. 639-648, 2018.

[88] M. Canakci and J. Van Gerpen, "Biodiesel production from oils and fats with high free fatty acids," Transactions of the ASAE, vol. 44, no. 6, p. 1429, 2001.

[89] M. Di Serio, R. Tesser, M. Dimiccoli, F. Cammarota, M. Nastasi, and E. Santacesaria, "Synthesis of biodiesel via homogeneous Lewis acid catalyst," Journal of Molecular Catalysis A: Chemical, vol. 239, no. 1-2, pp. 111-115, 2005.

[90] Y. P. S. Yadav, A. A. Chaturwedi, A. Sahu, A. Yadav, A. Fraynjiya, and R. Gautam, "Effect of Nozzle Geometry and Fuel Modification on Atomization and Emission Characteristics in CI Engine: A Review," in Emerging Trends in Mechanical and Industrial Engineering: Select Proceedings of ICETMIE 2022, pp. 13-32, 2023. [91] G. Vicente, M. Martınez, and J. Aracil, "Integrated biodiesel production: a comparison of different homogeneous catalysts systems," Bioresource technology, vol. 92, no. 3, pp. 297-305, 2004.

[92] H. Cao, Z. Zhang, X. Wu, and X. Miao, "Direct biodiesel production from wet microalgae biomass of Chlorella pyrenoidosa through in situ transesterification," BioMed research international, 2013.

[93] A. Javidialesaadi and S. Raeissi, "Biodiesel production from high free fatty acid-content oils: experimental investigation of the pretreatment step," APCBEE procedia, vol. 5, pp. 474-478, 2013

[94] A. Sagiroglu, S. Ş. Isbilir, M. H. Ozcan, H. Paluzar, and N. M. Toprakkiran, "Comparison of biodiesel productivities of different vegetable oils by acidic catalysis," Chemical Industry and Chemical Engineering Quarterly/CICEQ, vol. 17, no. 1, pp. 53-58, 2011.

[95] H. Lu, Y. Liu, H. Zhou, Y. Yang, M. Chen, and B. Liang, "Production of biodiesel from Jatropha curcas L. oil," Computers & Chemical Engineering, vol. 33, no. 5, pp. 1091-1096, 2009.

[96] H. A. Farag, A. El-Maghraby, and N. A. Taha, "Optimization of factors affecting esterification of mixed oil with high percentage of free fatty acid," Fuel processing technology, vol. 92, no. 3, pp. 507-510, 2011. https://doi.org/10.1016/j.fuproc.2010.11.004.

[97] Z. Helwani, M. R. Othman, N. Aziz, J. Kim, and W. J. N. Fernando, "Solid heterogeneous catalysts for transesterification of triglycerides with methanol: a review," Applied Catalysis A: General, vol. 363, no. 1-2, pp. 1-10, 2009.

[98] K. Jacobson, R. Gopinath, L. C. Meher, and A. K. Dalai, "Solid acid catalyzed biodiesel production from waste cooking oil," Applied Catalysis B: Environmental, vol. 85, no. 1-2, pp. 86-91, 2008.

[99] N. Mansir, Y. H. Taufiq-Yap, U. Rashid, and I. M. Lokman, "Investigation of heterogeneous solid acid catalyst performance on low-grade feedstocks for biodiesel production: A review," Energy Conversion and Management, vol. 141, pp. 171-182, 2017.

[100] M. R. Avhad and J. M. Marchetti, "A review on recent advancement in catalytic materials for biodiesel production," Renewable and sustainable energy reviews, vol. 50, pp. 696-718, 2015.

[101] A. Bajaj, P. Lohan, P. N. Jha, and R. Mehrotra, "Biodiesel production through lipase catalyzed transesterification: an overview," Journal of Molecular Catalysis B: Enzymatic, vol. 62, no. 1, pp. 9-14, 2010.

[102] K. T. Chen, J. X. Wang, Y. M. Dai, P. H. Wang, C. Y. Liou, C. W. Nien, et al., "Rice husk ash as a catalyst precursor for biodiesel production," Journal of the Taiwan Institute of Chemical Engineers, vol. 44, no. 4, pp. 622-629, 2013.

[103] X. Mo, E. Lotero, C. Lu, Y. Liu, and J. G. Goodwin, "A novel sulfonated carbon composite solid acid catalyst for biodiesel synthesis," Catalysis Letters, vol. 123, pp. 1-6, 2008.

[104] N. Viriya-Empikul, P. Krasae, W. Nualpaeng, B. Yoosuk, and K. Faungnawakij, "Biodiesel production over Ca-based solid catalysts derived from industrial wastes," Fuel, vol. 92, no. 1, pp. 239-244, 2012.

[105] Q. Shu, J. Gao, Z. Nawaz, Y. Liao, D. Wang, and J. Wang, "Synthesis of biodiesel from waste vegetable oil with large amounts of free fatty acids using a carbon-based solid acid catalyst," Applied Energy, vol. 87, no. 8, pp. 2589-2596, 2010.

[106] A. Birla, B. Singh, S. N. Upadhyay, and Y. C. Sharma, "Kinetics studies of the synthesis of biodiesel from waste frying oil using a heterogeneous catalyst derived from snail shell," Bioresource Technology, vol. 106, pp. 95-100, 2012.

[107] A. R. Yacob, M. K. A. A. Mustajab, and N. S. Samadi, "Calcination temperature of nano MgO effect on base transesterification of palm oil," International Journal of Chemical and Molecular Engineering, vol. 3, no. 8, pp. 408-412, 2009.

[108] J. Ji, J. Wang, Y. Li, Y. Yu, and Z. Xu, "Preparation of biodiesel with the help of ultrasonic and hydrodynamic cavitation," Ultrasonics, vol. 44, pp. e411-e414, 2006.

[109] J. P. Mikkola and T. Salmi, "Three-phase catalytic hydrogenation of xylose to xylitol—prolonging the catalyst activity by means of on-line ultrasonic treatment," Catalysis Today, vol. 64, no. 3-4, pp. 271-277, 2001.

[110] H. H. Mardhiah, H. C. Ong, H. H. Masjuki, S. Lim, and H. V. Lee, "A review on latest developments and future prospects of heterogeneous catalyst in biodiesel production from non-edible oils," Renewable and sustainable energy reviews, vol. 67, pp. 1225-1236, 2017.

[111] B. Fu, L. Gao, L. Niu, R. Wei, and G. Xiao, "Biodiesel from waste cooking oil via heterogeneous super acid catalyst SO42−/ZrO2," Energy & Fuels, vol. 23, no. 1, pp. 569-572, 2009.

[112] S. H. Teo, A. Islam, F. L. Ng, and Y. H. Taufiq-Yap, "Biodiesel synthesis from photoautotrophic cultivated oleoginous microalgae using a sand dollar catalyst," RSC Advances, vol. 5, no. 58, pp. 47140-47152, 2015.

[113] Y. Liu and T. J. Pinnavaia, "Assembly of wormhole aluminosilicate mesostructures from zeolite seeds," Journal of Materials Chemistry, vol. 14, no. 7, pp. 1099-1103, 2004.

[114] G. R. Chauhan, B. S. Chauhan, and H. C. Lim, "Influence of variation of injection angle on the combustion, performance and emissions characteristics of jatropha ethyl ester," Energy, vol. 254, p. 124436, 2022.

[115] S. K. Hoekman and C. Robbins, "Review of the effects of biodiesel on NOx emissions," Fuel Processing Technology, vol. 96, pp. 237-249, 2012.

[116] G. Knothe, "Dependence of biodiesel fuel properties on the structure of fatty acid alkyl esters," Fuel processing technology, vol. 86, no. 10, pp. 1059-1070, 2005.

[117] J. Orsavova, L. Misurcova, J. V. Ambrozova, R. Vicha, and J. Mlcek, "Fatty acids composition of vegetable oils and its contribution to dietary energy intake and dependence of cardiovascular on dietary intake of fatty acids," Int. J. Mol. Sci., vol. 16, no. 6, pp. 12871-12890, 2015. [Online]. Available: https://doi.org/10.3390/ijms160612871.

[118] S. K. Saroj, R. Gautam, and N. Shubhendu, "Reduction of free fatty acid of Jatropha oil using Taguchi approach," Int. J. Sci. Eng. Appl. Sci. (IJSEAS), vol. 2, no. 9.

[119] A. J. Folayan, P. A. L. Anawe, A. E. Aladejare, and A. O. Ayeni, "Experimental investigation of the effect of fatty acids configuration, chain length, branching and degree of unsaturation on biodiesel fuel properties obtained from lauric oils, high-oleic and high-linoleic vegetable oil biomass," Energy Reports, vol. 5, pp. 793-806, 2019.

[120] T. Řezanka and H. Řezanková, "Characterization of fatty acids and triacylglycerols in vegetable oils by gas chromatography and statistical analysis," Analytica chimica acta, vol. 398, no. 2-3, pp. 253-261, 1999.

[121] R. Gautam and N. Kumar, "Effect of ethanol addition on the properties of Jatropha ethyl ester," Energy Sources, Part A: Recovery, Utilization, and Environmental Effects, vol. 38, no. 23, pp. 3464-3469, 2016.

[122] R. D. Lanjekar and D. Deshmukh, "A review of the effect of the composition of biodiesel on NOx emission, oxidative stability and cold flow properties," Renewable and Sustainable Energy Reviews, vol. 54, pp. 1401-1411, 2016.

[123] S. M. Palash, M. A. Kalam, H. H. Masjuki, B. M. Masum, I. R. Fattah, and M. Mofijur, "Impacts of biodiesel combustion on NOx emissions and their reduction approaches," Renewable and Sustainable Energy Reviews, vol. 23, pp. 473-490, 2013.

[124] G. Lakshmi Narayana Rao, B. Durga Prasad, S. Sampath, and K. Rajagopal, "Combustion analysis of diesel engine fueled with jatropha oil methyl ester-diesel blends," International Journal of Green Energy, vol. 4, no. 6, pp. 645-658, 2007.

[125] M. Kumar, V. K. Singh, A. Sharma, N. A. Ansari, R. Gautam, and Y. Singh, "Effect of fuel injection pressure and EGR techniques on various engine performance and emission characteristics on a CRDI diesel engine when run with linseed oil methyl ester," Energy & Environment, vol. 33, no. 1, pp. 41-63, 2022.

[126] R. Gautam and N. Kumar, "Comparative assessment of performance, emission and combustion characteristics of blends of methyl and ethyl ester of jatropha oil and diesel in compression ignition engine," SAE Technical Paper, 2013-01-2664, https://doi.org/10.4271/2013-01-2664, 2013.

[127] R. Gautam and N. Kumar, "Comparative study of performance and emission characteristics of Jatropha alkyl ester/butanol/diesel blends in a small capacity CI engine," Biofuels, vol. 6, no. 3-4, pp. 179-190, 2015, DOI: 10.1080/17597269.2015.1068081.

[128] A. Shirneshan, "HC, CO, CO2, and NOx emission evaluation of a diesel engine fueled with waste frying oil methyl ester," Procedia-Social and Behavioral Sciences, vol. 75, pp. 292-297, 2013.

[129] A. N. Ozsezen, M. Canakci, A. Turkcan, and C. Sayin, "Performance and combustion characteristics of a DI diesel engine fueled with waste palm oil and canola oil methyl esters," Fuel, vol. 88, no. 4, pp. 629-636, 2009.

[130] R. Gautam and S. Kumar, "Performance and combustion analysis of diesel and tallow biodiesel in CI engine," Energy Reports, vol. 6, pp. 2785-2793, 2020.

[131] M. Özkan, "Comparative study of the effect of biodiesel and diesel fuel on a compression ignition engine's performance, emissions, and its cycle-by-cycle variations," Energy & Fuels, vol. 21, no. 6, pp. 3627-3636, 2007.

[132] R. Gautam, B. S. Chauhan, and H. C. Lim, "Influence of variation of injection angle on the combustion, performance and emissions characteristics of jatropha ethyl ester," *Energy*, vol. 254, 124436, 2022.

[133] S. Godiganur, C. H. S. Murthy, and R. P. Reddy, "6BTA 5.9 G2-1 Cummins engine performance and emission tests using methyl ester Mahua (Madhuca Indica) oil/ diesel blends," Renew Energy, vol. 34, pp. 2172–7, 2009.

[134] P. K. Srivastava and M. Verma, "Methyl ester of Karanja oil as an alternative renewable source of energy," Fuel, vol. 87, no. 8-9, pp. 1673-1677, 2008.

[135] V. Palash, M. A. Kalam, H. H. Masjuki, B. M. Masum, I. R. Fattah, and M. Mofijur, "Effect of coconut biodiesel blended fuels on engine performance and emission characteristics," Procedia Engineering, vol. 56, pp. 583-590, 2013.

[136] A. M. Abed, A. K. El Morsi, M. M. Sayed, A. A. El Shaib, and M. S. Gad, "Effect of waste cooking-oil biodiesel on performance and exhaust emissions of a diesel engine," Egyptian journal of petroleum, vol. 27, no. 4, pp. 985-989, 2018.

[137] C. Adhikesavan, D. Ganesh, and V. C. Augustin, "Effect of quality of waste cooking oil on the properties of biodiesel, engine performance and emissions," Cleaner Chemical Engineering, vol. 4, p. 100070, 2022.555

[138] R. C. Singh, R. Chaudhary, R. K. Pandey, S. Maji, A. Babbar, B. S. Chauhan, R. Gautam, et al., "Performance evaluation of an air-cooled diesel engine fuelled with neat neem oil and diesel blends," 2012.

[139] U. Rajak, T. S. Singh, T. N. Verma, P. K. Chaurasiya, S. Shaik, A. Afzal, and C. A. Saleel, "Experimental and parametric studies on the effect of waste cooking oil methyl ester with diesel fuel in compression ignition engine," Sustainable Energy Technologies and Assessments, vol. 53, p. 102705, 2022.

[140] D. Singh, D. Sharma, S. L. Soni, C. S. Inda, S. Sharma, P. K. Sharma, and A. Jhalani, "A comprehensive review of biodiesel production from waste cooking oil and its use as fuel in compression ignition engines: 3rd generation cleaner feedstock," Journal of Cleaner Production, vol. 307, p. 127299, 2021.

[141] S. Bhan, R. Gautam, and P. Singh, "An experimental assessment of combustion, emission, and performance behavior of a diesel engine fueled with a newly developed biofuel blend of two distinct waste cooking oils and metallic nanoparticle (Al2O3)," *Scientia Iranica*, vol. 29, no. 4, pp. 1853-1867, 2022

[142] Y. Ulusoy, R. Arslan, Y. Tekin, A. Sürmen, A. Bolat, and R. Şahin, "Investigation of performance and emission characteristics of waste cooking oil as biodiesel in a diesel engine," Petroleum Science, vol. 15, pp. 396-404, 2018.

[143] T. Mahmood, S. Hassan, A. Sheikh, A. Raheem, and A. Hameed, "Experimental Investigations of Diesel Engine Performance Using Blends of Distilled Waste Cooking Oil Biodiesel with Diesel and Economic Feasibility of the Distilled Biodiesel," Energies, vol. 15, no. 24, p. 9534, 2022.

[144] P. Yadav, N. Kumar, and R. Gautam, "Improvement in performance of CI engine using various techniques with alternative fuel," Energy Sources, Part A: Recovery, Utilization, and Environmental Effects, pp. 1-27, 2021.

[145] M. Kumar and N. A. Ansari, "Investigation of combustion, performance and emission of aluminium oxide nanoparticles as additives in CI engine fuels: a review," in Advances in Manufacturing and Industrial Engineering: Select Proceedings of ICAPIE 2019, 2021, pp. 1055-1063.

[146] S. Bhan, R. Gautam, P. Singh, and A. Sharma, "A comprehensive review of performance, combustion, and emission characteristics of biodiesel blend with nanoparticles in diesel engines," in Recent Trends in Thermal Engineering: Select Proceedings of ICCEMME 2021, pp. 73-88, 2022.

[147] A. M. Abdallah, A. A. Abdel-Rahman, and A. E. Elwardany, "Analysis of the impact of different nanoparticle metal oxides as fuel additives in compression ignition engine performance," Energy Reports, vol. 6, pp. 99-105, 2020.

[148] S. S. Hoseini, G. Najafi, B. Ghobadian, M. T. Ebadi, R. Mamat, and T. Yusaf, "Biodiesels from three feedstock: The effect of graphene oxide (GO) nanoparticles diesel engine parameters fuelled with biodiesel," Renewable Energy, vol. 145, pp. 190-201, 2020.

[149] Y. Devarajan, B. Nagappan, and S. Subbiah, "A comprehensive study on emission and performance characteristics of a diesel engine fueled with nanoparticle-blended biodiesel," Environmental Science & Pollution Research, vol. 26, no. 11, pp. 10662-10672, 2019.

[150] S. A. Razek, M. S. Gad, and O. M. Thabet, "Effect of aluminium oxide nano-particle in jatropha biodiesel on performance, emissions and combustion characteristics of DI diesel engine," International Journal for Research in Applied Science & Engineering Technology, vol. 5, no. 4, pp. 358-372, 2017.

[151] J. Sadhik Basha and R. B. Anand, "Effects of nanoparticle additive in the water-diesel emulsion fuel on the performance, emission and combustion characteristics of a diesel engine," International Journal of Vehicle Design, vol. 59, no. 2/3, pp. 164-181, 2012.

[152] M. K. Abbass and B. F. Sultan, "Effect of Al2O3 nanoparticles on corrosion behaviour of aluminium alloy (Al-4.5 wt% Cu-1.5 wt% Mg) fabricated by powder metallurgy," Engineering Structures & Technologies, vol. 11, no. 1, pp. 25-31, 2019.

[153] S. Kumar, P. Dinesha, and M. A. Rosen, "Effect of injection pressure on the combustion, performance and emission characteristics of a biodiesel engine with cerium oxide nanoparticle additive," Energy, vol. 185, pp. 1163-1173, 2019.

[154] D. Rangabashiam, J. V, and A. Rameshbabu, "Emission, performance, and combustion study on nanoparticle-biodiesel fueled diesel engine," Energy Sources, Part A: Recovery, Utilization, and Environmental Effects, vol. 45, no. 3, pp. 8396-8407, 2023.

[155] P. Anchupogu, L. N. Rao, and B. Banavathu, "Effect of alumina nano additives into biodiesel-diesel blends on the combustion performance and emission characteristics of a diesel engine with exhaust gas recirculation," Environmental Science and Pollution Research, vol. 25, pp. 23294-23306, 2018.

[156] V. Perumal and M. Ilangkumaran, "The influence of copper oxide nano particle added pongamia methyl ester biodiesel on the performance, combustion and emission of a diesel engine," Fuel, vol. 232, pp. 791-802, 2018.

[157] A. F. Chen, M. A. Adzmi, A. Adam, M. F. Othman, M. K. Kamaruzzaman, and A. G. Mrwan, "Combustion characteristics, engine performances and emissions of a diesel engine using nanoparticle-diesel fuel blends with aluminium oxide, carbon nanotubes and silicon oxide," Energy Conversion and Management, vol. 171, pp. 461-477, 2018.

[158] K. Nanthagopal, B. Ashok, A. Tamilarasu, J. Ajith, and M. Aravind, "Influence on the effect of zinc oxide and titanium dioxide nanoparticles as an additive with Calophyllum inophyllum methyl ester in a CI engine," Energy Convers Manag, vol. 146, pp. 8–19, 2017.

[159] S. Karthikeyan, A. Elango, and A. Prathima, "The effect of cerium oxide additive on the performance and emission characteristics of a CI engine operated with rice bran biodiesel and its blends," International Journal of Green Energy, vol. 13, no. 3, pp. 267-273, 2016.

[160] A. Anbarasu, A. Karthikeyan, and M. Balaji, "Performance and emission characteristics of diesel engine using alumina nanoparticle blended biodiesel emulsion fuel," Journal of Energy Resources Technology, vol. 138, no. 2, p. 022203, 2016.

[161] A. C. Sajeevan and V. Sajith, "Synthesis of stable cerium zirconium oxide nanoparticle–Diesel suspension and investigation of its effects on diesel properties and smoke," Fuel, vol. 183, pp. 155-163, 2016.

[162] A. K. Pandian, R. B. B. Ramakrishnan, and Y. Devarajan, "Emission analysis on the effect of nanoparticles on neat biodiesel in unmodified diesel engine," Environmental Science and Pollution Research, vol. 24, pp. 23273-23278, 2017.

[163] A. K. Agarwal, A. Dhar, J. G. Gupta, W. I. Kim, C. S. Lee, and S. Park, "Effect of fuel injection pressure and injection timing on spray characteristics and particulate size–number distribution in a biodiesel fuelled common rail direct injection diesel engine," Applied Energy, vol. 130, pp. 212-221, 2014.

[164] M. E. M. Soudagar, N. N. Nik-Ghazali, M. A. Kalam, I. A. Badruddin, N. R. Banapurmath, and N. Akram, "The effect of nano-additives in diesel-biodiesel fuel blends: A comprehensive review on stability, engine performance and emission characteristics," Energy Conversion and Management, vol. 178, pp. 146-177, 2018.

[165] A. M. Attia, A. I. El-Seesy, H. M. El-Batsh, and M. S. Shehata, "Effects of alumina nanoparticles additives into jojoba methyl ester-diesel mixture on diesel engine performance," in ASME International Mechanical Engineering Congress and Exposition, 2014, p. V06BT07A019.

[166] A. S. Aalam, C. G. Saravanan, and M. Kannan, "Experimental investigation on CRDI system assisted diesel engine fulled by diesel with nanotubes," American Journal of Engineering and Applied Sciences, vol. 8, no. 3, p. 380, 2015.

[167] R. Gautam, N. Kumar, and P. Sharma, "Comparative assessment of performance, emission and combustion characteristics of blends of methyl and ethyl ester of jatropha oil and diesel in compression ignition engine," SAE Technical Paper, 2013-01-2664, 2013.

[168] M. E. M. Soudagar, M. A. Mujtaba, M. R. Safaei, A. Afzal, W. Ahmed, N. R. Banapurmath, and S. N. Taqui, "Effect of Sr@ ZnO nanoparticles and Ricinus communis biodiesel-diesel fuel blends on modified CRDI diesel engine characteristics," Energy, vol. 215, p. 119094, 2021.

[169] C. S. Harsha, T. Suganthan, and S. Srihari, "Performance and emission characteristics of diesel engine using biodiesel-diesel-nanoparticle blends-an experimental study," Materials Today: Proceedings, vol. 24, pp. 1355-1364, 2020.

[170] V. Singh, T. Agarwal, N. Saroha, and R. Gautam, "Performance emissions and combustion analysis of CI engine using ethyl ester kusum oil and butanol blends," SAE Technical Paper, 2019-01-0568, 2019.

[171] S. Uslu, "Optimization of diesel engine operating parameters fueled with palm oil-diesel blend: Comparative evaluation between response surface methodology (RSM) and artificial

neural network (ANN)," Fuel, vol. 276, p. 117990, 2020. [Online]. Available: https://doi.org/10.1016/j.fuel.2020.117990.

[172] S. Kumar and P. Dinesha, "Optimization of engine parameters in a bio diesel engine run with honge methyl ester using response surface methodology," Measurement, vol. 125, pp. 224-231, 2018.

[173] A. Sharma, H. S. Pali, M. Kumar, N. K. Singh, Y. Singh, and D. Singh, "Study the effect of optimized input parameters on a CRDI diesel engine running with waste frying oil methyl ester-diesel blend fuel with ZnO nanoparticles: a response surface methodology approach," Biomass Conversion and Biorefinery, vol. 13, no. 14, pp. 13127-13152, 2023.

[174] A. Sharma, H. S. Pali, M. Kumar, N. K. Singh, E. A. Rahim, Y. Singh, and N. K. Gupta, "Effect of α-aluminum oxide nano additives with Sal biodiesel blend as a potential alternative fuel for existing DI diesel engine," Energy & Environment, pp. 0958305X221133257, 2022.

[175] Z. Win, R. P. Gakkhar, S. C. Jain, and M. Bhattacharya, "Parameter optimization of a diesel engine to reduce noise, fuel consumption, and exhaust emissions using response surface methodology," Proceedings of the Institution of Mechanical Engineers, Part D: Journal of Automobile Engineering, vol. 219, no. 10, pp. 1181-1192, 2005.

[176] R. Reitz and J. Von der Ehe, "Use of in-cylinder pressure measurement and the response surface method for combustion feedback control in a diesel engine," Proceedings of the Institution of Mechanical Engineers, Part D: Journal of Automobile Engineering, vol. 220, no. 11, pp. 1657-1666, 2006.

[177] C. A. Laforet, B. S. Brown, S. N. Rogak, and S. R. Munshi, "Compression ignition of directly injected natural gas with entrained diesel," International Journal of Engine Research, vol. 11, no. 3, pp. 207-218, 2010.

[178] T. Agrawal, R. Gautam, S. Agrawal, V. Singh, M. Kumar, and S. Kumar, "Optimization of engine performance parameters and exhaust emissions in compression ignition engine fueled with biodiesel-alcohol blends using Taguchi method, multiple regression and artificial neural network," Sustainable Futures, vol. 2, p. 100039, 2020.

[179] M. Ghanbari, L. Mozafari-Vanani, M. Dehghani-Soufi, and A. Jahanbakhshi, "Effect of alumina nanoparticles as additive with diesel–biodiesel blends on performance and emission characteristic of a six-cylinder diesel engine using response surface methodology (RSM)," Energy Conversion and Management: X, vol. 11, p. 100091, 2021.

[180] O. Khan, M. Z. Khan, B. K. Bhatt, M. T. Alam, and M. Tripathi, "Multi-objective optimization of diesel engine performance, vibration and emission parameters employing blends of biodiesel, hydrogen and cerium oxide nanoparticles with the aid of response surface methodology approach," International Journal of Hydrogen Energy, vol. 48, no. 56, pp. 21513-21529, 2023.

[181] H. Fayaz, M. A. Mujtaba, M. E. M. Soudagar, L. Razzaq, S. Nawaz, M. A. Nawaz, and A. Elfasakhany, "Collective effect of ternary nano fuel blends on the diesel engine performance and emissions characteristics," Fuel, vol. 293, p. 120420, 2021.

[182] P. M. Rastogi, A. Sharma, and N. Kumar, "Effect of CuO nanoparticles concentration on the performance and emission characteristics of the diesel engine running on jojoba (Simmondsia Chinensis) biodiesel," Fuel, vol. 286, p. 119358, 2021.

[183] C. Srinidhi, A. Madhusudhan, S. V. Channapattana, S. V. Gawali, and K. Aithal, "RSM based parameter optimization of CI engine fuelled with nickel oxide dosed Azadirachta indica methyl ester," Energy, vol. 234, p. 121282, 2021.

[184] S. Uslu, S. Simsek, and H. Simsek, "RSM modeling of different amounts of nano-TiO2 supplementation to a diesel engine running with hemp seed oil biodiesel/diesel fuel blends," Energy, vol. 266, p. 126439, 2023.

[185] S. A. Mirbagheri, S. M. S. Ardebili, and M. K. D. Kiani, "Modeling of the engine performance and exhaust emissions characteristics of a single-cylinder diesel using nano-biochar added into ethanol-biodiesel-diesel blends," Fuel, vol. 278, p. 118238, 2020.

[186] M. Kumar, N. A. Ansari, A. Sharma, V. K. Singh, R. Gautam, and Y. Singh, "Prediction of an optimum engine response based on different input parameters on common rail direct injection diesel engine: A response surface methodology approach," Scientia Iranica, vol. 28, no. 6, pp. 3181-3200, 2021.

[187] F. Hussain, M. E. M. Soudagar, A. Afzal, M. A. Mujtaba, I. R. Fattah, B. Naik, and S. A. Rahman, "Enhancement in combustion, performance, and emission characteristics of a diesel engine fueled with Ce-ZnO nanoparticle additive added to soybean biodiesel blends," Energies, vol. 13, no. 17, p. 4578, 2020.

[188] A. A. Yusuf, H. Dandakouta, I. Yahuza, D. A. Yusuf, M. A. Mujtaba, A. S. El-Shafay, and M. E. M. Soudagar, "Effect of low CeO2 nanoparticles dosage in biodiesel-blends on combustion parameters and toxic pollutants from the common-rail diesel engine," Atmospheric Pollution Research, vol. 13, no. 2, p. 101305, 2022.

[189] S. S. Lam, W. A. W. Mahari, C. K. Cheng, R. Omar, C. T. Chong, and H. A. Chase, "Recovery of diesel-like fuel from waste palm oil by pyrolysis using a microwave heated bed of activated carbon," Energy, vol. 115, pp. 791-799, 2016.

[190] T. Manchanda, R. Tyagi, and D. K. Sharma, "Comparison of fuel characteristics of green (renewable) diesel with biodiesel obtainable from algal oil and vegetable oil," Energy Sources, Part A: Recovery, Utilization, and Environmental Effects, vol. 40, no. 1, pp. 54-59, 2018.

[191] N. S. Sarvestani, M. Tabasizadeh, M. H. Abbaspour-Fard, H. Nayebzadeh, H. Karimi-Maleh, T. C. Van, and R. J. Brown, "Influence of doping Mg cation in Fe3O4 lattice on its oxygen storage capacity to use as a catalyst for reducing emissions of a compression ignition engine," Fuel, vol. 272, p. 117728, 2020.

[192] A. O. Emiroğlu, A. Keskin, and M. Şen, "Experimental investigation of the effects of turkey rendering fat biodiesel on combustion, performance and exhaust emissions of a diesel engine," Fuel, vol. 216, pp. 266-273, 2018.

[193] M. Ghanbari, Technology and design of internal combustion engines. Technical & Vocational University Press, Tehran, Iran, 2019.

[194] A. Heidari-Maleni, T. M. Gundoshmian, B. Karimi, A. Jahanbakhshi, and B. Ghobadian, "A novel fuel based on biocompatible nanoparticles and ethanol-biodiesel blends to improve diesel engines performance and reduce exhaust emissions," Fuel, vol. 276, p. 118079, 2020.

[195] P. Yadav, N. Kumar, and R. Gautam, "Improvement in performance of CI engine using various techniques with alternative fuel," Energy Sources, Part A: Recovery, Utilization, and Environmental Effects, pp. 1-27, 2021.

[196] A. Dhar and A. K. Agarwal, "Performance, emissions and combustion characteristics of Karanja biodiesel in a transportation engine," Fuel, vol. 119, pp. 70-80, 2014.

[197] S. N. A. Yusof, N. A. C. Sidik, Y. Asako, W. M. A. A. Japar, S. B. Mohamed, and N. M. A. Muhammad, "A comprehensive review of the influences of nanoparticles as a fuel

additive in an internal combustion engine (ICE)," Nanotechnology Reviews, vol. 9, no. 1, pp. 1326-1349, 2020.

[198] J. Wei et al., "Impact of aluminium oxide nanoparticles as an additive in diesel-methanol blends on a modern DI diesel engine," Applied Thermal Engineering, vol. 185, p. 116372, 2021.

[199] A. Prabu, "Nanoparticles as additive in biodiesel on the working characteristics of a DI diesel engine," Ain shams Engineering journal, vol. 9, no. 4, pp. 2343-2349, 2018.

[200] H. Venu and V. Madhavan, "Effect of Al2O3 nanoparticles in biodiesel-diesel-ethanol blends at various injection strategies: Performance, combustion and emission characteristics," Fuel, vol. 186, pp. 176-189, 2016.

[201] K. Subramani and M. Karuppusamy, "Performance, combustion and emission characteristics of variable compression ratio engine using waste cooking oil biodiesel with added nanoparticles and diesel blends," Environmental Science and Pollution Research, vol. 28, no. 45, pp. 63706-63722, 2021.

[202] G. Solero, "Experimental analysis of the influence of inert nano-additives upon combustion of diesel sprays," Nanoscience and Nanotechnology, vol. 2, no. 4, pp. 129-133, 2012.

[203] K. Fangsuwannarak and K. Triratanasirichai, "Effect of metalloid compound and bio-solution additives on biodiesel engine performance and exhaust emissions," American Journal of Applied Sciences, vol. 10, no. 10, p. 1201, 2013.

[204] J. S. Basha and R. B. Anand, "Performance, emission and combustion characteristics of a diesel engine using Carbon Nanotubes blended Jatropha Methyl Ester Emulsions," Alexandria Engineering Journal, vol. 53, no. 2, pp. 259-273, 2014.

[205] Ü. Ağbulut et al., "Impact of various metal-oxide based nanoparticles and biodiesel blends on the combustion, performance, emission, vibration and noise characteristics of a CI engine," Fuel, vol. 270, p. 117521, 2020.

[206] A. T. Hoang, "Combustion behaviour, performance and emission characteristics of diesel engine fuelled with biodiesel containing cerium oxide nanoparticles: A review," Fuel Processing Technology, vol. 218, p. 106840, 2021.

[207] E. Dobrzyńska et al., "Exhaust emissions from diesel engines fueled by different blends with the addition of nanomodifiers and hydrotreated vegetable oil HVO," Environmental Pollution, vol. 259, p. 113772, 2020.

[208] S. Gumus et al., "Aluminum oxide and copper oxide nanodiesel fuel properties and usage in a compression ignition engine," Fuel, vol. 163, pp. 80-87, 2016.

[209] S. Bhan, R. Gautam, and P. Singh, "Analyzing the impact of adding aluminium oxide and cerium oxide nanoparticles to waste cooking biodiesel on engine performance, combustion and emissions characteristics," Petroleum Science and Technology, pp. 1-29, 2022.

[210] S. Krishna kumar et al., "Influence of graphene nanoparticles and antioxidants with waste cooking oil biodiesel and diesel blends on engine performance and emissions," Energies, vol. 14, no. 14, p. 4306, 2021.

[211] G. S. Ganesan and S. Ramesh, "Effect of CeO2 nanopowder as an additive in WME-TPO blend to control toxic emissions from a light-duty diesel engine – An experimental study," Fuel, vol. 278, p. 118177, 2020.

[212] A. Afzal et al., "Blends of scum oil methyl ester, alcohols, silver nanoparticles and the operating conditions affecting the diesel engine performance and emission: an optimization study using Dragon fly algorithm," Applied Nanoscience, vol. 11, no. 9, pp. 2415-2432, 2021.

[213] M. A. Fayada and H. A. Dhahadb, "Effects of adding aluminium oxide nanoparticles to butanol-diesel blends on performance, particulate matter, and emission characteristics of diesel engine," Fuel, vol. 286, p. 119363, 2021.

[214] M. Nour et al., "Influence of adding aluminium oxide nanoparticles to diesel blends on the combustion and exhaust emission characteristics of a diesel engine," Experimental Thermal and Fluid Science, vol. 98, pp. 634-644, 2018.

[215] R. Gautam and N. Kumar, "Performance emission and combustion studies of diesel engine on Jatropha ethyl ester and its higher alcohol blends," International Journal of Global Warming, vol. 14, no. 2, pp. 159-169, 2018.

[216] H. Venu and V. Madhavan, "Effect of Al2O3 nanoparticles in biodiesel-diesel-ethanol blends at various injection strategies: Performance, combustion, and emission characteristics," Fuel, vol. 186, pp. 176-189, 2016.

[217] B. Ashok et al., "Experimental studies on the effect of metal oxide and antioxidant additives with Calophyllum inophyllum methyl ester in compression ignition engine," J Clean Prod, vol. 166, pp. 474–484, 2017.

[218] K. Nanthagopal et al., "An assessment on the effects of 1-pentanol and 1-butanol as additives with Calophyllum inophyllum biodiesel," Energy Convers Manag, vol. 158, pp. 70–80, 2018.

[219] M. Mirzajanzadeh et al., "A novel soluble nano-catalysts in diesel–biodiesel fuel blends to improve diesel engine's performance and reduce exhaust emissions," Fuel, vol. 139, pp. 374–82, 2015.

[220] S. Janakiraman et al., "Comparative behaviour of various nano additives in a diesel engine powered by novel Garcinia gummi-gutta biodiesel," Journal of Cleaner Production, vol. 245, p. 118940, 2020.

[221] P. Tamilselvan, N. Nallusamy, and S. Rajkumar, "A comprehensive review on performance, combustion and emission characteristics of biodiesel fuelled diesel engines," Renewable and Sustainable Energy Reviews, vol. 79, pp. 1134-1159, 2017.

[222] D. Sikha, R. Gautam, and S. Kumar, "Performance and Combustion Analysis of Diesel and Sesame Biodiesel in Small Capacity Diesel Engine," Design Engineering, pp. 4923-4938, 2021.

[223] V. Sajith, C. Sobhan, and G. Peterson, "Experimental investigations on the effects of cerium oxide nanoparticle fuel additives on biodiesel," Advances in Mechanical Engineering, vol. 2, p. 581407, 2010.

[224] D. Rangabashiam, S. Rathinam, G. Subbiah, J. B. Sajin, and S. Suresh Babu, "Emission behavior studies on the cause of ZnO nanoparticle inclusion in neat biodiesel," Energy Sources, Part A: Recovery, Utilization, and Environmental Effects, vol. 42, no. 16, pp. 1989–96, 2020.

[225] S. Krishnakumar et al., "Influence of graphene nanoparticles and antioxidants with waste cooking oil biodiesel and diesel blends on engine performance and emissions," Energies, vol. 14, no. 14, p. 4306, 2021.

[226] R. Gautam, N. Kumar, and P. Sharma, "Experimental Investigation on Use of Jatropha Oil Ethyl Ester and Diesel Blends in Small Capacity Diesel Engine," presented at the SAE Technical Paper, 2013, paper number 2013-24-0172.

[227] Afzal, A., €U. A_gbulut, M. E. M. Soudagar, R. K. Razak, A. Buradi, and C. A. Saleel. 2021. Blends of scum oil methyl ester, alcohols, silver nanoparticles and the operating conditions affecting the diesel engine performance and emission: An optimization study using Dragon fly algorithm. Applied Nanoscience 11 (9):2415–32. doi:10.1007/s13204-021-02046-5.

[228] V. Sajith, C. Sobhan, and G. P. Peterson, "Experimental investigations on the effects of cerium oxide nanoparticle fuel additives on biodiesel," Advances in Mechanical Engineering, vol. 2, p. 581407, 2010.

[229] V. Perumal and M. Ilangkumaran, "The influence of copper oxide nanoparticle added pongamia methyl ester biodiesel on the performance, combustion and emission of a diesel engine," Fuel, vol. 232, pp. 791-802, 2018.

[230] S. N. A. Yusof et al., "A comprehensive review of the influences of nanoparticles as a fuel additive in an internal combustion engine (ICE)," Nanotechnology Reviews, vol. 9, no. 1, pp. 1326-1349, 2020.

[231] M. A. Mujtaba et al., "Comparative study of nanoparticles and alcoholic fuel additives-biodiesel-diesel blend for performance and emission improvements," Fuel, vol. 279, p. 118434, 2020.

[232] S. Kumar, P. Dinesha, and M. A. Rosen, "Effect of injection pressure on the combustion, performance and emission characteristics of a biodiesel engine with cerium oxide nanoparticle additive," Energy, vol. 185, pp. 1163-1173, 2019.

[233] S. K. Yoon, J. C. Ge, and N. J. Choi, "Influence of fuel injection pressure on the emissions characteristics and engine performance in a CRDI diesel engine fueled with palm biodiesel blends," Energies, vol. 12, no. 20, p. 3837, 2019.

[234] A. Datta and B. K. Mandal, "Effect of compression ratio on the performance, combustion and emission from a diesel engine using palm biodiesel," in AIP Conference Proceedings, 2016, vol. 1754, no. 1, p. 030038.

[235] M. El_Kassaby and M. A. Nemit_allah, "Studying the effect of compression ratio on an engine fueled with waste oil produced biodiesel/diesel fuel," Alexandr Engineering Journal, vol. 52, no. 1, pp. 1-11, 2013.

[236] M. Ghanbari et al., "Effect of alumina nanoparticles as additive with diesel–biodiesel blends on performance and emission characteristic of a six-cylinder diesel engine using response surface methodology (RSM)," Energy Conversion and Management: X, vol. 11, p. 100091, 2021.

[237] M. E. A. Fahd et al., "Experimental investigation of the performance and emission characteristics of direct injection diesel engine by water emulsion diesel under varying engine load condition," Applied Energy, vol. 102, pp. 1042-1049, 2013.

[238] T. Kegl, A. K. Kralj, B. Kegl, and M. Kegl, "Nanomaterials as fuel additives in diesel engines: A review of current state, opportunities, and challenges," Progress in Energy and Combustion Science, vol. 83, p. 100897, 2021.

[239] T. Aina, "Influence of compression ratio on the performance characteristics of a spark ignition engine," Ph.D. dissertation, 2012.

[240] M. Hawi, A. Elwardany, M. Ismail, and M. Ahmed, "Experimental investigation on performance of a compression ignition engine fueled with waste cooking oil biodiesel–diesel blend enhanced with iron-doped cerium oxide nanoparticles," Energies, vol. 12, no. 5, p. 798, 2019.

[241] M. Canakci, C. Sayin, A. N. Ozsezen, and A. Turkcan, "Effect of injection pressure on the combustion, performance, and emission characteristics of a diesel engine fueled with methanol-blended diesel fuel," Energy & Fuels, vol. 23, no. 6, pp. 2908-2920, 2009.

[242] D. Sundaram, V. Yang, and R. A. Yetter, "Metal-based nanoenergetic materials: synthesis, properties, and applications," Progress in Energy and Combustion Science, vol. 61, pp. 293-365, 2017.

[243] A. I. EL-Seesy, H. Hassan, and S. Ookawara, "Performance, combustion, and emission characteristics of a diesel engine fueled with Jatropha methyl ester and graphene oxide additives," Energy Conversion and Management, vol. 166, pp. 674-686, 2018.

[244] K. Srinivas, B. B. Naik, and K. K. Radha, "Impact of fuel injection pressure and compression ratio on performance and emission characteristics of VCR CI engine fueled with palm kernel oil-eucalyptus oil blends," Materials Today: Proceedings, vol. 4, no. 2, pp. 2222-2230, 2017.

[245] S. Ramalingam, P. Chinnaia, and S. Rajendran, "Influence of compression ratio on the performance and emission characteristics of annona methyl ester operated DI diesel engine," Advances in Mechanical Engineering, vol. 6, p. 832470, 2014.

[246] A. Sharma, N. A. Ansari, A. Pal, Y. Singh, and S. Lalhriatpuia, "Effect of biogas on the performance and emissions of diesel engine fuelled with biodiesel-ethanol blends through response surface methodology approach," Renewable Energy, vol. 141, pp. 657-668, 2019.

[247] S. K. Yoon, J. C. Ge, and N. J. Choi, "Influence of fuel injection pressure on the emissions characteristics and engine performance in a CRDI diesel engine fueled with palm biodiesel blends," Energies, vol. 12, no. 20, p. 3837, 2019.

LIST OF PUBLICATIONS

International Journal

List of Publication Based on the Research work (present) Work

- **Paper published title on "**An Experimental Assessment of Combustion, Emissions, and Performance Behavior of Diesel Engine Fuelled With New Developed Biofuel Blend of Two Distinct Waste Cooking Oils and Metallic Nano-particle (Al_2O_3)" in Scientia iranica, *https://doi.org10.24200/SCI.2022.58882.5947.*

- **Paper published title on "**Analyzing the impact of adding aluminum oxide and cerium oxide nanoparticles to waste cooking biodiesel on engine performance, combustion and emissions characteristics" in petroleum and science technology. *https://doi.org/10.1080/10916466.2022.2136705* .

- **Paper published title on "**Application of response surface approach to optimize CI engine parameters fuelled by newly developed waste cooking biodiesel infused with Al_2O_3 nanoparticle" in environmental progress & sustainable energy. *https://doi.org/10.1002/ep.14151* .

International Conferences

- **Paper published title on "**A Comprehensive Review of Performance, Combustion, and Emission Characteristics of Biodiesel Blend with Nanoparticles in Diesel Engines". Recent Trends in Thermal Engineering. Lecture Notes in Mechanical Engineering. Springer, Singapore (2021). *https://doi.org/10.1007/978-981-16-3428-47* .

- **Paper published title on "**A Comprehensive Review of Performance, Combustion, and Emission Characteristics of Biodiesel-Fueled Diesel Engines". Recent Trends in Thermal Engineering. Lecture Notes in Mechanical Engineering. Springer, Singapore (2021). *https://doi.org/10.1007/978-981-16-3428-4.*

3rd International Conference
on
Computational & Experimental Methods in Mechanical Engineering
(ICCEMME-2021)
11th - 13th February, 2021

Certificate of Participation

Mr. Suraj Bhan

presented his/her research paper entitled

A Comprehensive review of performance, combustion and emission characteristics of biodiesel blend with nano particles in diesel engine

in ICCEMME-2021.

Prof. Satish Chand
Convener

Prof. (Dr.) Vinod Kr. Yadav,
Head-MED, GLBITM

Prof. Rajeev Agrawal
Conference Patron

SPONSOR BY: IFFCO   Technical Partner

Made for free with Certify'em

3rd International Conference
on
Computational & Experimental Methods in Mechanical Engineering
(ICCEMME-2021)
11th - 13th February, 2021

Certificate of Participation

Mr. Suraj bhan

presented his/her research paper entitled

A comprehensive review of performance , combustion and emission characteristics of biodiesel fueled diesel engine

in ICCEMME-2021.

Prof. Satish Chand
Convener

Prof. (Dr.) Vinod Kr. Yadav,
Head-MED, GLBITM

Prof. Rajeev Agrawal
Conference Patron

SPONSOR BY: IFFCO   Technical Partner

Made for free with Certify'em

BRIEF PROFILE

Suraj Bhan is an Assistant Professor in the Department of Mechanical Engineering at Noida International University, Greater Noida, a role he has held since December 4, 2023.

Teaching Experience:
- ➢ Assistant Professor, IIMT College of Engineering, Greater Noida (July 22, 2013 – December 1, 2023)
- ➢ Assistant Professor, VITS Ghaziabad (October 2009 – July 2011)
- ➢ Assistant Professor, ALPINE College of Engineering (August 16, 2011 – August 2012)
- ➢ Assistant Professor, ACME College of Engineering, Ghaziabad (September 9, 2012 – July 20, 2013)

Academic Background:
- ➢ Bachelor of Technology (B.Tech.): Uttar Pradesh Technical University (First Division)
- ➢ Master of Technology (M.Tech.): Alfalah University (Honorary degree for academic excellence)

He joined department of Mechanical Engineering Department, Delhi Technological University, Delhi-110042 as a PhD scholar in January 2019 and submitted his doctoral thesis on 9th February 2024.

Research Contribution: Primary areas of research interest include the development of alternative-fueled low emission engine/vehicles. His work explores the use of biodiesel and nanoparticle-enhanced blends, along with environmentally conscious engine modeling.

Ph.D. Thesis: "Experimental Investigation of Performance and Emission Characteristics of a Nano-Biofueled CI Engine".

He conducted his Ph.D. research at Delhi Technological University, where he investigated the performance and emission behaviors of CI engines fueled with waste cooking biodiesel blends and metallic nanoparticles.

His research involved:
- ➢ Comprehensive CI engine trials.
- ➢ Optimization of performance and emissions using Response Surface Methodology.
- ➢ Simulation of engine characteristics using Boost software.
- ➢ CFD modeling of diesel engine components using Auto Desk software.

Research Accomplishments
- ➢ Published three SCI/SCIE-indexed and two Scopus-indexed research papers.
- ➢ Two additional research papers are currently under review in SCI-indexed journals and one book chapter has published.
- ➢ Recognized with the *DTU Research Excellence Award 2024* for outstanding research contributions in 2023.

Suraj Bhan is a committed scholar with a robust academic background in mechanical engineering, dedicated to advancing sustainable energy solutions through innovative research.